Backman, J., Duncan, R. A., et al., 1988
Proceedings of the Ocean Drilling Program, Initial Reports, Vol. 115

4. SITES 705 AND 706[1]

Shipboard Scientific Party[2]

SITE 705

Hole 705A

Date occupied: 2100 L, 21 May 1987

Date departed: 2000 L, 22 May 1987

Time on hole: 23 hr

Position: 13°10.02′S, 61°23.02′E

Water depth (sea level; corrected m, echo-sounding): 2320.3

Water depth (rig floor; corrected m, echo-sounding): 2330.8

Bottom felt (m, drill pipe): 2318

Penetration (m): 27.5

Number of cores: 3

Total length of cored section (m): 27.5

Total core recovered (m): 19.2

Core recovery (%): 69.8

Oldest sediment cored:
Depth (mbsf): 27.5
Nature: coarse foraminiferal ooze
Age: late Pliocene
Measured velocity (km/s): not measured

SITE 706

Hole 706A

Date occupied: 2320 L, 22 May 1987

Date departed: 1035 L, 23 May 1987

Time on hole: 11 hr, 15 min

Position: 13°06.85′S, 61°22.26′E

Water depth (sea level; corrected m, echo-sounding): 2504.3

Water depth (rig floor; corrected m, echo-sounding): 2514.8

Bottom felt (m, drill pipe): 2517.0

Penetration (m): 47.5

Number of cores: 6

Total length of cored section (m): 47.5

Total core recovered (m): 39.3

Core recovery (%): 82.7

Oldest sediment cored:
Depth (mbsf): 47.5
Nature: calcareous nannofossil ooze
Age: early Oligocene
Measured velocity (km/s): not measured

Basement rocks:
Depth (mbsf): 47.5
Nature: vesicular plagioclase basalt
Age: early Oligocene?
Measured velocity (km/s): 3.5–4.0

Hole 706B

Date occupied: 1130 L, 23 May 1987

Date departed: 2400 L, 23 May 1987

Time on hole: 12 hr, 30 min

Position: 13°06.86′S, 61°22.26′E

Water depth (sea level; corrected m, echo-sounding): 2507.8

Water depth (rig floor; corrected m, echo-sounding): 2518.3

Bottom felt (m, drill pipe): 2507.8

Penetration (m): 43.7

Number of cores: 7

Total length of cored section (m): 43.7

Total core recovered (m): 29.4

Core recovery (%): 67.3

Oldest sediment cored:
Depth (mbsf): 36.7
Nature: calcareous nannofossil ooze
Age: early Oligocene
Measured velocity (km/s): not measured

Basement rocks:
Depth (mbsf): 36.7
Nature: vesicular basalt
Age: early Oligocene?
Measured velocity (km/s): 3.5–4.0

Hole 706C

Date occupied: 0915 L, 24 May 1987

Date departed: 0600 L, 26 May 1987

Time on hole: 44 hr, 45 min

Position: 13°06.84′S, 61°22.26′E

Water depth (sea level; corrected m, echo-sounding): 2519.0

Water depth (rig floor; corrected m, echo-sounding): 2529.5

Bottom felt (m, drill pipe): 2518.0

Penetration (m): 121.7

Number of cores: 9

Total length of cored section (m): 77.4

Total core recovered (m): 19.7

Core recovery (%): 25.5

Oldest sediment cored:
Depth (mbsf): 44.3
Nature: calcareous nannofossil ooze

[1] Backman, J., Duncan, R. A., et al., 1988. *Proc. ODP, Init. Repts.*, 115: College Station, TX (Ocean Drilling Program).
[2] Shipboard Scientific Party is as given in the list of Participants preceding the contents, with the addition of Isabella Premoli Silva and Silvia Spezzaferria, Dipartimento di Scienze della Terra, Universitá di Milano, Via Mangiagalli 34, I-20129 Milano, Italy.

Age: early Oligocene
Measured velocity (km/s): not measured

Basement rocks:
Depth (mbsf): 44.85
Nature: vesicular basalt
Age: early Oligocene?
Measured velocity (km/s): 3.5–4.0

SITE 705

Principal results: Site 705 is located in the western subtropical Indian Ocean at 13°10.02′S, 61°23.02′E at water depths of 2307.5 m on relatively gently sloping terrain. The site lies on the eastern shoulder of the Mascarene Plateau, at the northeastern margin of the Nazareth Bank (Fig. 1). This site is approximately 30 nmi north and east of shallow-water carbonate banks and reefs. In the immediate region are predominantly biogenic sediments, deposited on the volcanic slopes and then dissected by numerous east-trending channels. Canyons have cut down through the sediments as deep as 200 m. The intervening sediment highs are characterized by moderately to poorly stratified reflective layers (see "Seismic Stratigraphy" section, this chapter, and Fig. 2). We chose the site from survey data to be in the center of a 6-nmi-wide sediment lobe, bounded by 200-m-deep, east-trending canyons (Fig. 2).

Our primary objective was to drill to basement and recover a sequence of volcanic rocks for radiometric dating, geochemical and petrological analyses, and paleomagnetic studies. We hope these studies will determine the origin of the Mascarene Plateau and further our knowledge of Cenozoic plate reconstructions for the Indian Ocean. A secondary objective will use the sediment cores of this southernmost site of Leg 115 to monitor time-dependent fluctuations, if any, of surface-water mass boundaries (Equatorial Water, Central Water) through the expected Neogene and Oligocene strata, along with carbonate dissolution at this moderately deep location.

We retrieved only three cores using the advanced hydraulic piston corer (APC) in Hole 705A; the interval, which was cored to 27.5 mbsf, yielded a recovery rate of 69.8%. Hole instability caused by continuous cave-ins of loose foraminiferal sands prevented further penetration.

The sedimentary sequence (0–27.5 mbsf) at Site 705 is composed of a single lithologic unit, consisting of homogeneous, coarse-grained foraminiferal oozes lacking sedimentary structures (see "Lithostratigraphy" section, this chapter). The calcareous nannofossil content increases to 50% in a single 5-cm-thick layer at about 6 mbsf. Fragments and whole tests of pteropods occur in the uppermost 1.5 m of the sequence. Opaline silica is present only as traces of diatoms. Depositional rates averaged 5.2 m/m.y. during the past 2.85 Ma, but increased to over 20 m/m.y. in the lower part of the late Pliocene sequence. The deepest recovered sediment has an age which does not exceed 3.45 Ma (see "Sedimentation Rates" section, this chapter).

SITE 706

Principal results: Site 706 lies 3 nmi north of Site 705, at 13°06.85′S, 61°22.26′E, at water depths of 2506.5 m. Because of hole instability at Site 705 on the crest of a prominent sediment lobe, we decided to drill near the base of a canyon just to the north. Strong bottom reflections and side echoes on the precision depth recorder (PDR) over the site suggested that more consolidated sediments might be present at this location. A prominent ledge, 35 m above the canyon floor, was chosen as the drilling site (see "Seismic Stratigraphy" section, this chapter, Fig. 38).

Our objectives at Site 706 were identical to those at Site 705, although we realized that we could not reach our paleoceanographic goals because the site was located to avoid the upper Neogene coarse-grained, foraminiferal oozes encountered at Site 705. A total sediment thickness of about 50 m was estimated from the seismic stratigraphy.

Seven APC cores were raised from Hole 706A for a recovery rate of 82.7%. We ended coring at 47.5 mbsf, and upon retrieval of the deepest core, we found that a piece of basalt plugged the core catcher—the first basalt ever to be recovered using the APC technique! The ship then offset its position 10 m to the south to drill Hole 706B. Four APC cores were taken at Hole 706B. The fourth core advanced only 1.80 m, and the extended core barrel (XCB) system was used for the remaining three cores, down to a final depth of 43.7 m. The recovery was 67.3%. Core 115-706B-7X recovered material only in the core catcher, again basalt, overlain by 0.2 m of loose pebbles.

The final hole, Hole 706C, was drilled 20 m to the north of Hole 706B. The drill string was tripped, and the APC/XCB system was exchanged for the rotary core barrel (RCB). Hole 706C was washed down to a level just above the sediment/basalt contact (44.3 mbsf). This was followed by eight RCB cores, which recovered 0.55 m of sediment in the top of Core 115-706C-2R, and thereafter basalt to a terminal depth of 121.7 mbsf. Of a total penetration of 77.4 m into the basalt, 19.7 m were recovered (25.5%).

The stratigraphic section at Site 706 consists of loose foraminiferal sands and oozes followed by breccias composed of shallow-water limestone and volcanic rock fragments, overlying vesicular basalts. We perceived four dominant lithologies and age assignments in the stratigraphic sequence.

Unit 1 (0–4.0 mbsf) consists of coarse calcareous nannofossil-bearing foraminiferal ooze of Pleistocene age.

Unit 2 (4.0–47.0 mbsf) is composed of calcareous nannofossil ooze containing numerous volcanic-ash layers of early Oligocene age.

Unit 3 (47.0–47.5 mbsf) contains basalt, shallow-water limestone gravel, and breccia, which in turn contain basalt clasts with sulfide cement. Sediments in this unit are of early Oligocene age.

Unit 4 (47.5–121.7 mbsf) is composed of vesicular and massive plagioclase basalt flows of early Oligocene age.

Visual observation of a succession of distinct lithostratigraphic markers was used to correlate Hole 706A with Hole 706B; Hole 706C was washed down to basement. About 90% of the 47.5-m-long sediment sequence was probably deposited in less than 1 m.y. during the early Oligocene, entirely within Chron C12R. Since no biostratigraphic zonal boundaries were observed, the shipboard interhole correlations depend primarily on lithostratigraphic data.

The lithostratigraphic markers consist of the Pleistocene/Oligocene unconformity, a sharp change from yellow to green nannofossil ooze 3.5 m below the unconformity, and five prominent ash layers in the green ooze. One of these ash layers occurs only in Hole 706B, despite the fact that the corresponding depth interval was recovered in Hole 706A. Apart from this discrepancy, the lithostratigraphic markers suggest that there is no major offset in relative depth position between the two holes, and that a nearly complete composite section was recovered from the mud line to 47.0 mbsf.

The lithostratigraphic resolution attainable with magnetic susceptibility measurements, however, is on the scale of a few centimeters. Shipboard susceptibility data solved the problem of the missing ash layer in Hole 706A and added substantial insight into the hole-to-hole correlation (see "Paleomagnetics" section, this chapter). Over 60 significant tie points were identified, and 2 gaps were observed in the sediment section, one in Hole 706A at about 18 mbsf and another in Hole 706B at about 13 mbsf. The position of these gaps strongly suggests that they are related to recovery problems associated with the core boundaries.

The geologic column at Site 706 begins with a basement sequence of basaltic lava flows. These are thin, vesicular flows near the basalt-sediment interface which become noticeably more massive with depth. The chilled margins and thin, baked sediment interbeds provide evidence that all flows were erupted below sea level. We recognized 32 flow units on the basis of these glassy chilled margins. From their mineralogy, the basalts can be grouped into several magma types, all dominated by plagioclase and varying amounts of subordinate augite and olivine phenocrysts. The basalt is overlain by a coarse gravel which includes pebbles of reef limestone of Eocene to Oligocene age and rounded nodules of pyrite-cemented volcanic sandstone. Delicate, fresh glass shards enclosed in the sulfide attest to the rapid deposition and cementation of this material. The presence of "framboids" suggests that the pyrite was deposited by sulfur-reducing bacteria.

Lying immediately above the gravel is a 40-m sequence of calcareous nannofossil oozes and chalks interbedded with volcanic ashes. These ashes are generally a few centimeters thick and often contain unaltered shards of glass and fresh crystals of feldspar and pyroxene. An additional constituent is very fine particulate pyrite, which gives the ash layers a black to dark-gray color. Several ash layers have been disturbed by bioturbation upward and downward. There are four to five ash layers per meter through this unit, or one event every

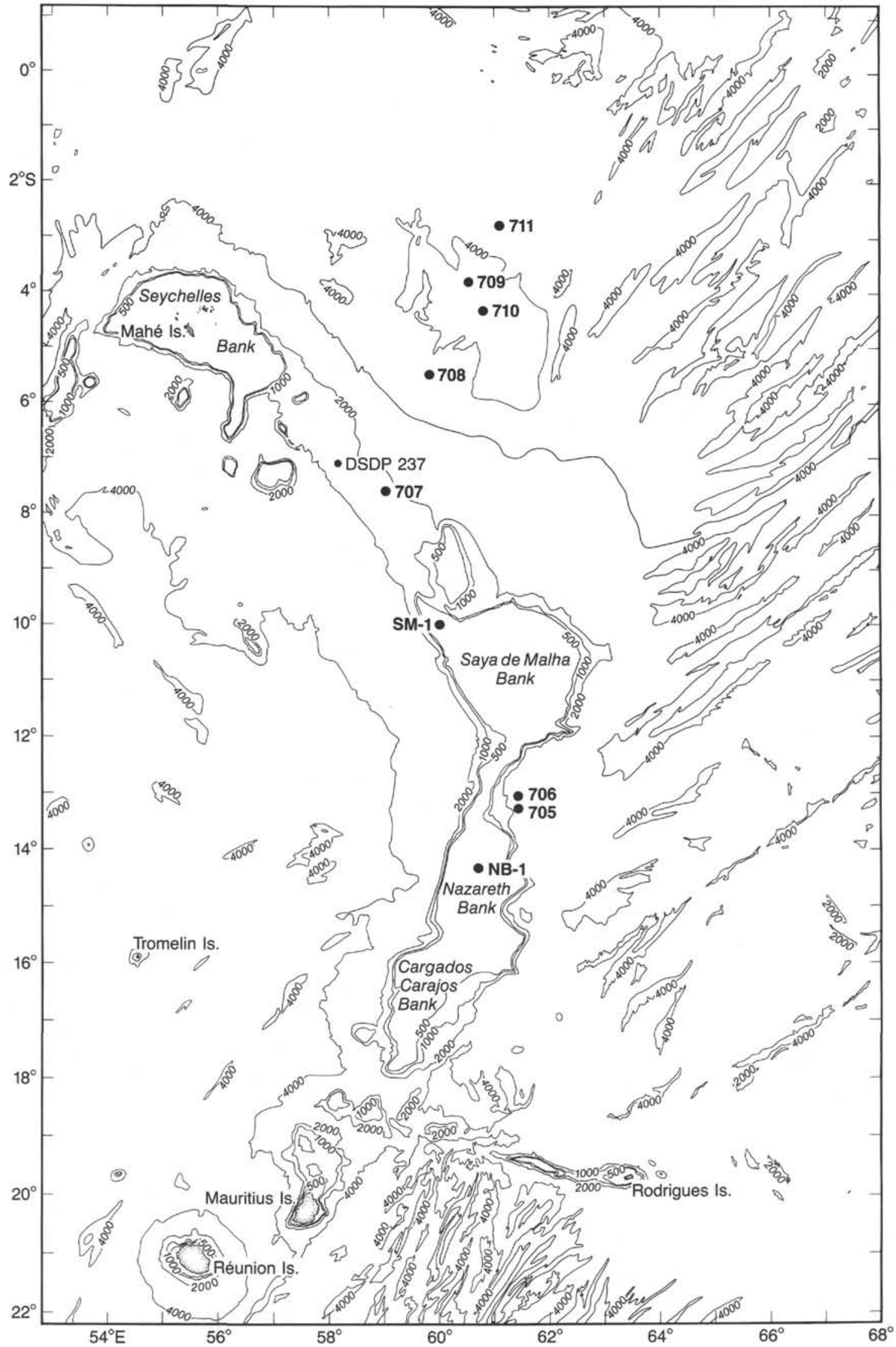

Figure 1. Bathymetric map of the western Indian Ocean (after Fisher et al., 1971) showing the location of sites drilled during Leg 115 in the vicinity of the Mascarene Plateau. Sites 705 and 706 are on the eastern shoulder of the ridge, at the northeastern margin of the Nazareth Bank. Depth in meters.

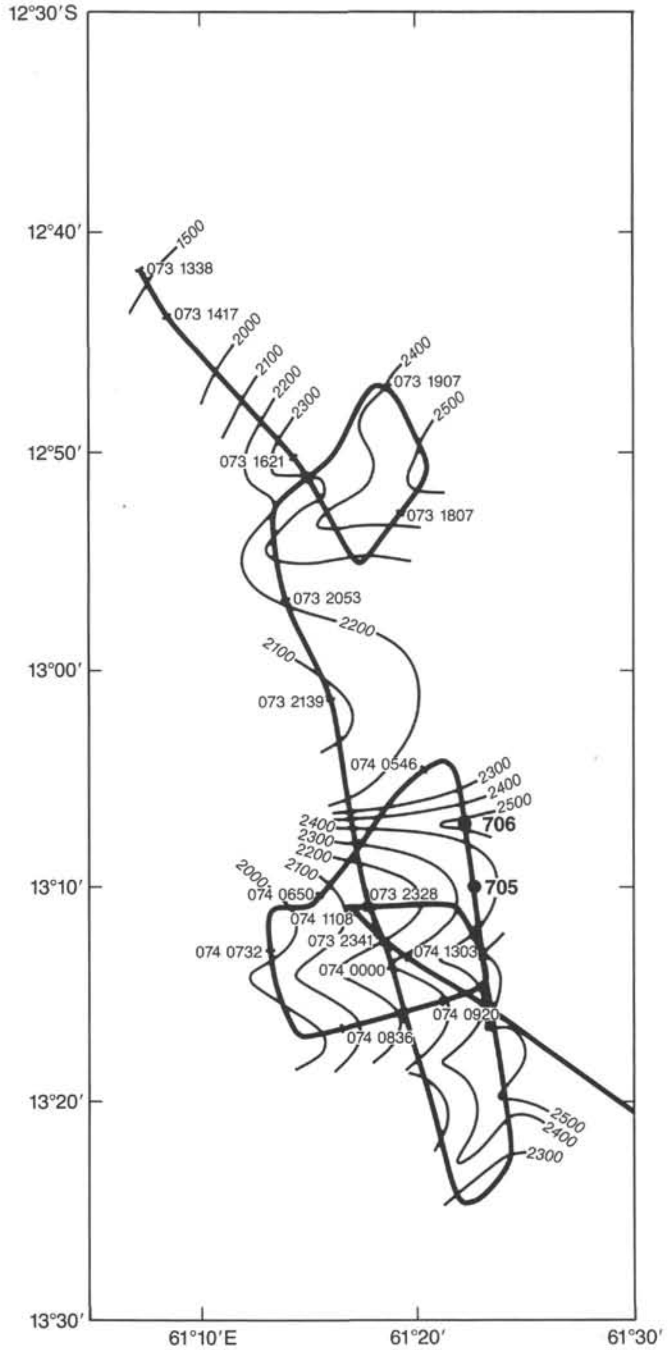

Figure 2. Detailed bathymetric survey in the area of Sites 705 and 706, conducted by the *Charles Darwin* in March 1987. The ship's track line and interpolated depth contours (meters) are shown. The region is characterized by sediment lobes bounded by west-trending canyons. Site 705 is located on the crest of one such sediment high, while Site 706 is close to the base of a 200-m-deep canyon.

6000–7000 yr, assuming the 34-m/m.y. sedimentation rate calculated from stratigraphic analysis.

The Oligocene nannofossil oozes and chalks consist almost exclusively of nannofossils (90%–100%) with less than 10% foraminifers. Benthic foraminifers indicate that the seafloor was shallower than it is now by 700–2000 m during early Oligocene times. At about 4 m below the top of this unit, there is a distinct color change from buff brown-yellow above to gray-green below, indicating a probable change in oxidation state.

The combined bio- and magnetostratigraphic information obtained from Holes 706A and 706C provide the basis for age estimates of the basalt and lowermost sediment at Site 706. The lower Oligocene nannofossil oozes are uniformly reversely magnetized, and all biostratigraphic indicators are consistent with deposition and magnetization of these sediments during the early portion of Chron C12R. The basalts, on the other hand, are all normally magnetized, and baked sediments interlayered with the flows contain *Ericsonia formosa*, but no Eocene elements. This indicates that the volcanic rocks were erupted during Chrons C13N-1 through C13N-2 (35.3–35.9 Ma; Berggren et al., 1985a). Calculating from the extremes of this age range, the minimum volcanic accumulation rate is about 120 m/m.y. If the basalts were magnetized entirely during Chron C13N-1, this rate would have been in excess of 380 m/m.y. (Fig. 3).

Figure 4 illustrates a reconstruction of the western Central Indian Ocean at 36 Ma, the time of eruption of basaltic lava flows at Site 706. At this time, the Central Indian Ridge began spreading and the Réunion hotspot was centered beneath one of its segments. Shortly afterward, the spreading ridge migrated to the northeast, and the hotspot's volcanic trail has since been recorded only on the African plate.

A major hiatus occurs at the top of the nannofossil ooze, where Pleistocene foraminiferal sands overlie the lower Oligocene sequence. The Pleistocene unit is about 4 m thick and of uniform age (<85 k.y.). Coarser sediment occurs at the base of this unit where we found pebbles of shallow-water limestone. These were probably eroded from the Nazareth Bank or Saya de Malha Bank. From the location of Site 706 near the base of a major canyon and from the uniform age and size sorting of fragments, we interpreted this unit as a grain flow that traveled eastward down the shoulder of the Mascarene Ridge.

Paleomagnetic measurements on split cores and discrete samples yield a paleolatitude of 26° ± 4° for sediments from Site 706. This implies that this site was about 5° south of the present location of hotspot activity at Réunion Island. However, we expected a component of true polar wander in this direction. Since the paleolatitude of the Deccan Traps (Western India) is somewhat further south (29° to ±4°S; Courtillot et al., 1986), the results imply that the hotspot moved slowly north between 67 Ma and the present.

BACKGROUND AND OBJECTIVES

The Mascarene-Chagos-Laccadive volcanic lineament is a major aseismic ridge system in the central Indian Ocean basin. It connects young volcanic activity in the vicinity of Réunion Island with the massive volumes of continental flood basalt erupted along India's western margin near the time of the Cretaceous/Tertiary boundary. This lineament parallels the remarkable Ninetyeast Ridge, and the two together record the northward motion of the Indian subcontinent away from stationary hotspots near Réunion and Kerguelen Islands, respectively (Fig. 5).

The southern, younger end of this trend is formed by the Mascarene Plateau, a broad, arcuate, elevated ridge that sweeps northward from Mauritius to the Nazareth Bank and then westward through the Saya de Malha Bank to the Seychelles Islands. The Nazareth Bank, Cargados Carajos Bank, and Soudan Bank form a series of shallow, broad carbonate platforms which trend northward from the islands of Réunion and Mauritius. Age determinations on rocks from the islands show that volcanic activity becomes progressively older to the northeast (McDougall and Chamalaun, 1969; McDougall, 1971). The carbonate banks are built on volcanic pedestals. Industry drilling on the Nazareth Bank penetrated 1700 m of shallow-water limestone before intersecting volcanic rocks (Meyerhoff and Kamen-Kaye, 1981).

Duncan (1981) and Morgan (1981) have proposed that hotspot activity near Réunion has persisted since Cretaceous time and has left a volcanic trail, first on the rapidly moving Indian plate and now on the slower moving African plate. This simple model predicts that the age of volcanic rocks along the trace increases from south to north. In addition, we expect that volcanic rocks recovered from the Mascarene Plateau should show geochemical and petrological similarities to rocks from Réunion

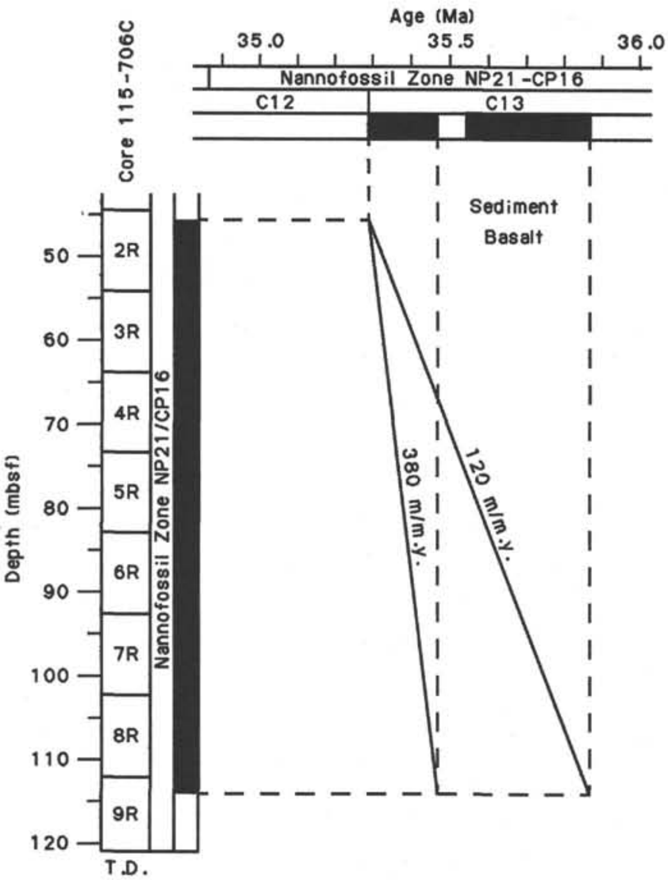

Figure 3. Age-depth constraints on the basalt recovered from Hole 706C. The rates suggested represent minimum sedimentation rates, according to magnetostratigraphy.

and Mauritius and to Deccan Trap basalts. Alternative models have proposed that the lineament is due to volcanic activity along a transform fault associated with early Tertiary seafloor spreading (Fisher et al., 1971; McKenzie and Sclater, 1971), or that the Mascarene Plateau is a submerged Paleozoic island arc (Meyerhoff and Kamen-Kaye, 1981).

Site 706 lies on the northern margin of Nazareth Bank, on a gentle east-dipping slope beyond the edge of carbonate reef formation. Reconstruction of the central Indian Ocean basin for Anomaly 13 time (36 Ma) closes up the Central Indian Ridge and joins the Nazareth Bank with the Chagos Bank (McKenzie and Sclater, 1971, and Fig. 6). This is strong evidence that the southeastern Mascarene Plateau and the Chagos to Maldive to Laccadive Islands ridge system are genetically related. We planned the drilling at Site 706 to test this connection by recovering basement volcanic rocks for age determinations and geochemical/petrological analyses. Paleomagnetic studies on the cored samples would determine the latitude at which basalts and immediately overlying sediments were magnetized; if our theories prove correct, that should be the latitude of the Réunion hotspot.

A secondary drilling objective at this location was to recover sediments from this southernmost site of Leg 115 to monitor time-dependent fluctuations of surface-water mass boundaries through the expected Neogene and upper Paleogene strata. In addition, we intend to examine carbonate dissolution at this moderately deep location for comparison with sediments from the equatorial depth-transect drilling planned later in the leg.

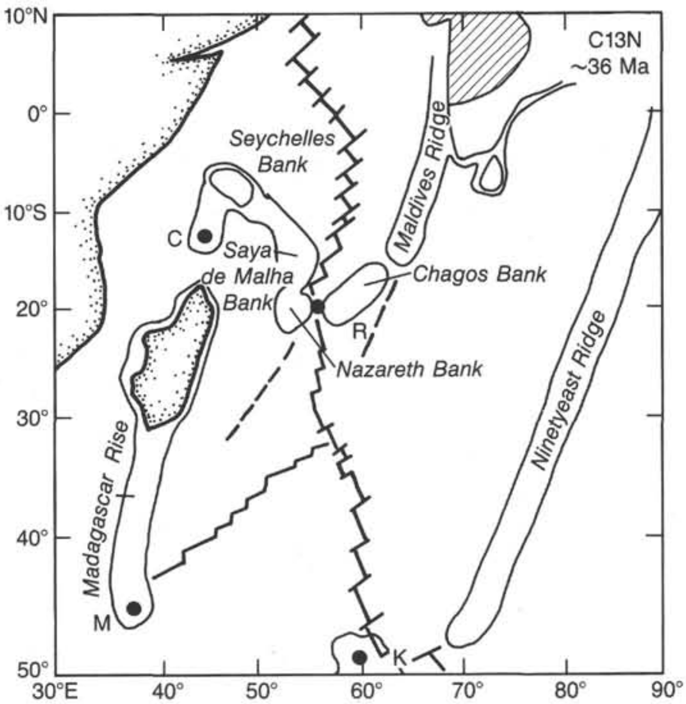

Figure 4. Plate reconstruction for the western central Indian Ocean for 36 Ma, in the fixed hotspot reference frame. Site 706 basalts were erupted over the Réunion hotspot at this time, when a segment of the Central Indian Ridge lay above the hotspot.

OPERATIONS

Leg 115 Drilling Plan

Leg 115 was initially planned to last 42 days with two main programs: (1) penetration and recovery of volcanic basement rocks on the Mascarene Plateau and (2) recovery of complete and undisturbed sediments by APC coring along a paleoceanographic depth transect consisting of four sites in equatorial waters. While in Port Louis, Mauritius, we learned that the government of Mauritius had rescinded permission to drill in their territorial waters. Therefore, we changed the first site we planned to drill to north of the Nazareth Bank, since the two southernmost sites we originally planned to drill were within Mauritian territorial waters.

Mauritius to Site 705 (MP-3)

The anchor was hoisted at 2115 hours, 19 May 1987, and the *JOIDES Resolution* was under way for Site MP-3. We suspended work on the drilling floor during transit due to heavy seas.

On the approach to Site MP-3, the seismic equipment was streamed for the pre-site survey and a beacon was dropped at 2100 hours, 21 May, establishing Site 705. A distance of 478 nmi was covered in 46.5 hrs (including surveying time over Site MP-1).

Site 705

Hole 705A

As the bottom hole assembly (BHA) was lowered to the seafloor, the drill string was rabbited and the downgraded joints removed.

The mud line was established at 2307.5 m water depth. After recovering three APC cores of foraminiferal sand, with the BHA

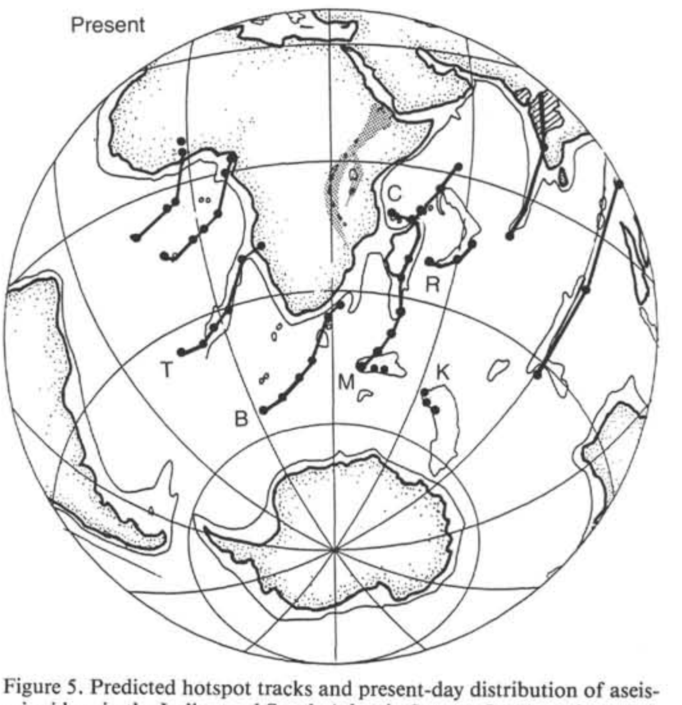

Figure 5. Predicted hotspot tracks and present-day distribution of aseismic ridges in the Indian and South Atlantic Oceans. Letters refer to Réunion (R), Comores (C), Kerguelen (K), Bouvet (B), Marion (M), and Tristan (T) hotspots. The present outcrop of flood basalts of the Deccan Traps is shown as the area of diagonal lines in western India (from Emerick, 1985).

beginning to stick after the second core, we decided to abandon Hole 705A.

Total penetration was 27.5 mbsf to 2335 m with 19.2 m of core recovered, for a recovery rate of 69.8% (Table 1).

Site 705 to Site 706

We relocated the ship 3 nmi north-northwest of Site 705 to initiate Site 706. The BHA was pulled above the mud line 100 m, and the ship was moved in the dynamic positioning (DP) mode to the new location. A retrievable beacon was dropped at 2320 hr, 22 May, to establish Site 706.

Hole 706A

The BHA was again lowered to the seafloor, and APC coring commenced with a water core on the first attempt. The second attempt established the mud line at 2506.5 m. After 41.1 m of penetration, recovering foraminiferal sand and "blue-green" clay, the water sampler temperature probe (WSTP), formerly called the pore-water sampler (PWS), was successfully deployed by free-falling. On Core 115-706A-6H, approximately 10 cm of basalt were recovered at 2554 m (47.5 mbsf).

With our objectives met, we pulled the BHA clear of the mud line and offset the ship 10 m south to initiate Hole 706B. Total penetration in Hole 706A was 47.5 mbsf to 2554 m, with 39.3 m of core recovered for a recovery rate of 82.7% (Table 1).

Hole 706B

The BHA was again lowered to the seafloor, and the mud line was established at 2497.3 m. Overlap APC coring to 2520.3 m (23 mbsf) recovered 22.3 m of foraminiferal sand and "blue-green" clay for an APC recovery rate of 99.6%. With penetration falling off, we decided to change to the extended core barrel (XCB) system.

We recovered 7.12 m of foraminiferal sand and clay with XCB coring from 2520.3 to 2541.6 m for an XCB recovery rate of 33.4%. On Core 115-706B-7X, 0.52 m of basalt was recovered. Once we reached basement and had met our objectives, we tripped the APC/XCB BHA to change to the rotary core barrel (RCB) system and offset the ship 20 m north to establish Hole 706C. Total penetration was 43.7 mbsf to 2541.6 m, with 29.4 m of core taken for a total recovery rate of 67.3% (Table 1).

We deployed the experimental XCB shoes with seal (one shoe with 1/4-in. jets, one with 3/32-in. jets). The experimental shoes presented no problems during retrieval with the sand line. We were able to recover full cores of sand and clay, using 40 spm at 700 psi. The test whether this mechanism improved recovery, however, was inconclusive due to the morphology of the hole (i.e., sand directly on top of basement). Therefore, we rescheduled this test for later holes.

Hole 706C

The BHA was lowered to the seafloor (2507.5 m), and the hole was washed down 44.3 m (2551.8 m) to begin RCB coring. Coring with the RCB system advanced the hole to 2629.2 m (121.7 mbsf).

During retrieval of Core 115-706C-4R, the drill string became stuck and circulation was lost. We believe that loose sand and rubble on top of the basalt fell into the hole and caused the problem. The drill string was worked for 1.5 hrs and was finally freed. We retrieved the core barrel and swept the hole with 30 bbl of mud. The hole was swept after we retrieved each core barrel thereafter. Total depth of penetration was 121.7 mbsf to 2629.2 m, with 77.4 m of basement cored and 19.7 m of basalt recovered, for a total recovery rate of 25.5% (Table 1).

Site 706 to Site 707 (CARB-1B)

Since the time scheduled for Site 706 was exhausted, the drill string was tripped and the beacon recalled and recovered at 2130 hrs, 25 May. We set a course for Site CARB-1B, a new site determined by the Co-Chiefs and approved by the Ocean Drilling Program (ODP) while en route.

LITHOSTRATIGRAPHY

Introduction

Due to the proximity of Site 705 to Site 706 (less than 5 km) and the similarity between the sedimentary facies of Hole 705A and the upper part of Holes 706A and 706B, both sites are described together. Two major sedimentary units are recognized in the combined sites.

We cored very pale brown (10YR 8/3) to yellowish tan (2.5Y 7/2) foraminiferal oozes with the APC in Hole 705A and in the upper part of Holes 706A and 706B. These oozes are considered as a single Unit I of Pliocene-Pleistocene age. Light greenish gray (5GY 7/1) to greenish gray (5GY 6/1) nannofossil oozes and chalks, interbedded with distinct unaltered and less distinct, bioturbated and altered volcanic-ash layers cored in the lower part of Holes 706A and 706B, are considered as a separate Unit II of early Oligocene age. Sediments in Hole 706C were mostly washed away during drilling in order to advance more quickly to the basement objective.

Unit I: Cores 115-705A-1H to -3H (0–27.5 mbsf); Core 115-706A-1H to Section 115-706A-2H-2, 9 cm (0–4.09 mbsf); and Sections 115-706B-1H-1 to 115-706B-1H-3, 30 cm (0–3.3 mbsf); Age: Pleistocene-Pliocene.

Unit I in both Sites 705 and 706 consists of foraminiferal oozes. In Hole 705A, 27.5 m of foraminiferal ooze was pene-

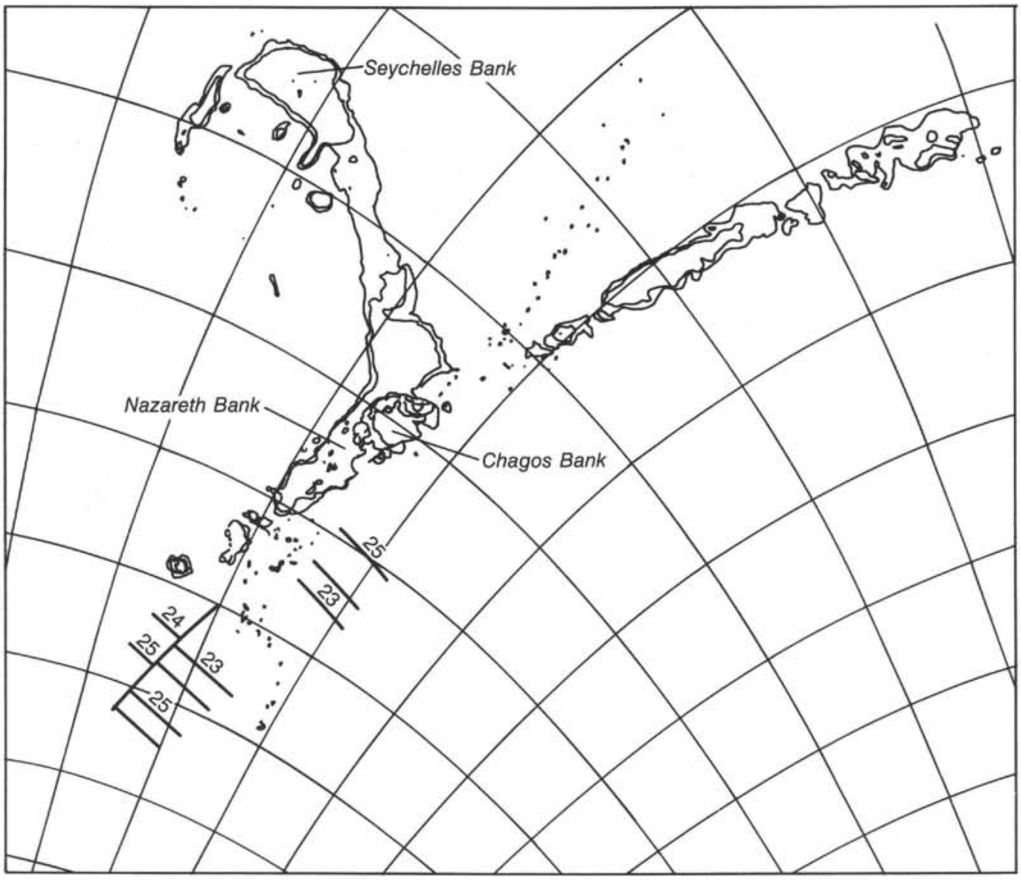

Figure 6. The fit of the Chagos Bank to the Mascarene Plateau by finite rotation, removing seafloor generated at the Central Indian Ridge between C13N time (36 Ma) and the present (from McKenzie and Sclater, 1971).

trated. The top 3.45 m consists of whitish orange (10YR 8/2) to very pale brown (10YR 8/4) foraminiferal ooze with more than 90% planktonic foraminifers; it could be called a foraminiferal sand. Pteropod tests and fragments occur only within the top section of Core 115-705A-1H (0–1.5 m). Below 3.45 m and to the bottom of Hole 705A (27.5 mbsf), the sediments become a nannofossil-bearing foraminiferal ooze, with nannofossils making up between 10% and 20% of the sediment. In a 5-cm-thick white (10YR 8/1) layer (Section 115-705A-1H-4, 139–144 cm), the nannofossil content is estimated to be 50% of the sediment and the ooze becomes a nannofossil-foraminiferal ooze. The cores do not show any obvious sedimentary structures and are quite homogeneous.

In summary, only a slight downcore variation in lithology is observed in Hole 705A. The sediment consists of a foraminiferal ooze at the top, an almost pure sand with some pteropod tests and fragments, which grades downcore into a slightly finer, incompletely winnowed sediment, becoming in one section a nannofossil-foraminiferal ooze. We interpreted Unit I in Hole 705A as a winnowed ooze with only minor reworking. The systematic age increase downcore within Unit I (see "Biostratigraphy" section, this chapter) strengthens this interpretation.

Unit I in Holes 706A and 706B is thinner (3.3 and 4.09 m) than in Hole 705A. It consists of a light gray to yellowish tan (10YR 7/2, 10YR 8/2, and 2.5Y 7/2), homogeneous, medium- to coarse-grained foraminiferal ooze with pteropod tests and fragments scattered throughout as well as rare echinoderm spines and coral fragments. In both Holes 706A and 706B, the coarser sediment occurs at the base of Unit I, where pebble-sized round fragments of shallow carbonate limestone are found (see Fig. 7). Based on thin-section observations, these limestone pebbles are Paleogene shallow-water reefal facies (see "Biostratigraphy" section, this chapter) which were probably eroded from the flanks of the Nazareth Bank, where a 1600-m-thick sequence of Eocene to Pliocene carbonates was drilled previously (Meyerhoff and Kamen-Kaye, 1981). Unit I in Holes 706A and 706B is interpreted to be part of a grain-flow layer that traveled eastward down a large canyon away from the north-trending Mascarene Ridge, before being deposited on the canyon floor. The uniform Pleistocene age of Unit I (see "Biostratigraphy" section, this chapter) supports this interpretation. In Holes 706A and 706B, Unit I is separated from Unit II by a lithologic and biostratigraphic unconformity (see "Biostratigraphy" section, this chapter, and Fig. 7).

Unit II: Section 115-706A-2H-2, 9 cm, to Core 115-706A-6H (4.09–47.5 mbsf); Section 115-706B-1H-3, 30 cm, to Core 115-706B-6X (3.3–36.7 mbsf); Age: Early Oligocene.

Unit II consists of a sequence of nannofossil ooze that grades into nannofossil chalk downcore. This sequence is 43.4 m thick in Hole 706A and 33.4 m thick in Hole 706B where it directly overlies oceanic basaltic basement. The nannofossil oozes and chalks are interbedded with distinct unaltered and less distinct, bioturbated and altered volcanic-ash layers which are generally a few centimeters thick. The carbonate fraction is composed almost exclusively of nannofossils (90%–100%), with foraminifers consistently making up less than 10% of the sediment. Nan-

Table 1. Coring summary, Sites 705 and 706.

Core no.	Date (May 1987)	Time (local)	Depth (mbsf)	Cored (m)	Recovered (m)	Recovery (%)
115-705A-						
1H	22	1445	0–8.5	8.5	8.33	98.0
2H	22	1545	8.5–18.0	9.5	8.43	88.7
3H	22	1645	18.0–27.5	9.5	2.40	25.2
115-706A-						
1H	23	0330	0–2.5	2.5	2.57	102.8
2H	23	0415	2.5–12.2	9.7	8.03	82.8
3H	23	0530	12.2–21.9	9.7	8.48	87.4
4H	23	0630	21.9–31.5	9.6	7.42	77.3
5H	23	0715	31.5–41.1	9.6	9.38	97.7
6H	23	0800	41.1–47.5	6.4	3.40	53.1
115-706B-						
1H	23	1200	0–5.7	5.7	5.70	100.0
2H	23	1300	5.7–12.7	7.0	7.00	100.0
3H	23	1415	12.7–20.6	7.9	7.88	99.7
4H	23	1515	20.6–22.4	1.8	1.74	96.6
5X	23	1715	22.4–27.1	4.7	3.50	74.4
6X	23	1900	27.1–36.7	9.6	3.10	32.3
7X	23	2045	36.7–43.7	7.0	0.52	7.4
115-706C-						
1W	24	1045	0–44.3	44.3	0.25	0.6
2R	24	1415	44.3–53.9	9.6	2.44	25.4
3R	24	1600	53.9–63.6	9.7	1.83	18.8
4R	24	2100	63.6–73.2	9.6	2.55	26.5
5R	25	0115	73.2–82.9	9.7	3.19	32.9
6R	25	0500	82.9–92.6	9.7	1.20	12.4
7R	25	0825	92.6–102.3	9.7	3.90	40.2
8R	25	1230	102.3–112.0	9.7	2.90	29.9
9R	25	1830	112.0–121.7	9.7	1.71	17.6

nofossil oozes in the top few meters of Unit II in both Holes 706A and 706B are pale yellow (2.5Y 7/4), indicating possible oxidizing conditions. At 7.4 mbsf in Hole 706A (Sample 115-706A-2H-4, 40 cm) and at 7.17 mbsf in Hole 706B (Sample 115-706B-2H-1, 147 cm), the color changes abruptly to a more greenish gray (5GY 6/1) to light greenish gray (5GY 7/1), indicating possible reducing conditions for most of Unit II.

Ash layers are easily distinguished from the nannofossil oozes/chalks by their darker colors (Fig. 8). Ash layers include distinct black (10YR 2/1, N4) to dark gray (N2) layers several centimeters thick, usually characterized by a sharp bottom contact and a gradational top boundary. Also present are less distinct ash layers characterized by both gradational lower and upper contacts; colors are dark greenish gray (5GY 4/1) and greenish gray (5GY 6/10) to pale green (5G 6/2). Distinct unaltered ash layers consist of volcanic glass, clays, opaque minerals (mainly pyrite), fresh feldspar, and pyroxene crystals as well as traces of olivine. Alteration and bioturbation of thinner ash layers produce less distinct layers ranging in color from the dark tones of pure ash to the greenish gray color of the intervening nannofossil oozes and chalks. Centimeter-scale faulting is also observed in some of the layers (Fig. 9).

In some well-developed ash layers, pyrite occurs in abundance (e.g., Sample 115-706A-5H-3, 52–53 cm). Presumably this pyrite forms as a result of diagenetic, microbial reduction of pore-water sulfate to sulfide which combines with iron derived from the ashes. The average frequency of ash layers is four to five per meter of core or one layer every 6000–7500 years, assuming sedimentation rates of 34 m/m.y. (see "Sedimentation Rates" section, this chapter). Visual correlation of distinct as well as less distinct ash layers between Holes 706A and 706B is difficult if based on the core description only. The correlation becomes more straightforward when using whole-core magnetic susceptibility profiles (see "Paleomagnetics" section, this chapter).

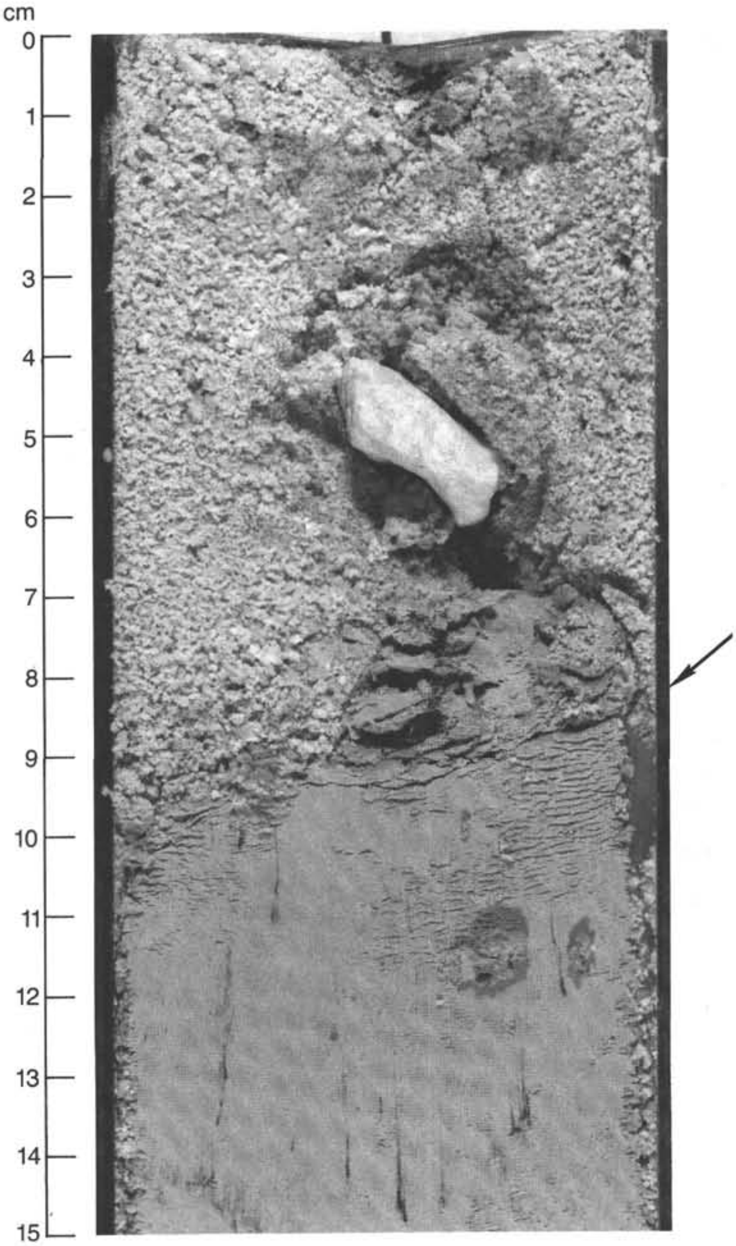

Figure 7. Lithologic and biostratigraphic unconformity; Pleistocene foraminiferal ooze overlies a lower Oligocene nannofossil ooze. Note pebble-sized fragment of Paleogene shallow carbonate limestone just above the unconformity (115-706A-2H-2, 0–15 cm).

BIOSTRATIGRAPHY

Introduction

The 27.5-m-thick sedimentary sequence penetrated at Site 705 consists of an upper Pliocene–Pleistocene foraminiferal ooze, whereas at Site 706 the 47.5-m-thick sequence consists of 3.8 m of Pleistocene foraminiferal ooze unconformably overlying 44 m of lower Oligocene nannofossil ooze.

Calcareous plankton are abundant and generally well preserved in both the Pliocene-Pleistocene and Oligocene intervals. Benthic foraminifers are also well preserved. They are rare in the Pliocene-Pleistocene sediments and abundant in the Oligocene. The entire sequence is barren of siliceous microfossils.

A biostratigraphic summary for Sites 705 and 706 is given in Figures 10 and 11.

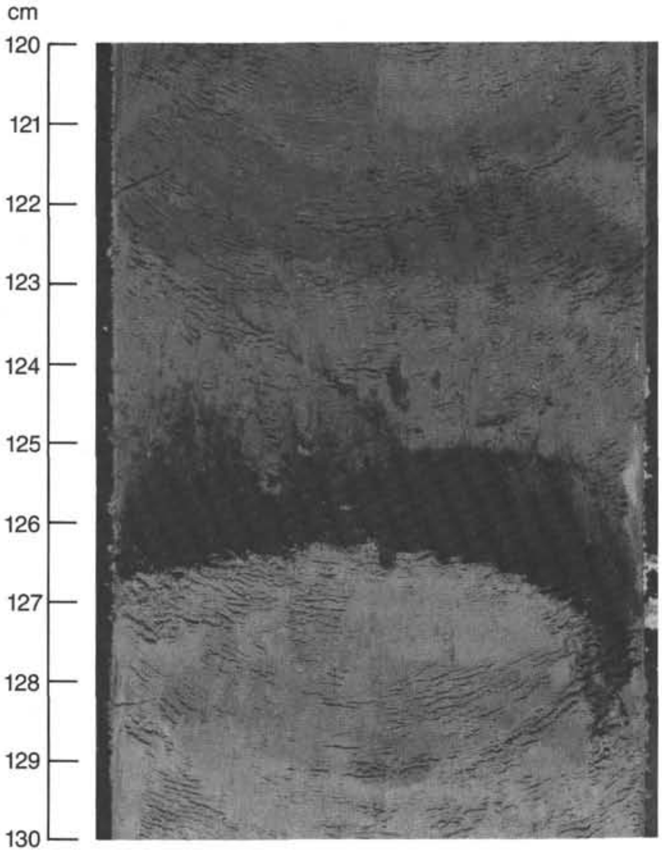

Figure 8. Example of a centimeter-thick ash layer with sharp bottom contact and gradational upper boundary (115-706A-2H-5, 120–130 cm).

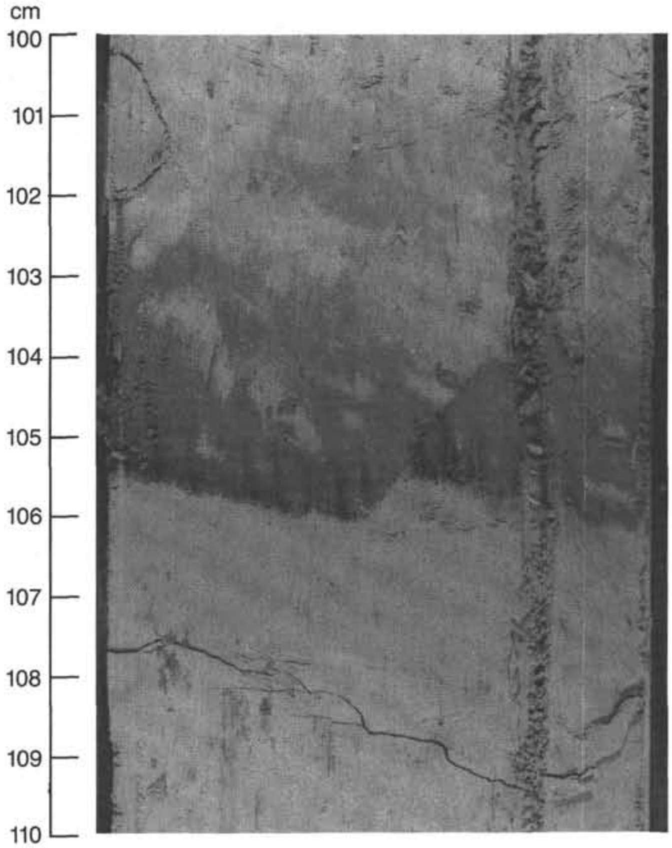

Figure 9. Example of an ash layer displaced by centimeter-scale faulting (115-706A-4H-1, 100–110 cm).

Calcareous Nannofossils

Site 705

Hole 705A

The three cores retrieved from Hole 705A yielded abundant Pleistocene to "middle" Pliocene calcareous nannofossils. The preservation is good in the upper four sections of Core 115-705A-1H and becomes moderate in deeper cores with evidence of slight dissolution. In addition, discoasters show the effects of overgrowth below the lower part of Core 115-705A-2H, with this overgrowth increasing substantially toward the bottom of the sequence.

Core 115-705A-1H contains a well-diversified Pleistocene coccolith assemblage in which gephyrocapsids are dominant. Other major components of the assemblage are *Calcidiscus leptoporus, Florisphaera profunda, Syracosphaera* spp., and *Umbilicosphaera sibogae*. Despite the somewhat winnowed nature of this lithologic sequence and the low sedimentation rate, the occurrence of reworked forms is surprisingly low. The relative abundance of *Emiliania huxleyi* is less than 10% in Sample 115-705A-1H-1, 2–3 cm, which suggests that the uppermost part of the Pleistocene sequence is missing at this site. Sample 115-705A-1H-1, 130–131 cm, however, also contains common *E. huxleyi*; therefore, we assigned Section 115-705A-1H-1 to the latest Quaternary Zone CN15.

Sample 115-705A-1H-2, 130–131 cm, does not contain *E. huxleyi* and *Pseudoemiliania lacunosa*; thus, it was assigned to Subzone CN14b. We observed the last occurrence (LO) of *P. lacunosa* in Sample 115-705A-1H-3, 130–131 cm. Thierstein et al. (1977) have shown that this event is globally synchronous in tropical and subtropical waters, and Backman (pers. comm., 1987) recently gave it a revised age of 0.46 Ma.

In the lower four sections of Core 115-705A-1H, medium and large forms of *Gephyrocapsa oceanica* that have a vertically oriented bridge are abundant. These sections are assigned to the upper part of Subzone CN14a. Although small forms of the genus *Gephyrocapsa* are abundant, medium and large *Gephyrocapsa* are extremely scarce in Section 115-705A-1, CC. This is a typical assemblage in the small *Gephyrocapsa* Zone of Gartner (1977).

Sample 115-705A-2H-1, 130–131 cm, yielded common *G. oceanica* in addition to frequent *Helicosphaera sellii* and rare *Calcidiscus macintyrei*. The LO of *C. macintyrei*, which is not used in the zonal schemes of Martini (1971) and Okada and Bukry (1980), has an estimated age of 1.45 Ma and has been proven to be synchronous worldwide (Backman and Shackleton, 1983). The first occurrence (FO) of *G. oceanica* is the nannofossil event which best approximates the Pliocene/Pleistocene boundary and was estimated at 1.6 Ma (Rio et al., in press). Section 115-705A-2H-1, therefore, belongs to the basal part of Subzone CN14a (1.45–1.6 Ma).

In the underlying Sample 115-705A-2H-2, 130–131 cm, we identified the LO of *Discoaster brouweri*, which is a terminal Pliocene event. The Pliocene/Pleistocene boundary was identified, therefore, as well as the lower boundaries of Zone NN19 or CN14 between Samples 115-705A-2H-1, 130–131 cm, and 115-705A-2H-2, 130–131 cm. In Samples 115-705A-2H-3, 130–131 cm, and 115-705A-2H-4, 130–131 cm, *D. brouweri* and *Discoaster pentaradiatus* are present, indicating Zone NN17 or Subzone CN12c.

The LO of *Discoaster tamalis*, which defines the top of Subzone CN12a, was observed between Samples 115-705A-2H-4,

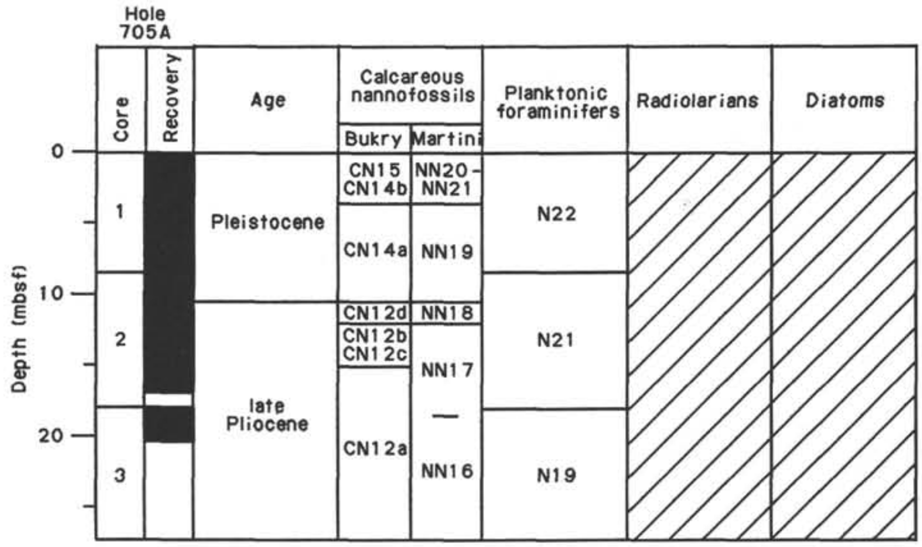

Figure 10. Biostratigraphic summary for Site 705. Black bars represent recovery in Hole 705A.

130–131 cm, and 115-705A-2H-5, 130–131 cm. *Reticulofenestra pseudoumbilica* or *Sphenolithus* spp. do not occur in any of the samples in Hole 705A. Therefore, the interval between Sample 115-705A-2H-5, 130–131 cm, and the bottom of the hole belongs to upper Pliocene Subzone CN12a.

The upper Pliocene–Pleistocene sequence of nannofossil events observed in the sedimentary sequence of Hole 705A is remarkably regular, with little sign of reworking. This finding indicates that the sedimentation rate was rather constant, albeit somewhat reduced, by the winnowing effects of bottom currents from the late Pliocene to late Pleistocene, and that redeposition of sediment was nonexistent or very limited at this site.

The change in preservation, from slight to near zero dissolution above Section 115-705A-1H-4, may indicate a deepening of the carbonate-compensation depth (CCD) after middle Pleistocene time. The increasing signs of recrystallization in the lower section of the sequence are probably due to diagenetic effects in this almost pure carbonate sediment.

Site 706

Hole 706A

We recovered Pleistocene and early Oligocene sequences from this hole. The contact between these sequences was easily recognized at the uppermost part of Section 115-706A-2H-2 by a sharp change of lithology from an upper yellowish brown foraminiferal sand to a lower gray-colored calcareous ooze.

The lithology of the Pleistocene sequence is identical with that of Hole 705A, with well- to moderately well-preserved nannofossils abundant to common in this sequence. As we observed in Hole 705A, the preservation of nannofossils is good in the top part of the section, but it becomes moderate in the lower part with some evidence of dissolution.

The sample taken from the bottom of this Pleistocene sequence yields abundant *Emiliania huxleyi*, and the entire Pleistocene sequence can be assigned to Zone CN15. In Sample 115-706A-1H-1, 130–131 cm, *E. huxleyi* constituted 34% of the flora, while *Gephyrocapsa* species accounted for only 19%. In terms of relative abundance, *E. huxleyi* is known to overtake *Gephyrocapsa caribbeanica* after 85,000 k.y. in tropical and subtropical waters (Thierstein et al., 1977). It also appears to be more abundant than *G. caribbeanica* in Sample 115-706A-1H-1, 130–131 cm, and Section 115-706A-1H, CC, whereas it is slightly less abundant than *G. caribbeanica* in Sample 115-706A-2H-2, 3 cm. The datum level of 0.085 Ma, therefore, is placed between Section 115-706A-1H, CC, and Sample 115-706A-2H, 3 cm.

At the unconformity between the Pleistocene and Oligocene sequences (at approximately Sample 115-706A-2H-2, 7–9 cm), we recovered a piece of white limestone. Strongly overgrown specimens of *Cyclicargolithus floridanus* were observed in this sample. Since no other species are recognizable, the age of this limestone cannot be determined to better than middle Eocene to early middle Miocene, which represents the entire range of *C. floridanus*.

The entire Oligocene sediment sequence contains very abundant nannofossils. The preservation of nannofossils is generally moderate except at the very bottom of the sequence where the preservation is good. We detected no signs of dissolution within the sequence, although moderate to severe recrystallization is evident in certain intervals.

Cyclicargolithus floridanus is the most abundant species, occupying from 40% to 60 % of the total assemblage in the Oligocene sequence. Other major species include *Braarudosphaera bigelowii, Coccolithus pelagicus, Dictyococcites bisectus, Helicosphaera compacta, H. euphratis, H. reticulata, Sphenolithus moriformis*, and *S. predistentus*. *Sphenolithus distentus* is rare in the upper part and becomes common in the middle to lower part of this section.

Because *S. distentus* is present and its descendant species *Sphenolithus ciperoensis* is absent, the entire Oligocene sequence between Sample 115-706A-2H-2, 10 cm, and Section 115-706A-6H, CC, is assigned to the upper lower Oligocene Zone CP18. In the lower samples of this interval, rare specimens of *Ericsonia formosa* occur sporadically. The extinction of *E. formosa* defines the base of Subzone CP16c. Since well-developed forms of *S. distentus* are commonly present, *E. formosa* observed in these samples are regarded as reworked.

Hole 706B

We cored this hole in order to recover a duplicate interval of the section recovered at Hole 706A. Although the Pleistocene sequence recovered from Hole 706B was almost twice as long as the one retrieved from Hole 706A, the nannofossil assemblages were practically identical in these two sequences. *Emiliania huxleyi* is abundant in Sample 115-706B-1H-1, 130–131 cm, and less abundant in Sample 115-706B-1H-2, 130–131 cm, suggesting an age of 0.085 Ma between these two samples.

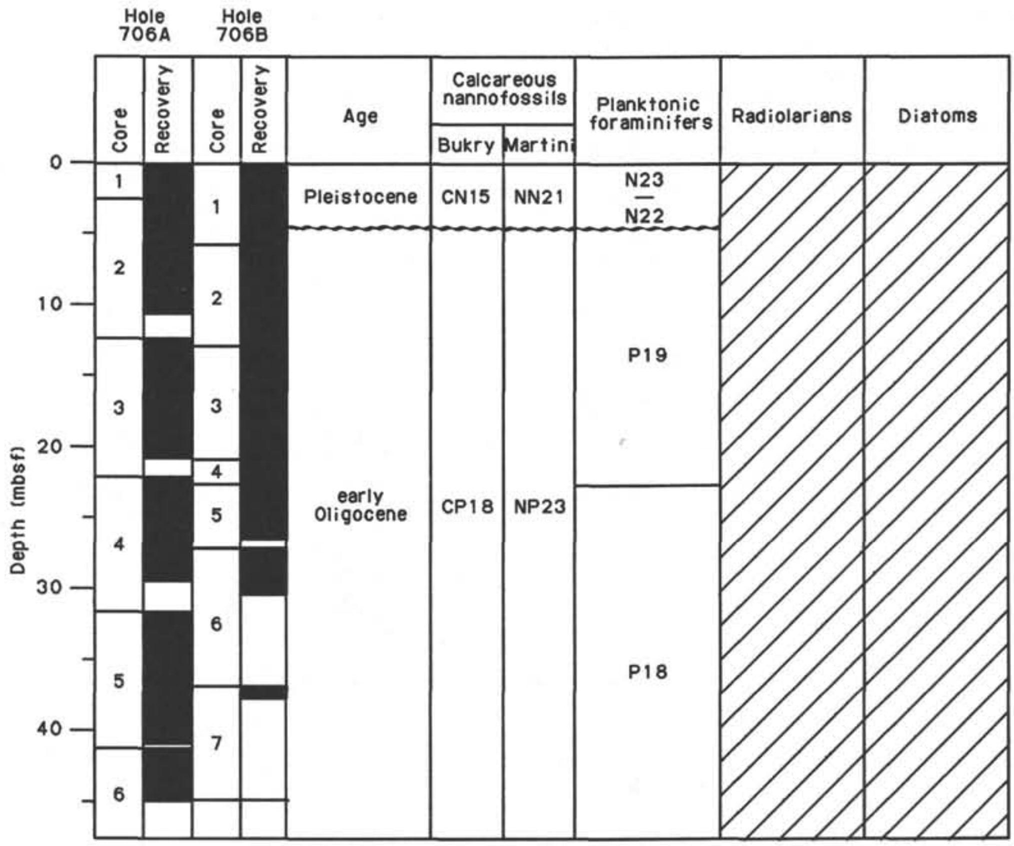

Figure 11. Biostratigraphic summary for Site 706. Black bars represent recovery in Holes 706A and 706B.

Because the Oligocene sequence recovered from this hole is identical to that of Hole 706A, detailed observations of the assemblages were not attempted except to confirm the absence of *Sphenolithus ciperoensis* and the occurrence of *Sphenolithus distentus* at the bottom of the sequence. These results were confirmed in Sample 115-706B-1H-1, 130–131 cm, as well as in all seven core-catcher samples. Therefore, this interval is assigned to Zone CP18, corresponding to the upper part of the lower Oligocene.

Hole 706C

The upper part of Section 115-706C-2R-1 recovered approximately 50 cm of sediment. The sample taken from the bottom of this sediment sequence yields a nannofossil assemblage nearly identical to that of Section 115-706A-6H, CC, and the state of preservation is also identical. Sediments deposited directly above the basalt are of late early Oligocene age (Zone CP18: 30.2–34.2 Ma). The basal age of this zone is 34.2 Ma, according to the chronology of Berggren et al. (1985c). This age, however, differs from the estimate of Backman (1987), who identified the LO of *Reticulofenestra umbilica* (marking the upper boundary of Zone CP17) at 33.8 Ma. Since Backman (1987) did not report the age of the LO of *S. distentus*, the age of the sediment directly overlying the basalt cannot be clarified any further at this stage.

After penetrating approximately 77 m into the basalt layer, the deepest core (115-706C-9R) recovered approximately 1.7 m of basalt. There are several layers of sediment occurring as baked-in chalk/limestones within this basalt sequence, containing moderate to severely recrystallized nannofossils. The nannofossil assemblage observed in Sample 115-706C-9R-1, 73–74 cm, is similar to that of the Oligocene sedimentary sequence recovered from directly above the basalt. *Cyclicargolithus floridanus* is a dominant component, constituting approximately two-thirds of the flora. Other major species are *Coccolithus pelagicus, Dictyococcites bisectus, Sphenolithus moriformis*, and *S. predistentus*. *Sphenolithus distentus*, which is a major component of the flora in Sample 115-706C-2R-1, 54 cm, and Section 115-706C-2R, CC, was not observed in Samples 115-706C-9R-1, 73–74 cm, and 115-706C-9R, 100 cm.

As we mentioned earlier, rare and sporadic specimens of *Ericsonia formosa*, regarded as reworked, occur in the bottom sequence of Hole 706A. *Ericsonia formosa*, whose LO defines the base of Subzone CP16c, is also present in these two samples of Core 115-706C-9R, but in higher abundance (i.e., "few" to "common"). Because we did not observe *Reticulofenestra umbilica*, whose LO defines the base of Zone CP17, it is again possible to consider these *E. formosa* as reworked. According to Backman (1987), however, the LO of *R. umbilica* is less reliable than the LO of *E. formosa*. We did not observe such Eocene *Discoaster* species as *D. barbadiensis* or *D. saipanensis*, but a few specimens of *Ericsonia subdisticha* (top of acme interval defines the base of Subzone CP16b) were recognized.

Considering the occurrence and absence of key species, the nannoflora observed in the two samples of Core 115-706C-9R are tentatively referred to the lower Oligocene Subzone CP16b or CP16c. The age of the sediment recovered within the basalt layer, and hence the age of the basalt itself, therefore, is tentatively estimated to range between 33.8 and 35.9 Ma.

Planktonic Foraminifers

Site 705

In the three Pliocene-Pleistocene cores recovered in Hole 705A, planktonic foraminifers are abundant and well preserved. They yield warm-water assemblages typical of this tropical area.

Section 115-705A-1H, CC, is assigned to foraminiferal Zone N22. The assemblage is dominated by *Globorotalia tumida* and *Neogloboquadrina dutertrei*. Very rare *Globorotalia truncatulinoides* indicate a Pleistocene age. Few *Globorotalia tosaensis* indicate an age older than 0.6 Ma.

Section 115-705A-2H, CC, assigned to the upper Pliocene Zone N21, contains common *Dentoglobigerina altispira*, right-coiling *Globorotalia limbata*, and rare *Globigerinoides fistulosus*, a typical middle Pliocene association of the tropical Indian Ocean. This association allows a precise age assignment of approximately 2.9 Ma for this level; both the last appearance datum (LAD) of *D. altispira* and the first appearance datum (FAD) of *G. fistulosus* are dated at 2.9 Ma. The presence of rare *G. tosaensis* is in agreement with this age since this species first appears at 3.1 Ma. A few individuals referable to *Sphaeroidinellopsis* would indicate a slighty older age (LAD *Sphaeroidinellopsis* = 3.0 Ma). However, these rare specimens are transitional with forms of *Sphaeroidinella dehiscens* that show a tendency toward a dorsal opening.

We assigned Section 115-705A-3H, CC, to the lower Pliocene Zone N19. It contains an assemblage similar to Section 115-705A-2H, CC, with common *D. altispira* and right-coiling *G. limbata*. However, in contrast to Section 115-705A-2H, CC, *G. fistulosus* is absent and *Sphaeroidinellopsis subdehiscens* is quite common. This sample is thus older than 3 Ma. A few *Globorotalia crassaformis* indicate an age younger than 4.3 Ma.

In these three samples, a number of yellowish stained specimens, the same age as the rest of the fauna, commonly occur. This staining probably results from oxidation, indicating that the specimens are probably transported.

Site 706

Section 115-706A-1H, CC, contains abundant and well-preserved planktonic foraminifers. Molluscs and pteropod fragments are also common. This tropical foraminiferal assemblage is dominated by *Globorotalia menardii, G. tumida, Pulleniatina obliquiloculata*, and *Globigerinoides sacculifer*. The presence of rare *Globorotalia truncatulinoides* indicates a Pleistocene age younger than that of Section 115-705A-1H, CC, however. The absence of *Globorotalia tosaensis* indicates an age younger than 0.6 Ma. We assigned the sample to the upper Pleistocene zonal interval N23–N22. Rare pink-walled *Globoturborotalia rubescens* and *Globigerinoides ruber* are present, as they are at other DSDP sites in the Western Indian Ocean containing upper Pleistocene sediments older than 125,000 years (Isotopic Stage 5e).

Abundant and generally well-preserved Oligocene age planktonic foraminifers were recovered in Section 115-706A-2H, CC, through Sample 115-706A-6H-5, 86 cm. The presence of *Globoquadrina sellii, Pseudohastigerina barbadoensis*, and *Globigerina ampliapertura* places all samples within the lower Oligocene Zone P19 of Blow (1969), which corresponds to the top of Zone P18 of Berggren et al. (1985c). The planktonic foraminiferal faunas were similar in all these core catchers, only the proportions of constituent species varied. Frequently found age-diagnostic species included *Turborotalia pseudoampliapertura, G. ampliapertura, Streptochilus cubensis, P. barbadoensis*, and the *Globoquadrina tripartita* group. Moreover, the high-spired subbotinids *Subbotina praeturritillina* and *S. corpulenta* occurred in the bottom two cores.

Equivalent levels were cored in Hole 706B where Sample 115-706B-3H-5, 86 cm, can be attributed to Zone P19 and Sample 115-706B-4H-1, 86 cm, to Zone P18.

A tropical environment is indicated by the high proportion of the *T. pseudoampliapertura* group, accompanied by *G. ampliapertura* and the related species, *T. increbescens*, and by the paucity of the cool-preferring groups of catapsydracids, globigerinids, and globorotalids. A stratified tropical, rather than a eutrophic, surface water is further indicated by the lack of the *Globoquadrina baroemoensis* group and mesopelagic species, which would be expected to reach nearly a third of the assemblage in eutrophic or vigorously circulating water masses. A relatively deep thermocline is indicated both by the dominance of the tropical indigenous forms as well as by the diversification of the turborotaliids. That is, niche differentiation at the warmest levels suggests a deep tropical thermocline (Kennett et al., 1985).

Benthic Foraminifers

Site 705

Benthic foraminifers, while generally well preserved, were very rare in the planktonic foraminiferal oozes in core catchers from Hole 705A. Benthic foraminifers averaged from 5 to 10 specimens per 10 cm^3 of washed sample. The generally cosmopolitan species included *Uvigerina auberiana, Globocassidulina subglobosa, Planulina wuellerstorfi, Cassidulina laevigata, Pyrgo murrhina, Oridorsalis umbonatus, Bulimina rostrata*, and *Gyroidinoides nitidus*. The only species to occur in all three core catchers was *P. wuellerstorfi*. Only juveniles of *C. laevigata* and *G. subglobosa* were found.

Features of these miniscule faunas which suggest a well-oxidized environment include (1) the yellowish coloration of *P. wuellerstorfi* and (2) the presence of the finely hispid *U. auberiana*. The fact that these forms occur at all depths and latitudes, and that all except *U. auberiana* are solution-resistant forms, makes an analysis of paleodepth speculative. The lack of any characteristically upper or upper middle bathyal faunal elements indicates that this is a lower intermediate- or deep-water fauna.

Site 706

Well-preserved benthic foraminifers were infrequent in the Pleistocene carbonate sands at Site 706, but common to abundant in the fine-grained Oligocene age sediments in Cores 115-706A-2H through -6H. Throughout the sequence, numerous other fossils accompanied the foraminifers. In the Pleistocene these included pteropods, microgastropods, micropelecypods, echinoid spines, sponge spicules, and otoliths.

Pleistocene faunas included the cosmopolitan species *Uvigerina auberiana, Globocassidulina subglobosa, Hoeglundina elegans*, and *Planulina wuellerstorfi*.

Oligocene benthic foraminifers were well preserved, large in size, and abundant in most samples. *In-situ* species in all core catchers were roughly the same, with only their proportions changing from one sample to the next. The most common species were *Uvigerina bortotara, U. mexicana, Marginulina fragaria, Vulvulina jarvisi, Bulimina tuxpamensis, Brizalina tectiformis, Osangularia mexicana, Planulina pseudowuellerstorfi, Hanzawaia ammophila*, and *Heterolepa mexicana*. Typical cosmopolitan species such as *Globocassidulina subglobosa, Oridorsalis umbonatus*, and *Vulvulina spinosa* are either rare or not present in these faunas.

All samples contained exotic elements. These were most common and variable in Section 115-706A-3H, CC, where wood fragments, pelecypod fragments, hystrichospheres, quartz, and glass fragments were found. Rock and quartz fragments became more abundant near the bottom of the hole and were greatest in the lowest core catcher, Section 115-706B-7H, CC. Redeposited benthic foraminifers included shallow-water and shelf forms, such as *Tretomphalus* in Section 115-706A-2H, CC, and numerous corroded large nodosariids, marginulinids, and plectofrondicularids which represent upper bathyal depths. The very high rate of sedimentation may be partially attributable to sediment transport down the canyon wall.

During the Oligocene, Site 706 was situated slightly shallower than its current depth of approximately 2500 m. The *in-*

situ benthic foraminifers represent a middle bathyal environment, that is, paleodepths from ~600 to 1800 m. This type of fauna has been found at other mid-ocean, intermediate-depth sites such as Site 526 on the Walvis Ridge and Site 516 on the Rio Grande Rise (Tjalsma, 1983; Boersma, 1984). Redeposited nodosariids, marginulinids, and the large costate plectofrondiculariids were derived from upper bathyal depths, from ~250 to 600 m. The lack of a true "Midway" fauna suggests that these forms inhabited the lower end of this depth range. Hystrichospheres and *Tretomphalus* inhabited a nearshore environment, thus demonstrating redeposition from shelf depths of less than ~250 m.

Thin sections of limestone pebbles found just above the Oligocene/Pleistocene unconformity in Hole 706B were examined. They show a reefal shallow-water facies containing calcareous algae (*Archaeolithothamnium*) and larger benthic foraminifers. Miliolids are common. The presence of *Discocyclina* sp. and *Ranikothalia* sp. indicates a Paleocene to Eocene age for these displaced limestone pebbles.

Radiolarians

Hole 705A

One sample was examined from each of the three core catchers. All samples were barren of identifiable radiolarians.

Holes 706A and 706B

Samples were prepared and examined for radiolarians from the core catchers of Cores 115-706A-4H through -6H and Cores 115-706B-1H through -4H. All samples were barren of identifiable radiolarians except for Section 115-706B-3H, CC, which contained a single specimen of *Dictyoprora pirum*. This species is diagnostic of the latest Eocene and Oligocene, and its presence is consistent with the stratigraphic evidence provided by calcareous microfossils at this site.

Diatoms

Hole 705A

One sample from each of the three core-catchers (Sections 115-705A-1H, CC, 115-705A-2H, CC, and 115-705A-3H, CC) was examined. All samples were barren of identifiable diatoms.

Hole 706A

All processed core-catcher samples from Hole 706A were barren of diatoms. An additional sample from a prominent ash layer (Sample 115-706A-3H, 52–53 cm) yielded no diatoms. The sample, however, contained fairly common sponge spicules, together with poorly preserved radiolarian fragments.

Hole 706B

Seven core-catcher samples from Cores 115-706B-1H through -7X were prepared for diatom analyses. All samples were barren of opaline silica except for Section 115-706B-5X, CC, which contained a fair number of sponge spicules as well as a few radiolarian and diatom fragments that showed a high degree of dissolution.

Hole 706C

One sample (Section 115-706C-2R, CC) taken from sediment in the core liner overlying the basalt also proved to be barren of diatoms.

PALEOMAGNETICS

Site 705 Hole Summary

We considered the poorly consolidated material recovered at Site 705 unlikely to produce reliable results; thus, we did not investigate the paleomagnetism of these sediments.

Site 706 Hole Summary

We used two standard techniques to examine the paleomagnetic properties of the material recovered at this site: (1) pass-through cryogenic magnetometer measurement of split-core sections and (2) measurements of discrete samples. All APC core sections from Holes 705A, 706A, and 706B were run through the cryogenic magnetometer except for some of the uppermost sections containing poorly consolidated Pleistocene material. We did not use the orienting device at this site. Pass-through measurements were taken before and after 5.0-mT demagnetization treatment. In addition, 37 discrete samples of Oligocene-age sediment and 23 basalt minicores were subjected to full progressive demagnetization.

Results

The pass-through magnetometer record contains some intervals which are reasonably consistent and others which are highly erratic (Fig. 12). In general, inclination varies from moderate to steeply downward, and the declination is reasonably consistent within each core. Only Core 115-706A-4H proved an exception. There, the declination of Sections 115-706A-4H-1 and 115-706A-4H-2 are markedly different from the rest of the core (Fig. 13).

Progressive alternating-field (AF) demagnetization of sedimentary samples often indicates a large-amplitude, low-coercivity component (Fig. 14). This behavior was consistently revealed with progressive demagnetization: the softer component (when present) is almost exclusively directed steeply downward. Fortunately, this obvious magnetic overprint is readily removed with a 5–10-mT demagnetizing field, leaving a magnetization which generally displays univectorial decay to the origin.

Most of the discrete sediment samples demagnetized displayed a well-defined, high-coercivity component directed downward at a moderate angle. Despite its having some similarity to the direction of the overprint, this component was usually easy to distinguish. Most of these samples (31 of 37) show stable demagnetization trajectories. Principal component analysis of the demagnetization data gives a consistent set of directions (shown in Table 2). The average inclination of these directions (excluding Sample 115-706B-4H-1, 112 cm, which appears anomalously shallow) is 43.5° (SD = 10.3°).

In addition, progressive demagnetization of 23 of the basalt samples shows good magnetic behavior with little evidence of spurious overprinting. The preliminary results suggest that a normal polarity (negative inclination) may be recorded in the basalts recovered (Fig. 15), but the direction of the high-coercivity component is not well defined: the inclination varies between −0.8° and −62.4° (Table 3). The mean inclination of the basalt samples is −20.8° (SD = 16.2°).

Discussion

Because the sediment magnetic overprint appears to point steeply downward, it seems unlikely to be the result of the present-day field (which at this site points upward at 43°). Rather, it is more likely associated with some intense vertical field generated by either the core barrel or the drill string.

Regardless of its origin, the presence of the overprint certainly explains the many steep positive directions determined with the pass-through system. Moreover, it might account for

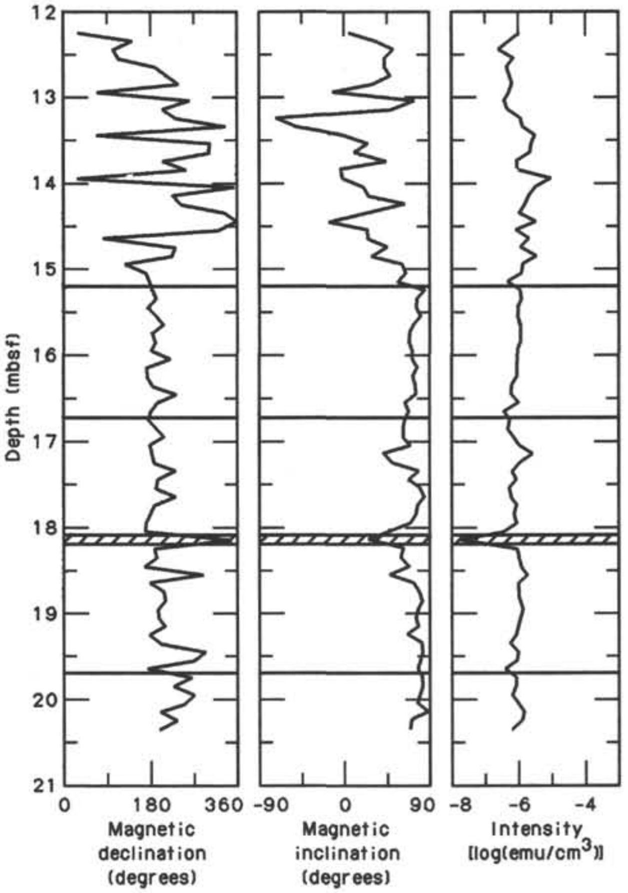

Figure 12. Example of pass-through magnetometer record (Core 115-706A-3H) after treatment by a 50-Oe demagnetizing field. Declination is given with respect to double line on the core liner only. Shaded areas indicate segments of core not measured.

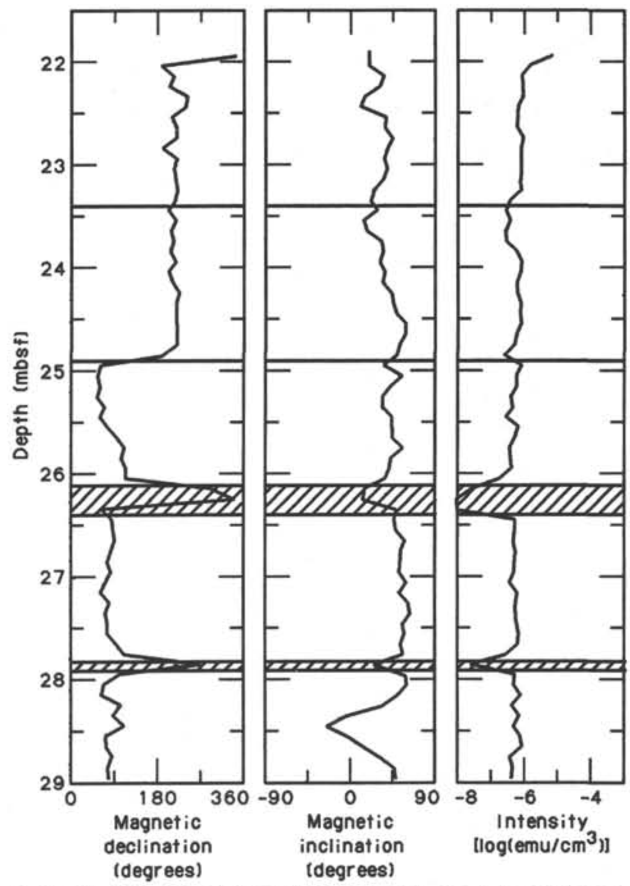

Figure 13. Example of pass-through magnetometer record (Core 115-706A-4H) after treatment by a 50-Oe demagnetizing field. Plot conventions as in Figure 12.

the variation in the pass-through data. In some sections of core, the overprint may be largely removed with 5-mT demagnetization; in other sections, it might be only partially removed. This then would produce an erratic record which varies between moderately and steeply downward directions.

Although the overprint would tend to mask any reversal pattern, the progressive demagnetizations show that the sediments are primarily (if not entirely) of reverse polarity. Furthermore, the only suggestive declination shift seen in the pass-through data (Core 115-706A-4H) coincides with a section break and thus is probably spurious. The pass-through record does show a few intervals which might be of normal polarity; however, an adequate test would require more detailed demagnetizations of discrete samples from these suspected normal polarity intervals.

In any case, it appears that the recovered core sections are dominantly of reverse polarity. Since biostratigraphic analysis indicates that these sediments are of early Oligocene age, we tentatively suggest that the sediments may be recording some portions of the relatively long (2.4 m.y.) reversed period between Chrons C12N and C13N. We cannot, of course, rule out the possibility that the sediments record some other reverse polarity interval; however, this alternate interpretation seems to require an unreasonably high sedimentation rate.

Despite not having uncovered any reversals within the sediments, we suggest that the high-coercivity component (Table 2) may well record a primary direction. To average these data rigorously requires a statistical technique for treating inclination-only data. The maximum-likelihood technique gives an average of 44.4° (N = 31, kappa = 30.5, alpha 95 = 4.7°). Note that this average excludes the anomalous Sample 115-706B-4H-1, 112 cm. Assuming a geocentric axial dipole field, the average inclination corresponds to a paleolatitude of 26.1°. The 4.7°, alpha-95 estimate suggests that the statistical error limits on this paleolatitude estimate are about 4°.

The basalt results appear somewhat problematic. The scatter in directions is much larger than would be expected from secular variation. The reason for this behavior is unclear, but it may be caused by a chemical remagnetization associated with some relatively recent alteration. The measured inclinations might then represent several different episodes of magnetization acquisition. The maximum-likelihood estimate of the mean inclination of the basalt samples is −24.2° (N = 20, kappa = 10.2, alpha 95 = 10.5°); however, the paleolatitude estimated from this mean (12.7° ± 6.0°) may not be very meaningful.

Magnetic Susceptibility

We performed whole-core magnetic susceptibility measurements on all sections of cores recovered from Holes 705A, 706A, and 706B. Measurements were made at intervals of 3 cm in the undisturbed upper Pleistocene and lower Oligocene sections from Holes 706A and 706B, and at 5-cm intervals throughout Hole 705A and in the uppermost "soupy" foraminiferal ooze horizons of late Pleistocene age in Holes 706A and 706B. Susceptibility measurements were made using a Bartington Instruments' susceptibility meter (type MS1) connected to a whole-core, pass-through, loop-type sensor (type MS2C) of 80-mm inner diameter.

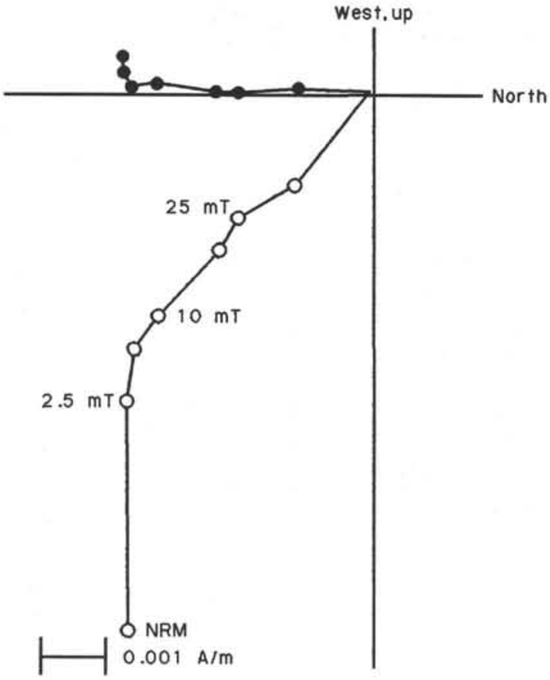

Figure 14. Zijderveld orthogonal projection diagram of a sample subjected to alternating-field (AF) demagnetization. Open points represent projection in the vertical plane; closed points, in the horizontal plane. NRM = natural remanent magnetization.

Table 2. Directions of primary component of magnetization in Oligocene sediments from Site 706 as determined with principal component analysis.

Sample interval (cm)	Number of samples	MAD	Declination (degrees)	Inclination (degrees)
115-706A-				
2H-4, 114	3	3.6	215.5	29.2
2H-5, 114	4	0.8	208.7	41.5
2H-6, 42	4	3.3	175.1	70.3
3H-1, 114	4	2.8	175.3	47.8
3H-2, 114	5	3.4	180.7	33.0
3H-3, 114	5	1.7	182.5	47.4
3H-4, 114	3	1.2	169.2	50.6
3H-5, 114	4	3.3	177.5	43.9
3H-6, 58	5	2.8	173.6	56.7
4H-1, 114	5	3.6	222.7	50.4
4H-2, 114	6	1.1	216.0	44.8
4H-3, 114	3	1.0	111.7	41.9
4H-4, 114	5	3.2	96.6	58.0
4H-5, 94	4	4.7	73.7	52.7
5H-1, 114	5	3.4	264.7	51.2
5H-2, 114	4	1.6	247.2	54.7
5H-6, 114	5	1.2	263.5	53.9
6H-1, 114	3	2.5	34.0	36.2
6H-2, 114	4	1.9	105.0	38.6
115-706B-				
1H-3, 114	3	1.6	93.3	39.6
1H-4, 85	5	1.9	90.1	37.6
2H-1, 114	8	3.1	334.9	24.8
2H-3, 114	4	2.4	323.9	47.5
2H-4, 114	4	2.1	326.2	24.4
3H-1, 98	3	2.4	215.4	49.8
3H-2, 98	4	3.7	227.5	32.3
3H-3, 98	5	1.3	212.9	31.1
3H-4, 98	3	1.1	226.4	38.2
3H-5, 98	4	1.1	209.6	37.9
4H-1, 112	4	2.7	8.5	2.8
6X-2, 114	4	3.1	165.6	46.3

Note: MAD = mean angular deviation of fit.

Site 705

Figure 16 shows the results of whole-core susceptibility measurements made on the highly disturbed core material recovered from Site 705. Susceptibility values are extremely low (1-3 $\times$ 10^{-6} cgs) throughout the middle Pleistocene and middle Pliocene horizons of the sequence, with three exceptions: two small peaks in susceptibility at 2.8 and 9.8 mbsf, and one much larger-scale deflection of the susceptibility profile at 19.4 mbsf. The two minor susceptibility peaks are illustrated more clearly in Figure 17, which shows that portion of the susceptibility profile of Hole 705A in which these features occur, plotted on an expanded scale. Neither of these two peaks in susceptibility correspond to any feature of the lithostratigraphic record of this hole recorded by visual examination of split-core sections. We observed "stained" (ferric-oxide coated) foraminifer tests throughout the sequence, however, so the two small peaks in the susceptibility profile of Hole 705A may possibly correspond to an increase in the proportion of "stained" relative to "nonstained" foraminifer tests in the sediment at these points in the sequence.

Contrasting with the two minor peaks that occur in the upper sections of the susceptibility profile of Hole 705A is a much larger-scale deflection of the susceptibility curve that occurs between 17 and 19.5 mbsf and culminates at a depth of 19.4 m with a peak susceptibility value of 3.75 $\times$ 10^{-4} cgs. The significant increase in susceptibility values, however, is entirely an artifact of downhole contamination by small particles of brown rust scraped from the drill pipe. Similar problems of pipe-rust contamination were also experienced during shipboard susceptibility measurements made on Leg 101 (Sager, 1986). The dissemination of rust flakes throughout the upper horizons of the first section of each APC core drastically affects not only susceptibility values but also natural-remanent-magnetization (NRM) data from the core. For this reason, and also because of the "soupy," unconsolidated, highly disturbed condition of the core material recovered from Hole 705, we did not make paleomagnetic measurements at this site.

Site 706

Whole-core magnetic susceptibility is proportional to the volume concentration of magnetizable material which the sediment contains. Magnetizable sedimentary components are principally lithogenic and include not only the NRM-carrying, ferromagnetic minerals like (titano)magnetite, (titano)maghemite, hematite, goethite, and pyrrhotite, but also paramagnetic minerals like clays (particularly chlorite and smectite), ferromagnesian silicates, and authigenic ferromagnesian-oxyhydroxide colloidal complexes which often occur in pore waters. Biogenic carbonate and siliceous components, in contrast, are diamagnetic (i.e., they exhibit negative susceptibility values). Accordingly, whole-core susceptibility profiles often reflect downhole variations in lithology, that is, changes in the ratio of biogenic (diamagnetic) to lithogenic (paramagnetic and ferromagnetic) constituents in the sediment. Whole-core susceptibility measurements have been used, therefore, in previous studies (e.g., Robinson, 1986) to provide a simple, rapid, nondestructive method of regional-scale lithostratigraphic correlation between sites.

The principal objective of the whole-core susceptibility measurements made at Site 706, therefore, was to correlate Hole 706A and Hole 706B to each other with a high degree of lithostratigraphic resolution. The resulting lithostratigraphic framework could then, in effect, be calibrated by shipboard biostrati-

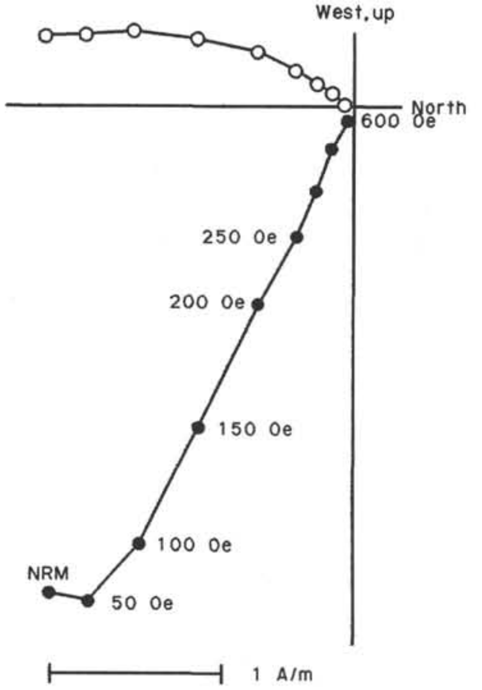

Figure 15. Zijderveld diagram of a basalt sample subjected to alternating-field (AF) demagnetization. Open points represent projection in the vertical plane; closed points, in the horizontal plane. NRM = natural remanent magnetization.

Table 3. Directions of primary component of magnetization in basalt samples from Site 706 as determined with principal component analysis.

Sample interval (cm)	Number of samples	MAD	Inclination (degrees)	Intensity (%)	Hard rock unit
115-706C-					
2R-1, 79-81 (Piece 4)	4	0.6	−12.2	9.966	1
2R-1, 105-107 (Piece 8)	5	1.7	−5.1	0.578	2
2R-2, 28-30 (Piece 6)	4	4.0	−34.5	6.749	4
2R-2, 52-54 (Piece 9)	3	2.4	−0.8	3.297	5
2R-2, 75-77 (Piece 12)	4	1.1	−11.1	5.240	6
2R-2, 144-146 (Piece 24)	4	1.2	−15.1	4.736	10
3R-1, 83-85 (Piece 12)	4	1.3	−22.1	4.085	12
3R-2, 45-47 (Piece 6)	3	0.1	−9.2	3.838	12
4R-2, 117-119 (Piece 15)	3	3.8	−31.4	3.118	12
5R-1, 82-84 (Piece 7)	5	3.0	−38.1	0.980	14
5R-2, 54-56 (Piece 8)	3	2.8	−5.2	0.519	15
5R-2, 135-137 (Piece 22)	6	1.9	−57.9	6.976	17
5R-3, 13-15 (Piece 2)	5	5.7	−47.5	0.397	18
5R-3, 54-56 (Piece 7)	4	2.0	−24.7	1.372	19
5R-3, 79-81 (Piece 10)	4	5.0	−62.4	2.050	20
6R-1, 48-50 (Piece 2)	6	3.9	−54.7	2.704	20
6R-2, 16-18 (Piece 2)	6	2.4	−42.8	3.256	21
8R-1, 34-36 (Piece 6)	4	3.2	−5.4	10.657	26
8R-1, 96-98 (Piece 14)	5	0.7	−19.4	13.223	27
8R-2, 80-82 (Piece 6)	6	1.2	−10.2	11.940	28
8R-3, 27-29 (Piece 3)	7	1.2	−2.0	8.712	29
9R-1, 27-29 (Piece 4)	8	1.2	−25.1	5.131	31
9R-2, 32-34 (Piece 4)	5	1.4	−24.9	4.638	32

Note: MAD = mean angular deviation of fit.

graphic and paleomagnetic data. Alternatively, the high-resolution susceptibility records of the cores could be used for purposes of interhole correlation in between biostratigraphic/paleomagnetic control points, thus enabling us to pinpoint the positions at which these marker horizons can be identified in each hole.

Magnetizable Material in Holes 706A and 706B

Contamination of the cores by particles of drill-pipe rust did not appear to be a problem at Site 706. The dominant magnetizable constituents responsible for downhole susceptibility variations at this site are most probably as follows:

1. In what appeared to be normally oxidized (i.e., light yellowish brown or buff-colored), foraminifer-nannofossil ooze horizons, the principal contribution to the generally low susceptibility values (10^{-6}–10^{-5} cgs) which these intervals exhibit is most probably made by the goethite and Fe(II)/Fe(III) ions that occur mainly in the lattices of clay minerals in the sediment.

2. In virtually all of the black, unaltered volcanic-ash (tephra) bands, the principal magnetizable constituent is most likely to be primary (titano)magnetite, which would account for the extremely high values of susceptibility (1-3 $\times$ 10^{-4} cgs) which these intervals exhibit. An exception to this, however, is the absence of a peak in the susceptibility profile of Hole 706A in response to the volcanic-ash band at 5.5 mbsf, which we presume consists mainly of glass shards and/or halmyrolytic clay minerals.

3. Pyrite is the principal magnetizable constituent in the greenish gray, muddy, foraminifer-nannofossil ooze horizons. Much of the magnetizable material in these horizons has probably been formed postdepositionally by anoxic or suboxic degradation of volcanic ash which was deposited more slowly than the tephra associated with the discrete, black volcanic-ash bands, and was therefore more diluted by the rain of pelagic sediment. We observed frequent deposits of pyrite in the degraded ash-rich horizons during our visual examination of split-core sections (see "Lithostratigraphy" section, this chapter). Further contributions to the susceptibility of these horizons may also be made by other volcanogenic constituents, both unaltered (i.e., labile minerals) and degraded (e.g., halmyrolitic clays). The generally much lower susceptibility values associated with the degraded volcanic-ash-rich horizons (1-3 $\times$ 10^{-5} cgs), relative to those values exhibited by the unaltered volcanic-ash bands, may be attributed to several decreases in the order of magnitude in the magnetic susceptibility of titanomagnetite grains when they become diagenetically altered to pyrite under conditions of negative Eh, low pH, and high pS^{2-} (Karlin and Levi, 1983, 1985; Canfield and Berner, 1987). For example, the specific susceptibility of stoichiometric titanomagnetite ($Fe_{3-x}Ti_xO_4$, where x = 1) is given by Carmichael (1982) as 0.41-1.2 $\times$ 10^{-4} SI, whereas the same author lists the susceptibility of pyrite as 1-110 (Av = 33) $\times$ 10^{-8} SI units.

Correlation between Holes 706A and 706B

The high-resolution magnetic susceptibility profiles obtained from Holes 706A and 706B (Figs. 18 and 19) ease precise intercorrelation between these holes, thus revealing the presence in each hole, at different depths, of an additional hiatus to that which occurs in each hole between the upper Pleistocene foraminifer-ooze horizons at the top of each sequence and the underlying lower Oligocene oozes and volcanogenic muds which comprise most of the two sequences. Figures 18 and 19, in general, show that unaltered volcanic-ash bands stand out as major, first-order peaks (ca. 100–300 $\times$ 10^{-6} cgs) in the susceptibility profiles of each hole, superimposed on background susceptibility fluctuations which correspond to normally oxidized foraminifer-nannofossil ooze horizons. Secondary peaks in the susceptibility profiles (ca. 30–70 $\times$ 10^{-6} cgs) correspond to reduced (greenish gray colored), degraded volcanic-ash-rich horizons. Correlation between the susceptibility profiles of each hole (Figs. 20 and 21) is based on the relative position, intensity, and configuration of first- and second-order deflections of the susceptibility profile (and intervening troughs), corresponding to all lithostratigraphic variations within each hole and not merely to

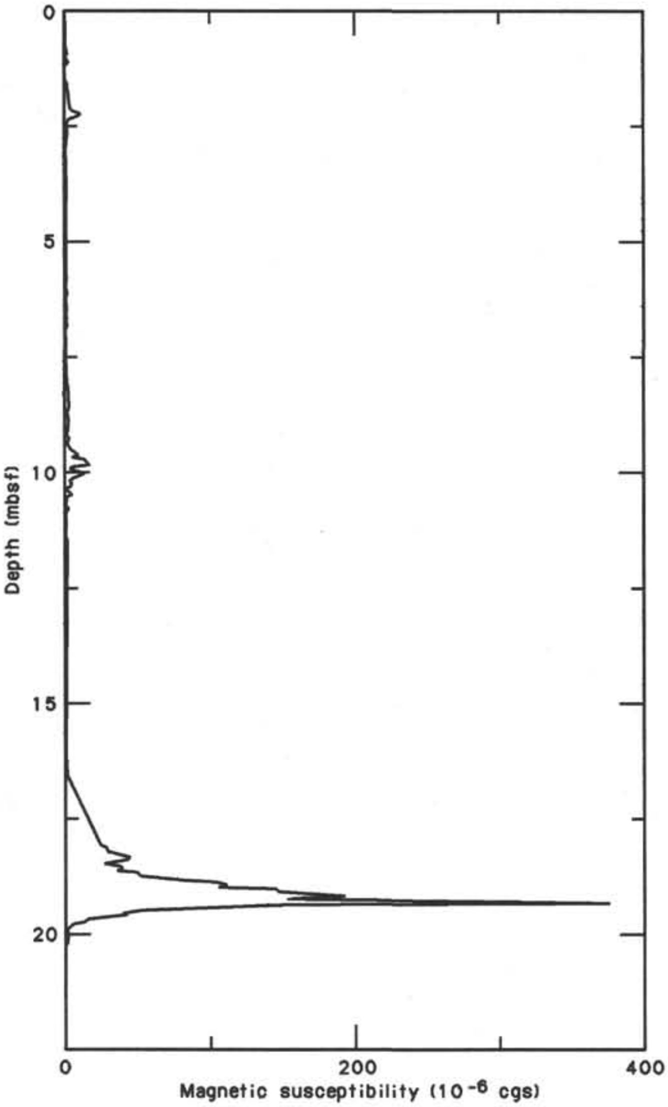

Figure 16. Whole-core magnetic susceptibility profile of Hole 705A.

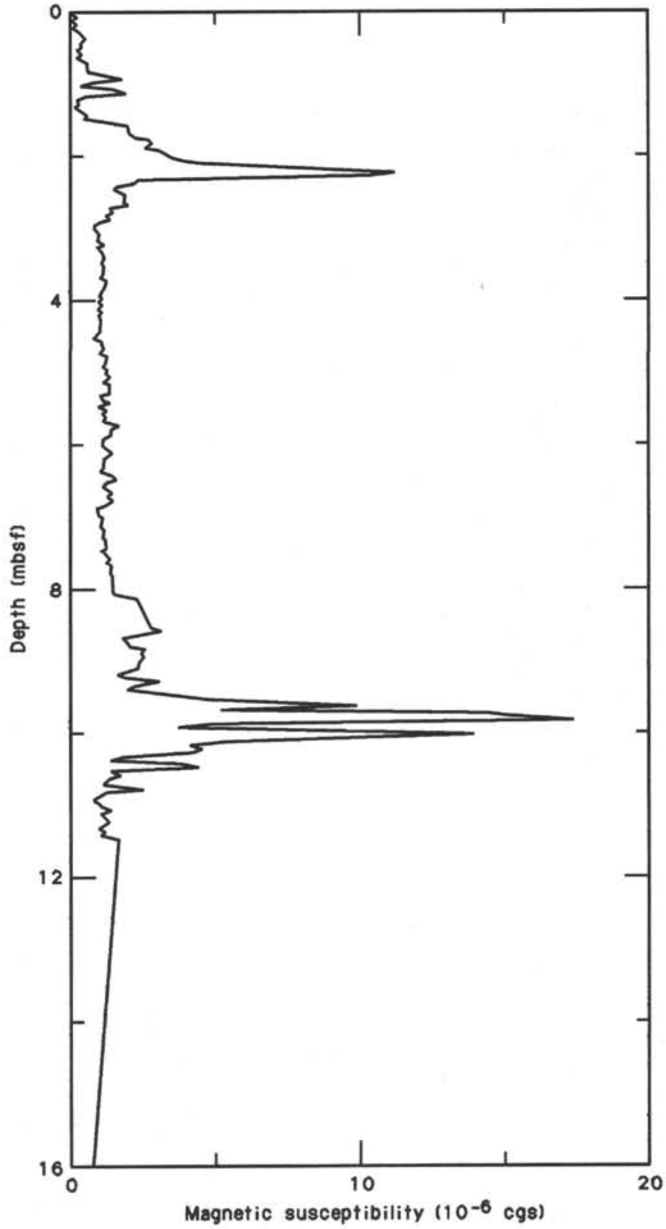

Figure 17. Whole-core magnetic susceptibility profile of the upper sections of Hole 705A.

the cross-matching of susceptibility peaks correlatable with volcanic-ash bands.

The highly detailed susceptibility records from each hole make visual identification of the intricacies of fine-scale lithostratigraphic correlation extremely difficult when the profiles are plotted on the scales used in Figures 18 and 19. Therefore, we have replotted selected subsections from each profile on the expanded scales in Figures 20 and 21 in order to illustrate the extent of correlation between the susceptibility records of these holes better.

In Figures 20 and 21, the principal points of correlation between the susceptibility profiles of Holes 706A and 706B are letter coded as follows: P_1, P_2, P_3, etc., for susceptibility peaks, and T_1, T_2, T_3, etc., for the intervening troughs. Detailed inspection of the configuration of the susceptibility profiles shown in Figures 20 and 21 reveals that several features of the profile of Hole 706A between 10.5 and 14.5 mbsf are absent from the susceptibility record of Hole 706B. Similarly, in Hole 706B, several prominent susceptibility peaks, corresponding both to unaltered and degraded volcanic-ash-rich horizons between 16 and 18 mbsf, are absent from the susceptibility profile of Hole 706A. The absence of these intervals can only be explained by the presence of an hiatus in the stratigraphic record of each hole (see Fig. 22).

The number-coded correlation points identified in the susceptibility plots shown in Figures 20 and 21, together with intervening correlation points which are not identified in these figures, are listed in Table 4; they are also illustrated graphically in the form of a "fence" diagram in Figure 22 and in the form of a Shaw correlation diagram in Figure 23. The positions in the sequence at which hiatuses occur in each hole are clearly apparent in each of the two types of correlation diagrams. In Hole 706A the hiatus occurs at about 17.75 ± 0.25 mbsf; in Hole 706B the hiatus occurs at about 12.9 ± 0.2 mbsf. Over distances as short as that between Holes 706A and 706B, the presence of hiatuses at different levels in each of the two recovered sequences is most likely attributable to winnowing by strong bottom currents or possibly to slumping.

Conclusions

The high degree of lithostratigraphic correlation achieved between Holes 706A and 706B, based on whole-core susceptibility

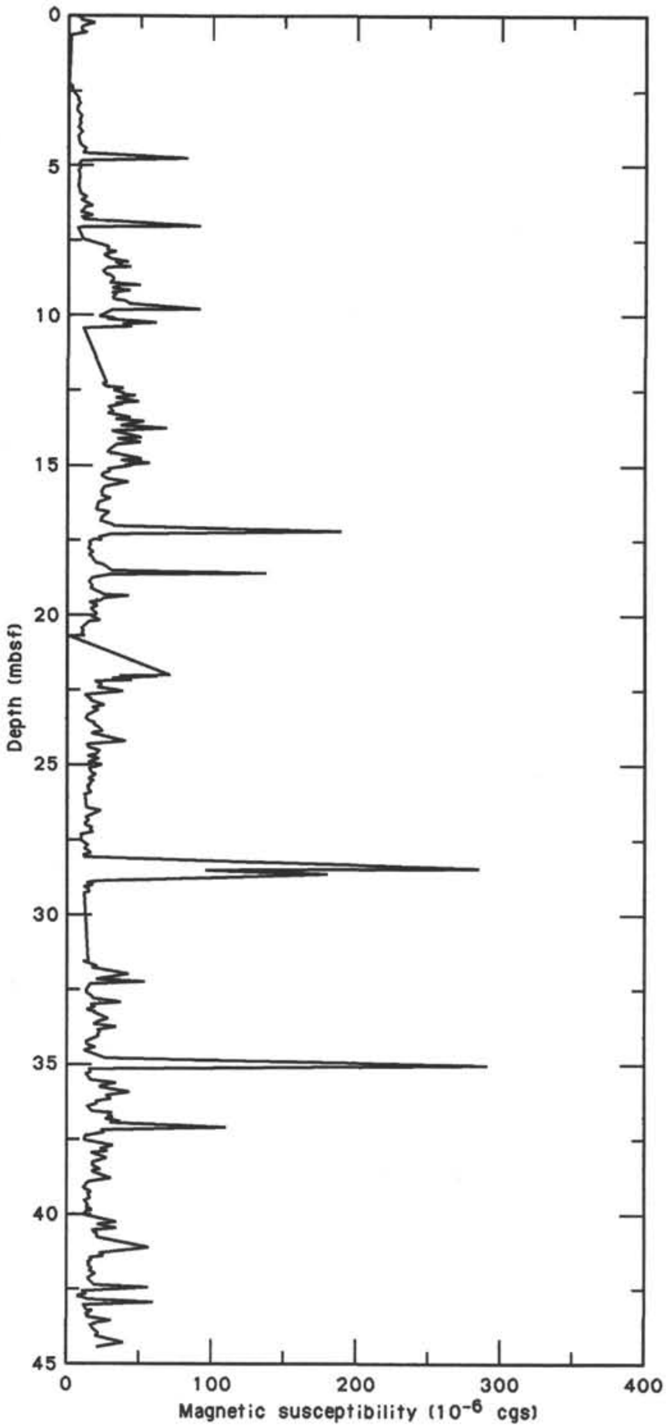

Figure 18. Whole-core magnetic susceptibility profile of Hole 706A.

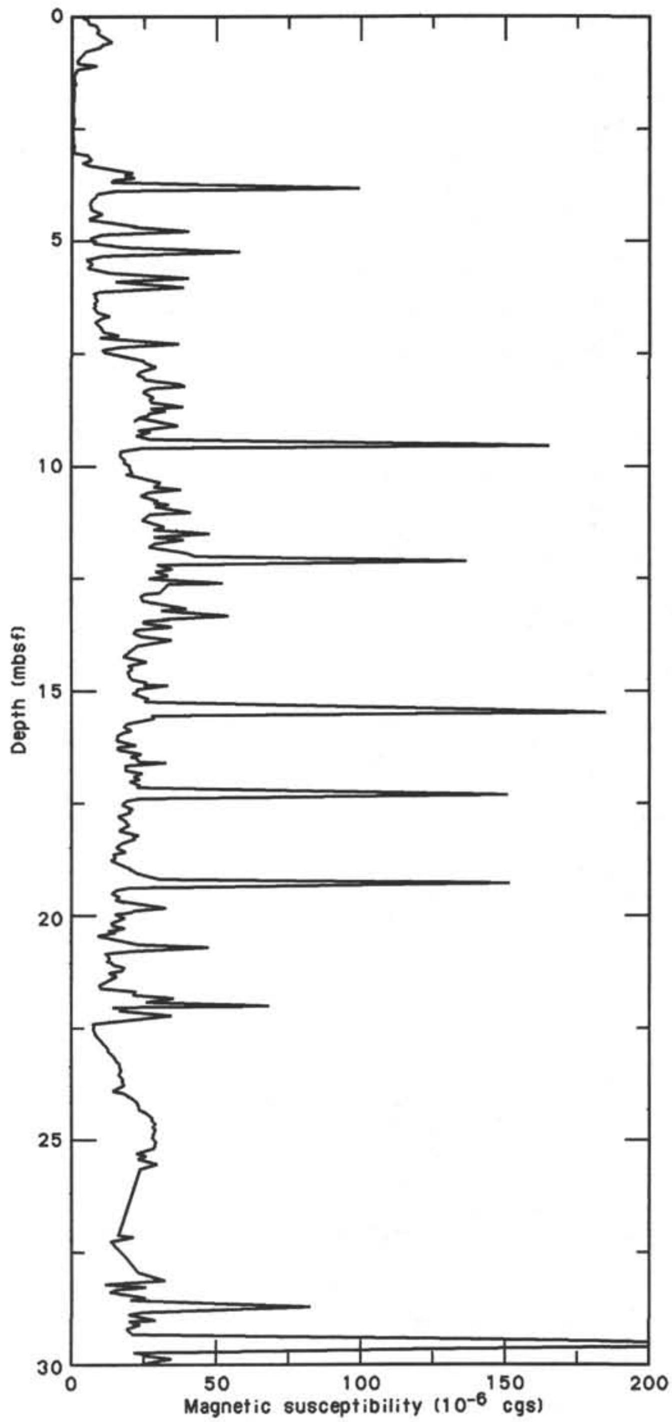

Figure 19. Whole-core magnetic susceptibility profile of Hole 706B.

profiles obtained from each hole, clearly illustrates the effectiveness with which this simple, rapid, and nondestructive magnetic measurement can be used to assist more conventional biostratigraphic and paleomagnetic techniques in establishing stratigraphic control in deep-sea sediment sequences. The presence of hiatuses at different levels in the two sequences recovered from Site 706, as revealed by detailed correlation between the high-resolution susceptibility profiles of each hole, also clearly emphasizes the need for double APC coring in order to obtain a complete stratigraphic record from any given site.

SEDIMENTATION RATES

Site 705

The sedimentation rates for Site 705 are based entirely on foraminiferal and calcareous nannofossil datum levels, as recorded in Table 5 and illustrated in Figure 24. We have indicated the uncertainty in sub-bottom depths (mbsf) between which each event occurs. We have also given the estimated age of each event, according to the chronology of Berggren et al. (1985b).

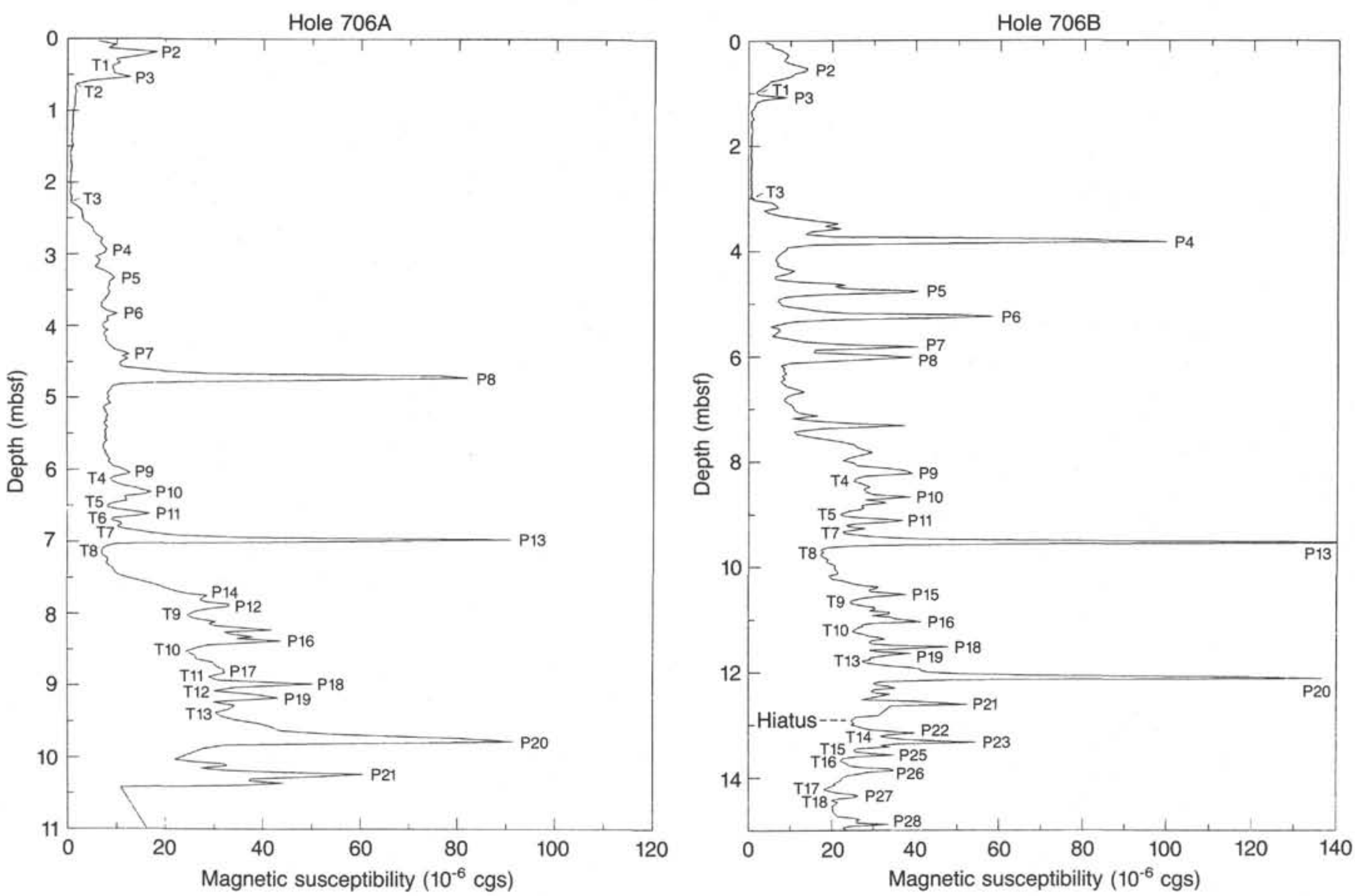

Figure 20. Correlatable features between the whole-core magnetic susceptibility profiles of the upper sections of Holes 706A and 706B.

Sphenolithus spp. are not found at all in this hole (see Table 5). Thus, their extinction event (3.45 Ma) must lie below the lowest sediment recovered, at 27.5 mbsf.

Site 706

In Hole 706A, only one magnetostratigraphic and three nannofossil datum levels provide constraints on determining sedimentation rates (Fig. 25). These datum levels are as follows:

1. *Emiliania huxleyi* extends at least down to 3.80 mbsf. Minimum sub-bottom depth for this event, therefore, is 3.80 m. We cannot determine the maximum depth because of the presence of an unconformity (see Table 6).
2. *Sphenolithus ciperoensis* was not found in the Oligocene interval (>3.80 mbsf); thus, its position lies above the uppermost Oligocene sediment recovered, at 3.80 mbsf (Table 6).
3. *Sphenolithus distentus* is present throughout the Oligocene interval (3.80–47.5 mbsf); thus, its first appearance lies below the lowest depth cored, at 47.5 mbsf (Table 6).

These constraints may be combined with the paleomagnetic observations in the Oligocene (3.8–47.5 mbsf) in order to estimate minimum sedimentation rates for each of the two principal stratigraphic intervals recovered.

For the upper Pleistocene interval (0–3.8 mbsf), the minimum sedimentation rate is 3.8 m per 0.27 m.y., or 15 m/m.y. For the Oligocene (3.8–47.5 mbsf), on the other hand, the reversed magnetic polarity throughout the interval suggests an age entirely within Chron C12R. The age of the C12N/C12R polarity reversal is 32.90 Ma (Berggren et al., 1985c); therefore, Oligocene sediments can be no younger than 32.90 m.y. and no older than 34.2 m.y. (the basal age of Zone CP18). Thus, the minimum sedimentation rate for the Oligocene interval is 44.7 m in 1.3 m.y., or 34 m/m.y.

GEOCHEMISTRY

Site 705

Interstitial Water Geochemistry

Samples for interstitial waters were collected from two cores in Hole 705A (4.45 and 12.95 mbsf; Table 7 and Fig. 26). These samples showed only slight changes with respect to surface seawater. Calcium increased from 10.34 to 11.61 mmol/L, whereas Mg^{2+} decreased over the same interval. Alkalinity increased slightly from 2.32 to 3.03 mmol/L, perhaps related to a small decrease in the concentration of SO_4^{2-} and consequent oxidation of organic material. The largest changes in any measured constituent occurred in dissolved SiO_2, which increased from normal surface values of 17–18 μmol/L to over 250 μmol/L. Although it is possible that the changes we observed in calcium and magnesium are the result of basement alteration reactions (Gieskes, 1981; Gieskes and Lawrence, 1981; McDuff, 1981), limited penetration precluded testing of this idea.

X-ray Diffraction, Carbonate, and Organic Carbon Analyses

X-ray analysis of the small number of samples showed them to be composed almost entirely of low-magnesium calcite (Table 8).

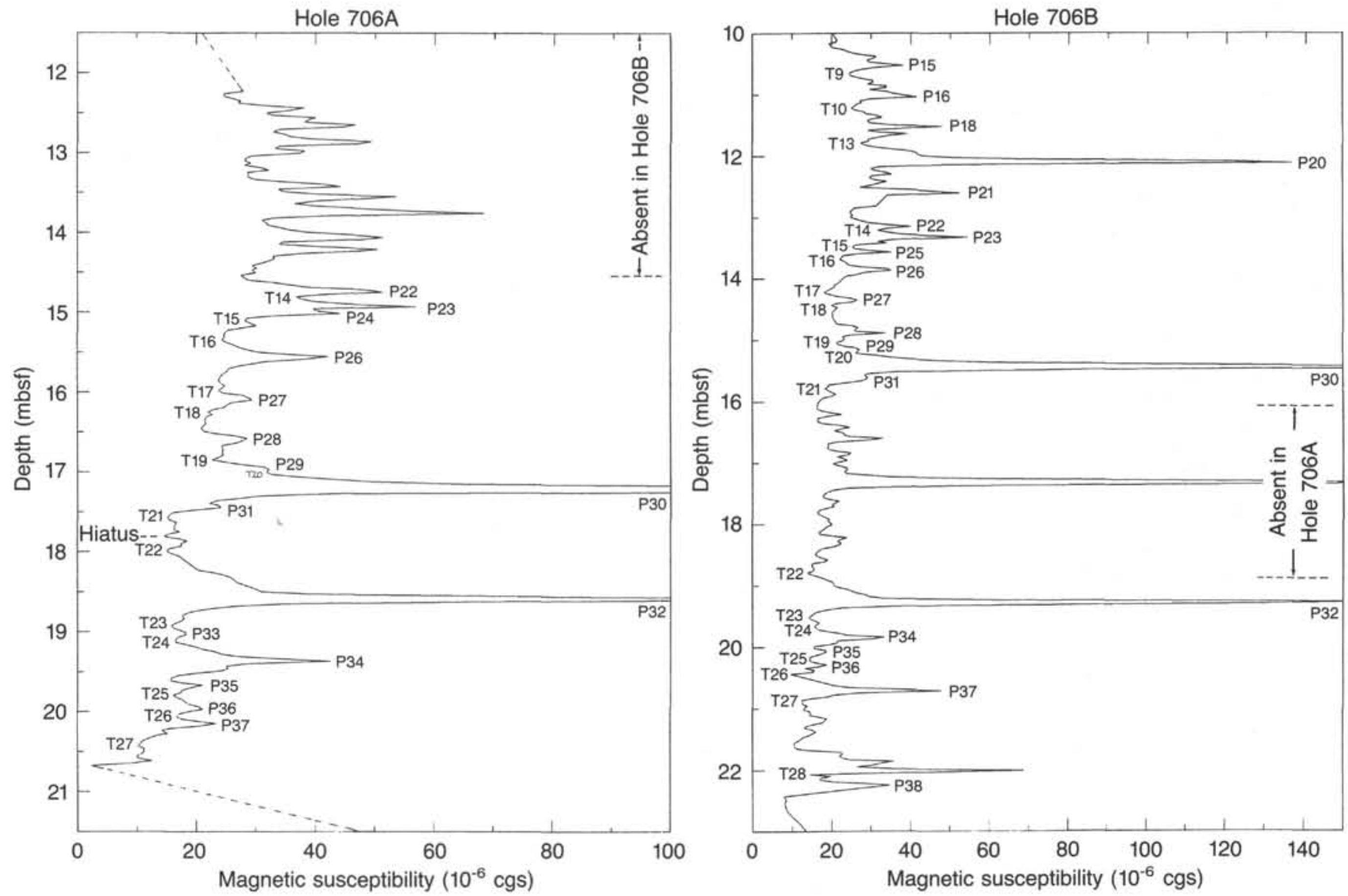

Figure 21. Correlatable features between the whole-core magnetic susceptibility profiles of the middle sections of Holes 706A and 706B.

Specific exceptions to this occurred at 5.01 and 13.28 mbsf where small amounts of dolomite were detected; concentrations of this mineral did not, however, exceed 4%. The origin of the dolomite is uncertain, but it is not believed to be forming at the present time since geochemical conditions in the sediment cannot be considered unusually favorable for dolomite formation.

Carbonate analyses (Table 9) reveal a decrease in the percent carbonate from surface values of 94.9% to 83.4% at 16.28 mbsf. The percentage of organic carbon (Table 9) is practically at or below detection limits throughout the hole, with the exception of one sample at 16.28 mbsf.

Volatile Hydrocarbon Gases

Head-space analyses for methane (C_1), ethane (C_2), and higher hydrocarbons (C_N) showed concentrations typical of normal atmospheric levels.

Site 706

Interstitial Water Samples

Interstitial water samples were collected from Cores 115-706A-2H through -6H. In addition, the downhole water sampler was used below Core 115-706A-6H. No water samples were collected from either Hole 706B or 706C (Table 7 and Fig. 27).

Calcium and Magnesium

The limited thickness of sediment overlying basement at Site 706 increased the probability that calcium- and magnesium-concentration gradients would be visible as a result of basaltic alteration and the upward diffusion of these elements. In fact, Ca^{2+} concentrations do increase from surface values of 10.34 mmol/L to 13.93 mmol/L at 37.45 mbsf, while Mg^{2+} concentrations decrease to 49.82 mmol/L over the same interval. The inverse relationship between Ca^{2+} and Mg^{2+} has a slope of approximately -1 and is less negative than that normally suggested for sediments overlying basaltic basement (i.e., -1.5; McDuff, 1981; Baker, 1986), but lower than that for sediments overlying presumed silicic rocks (Fig. 27). In order to compare previous sites drilled in the same general area of the Indian Ocean, we have compiled Table 10 of the downhole calcium/magnesium gradients at Sites 232 through 245 (data from Gieskes, 1974; Sandstrom and Gieskes, 1974).

These data suggest that the basement to the east of the Mascarene Plateau is basaltic, but that the plateau itself (represented by Site 237) is underlain by rocks of a more felsic composition because the calcium/magnesium gradient is $\ll 1$.

Alkalinity, Sulfate, and Silica

Alkalinity and sulfate concentrations show only small deviations from surface seawater values downhole. Alkalinity decreases from 2.38 mmol/L at 9.95 mbsf to 1.64 at 44.05 mbsf. No changes occur in the dissolved SO_4^{2-} concentration. The absence of a change in the sulfate concentration suggests that the abundant pyrite observed (see "Basement Rocks" section, this chapter) did not form in the recent geological past.

Hole 706A is characterized by high silica concentrations at very shallow depths. The rapid rise in concentration is a result of the dissolution of either biogenic silica or abundant ash ob-

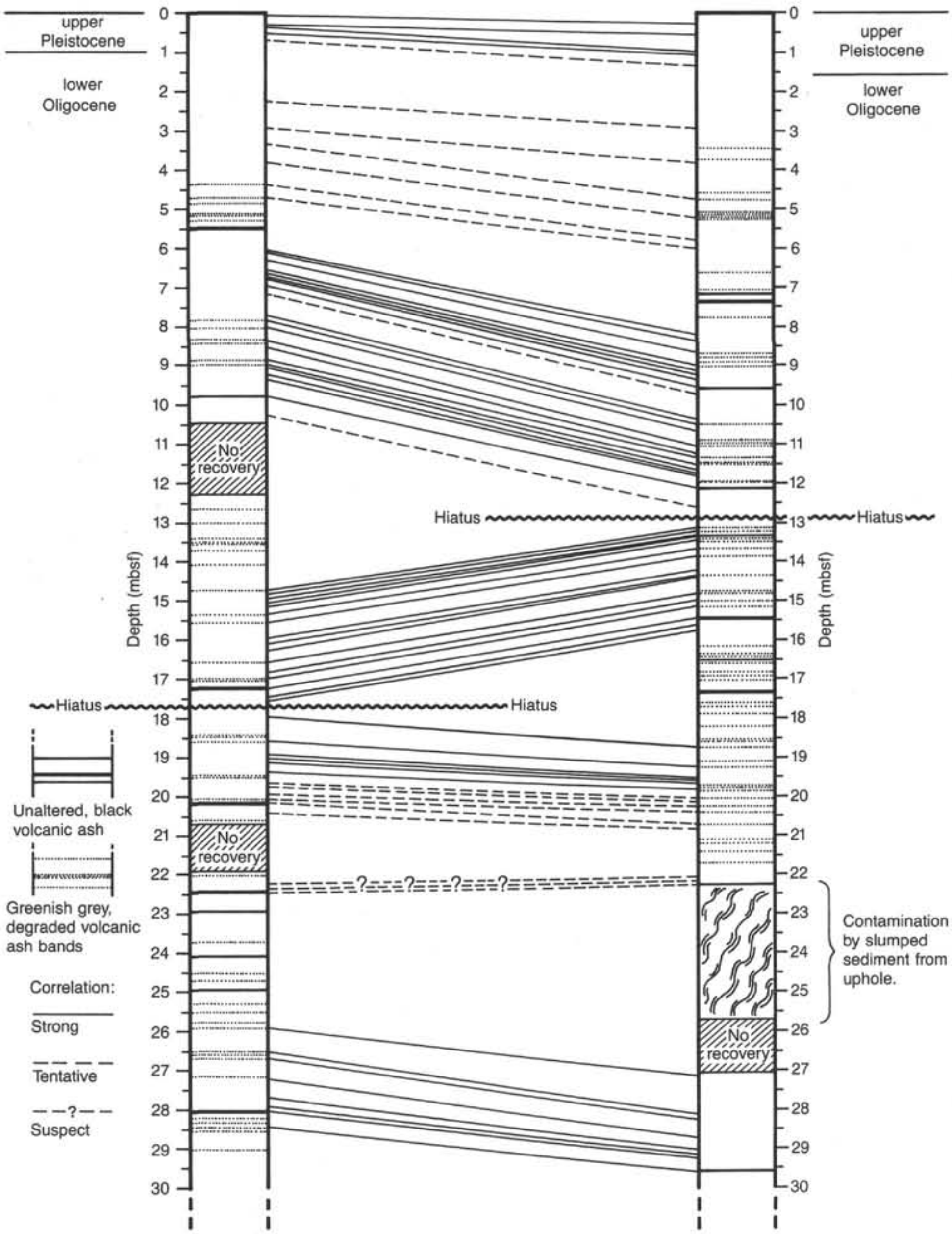

Figure 22. "Fence" diagram showing the correlation between Holes 706A (left) and 706B (right) based on whole-core magnetic susceptibility profiles. This figure also shows the position of unaltered and degraded volcanic-ash-rich horizons in each sequence, taken from core description data.

served throughout the core (see "Lithostratigraphy" section, this chapter). With increasing depth, levels of silica actually decrease, perhaps because of the formation of some authigenic silicate phases.

Salinity and chloride concentrations show slight increases with depth, perhaps related to incorporation of water into silicate phases.

Results from Downhole Water Sampler

Water retrieved from the downhole water sampler proved to be normal ocean water. This can be seen from a comparison of practically all the geochemical parameters measured (Fig. 27). It is perhaps most obvious in the concentration of silica, which falls from approximately 500 μmol/L in Core 115-706A-6H to the failure to retrieve *in-situ* sediment pore water was because the tool may not have been properly latched to the drill string and therefore did not penetrate the sediments.

Organic Geochemistry

Head-space analyses for volatile hydrocarbon gases in Holes 706A revealed no detectable concentration of any species.

X-ray Mineralogy, Carbonate, and Organic Carbon Analyses

Quantitative X-ray analyses revealed that the carbonate soluble fraction of the samples measured in Hole 706A consisted entirely of low-magnesium calcite, with the exception of one sample which contained a small amount of aragonite (Table 8).

Table 4. Lithostratigraphic correlation points between Holes 706A and 706B, based on the whole-core magnetic susceptibility profiles of each hole.

Correlation point	Depth in Hole 706A (mbsf)	Depth in Hole 706B (mbsf)	Strength of correlation (rank)
P1	0.08	0.28	3
P2	0.18	0.53	2
T1	0.38	0.98	3
P3	0.53	1.08	2
T2	0.68	1.38	4
T3	2.28	2.98	4
P4	2.93	3.83	4
P5	3.33	4.77	4
P6	3.83	5.25	4
P7	4.39	5.83	4
P8	4.72	6.03	4
P9	6.04	8.23	3
T4	6.13	8.38	3
P10	6.31	8.68	3
T5	6.52	9.00	3
P11	6.61	9.12	3
T6	6.70	9.21	3
P12	6.76	9.27	3
T7	6.79	9.33	3
P13	6.97	9.54	3
T8	7.18	9.75	4
P14	7.75	10.38	3
P15	7.87	10.53	2-3
T9	8.02	10.67	2-3
P16	8.38	11.04	3
T10	8.53	11.22	2-3
P17	8.83	11.37	3
T11	8.88	11.43	3
P18	8.98	11.52	2-3
T12	9.08	11.58	3
P19	9.18	11.64	2-3
T13	9.38	11.79	2-3
P20	9.78	12.12	1-2
P21	10.24	12.61	4
P22	14.75	13.15	2-3
T14	14.81	13.21	2
P23	14.93	13.33	2
P24	15.02	13.42	3
T15	15.11	13.48	3
P25	15.17	13.57	3
T16	15.35	13.69	2-3
P26	15.56	13.87	2
T17	15.98	14.23	2-3
P27	16.10	14.35	2-3
T18	16.25	14.44	2
P28	16.58	14.89	3
T19	16.85	15.04	2-3
P29	16.97	15.16	3
T20	17.00	15.22	3
P30	17.21	15.46	1
P31	17.45	15.61	2-3
T21	17.57	15.79	2-3
T22	17.99	18.79	2-3
P32	18.59	19.27	1
T23	18.92	19.51	2-3
P33	19.03	19.60	2-3
T24	19.13	19.66	2-3
P34	19.37	19.84	2
P35	19.67	20.08	4
T25	19.79	20.17	4
P36	19.97	20.29	4
T26	20.06	20.44	4
P37	20.15	20.72	4
T27	20.43	20.87	4
T28	22.23	22.27	5
T29	22.35	22.16	5
P38	22.47	22.25	5
P39	25.92	27.18	4
P40	26.52	28.13	3-4
T30	26.76	28.23	3-4
P41	26.88	28.28	3-4
P42	27.24	28.73	3-4
P43	27.69	29.03	3-4
T31	27.78	29.08	3-4
P44	27.93	29.16	3-4
T32	28.02	29.23	3
P45	28.41	29.58	2

Note: Correlation ranks (subjective assessment): 1 = very strong, 2 = strong, 3 = probable, 4 = tentative, 5 = dubious.

Scans of the samples between 3° and 65° 2θ revealed the presence of pyrite in only a few of the samples; no other phases were detected.

The carbonate content of sediments in Holes 706A and 706B (Table 11 and Figure 28) varies between 60% and 90%. Organic carbon content (Table 11) was at or below detection limits, as at Site 705.

BASEMENT ROCKS

Introduction

We recovered volcanic basement from all three holes (706A, 706B, and 706C) at Site 706. At Hole 706A a basalt cobble was sampled by the core catcher of Core 115-706A-6H at a depth of 47.5 mbsf. No further recovery was attempted. At Hole 706B pyrite-cemented volcanic sandstone pebbles and half a meter of basalt were recovered in Core 115-706B-7X. We then ended drilling and tripped the pipe to begin rotary coring. Hole 706C was washed to basement and then drilled 77.4 m into basement, recovering 19.7 m of volcanic material.

The basement rocks from all three holes are slightly to moderately altered, fine-grained, vesicular basalts. This section summarizes the description of these samples based on recovery, lithostratigraphy, vesicularity, grain size, alteration, and phenocryst type and abundance that we compiled on visual core and thin-section description forms. The results of XRF analyses for basalts from the three holes are shown in Table 12.

Hole 706A

The one piece of vesicular, fine-grained basalt that was recovered represents the topmost volcanic unit. This sample is nearly identical in its phenocryst assemblage, alteration, and vesicularity to 115-706C-2R-2 (Piece 1 through 3; Unit 3) in Hole 706C, and is similar to 115-706B-7X, CC (Piece 6, 5–60 cm) in Hole 706B (Unit 7), except that Piece 6 is more altered. While the majority of basalts recovered in these three holes are mineralogically similar, the single piece from Hole 706A, Piece 6 from Hole 706B, and Unit 3 from Hole 706C appear to contain no olivine, whereas most other basalt samples have small amounts of olivine that have been completely altered to clay minerals.

Hole 706B

The extended core barrel (XCB) recovered carbonate sediment, pebbles of limestone, chert, and basalt, and sulfide-cemented volcanic sands directly above basement, as well as six pieces of basalt totaling 0.5 m. The sulfide sandstone appears to have formed in place by the action of sulfate-reducing bacteria which precipitated pyrite framboids that cemented clasts of lithic fragments, glass, and mineral grains. The glass fragments have delicate shapes that would not survive transport and were presumably formed by an explosive submarine eruption, such as that described for seamounts on the East Pacific Rise (Batiza et al., 1984). The presence of large amounts of sulfur suggests proximity to hydrothermal activity. Alternatively, the pebbles may have been transported to this location.

The basalt pieces from Hole 706B are similar to most other basalts of Holes 706A and 706C. Perhaps most surprising is the low degree of alteration in 115-706B-7X, CC (Pieces 2 and 7; Units 3 and 8). This may indicate that the system was sealed shortly after the eruption of these flows. Fresh glass occurs in both of these pieces.

Hole 706C

The largest section of basalt was recovered in this hole. We defined 32 units by changes in lithology and/or the presence of basalt pieces with glassy chilled margins. Some original flow units may be missing altogether because we recovered only 25%

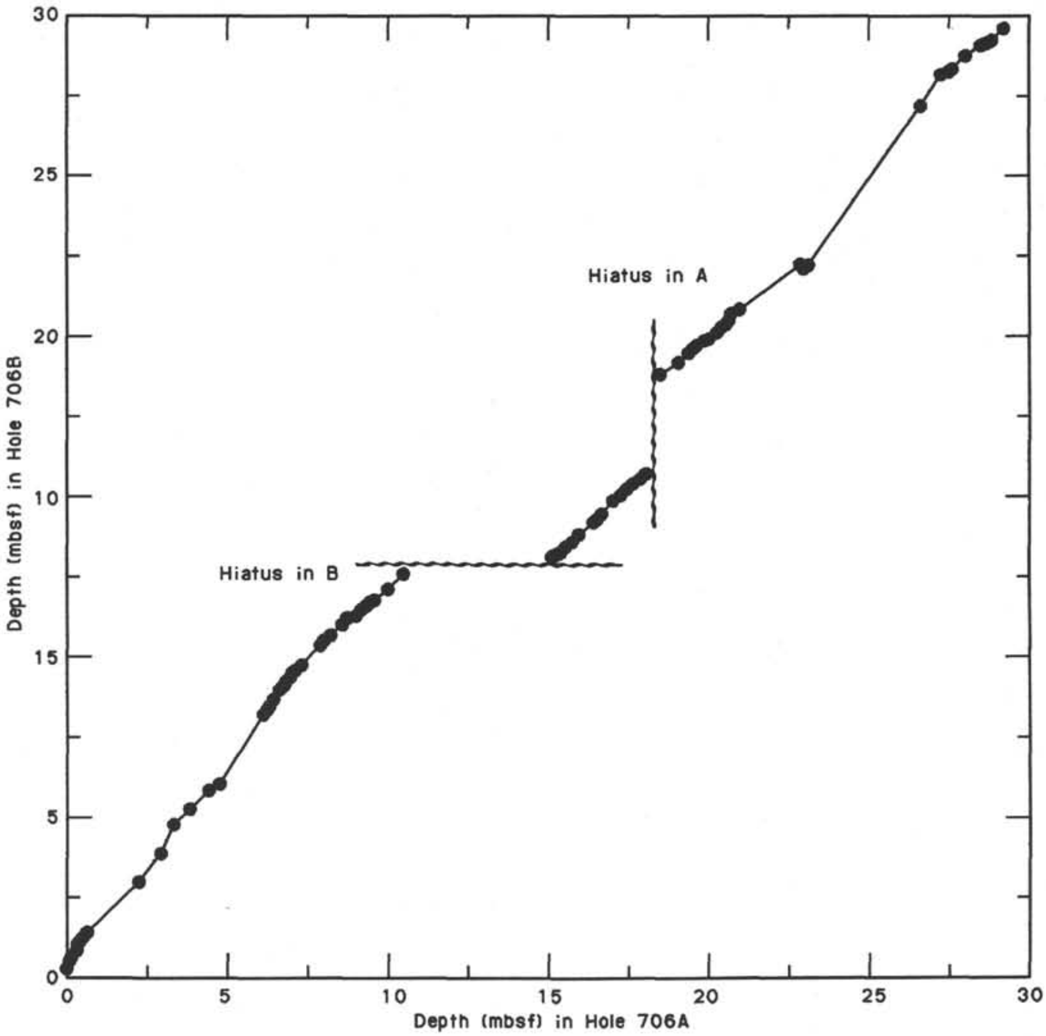

Figure 23. Shaw correlation diagram showing the relationship between the lithostratigraphic records of Holes 706A and 706B, based on whole-core magnetic susceptibility profiles of each hole.

of the basement drilled. On the other hand, some of our "units," especially those defined by chilled contacts, may represent pillows or multiple chilled contacts produced within a single flow unit.

The lithostratigraphy, vesicularity, grain size, alteration, and abundance of plagioclase, augite, and olivine are shown in Figure 29. The length of each unit shown in Figure 29 is in proportion to its recovered length. Rubble recovered in Core 115-706C-7R was assigned to Unit 24 and is not shown in Figure 29. Samples from 115-706C-7R, CC (Pieces 1, 2, and 4), representing Units 22, 23, and 25, were not examined in thin section.

Basalts composing Units 1-30 appear to be very similar. The most common rock type contains 0.5-mm plagioclase (typically An_{60-65}, determined optically) and 0.4-mm clinopyroxene (augite) microphenocrysts (commonly 15 and 7 modal percent, respectively) with altered olivine phenocrysts comprising 1%-2% of most samples. The total percentage of phenocrysts varies from about 5% to over 40% (Fig. 29). Both the plagioclase and augite phenocrysts commonly display zoning. Augite often forms glomeroporphyritic aggregates that subophitically enclose plagioclase and, in some units (e.g., Unit 10), appears light purple, especially near the edges, which is quite in harmony with higher concentrations of TiO_2 in those rocks. Olivine was present in most of the units but has been completely altered to clay or iddingsite; however, fresh olivine does occur in at least one flow. Iron-rich spinel also occurs as microphenocrysts in some of the lavas.

The majority of samples are fine grained; quenched borders show well-preserved glass, grading into an opaque crystalline groundmass in the interior. Needles of clinopyroxene and an iron-titanium-oxide phase radiate from the edges of phenocrysts in the cryptocrystalline groundmasses. These textures formed probably by quenching. Unit 13 (Sample 115-706C-4R-3, Piece 1, 0-25 cm) is the only medium-grained sample recovered, is one of the least vesicular (10%), and also has the highest modal abundance of phenocrysts (50%). Unit 31 is distinct in having the highest inferred olivine percentages. Units 31 and 32 appear to be distinct from the others, with large, white, somewhat equant plagioclase phenocrysts ($\leq$7 mm), and low pyroxene phenocryst percentages.

Alteration

All samples show signs of alteration, ranging commonly from 10% to 50%. In the slightly altered samples (2%-10% alteration minerals), the olivine has been replaced by iddingsite, possibly including hematite, and there is some replacement of glass in the groundmass by clay minerals. In the moderately to highly altered rocks (10%-80% altered), the olivine, glass, and ground-

Table 5. Biostratigraphic datum levels, Hole 705A.

Species event	Depth (mbsf)	Age (Ma)
FO *E. huxleyi* (N)	1.80–2.80	0.27
LO *P. lacunosa* (N)	2.80–4.30	0.46
LO *G. tosaensis* (F)	0.01–8.50	0.60
LO *C. macintyrei* (N)	8.50–9.80	1.45
FO *G. oceanica* (N)	9.80–11.30	1.60
LO *D. brouweri* (N)	9.80–11.30	1.89
FO *G. truncatulinoides* (F)	0.01–8.50	1.90
LO *D. pentaradiatus* (N)	12.80–14.30	2.35
LO *D. tamalis* (N)	14.30–15.80	2.65
LO *G. altispira* (F)	8.50–18.00	2.90
FO *G. fistulosus* (F)	8.50–18.00	2.90
LO *Sphaeroidinellopsis* (F)	18.00–27.50	3.00

Note: FO = first occurrence, LO = last occurrence, N = nannofossil, and F = foraminifer.

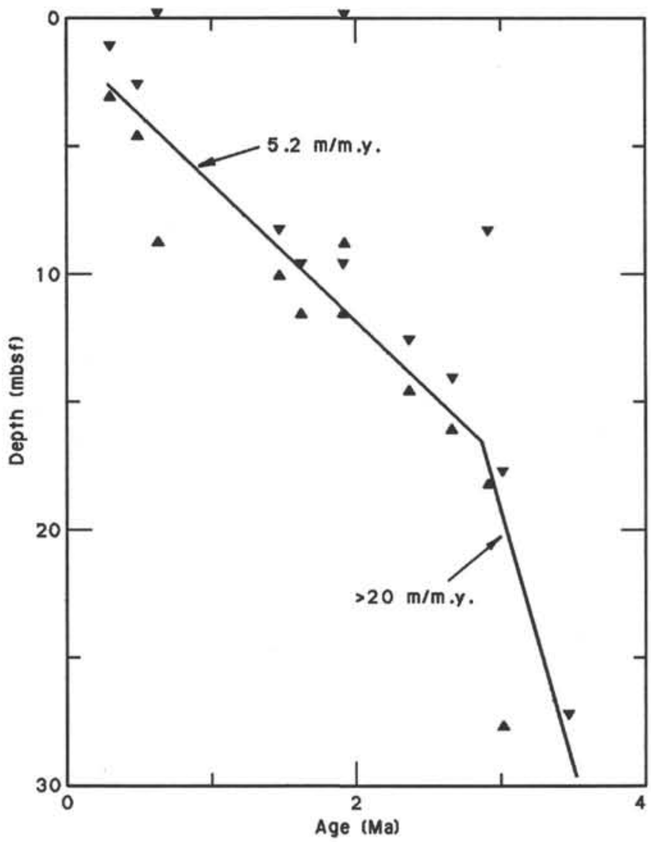

Figure 24. Sedimentation-rate curve for Hole 705A.

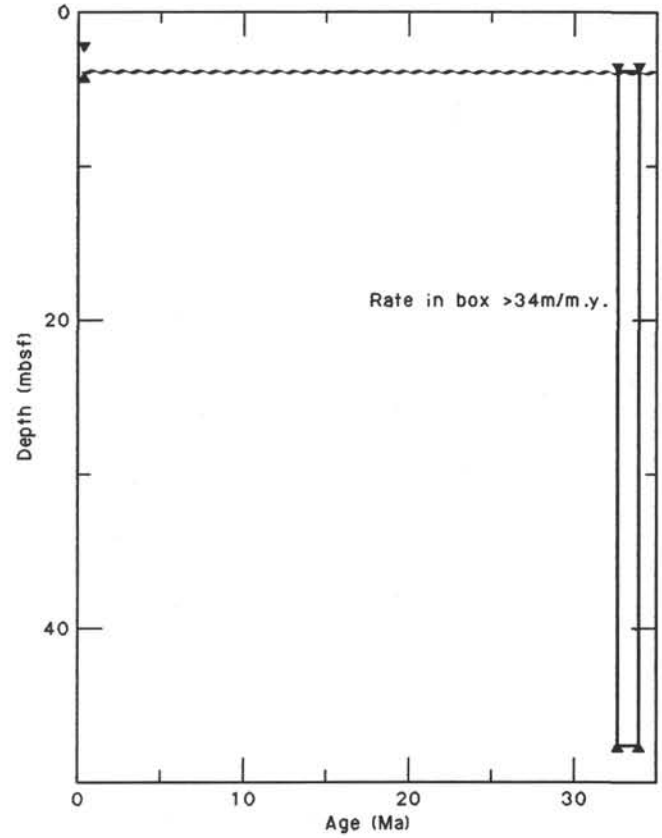

Figure 25. Sedimentation-rate curve for Hole 706A.

Table 6. Biostratigraphic and magnetostratigraphic datum levels, Hole 706A.

Species event	Depth (mbsf)	Age (Ma)
FO *E. huxleyi* (N)	3.80	0.27
FO *S. ciperoensis* (N)	—	30.20
FO *S. distentus* (N)	47.50	34.20
Chron C12R	3.80	32.90

Note: FO = first occurrence and N = nannofossil.

mass have been replaced by clay. Plagioclase and augite microphenocrysts always appear pristine, and fresh glass is common at unit boundaries.

Alteration minerals observed include green clay (celadonite), light purple and brown iron oxides and hydroxides (goethite and hematite), and clay minerals (illite/montmorillinite?), pyrite, calcite, and a clear colorless mineral forming prismatic crystals. The latter may be a zeolite (phillipsite?) or selenite; it tends to occur in vugs or large vesicles close to contacts between units (i.e., on glassy samples). The iron oxides/hydroxides appear as a coating on vesicle interiors. Vesicles and fractures through the samples host the green and brown alteration minerals (tentatively identified as celadonite and limonite), which occur as alternating bands or layers growing one on top of the other. Vesicles near fractures tend to be more completely filled with alteration minerals than those in the rock interior. Pyrite was locally observed filling a small percentage of vesicles. We observed calcite in Units 31 and 32 apparently replacing olivine and filling the centers of vesicles.

Discussion

Based on chemical compositions, volcanic rocks from Site 706 are divided into two groups: high- and low-titanium basalts. The high-titanium basalts have lower Al_2O_3 and higher ferric-oxide contents than do typical ocean floor basalts, and they closely resemble rocks of the older alkaline group on Mauritius (Baxter, 1975). The low-titanium group, on the other hand, have compositions similar to ocean-floor basalts.

All volcanic rocks from Site 706 are characterized by their high content of plagioclase phenocrysts, and in this sense they are distinct from the basalts from Mauritius (Baxter, 1975) and

Table 7. Interstitial water analyses, Holes 705A and 706A.

Sample interval (cm)	Depth (mbsf)	Ca (mmol/L)	Mg (mmol/L)	Cl (mmol/L)	Al (mmol/L)	pH	Salinity (‰)	Si (µmol/L)	NH_3 (µmol/L)	SO_4 (mmol/L)
Seawater	0	10.34	55.42	571.88	2.32	8.36	34.6	17.80	8.30	30.16
115-705A-										
1H-3, 145-150	4.45	11.27	53.28	564.95	3.01	7.86	35.0	271.70	0	29.69
2H-3, 145-150	12.95	11.61	52.86	565.94	3.03	7.74	35.4	265.03	2.35	30.00
Seawater	0	10.34	55.43	571.88	2.32	8.36	34.2	17.80	8.30	30.16
115-706A-										
2H-2, 145-150	9.95	10.90	51.96	569.90	2.38	7.74	35.0	575.77	0	30.32
3H-3, 145-150	18.15	12.18	49.39	576.84	2.44	7.68	35.0	550.71	0	30.16
4H-4, 145-150	26.35	13.16	47.60	577.83	2.16	7.78	35.0	495.58	171.20	30.00
5H-5, 145-150	37.45	13.93	49.82	571.88	2.10	7.67	34.8	425.41	55.00	29.53
6H-6, 145-150	44.05	13.91	48.22	572.88	1.64	7.84	35.2	463.83	43.00	30.32
7W-7, 0-1	47.50	10.35	52.75	557.02	2.48	8.32	34.0	17.80	0	29.69

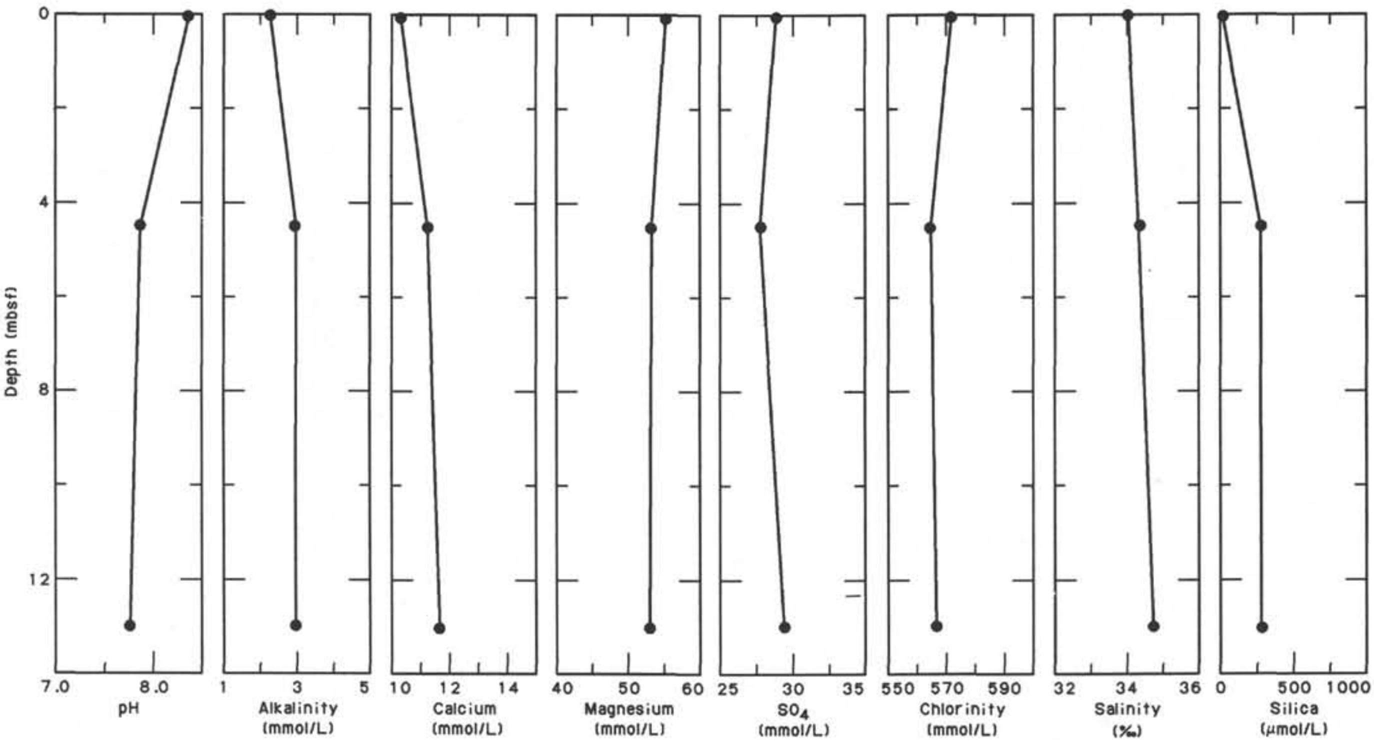

Figure 26. Summary of interstitial water analyses, Hole 705A, as a function of sub-bottom depth. Surface seawater is plotted at 0 mbsf.

Réunion (Upton and Wadsworth, 1972) which are dominated by olivine or olivine plus clinopyroxene. Only Rodrigues Island, 400 miles east of the south end of the Mascarene Plateau and connected to it by the Rodrigues Ridge, shows any affinities with Site 706. Rodrigues basalts are dominated by plagioclase and olivine phenocrysts with subordinate clinopyroxene (Baxter et al., 1985).

Unit 30, with the 9 modal percent olivine, is probably the most mafic unit in the suite, but the generally low olivine percentages indicate that most rocks are somewhat evolved. The feldspar-rich, clinopyroxene-poor samples from Units 31 and 32 indicate that these units contain the most evolved rocks in the suite.

Several of the contacts between flow units contained carbonate sediment with microfossils (Fig. 30). These fossils give an approximate date of early Oligocene for the lowermost flows that were recovered from Hole 706C. This corresponds with the magnetic anomaly Chron C13N (35–36 Ma), which is the age of the seafloor on which this part of the Mascarene Plateau is built. This indicates that the plateau was being built on zero-age crust at the Central Indian Ridge, in much the same way Iceland is forming today.

PHYSICAL PROPERTIES

Introduction

This section presents data for the following physical properties using the techniques outlined in the "Explanatory Notes" chapter: index properties, compressional- and shear-wave velocities, thermal conductivity, and undrained shear strength for the sediments from Holes 705A, 706A, and 706B. The measurements were taken on reasonably good quality APC samples.

Table 8. X-ray analyses, Holes 705A and 706A.

Sample interval (cm)	Depth (mbsf)	Calcite (%)	Aragonite (%)	Dolomite (%)	Quartz (%)
115-705A-					
1H-2, 56	2.06	100.00	0	0	0
1H-3, 145	4.45	100.00	0	0	0
1H-4, 51	5.01	96.14	0	3.86	100
2H-2, 28	10.28	100.00	0	0	0
2H-3, 145	12.95	100.00	0	0	0
2H-4, 28	13.28	98.00	0	2.00	0
2H-6, 28	16.28	100.00	0	0	0
115-706A-					
1H-1, 110	1.10	96.82	3.84	0	0
1H-3, 104	4.04	100.00	0	0	0
1H-4, 41	4.91	100.00	0	0	0
2H-1, 53	7.73	100.00	0	0	0
2H-4, 108	8.08	100.00	0	0	0
2H-5, 145	9.40	100.00	0	0	0
2H-5, 145	9.95	100.00	0	0	0
3H-3, 44	15.64	100.00	0	0	0
3H-4, 145	16.65	100.00	0	0	0
4H-3, 145	27.85	100.00	0	0	0
5H-5, 145	38.95	100.00	0	0	0
6H-2, 145	44.05	100.00	0	0	0

Table 9. Percent carbonate and organic carbon, Hole 705A.

Sample interval (cm)	Depth (mbsf)	Carbonate (wt%)	Organic carbon (%)
115-705A-			
1H-2, 56	2.06	94.9	—
1H-4, 51	5.01	92.5	0.02
1H-6, 18	7.68	91.1	0.13
2H-2, 28	10.28	94.6	—
2H-4, 28	13.28	94.9	0.01
2H-6, 28	16.28	83.4	1.19

Data are also presented for the bulk density, compressional-wave velocity, and thermal conductivity for selected samples of basalt recovered from Hole 706C.

Site 705

Index Properties

The index properties are presented graphically in Figures 31–33 and are tabulated in Table 13. One can see from these data that the downhole variations of the wet-bulk density in Hole 705A are small, ranging from 1.38 to 1.58 g/cm³. This reflects the homogeneous lithology of the foraminiferal sand (see "Lithostratigraphy" section, this chapter), reinforced by its uniform $CaCO_3$ content (Fig. 28). There is a slight linear decrease of wet-bulk density with depth (Fig. 31) and corresponding linear increases in the porosity and water content (Fig. 33).

Compressional-Wave Velocity

The compressional-wave velocity (V_p) of the foraminiferal oozes was measured by the *P*-wave logger only. It was not possible to use the Hamilton Frame velocimeter on the noncohesive sediments recovered. The *P*-wave logger had great difficulty in transmitting a compressional wave of 1 MHz through the sand-size sediment. Significant scattering occurred, resulting in a low signal-to-noise ratio. We have not given the V_p results because of their poor quality. In regions where a signal was detected, a velocity between 1500 and 1600 m/s was recorded.

Shear-Wave Velocity and Shear Strength

The shear-wave velocity (V_s) in the sands was evaluated at several locations using the bender transducer technique. The results are presented in Table 14. The recorded velocities (around 80 m/s) are not indicative of the true *in-situ* shear-wave velocities for a number of reasons: laboratory desiccation and capillary cohesion tending to increase V_s, coring disturbance, and the lack of overburden pressure tending to decrease V_s.

The foraminiferal sand was noncohesive, making it pointless to attempt to measure the shear strength. It was undoubtedly this lack of cohesion which caused the borehole walls to fail at Hole 705A.

Thermal Conductivity

Thermal conductivity was measured once per core by the needle-probe technique. The results from Site 705 are shown in Table 15. Measurements in the loose foraminiferal ooze are questionable.

Holes 706A and 706B

Index Properties

Index properties results for Holes 706A and 706B are plotted in Figures 31–33 and also are shown in Table 13. The variation in wet-bulk density values is more extensive than at Site 705, and all values are higher. For Hole 706B, wet-bulk densities obtained from discrete samples have been compared with the wet-bulk densities measured by GRAPE. The measurements from the two techniques agree fairly well over the entire section.

The wet-bulk densities of 2.06 and 1.13 g/cm³ occurring at depths 1.11 and 4.88 mbsf for Hole 706A are probably incorrect as neither the porosity nor the grain density vary significantly in adjacent measurements. Neglecting these measurements, the wet-bulk density fluctuates around 1.70 g/cm³, corresponding to a grain density of 2.60–2.80 g/cm³ (Fig. 32) and a porosity of 60%–75% (Fig. 33). The porosity shows an inverse correlation with the wet-bulk density and grain density. The grain density reflects the high carbonate content, similar to Site 705. However, the carbonate content varies between 85% and 60% in the upper 25 m in Hole 706A, and then rapidly increases to more than 85% at greater depths (Fig. 28).

Porosities and water contents match very well within Hole 706A and Hole 706B. In Hole 706A both properties are about 20% higher in the upper 20 m of the section than in Hole 706B (Fig. 33). Correlation between the two holes is especially good in the lower part of the sections.

Compressional-Wave Velocity

Compressional-wave velocities were evaluated using both the Hamilton Frame and the *P*-wave logger at Holes 706A and 706B. The results for V_p vs. depth are shown in Figure 34. Discrete measurements are given in Table 16. In general, the discrete and logger results are in good agreement.

Shear-Wave Velocity and Shear Strength

The shear-wave velocity (V_s) was measured at a number of locations in the stiff oozes encountered at Holes 706A and 706B. These results are presented in Table 14. Significant problems were encountered with the sediment cracking in between the transducers, resulting in low shear velocities. These data were disregarded, as were data collected in disturbed regions of core. No relationship of V_s with depth can be inferred from the data shown in Table 14.

Shear strength measurements were conducted in half-split cores using the motorized shear vane. The results for (maximum) shear strength for measurements at Holes 706A and 706B

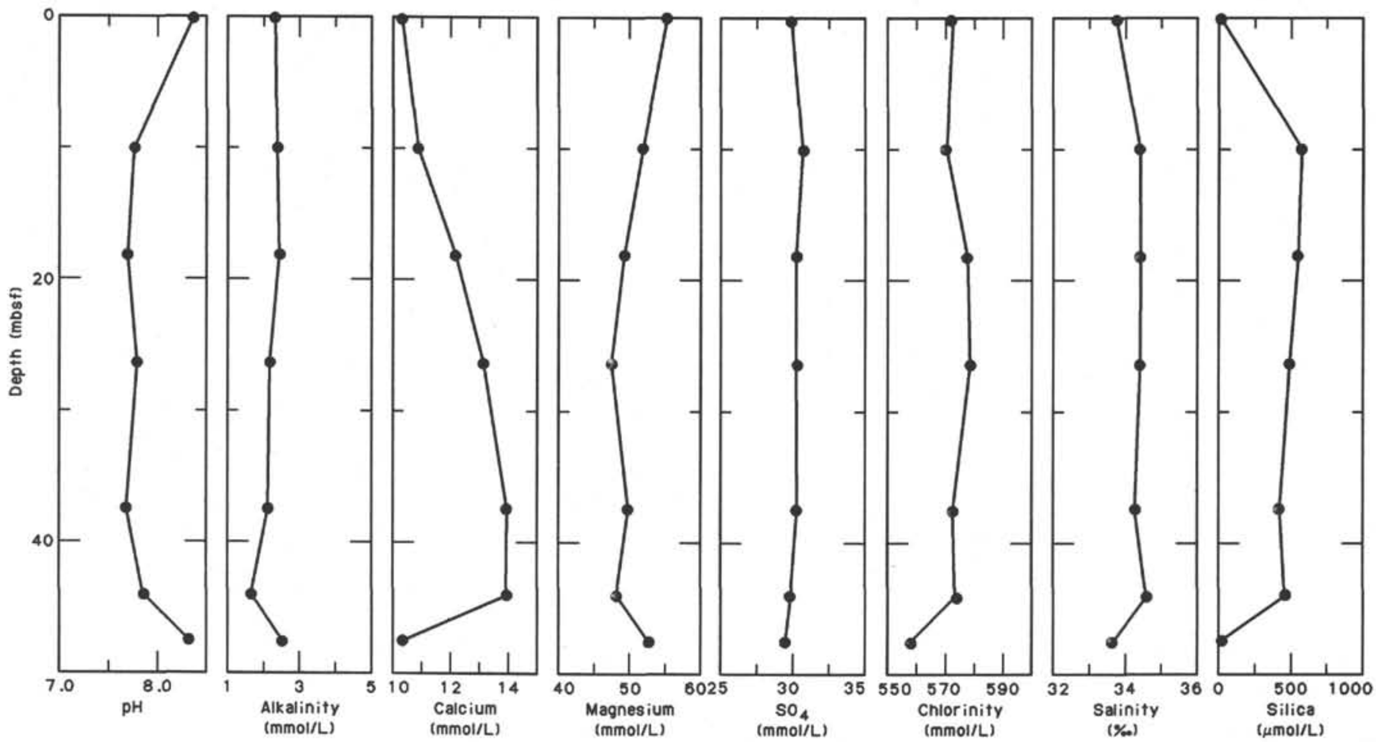

Figure 27. Summary of interstitial water analyses, Hole 706A, as a function of sub-bottom depth. Surface seawater is plotted at 0 mbsf. Data at the deepest sampling level apply to fluids recovered with the downhole water sampler.

Table 10. Downhole calcium/magnesium gradients at DSDP Sites 232 through 245.

Site	Calcium/magnesium gradient
232	−0.31
235	−0.94
236	−1.70
237	−0.57
706	−0.96
238	−1.47
239	−1.80
242	−1.64
245	−1.00

are shown in Figure 35 and in Table 17. These results show a range of values between 50 and 172 kPa. There is no obvious correlation between holes, nor to sediment lithology, nor to V_s.

Thermal Conductivity

In Holes 706A and 706B thermal conductivity was determined at every other section using the probe technique. Table 15 presents the results, which vary from 0.96 to 1.56 $W \cdot m^{-1} \cdot K^{-1}$. The overall trend shows an inverse correlation with water content, which is typical of marine sediments (Hamilton, 1974), and a direct correlation in these sediments with bulk density.

Hole 706C

Basement Section

Within the basement section drilled in Hole 706C, physical properties measurements were reduced to compressional-wave velocities, 2-min GRAPE density analyses, and thermal conductivity. The velocities were measured (in a direction perpendicular to the major core axis) on minicore samples (one per core) using the Hamilton Frame, while the thermal conductivity was evaluated using the half-space technique. The results of thermal conductivity measurements, compressional-wave velocities, and wet-bulk densities for Hole 706C are shown in Tables 18 and 19. Acoustic impedance values, calculated as the product of compressional-wave velocity and bulk density, are also listed in Table 18.

The low velocities of 3018–3958 m/s reflect the extraordinarily porous character of the basalts.

Summary

The physical properties of a Pleistocene foraminiferal sand, an Oligocene nannofossil ooze, and basement basalts were measured at Sites 705 and 706. Each lithologic unit had its own distinct characteristics.

The foraminiferal ooze was a noncohesive sand-grade material, with a porosity exceeding 70% and a calcium-carbonate content greater than 95%. It had a compressional-wave velocity similar to that for seawater, and a thermal conductivity of 1.08 $W \cdot m^{-1} \cdot K^{-1}$.

The underlying ooze was stiff and brittle (average cohesion of 150 kPa) with a porosity of less than 60%. It was further characterized by a compressional velocity of 2000 m/s and a shear velocity of 200 m/s. The thermal conductivity for this ooze averaged 1.25 $W \cdot m^{-1} \cdot K^{-1}$.

The basement basalts were of a low bulk density (2.4 g/cm^3) and had a low compressional-wave velocity (3–4 km/s) in comparison with typical basalts. They were characterized by a thermal conductivity of 1.30–1.38 $W \cdot m^{-1} \cdot K^{-1}$.

SEISMIC STRATIGRAPHY

Ocean drilling on the Mascarene Plateau is complicated by several factors. The objective of basement penetration and recovery cannot be achieved near the flat summit areas because

Table 11. Percent carbonate and organic carbon, Holes 706A and 706B.

Sample interval (cm)	Depth (mbsf)	Carbonate (wt%)	Organic carbon (%)
115-706A-			
1H-1, 110	1.10	87.8	0.08
2H-2, 88	4.88	68.0	0.04
2H-5, 145	9.40	71.7	—
3H-3, 44	15.64	64.1	0.07
3H-5, 68	18.88	79.2	—
4H-1, 50	22.40	67.3	—
4H-2, 138	24.78	85.3	—
4H-4, 63	27.03	85.6	—
5H-1, 93	32.43	86.9	—
5H-2, 105	34.05	85.6	0.02
5H-3, 94	35.44	91.9	—
5H-4, 98	36.98	83.0	—
5H-5, 93	38.43	85.5	—
5H-6, 55	39.55	90.2	—
6H-1, 61	41.71	79.2	—
6H-2, 106	43.66	78.4	0.02
115-706B-			
1H-3, 104	4.04	69.7	0.32
1H-4, 41	4.91	72.2	—
2H-1, 53	6.23	68.6	—
2H-2, 103	8.23	62.2	—
2H-3, 71	9.41	65.1	0.12
2H-4, 47	10.67	64.7	—
2H-5, 16	11.86	59.1	—
3H-3, 23	15.93	71.6	0.20
3H-4, 28	17.48	71.0	—
3H-5, 22	18.92	70.0	—
4H-1, 66	21.26	68.8	0.39
6X-2, 70	29.30	75.5	1.07

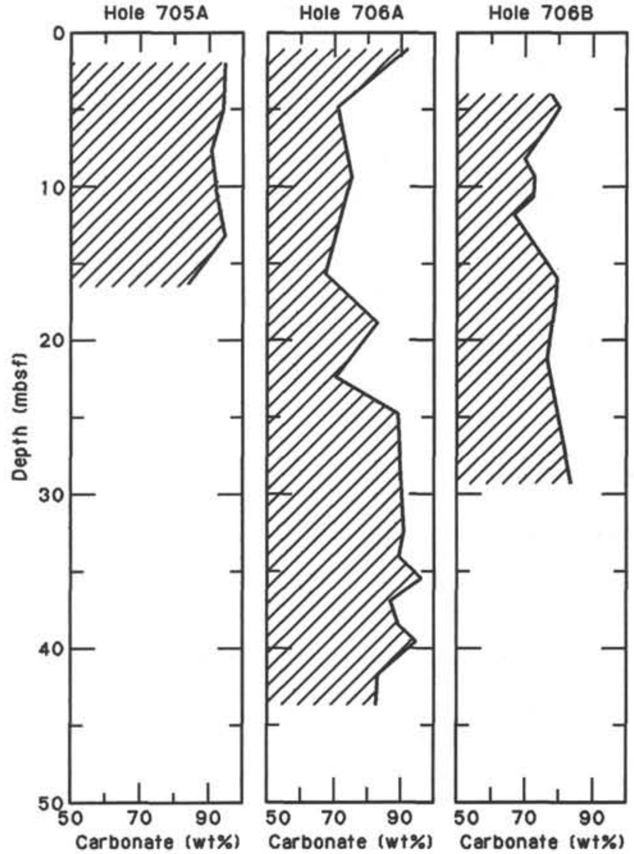

Figure 28. Carbonate content of samples for which the index properties were measured in Holes 705A, 706A, and 706B.

tremendously thick carbonate banks have grown up over the volcanic rocks as the ridge subsided. Industrial drilling has shown that over 2000 m of shallow-water carbonates overlie the Saya de Malha and Nazareth Banks (Meyerhoff and Kamen-Kaye, 1981). The flanks just below the carbonate buttresses are very steep and rugged, showing evidence of normal faulting and active downslope transport. Hence, the only real potential for locating successful sites is well down on the flanks where slopes are more gentle and pelagic sediments accumulate. Even here, erosion is active and sediment preservation is irregular. Figure 36 illustrates a typical profile across the Mascarene Plateau near Sites 705 and 706.

Sites 705 and 706 are located on a single-channel seismic (SCS), air-gun line (Fig. 37) run in March 1987 by the *Charles Darwin* cruise 21/87, and funded by the Natural Environmental Research Council of Great Britain and the U.S. National Science Foundation. The seismic and bathymetric surveys of this site showed a region of moderately to poorly stratified sediments which had been deeply dissected by west-to-east-trending canyons. A very strong reflector interpreted as volcanic basement underlies the entire area and, because of the active erosional environment, may actually crop out in the canyon floors.

On the approach to Site 705, we deployed the *JOIDES Resolution*'s SCS system in order to identify the planned drilling location. Our approach profile (Fig. 38) was recorded from an 80-in.[3] water gun, with a 10-s firing interval, and looks very similar to the *Darwin* profile on the same line. The 3.5- and 12-kHz depth profilers recorded some near-surface stratified sediments.

On the seismic records, most of the sediment highs show evidence of unconformities at depth, probably due to a history of channeling and slumping of sediments from the shallower slopes to the west. This has led to an extremely variable sediment cover and, over time, probably has produced irregular sediment preservation throughout the region. After loose-surface foraminiferal sands caused hole stability problems at Site 705, we found a surface with a stronger seismic reflectivity to drill at Site 706 on a prominent ledge about 35 m above the canyon floor to the north of Site 705 (Fig. 37). One can trace this ledge 6 nmi on additional *Darwin* crossings of the same canyon.

From the drilling at Site 706, we know that this strong surface reflector is lower Oligocene nannofossil ooze. Measured *P*-wave velocities for this material are 1.6 km/s. This could be the rather continuous strong reflector overlying basement in most parts of the surveyed area; if so, it is 50–80 m thick. The basement reflector is vesicular to massive basalt flows, which were penetrated 74 m at Site 706. Measured *P*-wave velocities for this material are from 3.5 to 4.0 km/s. Some steeply dipping reflectors within the basement appear on the *Darwin* survey and are consistent with strike-slip faulting parallel with transform faults extending southwestward from the Central Indian Ridge.

REFERENCES

Backman, J., 1987. Quantitative calcareous nannofossil biochronology of middle Eocene through early Oligocene sediment from DSDP Sites 522 and 523. *Geol. Bundestandt Abh. Austria*, 39:21–31.

Backman, J., and Shackleton, N. J., 1983. Quantitative biochronology of Pliocene and early Pleistocene calcareous nannofossils from the Atlantic, Indian, and Pacific Oceans. *Mar. Micropaleontol.*, 8:141–170.

Baker, P. A., 1986. Pore-water chemistry of carbonate-rich sediments, Lord Howe Rise, Southwest Pacific Ocean. *In* Kennett, J. P., and von der Borch, C. C., et al., *Init. Repts. DSDP*, 90: Washington (U.S. Govt. Printing Office), 1249–1256.

Batiza, R., Fornari, D. J., Vanko, D. A., and Lonsdale, P., 1984. Craters, calderas, and hyaloclastites on young Pacific seamounts. *J. Geophys. Res.*, 89:8371–8390.

Baxter, A. N., 1975. Petrology of the Older Series lavas from Mauritius, Indian Ocean. *Geol. Soc. Am. Bull.*, 86:1449–1458.

Baxter, A. N., Upton, B.G.J., and White, W. M., 1985. Petrology and geochemistry of Rodrigues Island, Indian Ocean. *Contrib. Mineral. Petrol.*, 89:90–101.

Berggren, W. A., Kent, D. V., Flynn, J. J., and Van Couvering, J. A., 1985a. Cenozoic geochronology. *Geol. Soc. Am. Bull.*, 96:1407–1418.

Berggren, W. A., Kent, D. V., and Flynn, J. J., 1985b. Jurassic to Paleogene: Part 2. Paleogene geochronology and chronostratigraphy. *In* Snelling, N. J. (Ed.), *The Chronology of the Geological Record*, London Geol. Soc. Mem., 10:141–195.

Berggren, W. A., Kent, D. V., and Van Couvering, J. A., 1985c. The Neogene: Part 2. Neogene geochronology and chronostratigraphy. *In* Snelling, N. J. (Ed.), *The Chronology of the Geological Record*, London Geol. Soc. Mem., 10:211–260.

Blow, W. H., 1969. Late middle Eocene to Recent planktonic foraminiferal biostratigraphy. *Proc. 1st Intl. Conf. Planktonic Microfossils*, 1: 199–422.

Boersma, A., 1984. Oligocene and other Tertiary benthic foraminifers from a depth traverse down Walvis Ridge, Deep Sea Drilling Project Leg 74, Southeast Atlantic. *In* Hay, W. W., Sibuet, J.-C., et al., *Init. Repts. DSDP*, 75: Washington (U.S. Govt. Printing Office), 1273–1300.

Canfield, D. E., and Berner, R. A., 1987. Dissolution and pyritization of magnetite in anoxic marine sediments. *Geochim. Cosmochim. Acta*, 51:645–659.

Carmichael, R. S., 1982. Magnetic properties of minerals and rocks. *In* Carmichael, R. S. (Ed), *Handbook of Physical Properties of Rocks* (Vol. 4): Boca Raton, FL (CRC Press).

Courtillot, V., Besse, J., Vandamme, D., Montigny, R., Jaeger, J.-J., and Cappetta, H., 1986. Deccan flood basalts at the Cretaceous/Tertiary boundary? *Earth Planet. Sci. Lett.*, 80:361–374.

Duncan, R. A., 1981. Hotspots in the southern oceans—an absolute frame of reference for motion of the Gondwana continents. *Tectonophysics*, 74:29–42.

Emerick, C. M., 1985. Age-progressive volcanism in the Comores Archipelago and northern Madagascar [Ph.D. dissert.]. Oregon State Univ., Corvallis.

Fisher, R. L., Sclater, J. G., and McKenzie, D. P., 1971. Evolution of the Central Indian Ridge, Western Indian Ocean. *Geol. Soc. Am. Bull.*, 82:553–562.

Gartner, S., Jr., 1977. Calcareous nannofossil biostratigraphy and revised zonation of the Pliocene. *Mar. Micropaleontol.*, 2:1–25.

Gieskes, J. M., 1974. Interstitial water studies, Leg 25. *In* Simpson, E.S.W., Schlich, R., et al., *Init. Repts. DSDP*, 25: Washington (U.S. Govt. Printing Office), 361–394.

————, 1981. Deep-sea drilling interstitial water studies: implications for chemical alteration of the ocean crust, Layers I and II. *Soc. Econ. Paleontol. Mineral. Spec. Publ.*, 32:149–167.

Gieskes, J. M., and Lawrence, J. R., 1981. Alteration of volcanic matter in deep sea sediments: evidence from the chemical composition of interstitial waters from deep sea drilling cores. *Geochim. Cosmochim. Acta*, 45:1687–1703.

Hamilton, E. L., 1974. Prediction of deep-sea sediment properties: state of the art. *In* Inderbitzen, A. L. (Ed.), *Deep-Sea Sediments—Physical and Mechanical Properties:* New York (Plenum), 1–44.

Karlin, R., and Levi, S., 1983. Diagenesis of magnetic minerals in recent hemipelagic sediments. *Nature*, 303:327–330.

————, 1985. Geochemical and sedimentological control of the magnetic properties of hemipelagic sediments. *J. Geophys. Res.*, 90: 10,373–10,392.

Kennett, J. P., Keller, G., and Srinivasan, M. S., 1985. Miocene planktonic foraminiferal biogeography and paleoceanographic development of the Indo-Pacific region. *In* Kennett, J. P. (Ed.), *The Miocene Ocean: Paleoceanography and Biogeography*, Geol. Soc. Am. Mem., 163:197–236.

McDougall, I., 1971. The geochronology and evolution of the young oceanic island of Réunion, Indian Ocean. *Geochim. Cosmochim. Acta*, 35:261–270.

McDougall, I., and Chamalaun, F. G., 1969. Isotopic dating and geomagnetic polarity studies on volcanic rocks from Mauritius, Indian Ocean. *Geol. Soc. Am. Bull.*, 80:1419–1431.

McDuff, R. E., 1981. Major cation gradients in DSDP interstitial waters: the role of diffusive exchange between seawater and upper oceanic crust. *Geochim. Cosmochim. Acta*, 45:1705–1713.

McFadden, P. L., and Reid, A. B., 1982. Analysis of paleomagnetic inclination data. *Geophys. J. R. Astron. Soc.*, 69:307–319.

McKenzie, D. P., and Sclater, J. G., 1971. The evolution of the Indian Ocean since the Late Cretaceous. *Geophys. J. R. Astron. Soc.*, 25: 437–528.

Martini, E., 1971. Standard Tertiary and Quaternary calcareous nannoplankton zonation. *In* Farinacci, A. (Ed.), *Proc. II Planktonic. Conf. Roma, 1971*: Rome (Ed. Tecnoscienza), 739–777.

Meyerhoff, A. A., and Kamen-Kaye, M., 1981. Petroleum prospects of the Saya de Malha and Nazareth Banks, Indian Ocean. *Am. Assoc. Pet. Geol. Bull.*, 65:1344–1347.

Morgan, W. J., 1981. Hotspot tracks and the opening of the Atlantic and Indian Oceans. *In* Emiliani, C. (Ed.), *The Sea* (Vol. 7): New York (Wiley), 443–487.

Okada, H., and Bukry, D., 1980. Supplementary modification and introduction of code numbers to the low-latitude coccolith biostratigraphic zonation (Bukry, 1973; 1975). *Mar. Micropaleontol.*, 5:321–325.

Rio, D., Backman, J., and Raffi, I., in press. *Calcareous Nannofossil Biochronology and the Pliocene/Pleistocene Boundary*: Cambridge (Cambridge Univ. Press).

Robinson, S. G., 1986. The late Pleistocene palaeoclimatic record of North Atlantic deep-sea sediments revealed by mineral-magnetic measurements. *Phys. Earth Planet. Inter.*, 42:22–47.

Sager, W. W., 1986. Magnetic-susceptibility measurements of metal contaminants in ODP Leg 101 cores. *In* Austin, J. A., Jr., Schlager, A. A., et al., *Proc. ODP, Init. Repts.*, 101: College Station, TX (Ocean Drilling Program), 39–45.

Sandstrom, M., and Gieskes, J. M., 1974. Interstitial water studies, Leg 24. *In* Fisher, R. L., Bunce, E. T., et al., *Init. Repts. DSDP*, 24: Washington (U.S. Govt. Printing Office), 799–810.

Thierstein, H. R., Geitzenauer, K. R., Molfino, B., and Shackleton, N. J., 1977. Global synchroneity of late Quaternary coccolith datum levels: validation by oxygen isotopes. *Geology*, 5:400–404.

Tjalsma, R. C., 1983. Eocene to Miocene benthic foraminifers from Deep Sea Drilling Project Site 516, Rio Grande Rise, South Atlantic. *In* Barker, P. F., Carlson, R. L., Johnson, D. A., et al., *Init. Repts. DSDP*, 72: Washington (U.S. Govt. Printing Office), 731–756.

Upton, B.G.J., and Wadsworth, W. J., 1972. Aspects of magmatic evolution of Réunion Island. *Phil. Trans. R. Soc. London.*, A-271:105–130.

Ms 115A-105

Table 12. Basalt major and trace element chemistry, Site 706.

Hole no. Core, Section Interval	115-706A 6H, CC 21–23	115-706B 7X, CC 22–24	115-706B 7X, CC 29–32	115-706C 2R-1 80–83	115-706C 2R-1 105–107	115-706C 2R-2 28–30	115-706C 2R-2 74–77	115-706C 2R-2 116–119	115-706C 2R-2 142–146	115-706C 3R-1 12–14	115-706C 3R-1 83–85	115-706C 3R-2 45–47	115-706C 4R-1 78–80	115-706C 4R-2 116–118	115-706C 4R-3 10–13	115-706C 5R-1 82–90
wt%:																
SiO_2	47.62	48.34	47.82	48.90	47.67	47.91	48.23	48.27	48.03	47.26	47.95	47.71	47.74	47.49	48.04	47.86
TiO_2	3.34	3.32	3.65	3.18	3.48	3.43	3.27	3.34	3.33	3.69	3.38	3.53	3.50	3.47	3.17	3.21
Al_2O_3	13.95	13.11	13.91	13.25	14.06	13.97	13.40	13.50	13.80	14.24	13.85	13.78	13.73	13.86	13.67	14.07
Fe_2O_3	15.22	16.44	15.69	16.28	15.45	15.62	16.52	16.69	15.33	16.23	15.23	15.99	15.81	15.37	15.65	15.23
MnO	0.18	0.23	0.20	0.20	0.20	0.19	0.18	0.21	0.20	0.19	0.19	0.19	0.19	0.22	0.20	0.21
MgO	5.06	5.06	4.68	6.08	4.86	5.01	4.72	5.66	5.15	4.20	4.88	4.91	5.58	5.58	5.65	5.71
CaO	10.32	9.75	10.04	8.96	10.11	9.48	9.47	9.26	10.25	10.44	10.35	10.02	9.57	10.35	10.35	9.75
Na_2O	2.72	2.19	2.40	2.13	2.63	2.72	2.48	2.46	2.65	2.58	2.66	2.71	2.50	2.74	2.61	2.61
K_2O	0.67	0.85	0.90	1.13	0.67	0.88	1.47	0.80	0.80	0.89	0.86	0.83	0.72	0.32	0.34	
P_2O_5	0.45	0.30	0.36	0.21	0.40	0.40	0.36	0.33	0.44	0.42	0.46	0.43	0.41	0.34	0.35	0.34
Total	99.53	99.59	99.65	100.32	99.53	99.61	100.10	100.52	99.98	100.14	99.81	100.10	99.75	99.74	100.03	99.84
Ignition loss	0.62	0.66	0.59	1.02	0.46	0.80	1.09	0.99	0.34	0.36	1.15	0.66	0.75	0.71	0.38	0.14
ppm:																
Nb	22.1	21.8	23.6	22.1	24.5	23.5	22.0	22.4	23.2	23.6	22.6	24.4	23.2	23.8	23.0	21.8
Zr	252.3	245.9	259.6	242.0	265.0	256.3	244.2	246.0	249.3	257.2	257.1	265.8	264.6	266.6	250.4	244.1
Y	52.8	41.2	47.9	38.5	50.5	47.4	41.9	42.3	48.1	59.4	51.5	50.1	51.1	44.4	43.2	42.3
Sr	275.0	222.6	255.5	211.0	276.4	276.5	258.6	233.6	275.0	283.3	276.7	270.7	250.1	279.8	271.6	282.8
Rb	11.9	16.5	9.2	17.8	10.1	15.6	39.4	10.1	15.4	15.9	17.1	18.7	13.0	1.4	3.5	2.0
Zn	164.1	156.4	146.0	225.0	152.0	137.8	138.2	147.7	143.1	125.5	142.4	150.2	159.9	281.3	137.1	134.4
Cu	100.5	112.5	128.0	119.8	148.2	126.8	117.8	118.2	145.7	167.7	128.3	120.6	139.3	128.7	122.9	117.3
Ni	62.6	47.1	69.2	36.9	48.6	48.7	37.0	44.2	58.9	30.5	43.8	45.1	48.9	45.7	48.1	50.7
Cr	45.9	31.4	28.9	34.2	31.0	29.1	31.2	29.7	27.5	28.2	28.9	20.1	22.4	23.8	33.4	35.2
V	426.2	415.0	451.9	405.3	452.1	426.4	398.4	405.4	422.4	457.8	431.9	437.0	429.5	421.6	393.9	412.2
Ce	56.8	33.9	53.3	36.7	55.4	57.5	47.5	44.0	47.3	72.8	59.3	51.0	46.2	53.7	50.0	50.7
Ba	124	139	124	107	116	120	113	116	136	141	121	134	109	126	138	134

Table 12 (continued).

Hole no.	115-706C	115-706C	115-706C	115-706C	115-706C	115-706C	115-706C	115-706C	115-706C	115-706C	115-706C	115-706C[a]	115-706C	115-706C	115-706C
Core, Section	5R-2	5R-2	5R-3	6R-1	6R-2	8R-1	8R-1	8R-2	8R-2	8R-3	9R-1	9R-1	9R-1	9R-1	9R-2
Interval	52-56	136-138	59-62	45-50	17-19	32-35	74-77	44-48	125-128	45-48	10-12	10-12	13-16	23-29	36-39
wt%:															
SiO_2	47.63	48.07	47.49	48.90	47.27	48.10	48.04	48.68	48.67	48.78	48.87	48.84	49.06	48.97	48.99
TiO_2	3.41	3.33	3.37	3.12	3.46	3.08	3.47	3.04	2.97	3.08	3.12	3.20	1.18	1.18	1.13
Al_2O_3	13.48	13.24	13.96	13.63	13.88	13.77	13.87	13.61	13.73	13.60	13.61	13.22	18.81	17.70	18.55
Fe_2O_3	16.01	16.44	14.89	15.46	16.16	14.10	14.34	15.28	15.18	15.09	15.55	16.47	9.16	10.30	9.94
MnO	0.20	0.19	0.19	0.20	0.23	0.25	0.20	0.18	0.18	0.22	0.20	0.22	0.13	0.15	0.13
MgO	5.10	5.15	5.76	5.98	5.55	5.89	5.82	5.16	5.25	5.68	5.98	5.35	6.04	6.16	5.52
CaO	10.07	9.11	10.34	9.02	10.30	10.88	10.70	9.84	10.35	10.59	9.02	9.27	13.24	12.86	13.10
Na_2O	2.50	2.53	2.67	2.24	2.67	2.71	2.73	2.64	2.49	2.62	2.36	2.25	2.20	2.17	2.21
K_2O	0.85	1.24	0.32	0.97	0.38	0.52	0.80	1.41	1.30	0.40	0.97	0.95	0.10	0.21	0.37
P_2O_5	0.48	0.38	0.44	0.22	0.36	0.38	0.38	0.36	0.36	0.36	0.22	0.25	0.10	0.10	0.11
Total	99.73	99.68	99.43	99.74	100.26	99.69	100.35	100.20	100.48	100.42	99.90	100.06	100.02	99.80	100.05
Ignition loss	0.88	0.63	0.82	0.61	0.22	1.84	1.17	0.77	0.99	0.43	0.43	1.43	0.72	0.77	1.01
ppm:															
Nb	23.6	23.4	22.9	23.5	23.7	22.6	22.5	22.6	21.6	23.8	22.6		6.5	6.5	6.9
Zr	265.8	257.8	255.4	262.5	265.1	248.1	245.8	245.7	235.6	257.3	246.3		65.7	65.3	62.0
Y	52.3	44.6	47.9	47.6	46.6	47.0	44.8	44.7	42.2	45.6	36.2		23.8	25.5	24.6
Sr	268.6	258.1	278.9	276.5	283.2	264.7	260.3	248.7	257.8	269.5	190.4		158.3	151.4	152.3
Rb	19.2	33.7	1.9	24.8	2.7	6.6	13.7	42.4	32.4	3.6	17.6		0.8	3.0	6.2
Zn	154.0	145.6	147.4	146.5	148.1	130.1	144.5	132.6	126.5	139.1	179.5		81.2	82.3	77.8
Cu	112.1	115.0	113.6	121.4	125.2	103.0	101.9	85.4	101.6	103.5	194.9		146.3	149.1	121.5
Ni	44.8	31.7	49.7	37.7	44.4	202.7	96.8	59.7	55.1	62.6	56.2		60.2	62.2	48.6
Cr	20.7	21.6	24.8	20.5	21.3	94.0	97.1	96.7	104.3	101.7	105.4		24.2	24.4	24.6
V	418.6	403.1	420.2	410.3	432.9	411.8	381.7	396.4	384.5	386.2	386.0		266.7	271.8	255.3
Ce	56.1	48.8	54.8	51.0	53.6	45.6	51.5	48.0	43.5	50.3	40.2		8.5	11.0	11.4
Ba	117	129	112	132	133	124	119	133	119	146	100		44	43	61

[a] These values represent duplicate measurements taken on this section interval for major elements only.

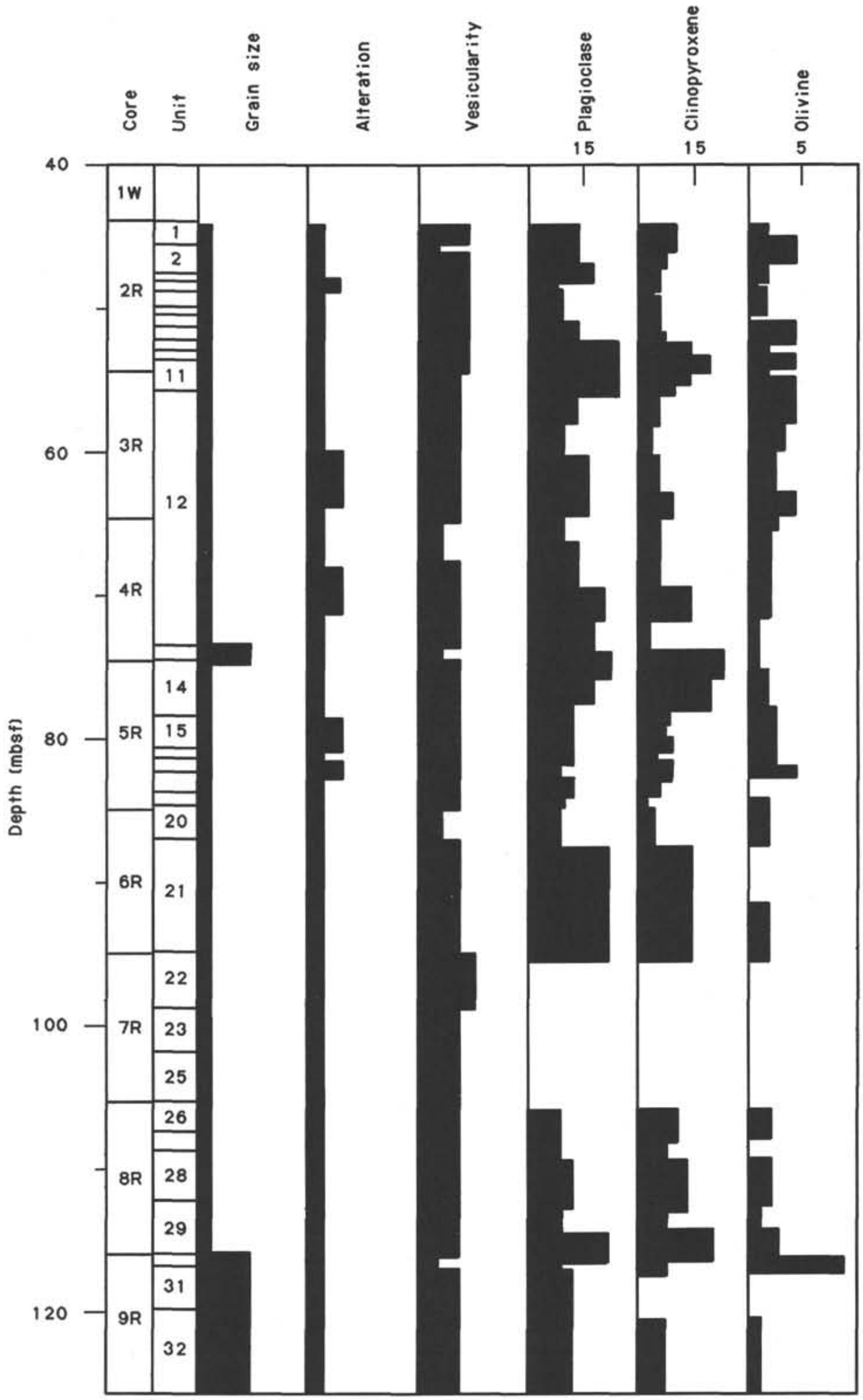

Figure 29. Graphic summary of the petrographic characteristics of basalts from Hole 706C. The first column shows the length of each core (1W, 2R, etc.), and the second column gives the stratigraphic positions and unit numbers. In the third column, grain size is indicated by bar length, with short bars representing fine grains and long bars, medium grains. Alteration is indicated in the fourth column, with a range of 0%–100%. Vesicularity increases from left to right from nonvesicular to highly vesicular. The columns headed plagioclase, clinopyroxene, and olivine refer to the modal percent of plagioclase, augite, and olivine phenocrysts.

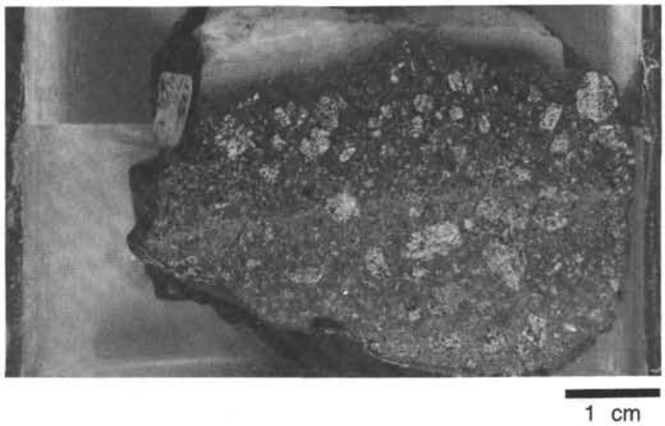

Figure 30. Photograph of the contact between flow Units 31 and 32 showing carbonate that is early Oligocene in age. Note the large feldspar phenocrysts in both units.

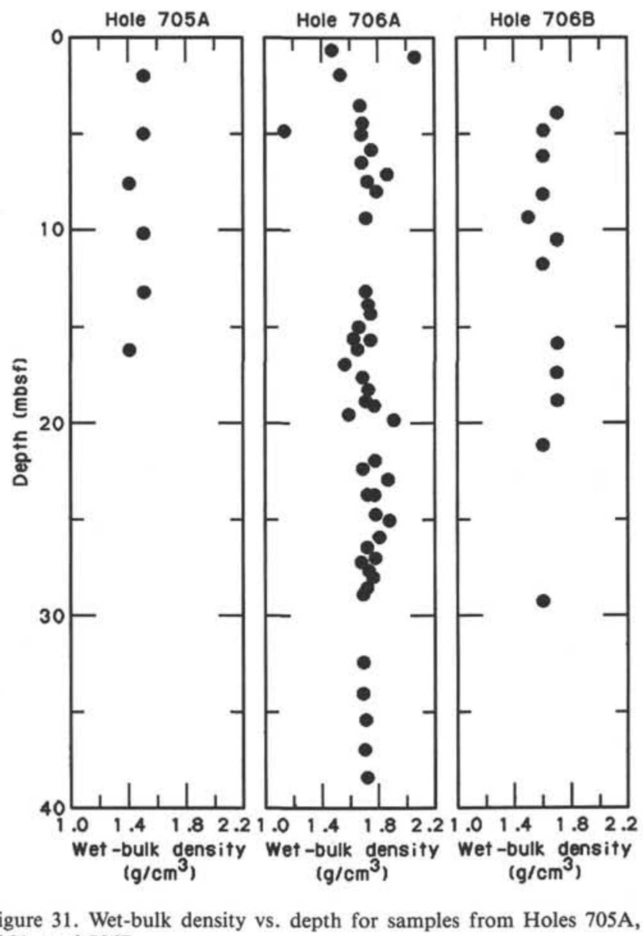

Figure 31. Wet-bulk density vs. depth for samples from Holes 705A, 706A, and 706B.

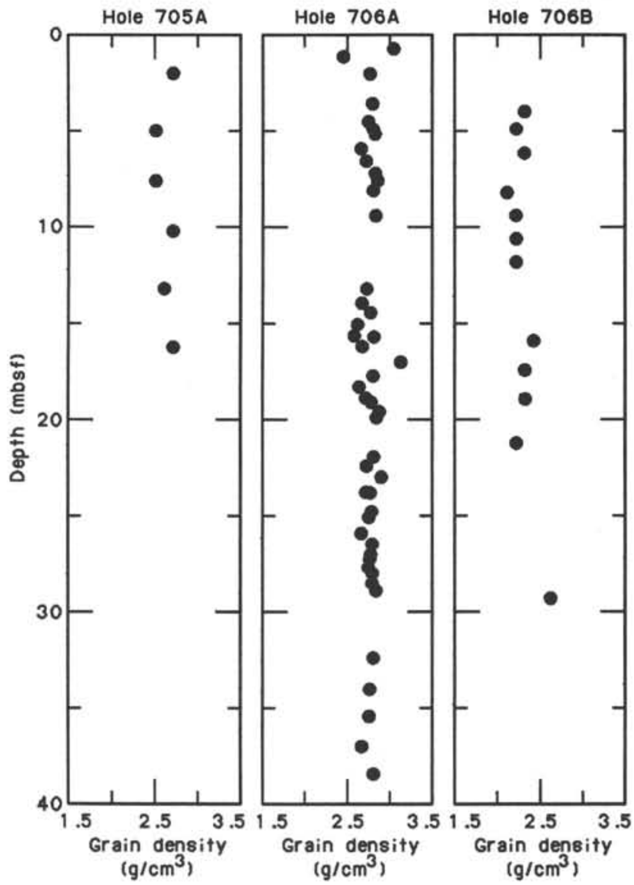

Figure 32. Grain density vs. depth for samples from Holes 705A, 706A, and 706B.

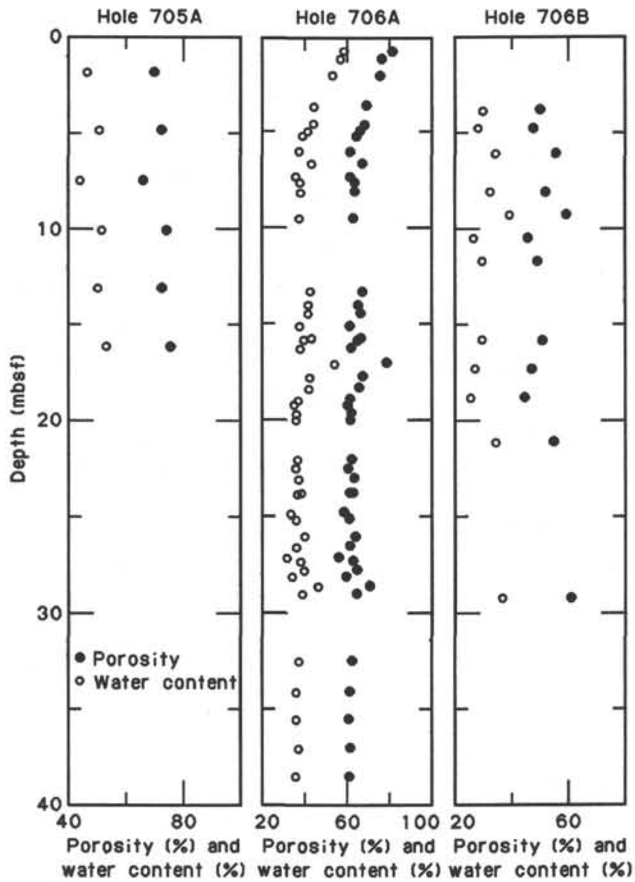

Figure 33. Porosity and water content vs. depth for samples from Holes 705A, 706A, and 706B.

Table 13. Index-properties data, Holes 705A, 706A, and 706B.

Section interval (cm)	Depth (mbsf)	Water content (%)	Porosity (%)	Wet-bulk density (g/cm^3)	Dry-bulk density (g/cm^3)	Grain density (g/cm^3)	Carbonate content (wt%)
115-705A-							
1H-2, 56	2.06	45.93	69.48	1.54	0.83	2.71	94.9
1H-4, 51	5.01	50.12	72.05	1.51	0.75	2.59	92.5
1H-6, 18	7.68	43.45	65.73	1.49	0.84	2.52	91.1
2H-2, 28	10.28	51.20	73.99	1.50	0.73	2.74	94.6
2H-4, 28	13.28	49.71	72.35	1.51	0.76	2.67	94.9
2H-6, 28	16.28	52.74	75.45	1.46	0.69	2.78	83.4
115-706A-							
1H-1, 70	0.70	58.21	80.73	1.47	0.61	3.03	
1H-1, 110	1.10	56.54	75.94	2.06	0.89	2.44	87.8
1H-2, 50	2.00	52.89	75.37	1.53	0.72	2.75	
2H-1, 108	3.58	44.47	68.78	1.67	0.93	2.78	
2H-2, 50	4.50	44.10	68.08	1.69	0.94	2.73	
2H-2, 88	4.88	41.31	66.00	1.13	0.66	2.79	68.0
2H-2, 110	5.10	39.21	64.20	1.68	1.20	2.81	
2H-3, 40	5.90	37.97	61.55	1.75	1.75	2.65	
2H-3, 105	6.55	43.48	67.37	1.68	0.95	2.71	
2H-4, 20	7.20	36.41	61.46	1.86	1.18	2.82	
2H-4, 52	7.52	28.31	63.55	1.72	1.06	2.84	
2H-4, 106	8.06	38.59	63.36	1.79	1.10	2.79	
2H-5, 90	9.40	37.83	62.89	1.71	1.06	2.82	71.7
3H-1, 100	13.20	43.11	67.12	1.71	0.97	2.72	
3H-2, 20	13.90	42.14	65.59	1.73	1.00	2.65	
3H-2, 68	14.38	42.03	66.41	1.74	1.01	2.76	
3H-2, 134	15.04	38.15	61.33	1.66	1.03	2.60	
3H-3, 44	15.64	43.63	66.34	1.62	0.91	2.57	64.1
3H-3, 52	15.72	40.09	64.91	1.74	1.04	2.80	
3H-3, 98	16.18	38.37	62.10	1.65	1.02	2.66	
3H-4, 28	16.98	54.27	78.51	1.56	0.71	3.11	
3H-4, 99	17.69	42.92	67.39	1.69	0.96	2.78	
3H-5, 8	18.28	42.41	65.65	1.73	1.00	2.62	
3H-5, 68	18.88	37.53	61.57	1.71	1.07	2.70	79.2
3H-5, 90	19.10	35.64	60.22	1.77	1.14	2.77	
3H-5, 138	19.58	36.67	62.06	1.59	1.01	2.86	
3H-6, 20	19.90	36.61	61.65	1.91	1.21	2.82	
4H-1, 6	21.96	37.40	62.16	1.78	1.11	2.79	
4H-1, 50	22.40	36.38	60.49	1.69	1.07	2.71	67.3
4H-1, 108	22.98	37.77	63.35	1.87	1.16	2.88	
4H-2, 37	23.77	37.24	61.71	1.77	1.11	2.75	
4H-2, 32	23.72	39.10	63.11	1.72	1.04	2.70	
4H-2, 138	24.78	34.14	58.67	1.78	1.17	2.77	85.3
4H-3, 18	25.08	36.62	61.02	1.88	1.19	2.74	
4H-3, 101,	25.91	40.48	64.00	1.81	1.08	2.65	
4H-4, 8	26.48	36.79	61.52	1.72	1.09	2.78	
4H-4, 63	27.03	32.21	56.44	1.78	1.21	2.76	85.6
4H-4, 83	27.23	38.74	63.19	1.68	1.03	2.75	
4H-4, 130	27.70	40.32	64.56	1.73	1.04	2.73	
4H-5, 12	28.02	34.90	59.50	1.76	1.14	2.78	
4H-5, 64	28.54	46.67	70.67	1.72	0.92	2.78	
4H-5, 102	28.92	39.53	64.56	1.69	1.02	2.82	
5H-1, 93	32.43	37.86	62.63	1.69	1.05	2.79	86.9
5H-2, 105	34.05	36.65	61.12	1.69	1.07	2.75	85.6
5H-3, 94	35.44	36.46	60.82	1.71	1.08	2.74	91.9
5H-4, 98	36.98	37.62	61.22	1.70	1.06	2.65	83.0
5H-5, 93	38.43	36.16	60.94	1.72	1.10	2.79	85.5
115-706B-							
1H-3, 104	4.04	30.07	49.60	1.70	1.19	2.32	69.7
1H-4, 41	4.91	28.63	47.20	1.67	1.19	2.26	72.2
2H-1, 53	6.23	34.42	54.91	1.63	1.07	2.35	68.6
2H-2, 103	8.23	32.88	51.39	1.60	1.08	2.18	62.2
2H-3, 71	9.41	39.30	58.80	1.53	0.93	2.23	65.1
2H-4, 47	10.67	27.20	45.32	1.71	1.24	2.25	64.7
2H-5, 16	11.86	29.91	48.69	1.67	1.17	2.25	59.1
3H-3, 23	15.93	29.82	50.63	1.73	1.21	2.45	71.6
3H-4, 28	17.48	27.48	46.77	1.75	1.27	2.35	71.0
3H-5, 22	18.92	25.92	44.42	1.76	1.30	2.31	70.0
4H-1, 66	21.26	34.65	54.60	1.62	1.06	2.29	68.8
6X-2, 70	29.30	36.79	60.18	1.66	1.05	2.63	75.5

Table 14. Shear-wave velocity data, Holes 705A, 706A, and 706B.

Section interval (cm)	Depth (mbsf)	V_s (m/s)
115-705A-		
1H-2, 49	1.99	85
1H-4, 56	5.06	75
115-706A-		
3H-3, 44	15.64	275
4H-4, 24	26.64	205
115-706B-		
2H-4, 41	10.61	180
3H-4, 26	17.46	219
3H-5, 24	18.94	298
4H-1, 67	21.27	270
6H-2, 72	29.32	262

Table 15. Thermal conductivity data, Holes 705A, 706A, and 706B.

Section interval (cm)	Depth (mbsf)	Thermal conductivity ($W \cdot m^{-1} \cdot K^{-1}$)
115-705A-		
1H-2, 40	1.9	1.152
2H-4, 85	13.8	1.021
115-706A-		
2H-2, 75	5.3	1.177
2H-4, 75	8.3	1.368
3H-4, 85	17.5	1.030
3H-6, 34	20.0	1.376
4H-2, 40	23.8	1.337
4H-4, 40	26.8	1.568
5H-2, 40	33.4	1.522
5H-4, 40	36.4	1.400
6H-2, 40	43.0	1.219
115-706B-		
1H-2, 40	1.9	0.966
1H-4, 40	4.9	1.188
2H-2, 40	7.6	1.187
2H-4, 40	10.6	1.206
3H-2, 40	14.6	2.086
3H-4, 40	17.6	1.480
5X-2, 110	25.0	0.958
6X-2, 80	29.4	1.379

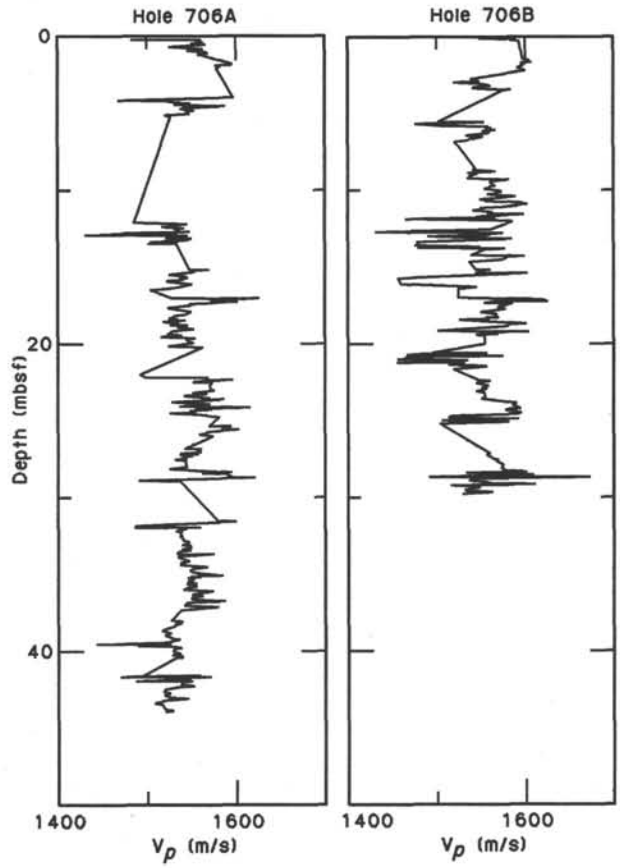

Figure 34. Compressional-wave velocity vs. depth at Holes 706A and 706B.

Table 16. Discrete compressional-wave velocity data, Hole 706A.

Section interval (cm)	Depth (mbsf)	V_p (m/s)
115-706A-		
2H-2, 110–112	5.10	1566
3H-3, 134–136	16.54	1556
3H-3, 98–100	16.18	1550
3H-5, 90–92	19.10	1542
3H-5, 138–140	19.58	1551
3H-6, 20–22	19.90	1593
4H-4, 8–10	26.48	1587
4H-4, 83–85	27.23	1548
4H-5, 12–14	28.02	1550
4H-5, 103–105	28.93	1580

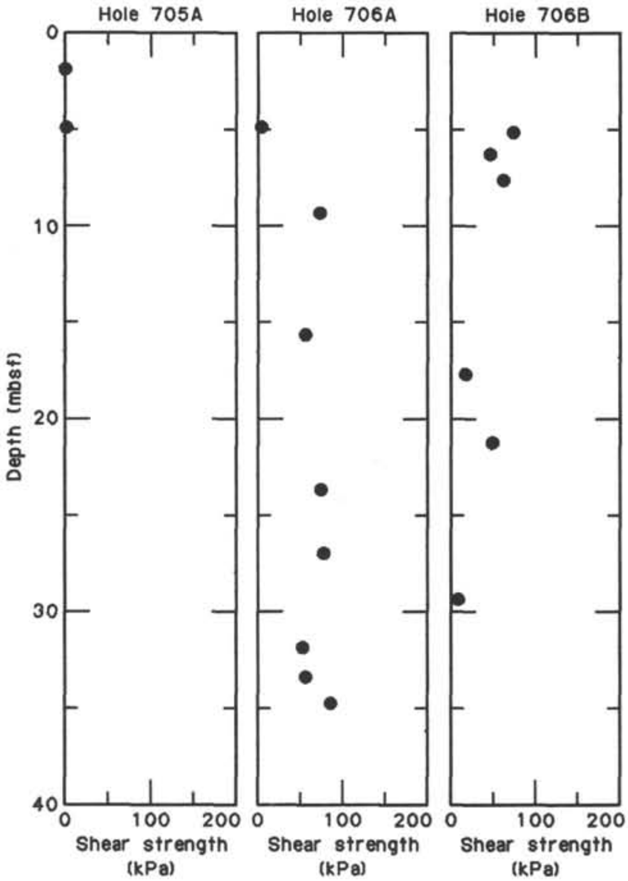

Figure 35. Shear strength vs. depth at Holes 705A, 706A, and 706B.

Table 17. Motorized shear strength data, Holes 706A and 706B.

Section interval (cm)	Depth (mbsf)	Peak (kPa)
115-706A-		
2H-2, 95	4.95	104.0
2H-5, 90	9.40	172.6
3H-3, 50	15.70	55.5
4H-2, 26	23.66	73.3
4H-4, 57	26.97	76.8
5H-1, 38	31.88	52.0
5H-2, 36	33.36	55.5
5H-3, 32	34.82	85.1
115-706B-		
1H-4, 70	5.20	74.7
1H-6, 32	6.32	47.3
2H-2, 45	7.65	62.8
3H-4, 50	17.70	118.6
4H-1, 62	21.22	49.7
6X-2, 73	29.33	9.4

Table 18. Compressional-wave velocity, wet-bulk density, and acoustic impedance data for basement rocks in Hole 706C.

Section interval (cm)	V_p (m/s)	Wet-bulk density (g/cm^3)	Acoustic impedance ($g/cm^2 \cdot s \cdot 10^5$)
115-706C-			
2R-1, 105	3378	2.33	7.87
3R-1, 83	3298	2.17	7.16
4R-2, 10	3868	2.33	9.01
5R-3, 14	3018	2.43	7.33
6R-1, 104	3958	2.53	10.01
8R-1, 41	3827	2.63	10.06

Table 19. Thermal conductivity data for basement rocks in Hole 706C.

Section interval (cm)	Depth (mbsf)	Thermal conductivity ($W \cdot m^{-1} \cdot K^{-1}$)
115-706C-		
3R-2, 14	55.5	1.38
6R-1, 134	84.2	1.30

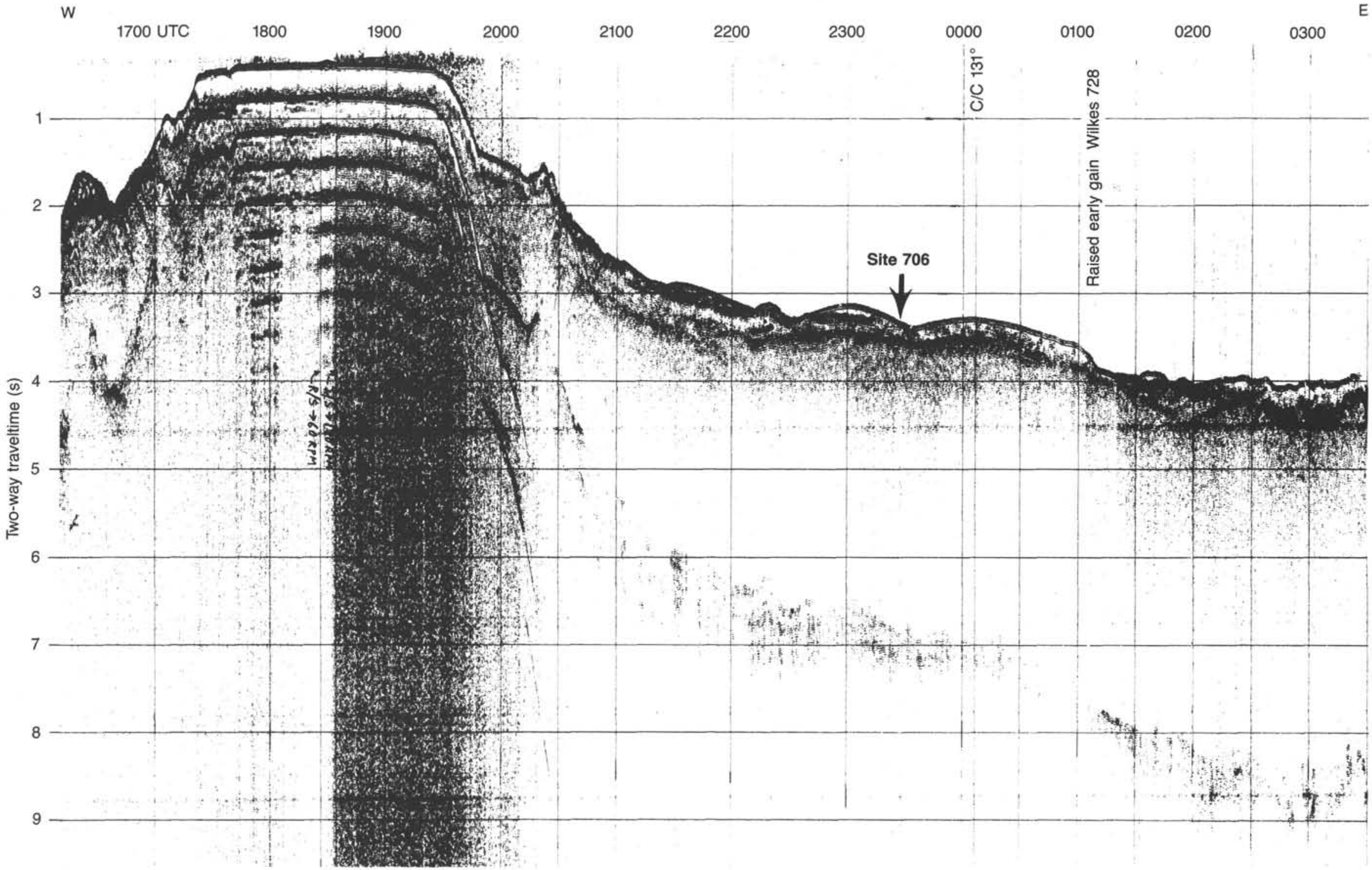

Figure 36. West-to-east, single-channel seismic (SCS) profile of the Mascarene Plateau at latitude 13°S (*Wilkes* 728, 27 August 1977). Thick, high-velocity carbonates over the central plateau produce a characteristic reverberation. The approximate position of Site 706 (slightly south of this profile) is shown.

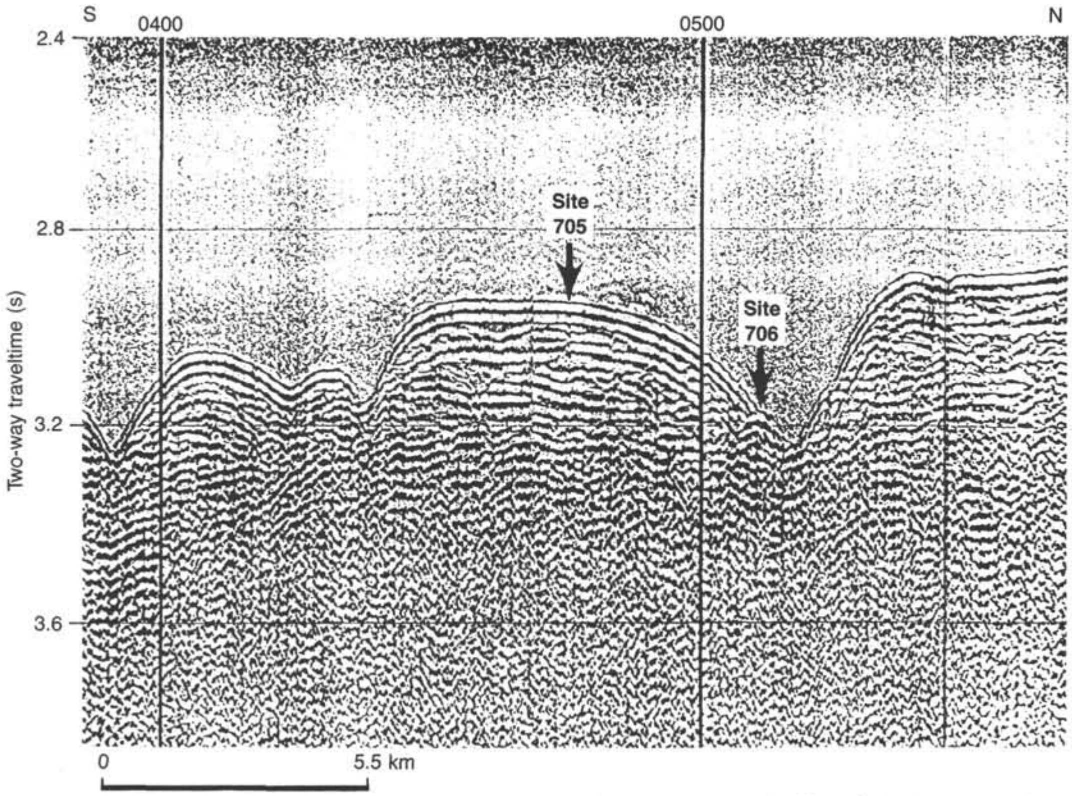

Figure 37. South-to-north, single-channel seismic (SCS) profile on the eastern shoulder of the Mascarene Plateau (*Charles Darwin* 21/87, 15 March 1987). This terrain is a pelagic apron cut by west-to-east canyons which carry mass flows from the eastern slopes of the plateau. The location of Sites 705 (in the center of one sediment lobe) and 706 (near one canyon floor) are shown.

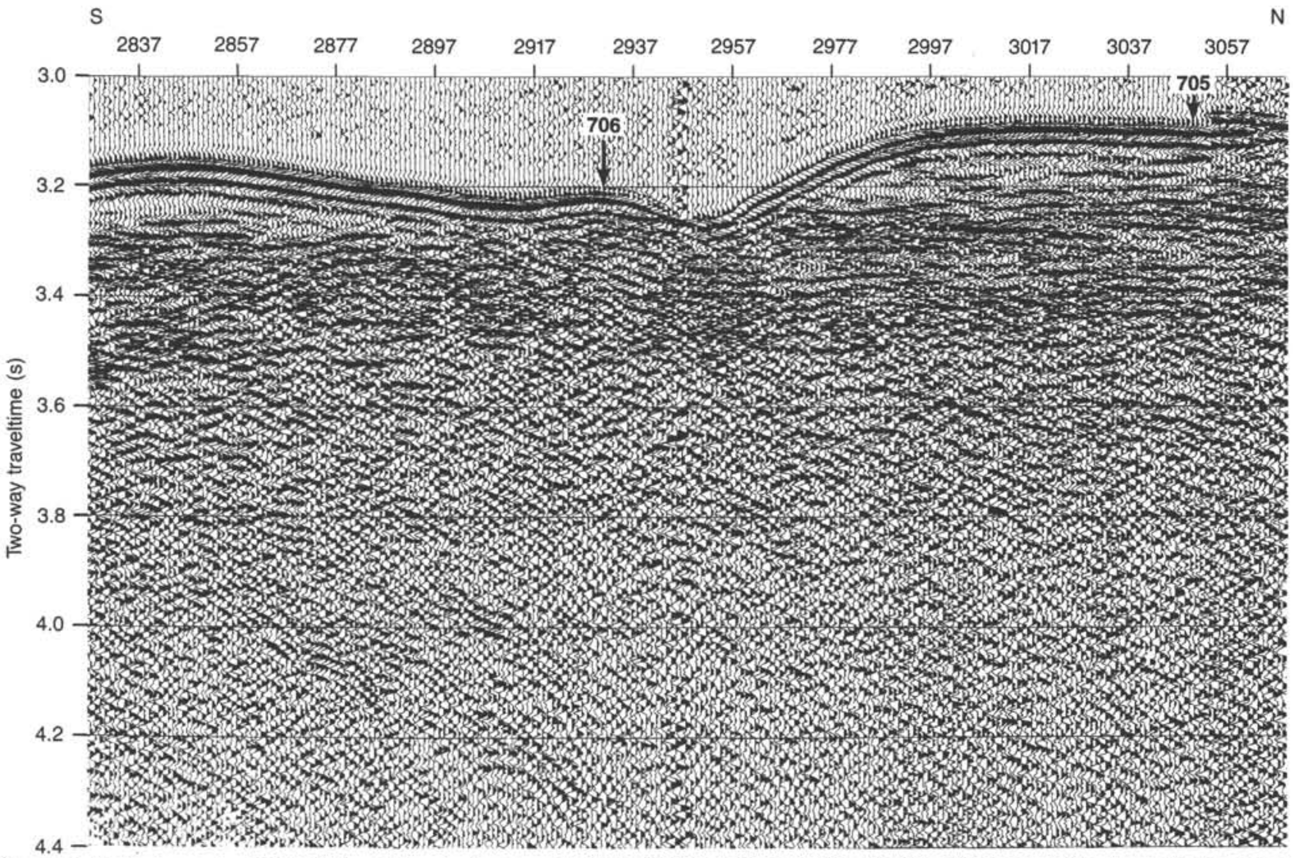

Figure 38. South-to-north, *JOIDES Resolution* single-channel seismic (SCS) profile over Site 705 (Site 706 lies 3 nmi to the north in a canyon similar to the position labeled [706]). Transparent foraminiferal sands overlie more reflective nannofossil oozes and highly reflective lava flows.

SITE 705 HOLE A CORE 1H CORED INTERVAL 2307.5-2316.0 mbsl; 0.0-8.5 mbsf

TIME-ROCK UNIT	FORAMINIFERS	NANNOFOSSILS	RADIOLARIANS	DIATOMS	PALEOMAGNETICS	PHYS. PROPERTIES	CHEMISTRY	SECTION	METERS	GRAPHIC LITHOLOGY	DRILLING DISTURB.	SED. STRUCTURES	SAMPLES
PLEISTOCENE	N 22	CN 15 (NN 21) AG; CN 14b (NN 20); CN 14a (NN 19)	Barren	Barren				1, 2, 3, 4, 5, 6	0.5, 1.0				*, *, IW, *, *
	AG	AM						CC					

BIOSTRAT. ZONE/ FOSSIL CHARACTER

LITHOLOGIC DESCRIPTION

FORAMINIFERAL OOZE and NANNOFOSSIL-BEARING FORAMINIFERAL OOZE

Major lithologies: Foraminiferal ooze (Sections 1 and 2, and Section 3, 0-45 cm) and nannofossil-bearing foraminiferal ooze (Section 3, 45-150 cm, and Sections 4-6), whitish orange to pale brown (10YR 8/2, 8/4, 7/3).

Minor lithologies:
a. Nannofossil foraminiferal ooze, white (10YR 8/1), Section 4, 140-145 cm.
b. Pteropods and pteropod fragments in Section 1.

Usually no visible structures except for some possible burrows.

SMEAR SLIDE SUMMARY (%):

	3, 30 D	3, 100 D	Z4, 144 M	5, 130 D
TEXTURE:				
Sand	95	90	50	80
Silt	4	8	45	16
Clay	1	2	5	4
COMPOSITION:				
Foraminifers	95	90	50	80
Nannofossils	5	10	50	20
Fish remains	—	—	Tr	Tr
Calcareous sponge spicules	—	—	Tr	—

Information on Core Description Forms, for ALL sites, represents field notes taken aboard ship. Some of this information has been refined in accord with post-cruise findings, but production schedules prohibit definitive correlation of these forms with subsequent findings. Thus the reader should be alerted to the occasional ambiguity or discrepancy.

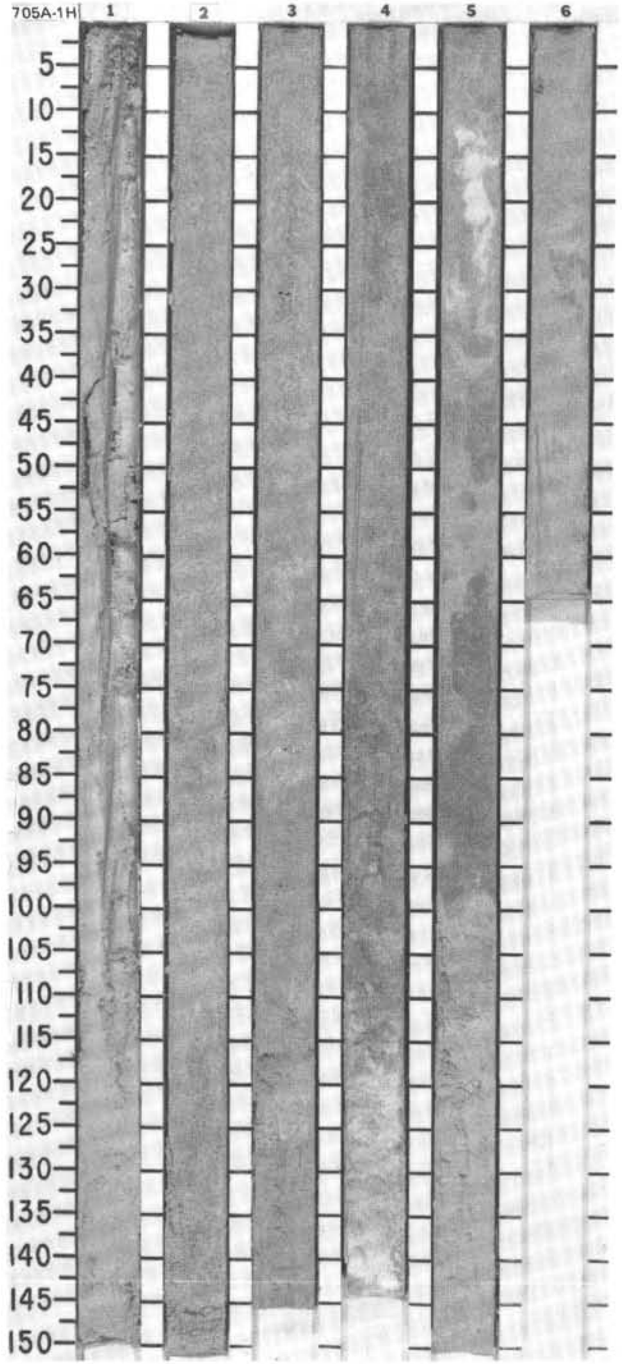

SITE 705 HOLE A CORE 2H CORED INTERVAL 2316.0-2325.5 mbsl; 8.5-18.0 mbsf

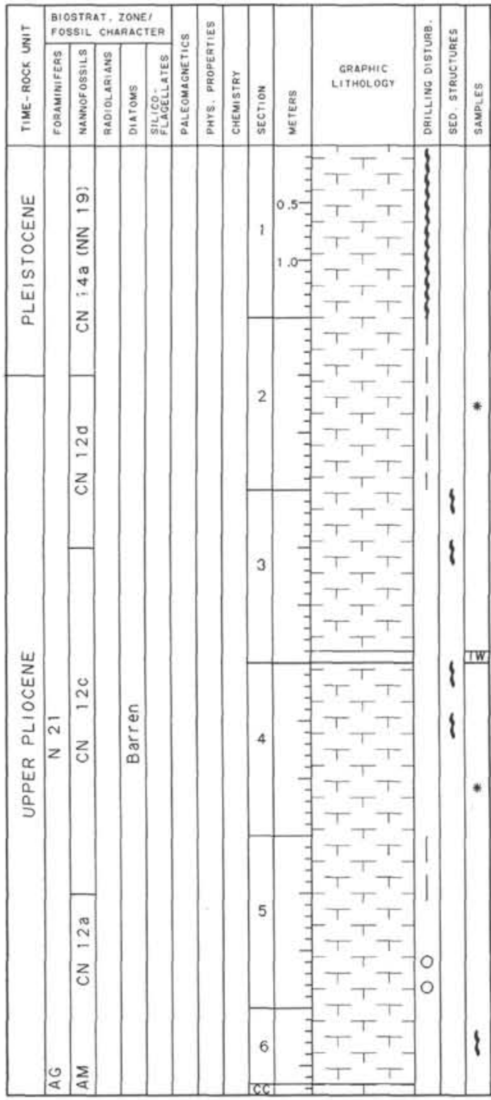

LITHOLOGIC DESCRIPTION

NANNOFOSSIL-BEARING FORAMINIFERAL OOZE

Major lithology: Nannofossil-bearing foraminiferal ooze, pale brown (10YR 8/3, 7/3), slightly mottled.

SMEAR SLIDE SUMMARY (%):

	2, 75 D	4, 100 D
TEXTURE:		
Sand	80	80
Silt	20	20
COMPOSITION:		
Foraminifers	80	80
Nannofossils	20	20

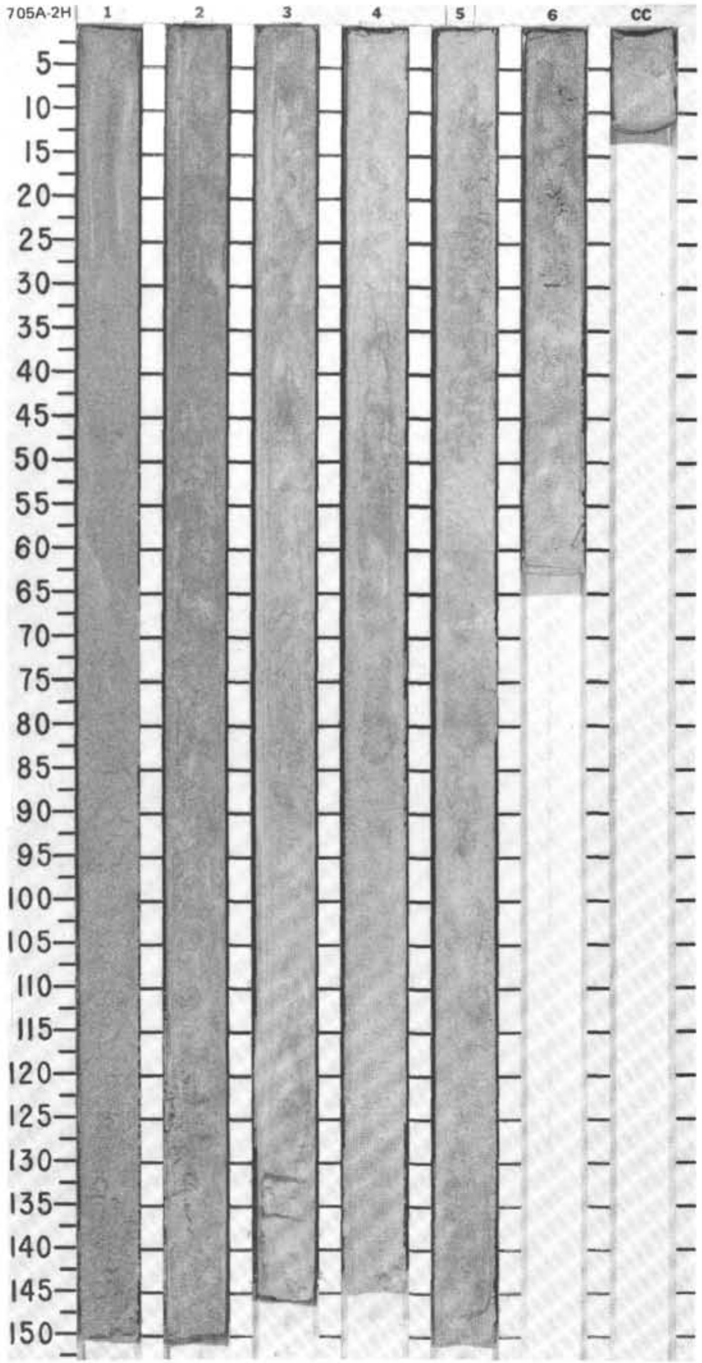

SITE 705 HOLE A CORE 3H CORED INTERVAL 2325.0-2335.0 mbsl; 18.0-27.5 mbsf

TIME-ROCK UNIT	BIOSTRAT. ZONE/ FOSSIL CHARACTER: FORAMINIFERS	NANNOFOSSILS	RADIOLARIANS	DIATOMS		PALEOMAGNETICS	PHYS. PROPERTIES	CHEMISTRY	SECTION	METERS	GRAPHIC LITHOLOGY	DRILLING DISTURB.	SED. STRUCTURES	SAMPLES	LITHOLOGIC DESCRIPTION
UPPER PLIOCENE	N 19 / AG	CN 12a / AM	Barren	Barren					1	0.5, 1.0					NANNOFOSSIL-BEARING FORAMINIFERAL OOZE Major lithology: Nannofossil-bearing foraminiferal ooze, pale brown (10YR 7/3).
									2						

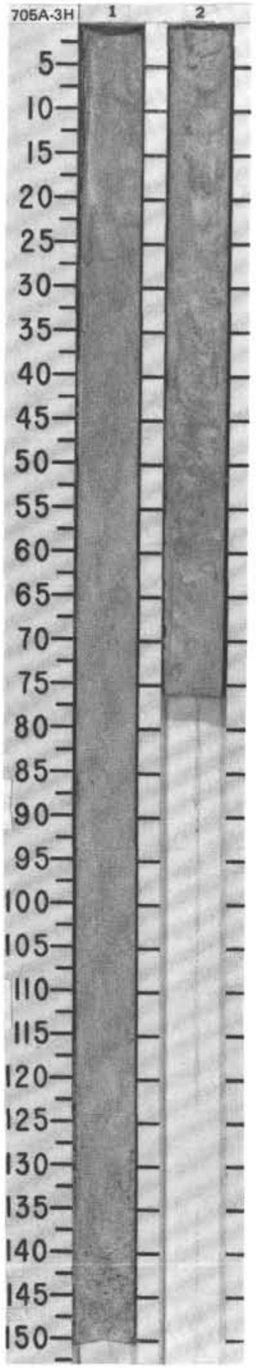

SITE 706 HOLE A CORE 1H CORED INTERVAL 2506.5-2509.0 mbsl; 0.0-2.5 mbsf

TIME-ROCK UNIT	BIOSTRAT. ZONE/FOSSIL CHARACTER: FORAMINIFERS	NANNOFOSSILS	RADIOLARIANS	DIATOMS	PALEOMAGNETICS	PHYS. PROPERTIES	CHEMISTRY	SECTION	METERS	GRAPHIC LITHOLOGY	DRILLING DISTURB.	SED. STRUCTURES	SAMPLES
UPPER PLEISTOCENE	AG N 23-N 22	CM AG CN 15 (NN 21)	Barren	Barren				1, 2, CC	0.5, 1.0				*

LITHOLOGIC DESCRIPTION

FORAMINIFERAL OOZE

Major lithology: Foraminiferal ooze, light gray to yellowish tan (10YR 7/2, 8/2, 2.5Y 7/2), homogenous, medium to coarse grained between 0-138 cm in Section 1, and coarse grained between 138-150 cm in Section 1.

Minor lithology: Pteropods and pteropod fragments scattered throughout.

SMEAR SLIDE SUMMARY (%):

	1, 90 D	2, 70 D
TEXTURE:		
Sand	95	95
Silt	4	4
Clay	1	1
COMPOSITION:		
Foraminifers	95	98
Nannofossils	5	2

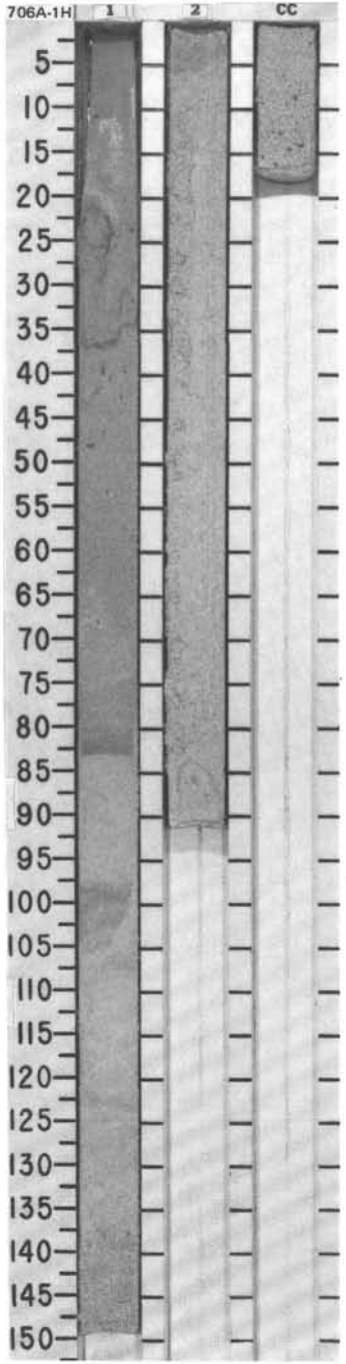

SITE 706 HOLE A CORE 2H CORED INTERVAL 2509.0-2518.7 mbsl; 2.5-12.2 mbsf

TIME-ROCK UNIT	BIOSTRAT. ZONE/FOSSIL CHARACTER: FORAMINIFERS	NANNOFOSSILS	RADIOLARIANS	DIATOMS	PALEOMAGNETICS	PHYS. PROPERTIES	CHEMISTRY	SECTION	METERS	GRAPHIC LITHOLOGY	DRILLING DISTURB.	SED. STRUCTURES	SAMPLES
PLEISTOCENE		CM CN 15						1	0.5, 1.0		O O O O		
LOWER OLIGOCENE	P 19	CP 18 (NP 23)	Barren	Barren				2, 3, 4, 5			⌇		#, *, *, *, *, *, IW
	AG	AM						CC					*

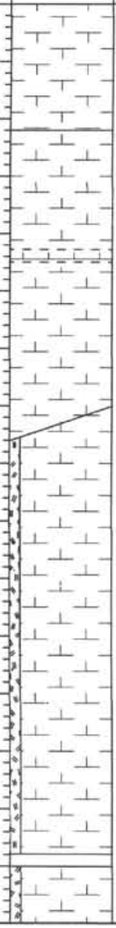

LITHOLOGIC DESCRIPTION

FORAMINIFERAL OOZE, NANNOFOSSIL OOZE, and NANNOFOSSIL OOZE WITH VOLCANIC ASH LAYERS

Major lithologies:

a. Foraminiferal ooze, yellowish tan (2.5Y 7/2), homogeneous, coarse-grained, with pteropods and pteropod fragments in Section 1 and Section 2, 0-9 cm. Large (2 cm) piece of limestone at the base of ooze.

Unconformity in Section 2, 9 cm.

b. Nannofossil ooze, below the unconformity, pale yellow (2.5Y 7/4) with a 3-cm-thick light yellowish brown (2.5YR 5/4) to brown (7.5YR 5/4) layer, distinguishable only by color change, and a 4-cm-thick nodular, well-indurated (chalk?) layer.

Angular (erosional) unconformity in Section 3, 75 cm.

Nannofossil ooze, pale yellow (2.5Y 7/4, oxidizing conditions), down to Section 4, 40 cm; and below is nannofossil ooze, greenish gray (5GY 6/1), with interbedded dark greenish gray (5G 4/1) to greenish gray (5GY 6/1) and black (10YR 2/1) ash layers.

Ash layers make up 10-15% of the core, and are rich in pyrite, feldspar, pyroxene, and glass. Unaltered ash layers in Section 3, 148-150 cm, Section 5, 124-126 cm, and CC, 30-32 cm.

SMEAR SLIDE SUMMARY (%):

	2, 18	2, 15	3, 148	4, 100	5, 125	5, 135	CC, 31
	M	D	M	D	M	D	M
TEXTURE:							
Sand	—	—	—	—	—	—	15
Silt	—	—	100	—	100	—	—
Clay	—	100	—	100	—	100	85
COMPOSITION:							
Quartz	—	—	—	—	—	—	5
Feldspar	—	—	—	—	—	—	5
Clay	—	—	—	1	—	Tr	—
Volcanic glass	—	—	60	—	70	—	10
Accessory minerals:							
Pyrite	—	—	40	—	30	—	10
Foraminifers	39	—	—	Tr	—	—	5
Nannofossils	—	100	—	98	—	100	65
Sponge spicules	—	Tr	—	1	—	—	—
Bioclasts	15	—	—	—	—	—	—
Red Algae	20	—	—	—	—	—	—
Bryozoans	10	—	—	—	—	—	—
Echinoderm fragments	3	—	—	—	—	—	—
Spar Cement	12	—	—	—	—	—	—
Micrite	5	—	—	—	—	—	—

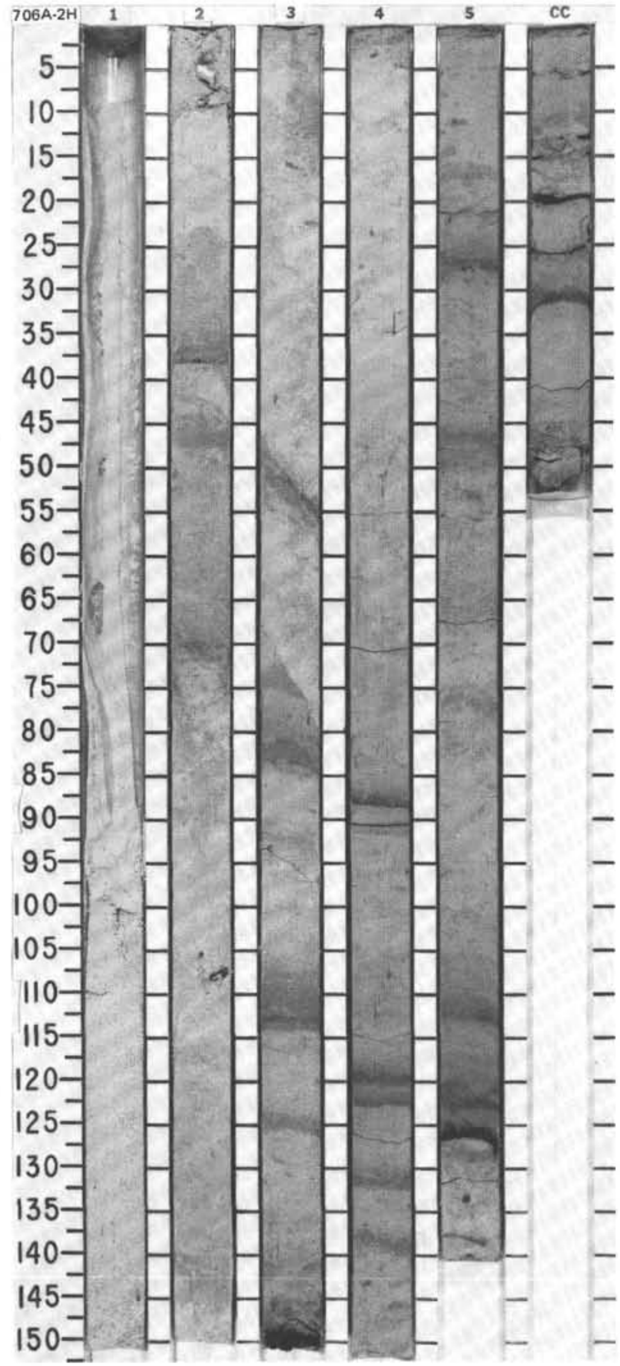

SITE 706 HOLE A CORE 3H CORED INTERVAL 2518.7-2528.4 mbsl; 12.2-21.9 mbsf

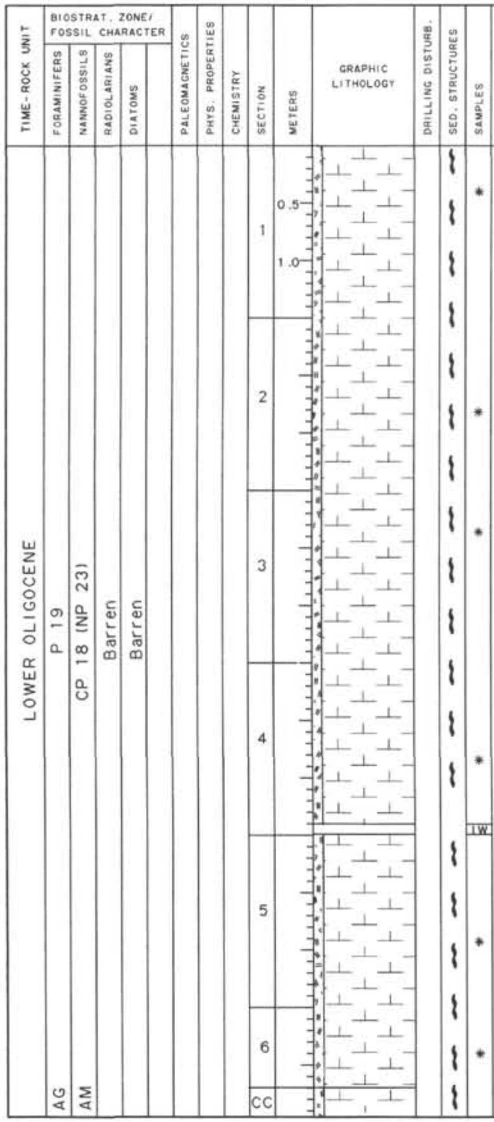

LITHOLOGIC DESCRIPTION

NANNOFOSSIL OOZE with VOLCANIC ASH LAYERS

Major lithology: Nannofossil ooze, greenish gray (5GY 6/1) in Sections 1-3, to light greenish gray (5G 7/1, 5GY 7/1) in Sections 4-6, with numerous interbedded dark greenish gray (5G 4/1), dark greenish gray (10YR 3/1), and dark gray (N4) volcanic ash layers averaging 2-4 cm in thickness.

Ash layers make up an estimated 10-15% of the core, based on the ash concentrations related to their original thickness and bioturbation. Ash layers are rich in pyrite, feldspar, pyroxene, and angular glass fragments. Most of the ash layers are highly altered, except for a fresh ash layer in Section 6, 50-52 cm.

SMEAR SLIDE SUMMARY (%):

	1, 46 M	2, 80 D	3, 38 D	4, 80 D	5, 90 D	6, 40 M
TEXTURE:						
Sand	—	—	—	—	5	5
Silt	5	—	30	—	5	5
Clay	95	100	70	100	90	90
COMPOSITION:						
Feldspar	Tr	—	—	—	—	—
Volcanic glass	10	—	5	—	—	Tr
Accessory minerals:						
Pyrite	—	—	5	—	Tr	—
Foraminifers	5	—	30	—	5	10
Nannofossils	85	100	60	100	95	90

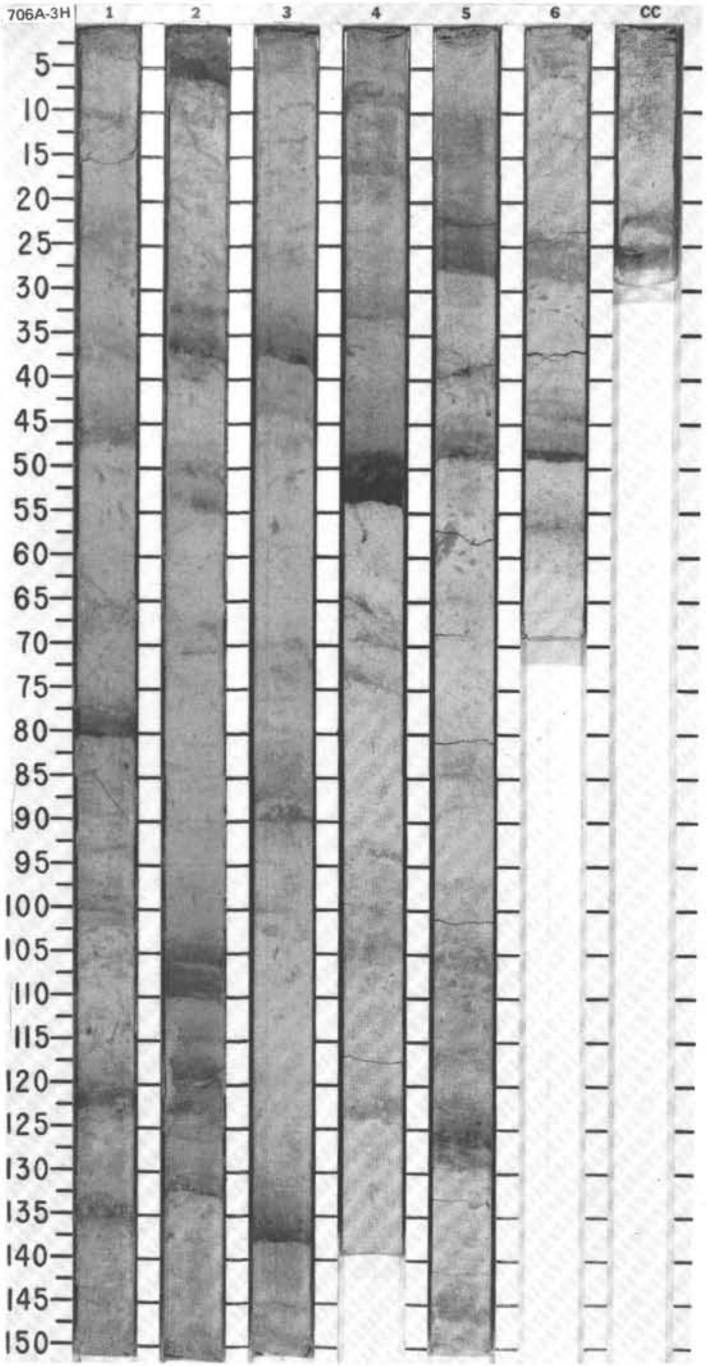

SITE 706 HOLE A CORE 4H CORED INTERVAL 2528.4-2538.0 mbsl; 21.9-31.5 mbsf

TIME-ROCK UNIT	FORAMINIFERS	NANNOFOSSILS	RADIOLARIANS	DIATOMS	PALEOMAGNETICS	PHYS. PROPERTIES	CHEMISTRY	SECTION	METERS	GRAPHIC LITHOLOGY	DRILLING DISTURB.	SED. STRUCTURES	SAMPLES
LOWER OLIGOCENE	P 19	CP 18 (NP 23)	Barren	Barren				1	0.5, 1.0				
								2					*
								3					OG, IW
								4					*, IW
								5					
	AG	AM						CC					

(BIOSTRAT. ZONE/ FOSSIL CHARACTER spans FORAMINIFERS, NANNOFOSSILS, RADIOLARIANS, DIATOMS.)

LITHOLOGIC DESCRIPTION

NANNOFOSSIL OOZE and NANNOFOSSIL CHALK, with VOLCANIC ASH LAYERS

Major lithology: Light greenish gray (5GY 7/1) nannofossil ooze and nannofossil chalk, with interbedded greenish gray (5GY 5/1, 6/1) altered ash layers, and unaltered, dark gray (N4) grading upward to greenish gray (5GY 5/1), distinct ash layers. General bioturbation throughout results in a mottled aspect. Some 2-5 cm thick harder chalk layers.

Unaltered, distinct ash layers in Section 1, 56-57 and 105-106 cm; Section 2, 66-67 cm; Section 3, 7-10 cm; and Section 5, 50-52 cm. Some of the layers show microfaulting.

SMEAR SLIDE SUMMARY (%):

	2, 65 M	4, 62 D
TEXTURE:		
Sand	45	5
Silt	50	5
Clay	5	90
COMPOSITION:		
Feldspar	Tr	—
Volcanic glass	90	—
Accessory minerals:		
Barite	Tr	—
Pyrite	5	—
Micrite	—	Tr
Foraminifers	Tr	10
Nannofossils	5	90

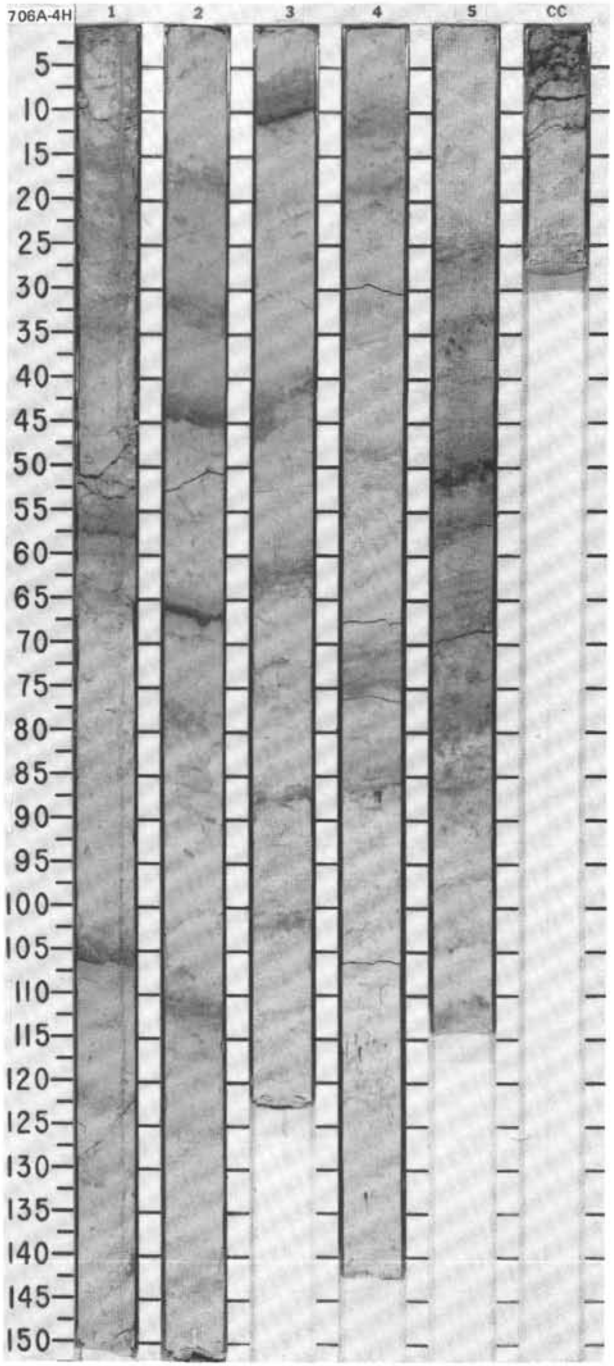

SITE 706 HOLE A CORE 5H CORED INTERVAL 2538.0-2547.6 mbsl; 31.5-41.1 mbsf

TIME-ROCK UNIT	FORAMINIFERS	NANNOFOSSILS	RADIOLARIANS	DIATOMS	PALEOMAGNETICS	PHYS. PROPERTIES	CHEMISTRY	SECTION	METERS	GRAPHIC LITHOLOGY	DRILLING DISTURB.	SED. STRUCTURES	SAMPLES
LOWER OLIGOCENE	P 19	CP 18 (NP 23)	Barren	Barren	Reversed			1, 2, 3, 4, 5, 6, CC	0.5, 1.0				*, *, IW, *
	AG	AM											

LITHOLOGIC DESCRIPTION

NANNOFOSSIL CHALK with VOLCANIC ASH LAYERS

Major lithology: Nannofossil chalk, light greenish gray (5GY 7/1), with interbedded (5-15% of core) pale green (5G 6/2) altered, indistinct volcanic ash layers, and black (N2) unaltered, distinct ash layers. Ash layers average 2-5 cm thick.

Mottled aspect due to bioturbation.

Unaltered, distinct ash layer at Section 3, 52-54 cm.

SMEAR SLIDE SUMMARY (%):

	3, 52 M	4, 14 D	5, 114 D
TEXTURE:			
Sand	30	5	5
Silt	45	—	5
Clay	25	95	90
COMPOSITION:			
Quartz	—	—	Tr
Feldspar	—	Tr	Tr
Volcanic glass	—	Tr	—
Accessory minerals:			
Pyrite	Tr	Tr	—
Zeolites	—	—	5
Foraminifers	5	5	5
Nannofossils	95	95	90

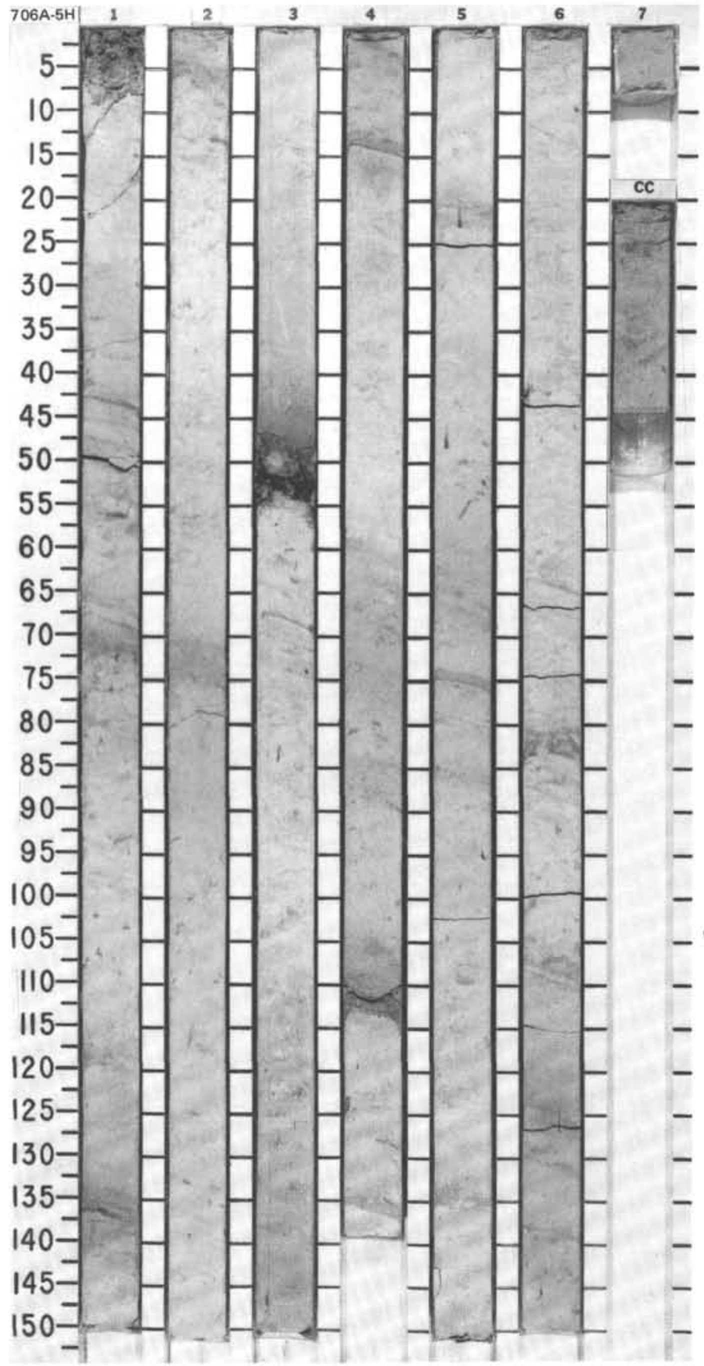

SITE 706 HOLE A CORE 6H CORED INTERVAL 2547.6-2551.0 mbsl; 41.1-47.5 mbsf

TIME-ROCK UNIT	FORAMINIFERS	NANNOFOSSILS	RADIOLARIANS	DIATOMS	PALEOMAGNETICS	PHYS. PROPERTIES	CHEMISTRY	SECTION	METERS	GRAPHIC LITHOLOGY	DRILLING DISTURB.	SED. STRUCTURES	SAMPLES
LOWER OLIGOCENE	AG P 19	AG CP 18 (NP 23)	Barren	Barren	Reversed			1	0.5, 1.0	VOID			*
								2					
								3					IW
								CC					*

LITHOLOGIC DESCRIPTION

NANNOFOSSIL CHALK with VOLCANIC ASH LAYERS

Major lithology: Nannofossil chalk, light greenish gray (5Y 7/1), with interbedded, indistinct pale green (5G 6/2, 7/2) and greenish gray (5G 5/1) altered volcanic ash layers, averaging 2-5 cm in thickness and making up 5-10% of the core.

General mottled aspect due to bioturbation.

A piece of fresh basalt was recovered from the CC.

SMEAR SLIDE SUMMARY (%):

	1, 66 D	CC, 3 M
TEXTURE:		
Sand	5	5
Silt	—	25
Clay	95	70
COMPOSITION:		
Clay	—	40
Volcanic glass	Tr	50
Accessory minerals:		
Zeolites	Tr	—
Pyrite	—	Tr
Foraminifers	5	5
Nannofossils	95	5
Sponge spicules	Tr	—

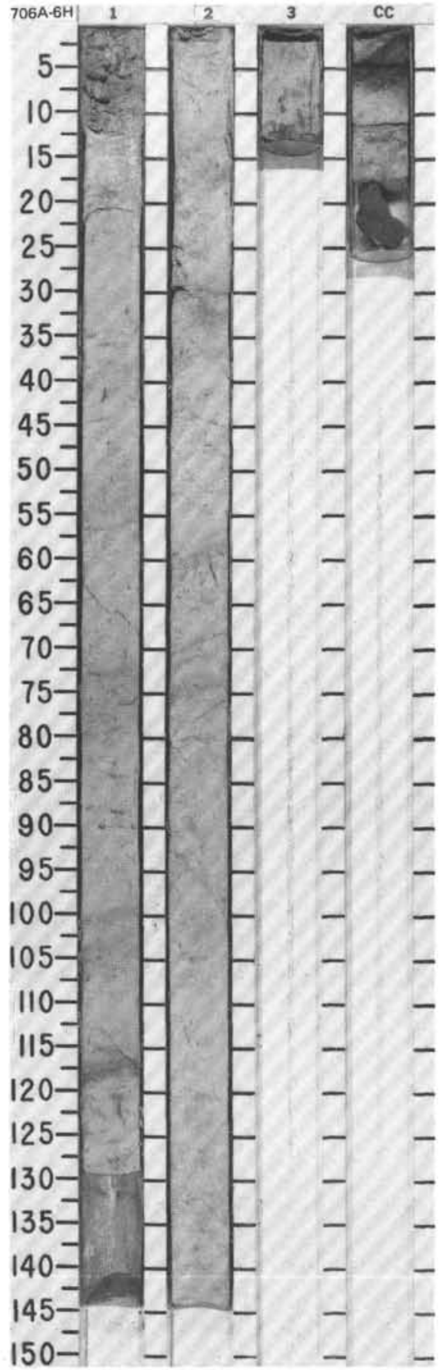

SITE 706 HOLE B CORE 1H CORED INTERVAL 2497.3-2503.0 mbsl; 0.0-5.7 mbsf

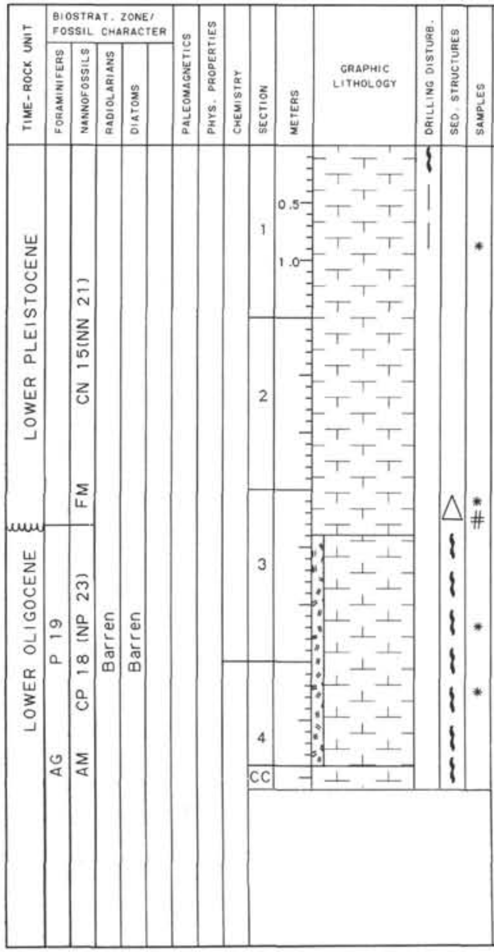

LITHOLOGIC DESCRIPTION

FORAMINIFERAL OOZE and NANNOFOSSIL OOZE, with VOLCANIC ASH LAYERS

Major lithology:

a. Foraminiferal ooze, white to very pale brown (10YR 8/2, 8/3), homogeneous, winnowed, and medium to coarse grained. Foraminifer ooze is slightly coarser toward its base (Section 3, 30 cm), with a few limestone (shallow water) cobbles, and a nannofossil ooze clast (possible drilling disturbance) from the underlying unit. Pteropods and pteropod fragments scattered throughout, along with echinoid spines(?). Unconformity at Section 3, 30 cm (sharp contact).

b. Nannofossil ooze, pale yellow (2.5Y 7/4, oxidized conditions), interbedded with several few-cm-thick, indistinct light yellowish brown (2.5Y 6/4) volcanic ash layers. Ash layers are rich in pyrite, feldspar, pyroxene, and glass.

SMEAR SLIDE SUMMARY (%):

	1, 85 D	3, 8 M	3, 20 M	3, 115 D	4, 12 D
TEXTURE:					
Sand	95	25		5	10
Clay	5	75		95	90
COMPOSITION:					
Feldspar	—	5	—	—	2
Clay	—	70	—	—	—
Volcanic glass	3	5	—	—	3
Calcite/dolomite	—	15	—	—	—
Foraminifers	95	—	—	5	5
Nannofossils	Tr	50	5	95	95
Radiolarians	1	—	—	—	—
Silicoflagellates	1	—	—	—	—
Bioclasts	—	—	10	—	—
Echinoderm fragments	—	—	2	—	—
Spar cement	—	—	3	—	—
Micrite	—	—	35	—	—

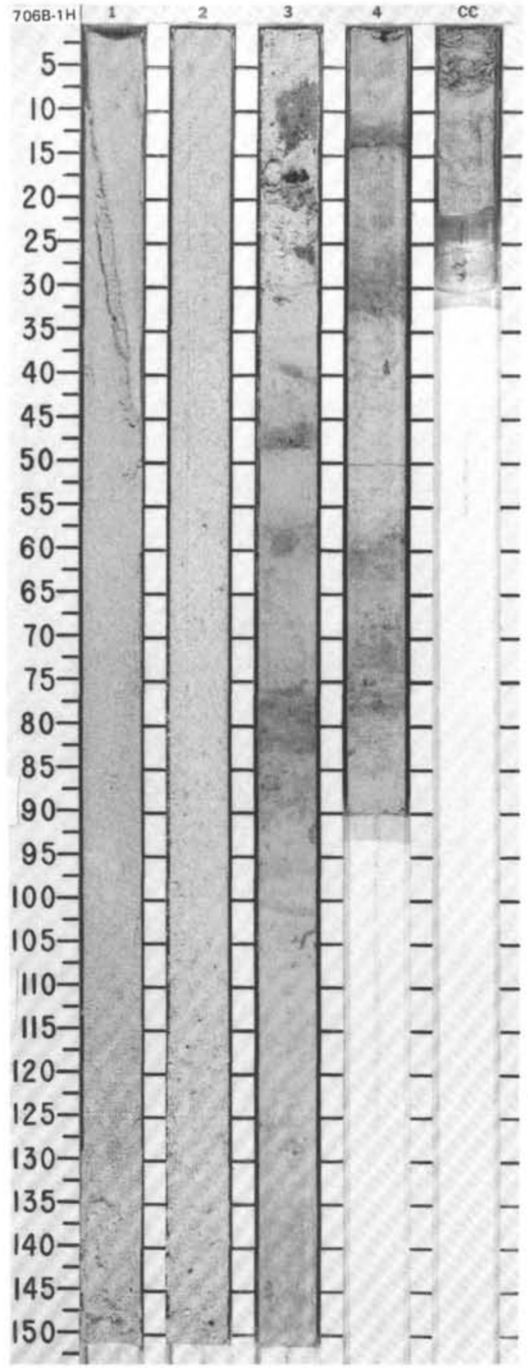

SITE 706 HOLE B CORE 2H CORED INTERVAL 2503.0-2510.0 mbsl; 5.7-12.7 mbsf

TIME-ROCK UNIT	FORAMINIFERS	NANNOFOSSILS	RADIOLARIANS	DIATOMS	PALEOMAGNETICS	PHYS. PROPERTIES	CHEMISTRY	SECTION	METERS	GRAPHIC LITHOLOGY	DRILLING DISTURB.	SED. STRUCTURES	SAMPLES
LOWER OLIGOCENE	P 19	CP 18 (NP 23)	Barren	Barren				1, 2, 3, 4, 5, CC	0.5, 1.0				
	AG	AM											

LITHOLOGIC DESCRIPTION

NANNOFOSSIL OOZE and NANNOFOSSIL CHALK, with VOLCANIC ASH LAYERS

Major lithology: Nannofossil ooze, pale yellow (2.5Y 8/4, 7/4, oxidized conditions) down to Section 1, 147 cm; then through a sharp contact to a light greenish gray (5GY 7/1, reduced conditions) nannofossil ooze, with interbedded greenish gray to dark greenish gray (5G 5/1, 4/1) altered, indistinct ash layers, and dark gray (5Y 4/1) to black (N2) unaltered, distinct ash layers. The background nannofossil ooze grades downcore to chalk. Gradual mottled aspect throughout due to bioturbation. Unaltered ash layers at Section 2, 13-15 cm; Section 3, 83-86 cm; and Section 5, 40-42 cm. Limestone clast at the very top of Section 1.

SMEAR SLIDE SUMMARY (%):

	1, 5 M	1, 57 D	2, 102 D	3, 86 M	4, 117 M
TEXTURE:					
Sand		5	5	—	—
Silt		—	—	100	100
Clay		95	95	—	—
COMPOSITION:					
Feldspar	—	—	—	1	3
Volcanic glass	—	—	—	98	1
Accessory minerals:					
Glauconite	—	—	—	1	1
Pyrite	—	—	—	—	25
Foraminifers	40	5	5	—	5
Nannofossils	—	95	95	Tr	65
Radiolarians	—	—	—	—	Tr
Sponge spicules	—	—	—	Tr	—
Bioclasts	5	—	—	—	—
Bryozoans	20	—	—	—	—
Red Algae	10	—	—	—	—
Ichinoderm fragments	Tr	—	—	—	—
Spar cement	10	—	—	—	—
Micrite	15	—	—	—	—

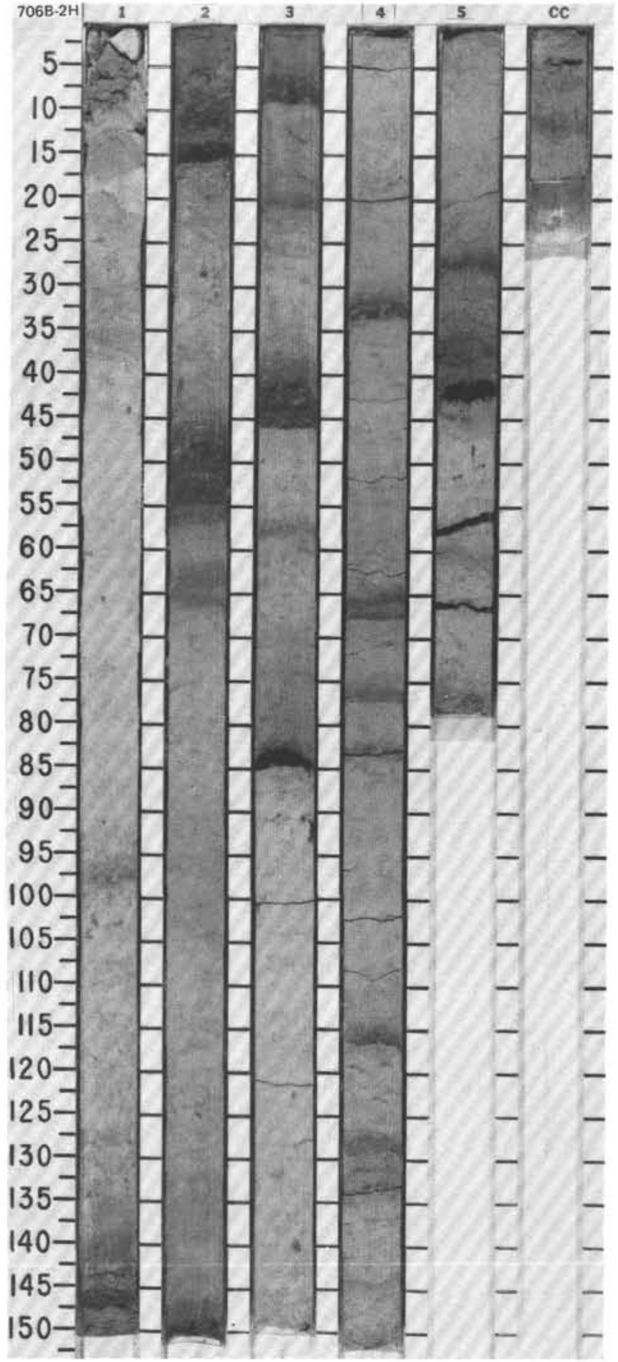

SITE 706 HOLE B CORE 3H CORED INTERVAL 2510.0-2517.9 mbsl; 12.7-20.6 mbsf

TIME-ROCK UNIT	FORAMINIFERS	NANNOFOSSILS	RADIOLARIANS	DIATOMS	PALEOMAGNETICS	PHYS. PROPERTIES	CHEMISTRY	SECTION	METERS	GRAPHIC LITHOLOGY	DRILLING DISTURB.	SED. STRUCTURES	SAMPLES	LITHOLOGIC DESCRIPTION
LOWER OLIGOCENE	P 19	CP 18 (NP 23)	Barren	Barren				1	0.5, 1.0					
								2						
								3						
								4						
								5						
	AG	AM						CC						

BIOSTRAT. ZONE/ FOSSIL CHARACTER

NANNOFOSSIL CHALK with VOLCANIC ASH LAYERS

Major lithology: Light greenish gray (5G 7/1) to greenish gray (5G 6/1) nannofossil chalk, with interbedded greenish gray to dark greenish gray (5G 5/1, 4/1), indistinct altered ash layers, and dark gray (5Y 4/1) to black (N2) unaltered ash layers with sharp basal contacts. Ash layers make up an estimated 10% of the core.

General mottled aspect throughout due to bioturbation.

Unaltered ash layers at Section 1, 63-65 cm; Section 2, 120-128 cm; Section 3, 73-74 cm; and Section 4, 10-16 cm.

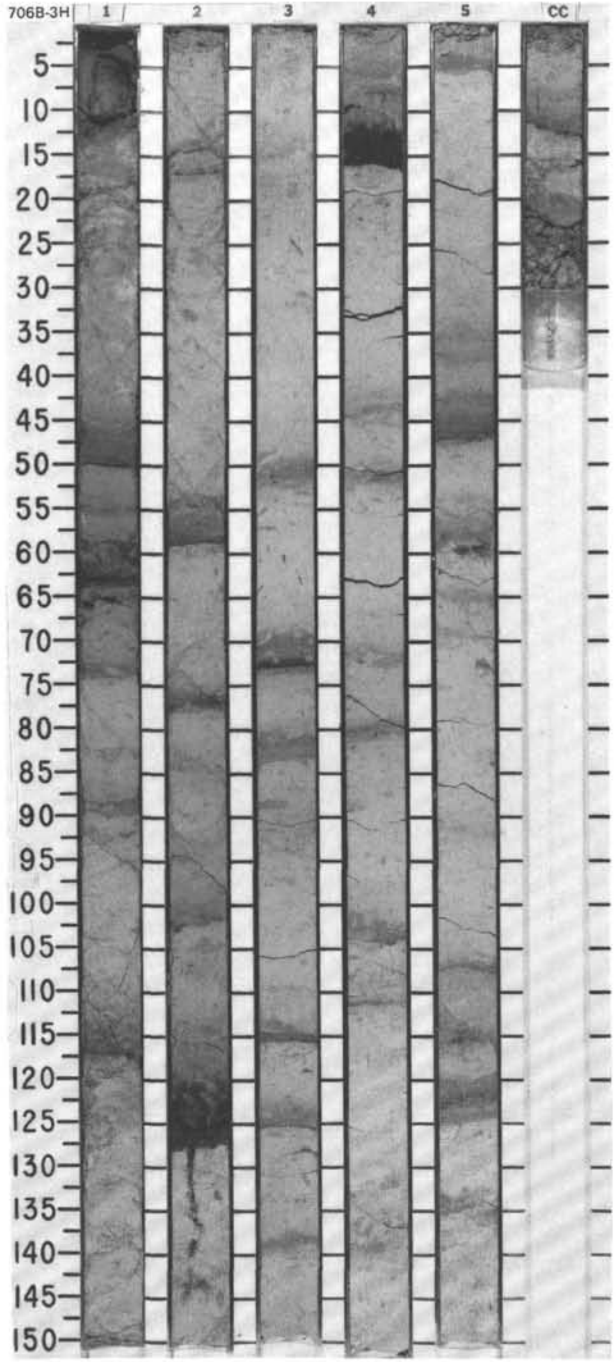

SITE 706 HOLE B CORE 4H CORED INTERVAL 2517.9-2519.7 mbsl; 20.6-22.4 mbsf

TIME-ROCK UNIT	FORAMINIFERS	NANNOFOSSILS	RADIOLARIANS	DIATOMS	PALEOMAGNETICS	PHYS. PROPERTIES	CHEMISTRY	SECTION	METERS	GRAPHIC LITHOLOGY	DRILLING DISTURB.	SED. STRUCTURES	SAMPLES	LITHOLOGIC DESCRIPTION
LOWER OLIGOCENE	P 19 / AG	CP 18 (NP 23) / AM	Barren	Barren				1, CC	0.5, 1.0					NANNOFOSSIL CHALK with VOLCANIC ASH LAYERS

NANNOFOSSIL CHALK with VOLCANIC ASH LAYERS

Major lithology: Nannofossil chalk, light greenish gray (5G 7/1) to greenish gray (5G 6/1); with interbedded greenish gray to dark greenish gray (5G 5/1, 4/1), indistinct, altered ash layers making up approximately 10% of the core.

General mottled aspect due to bioturbation.

SITE 706 HOLE B CORE 5X CORED INTERVAL 2519.7-2524.4 mbsl; 22.4-27.1 mbsf

TIME-ROCK UNIT	FORAMINIFERS	NANNOFOSSILS	RADIOLARIANS	DIATOMS	PALEOMAGNETICS	PHYS. PROPERTIES	CHEMISTRY	SECTION	METERS	GRAPHIC LITHOLOGY	DRILLING DISTURB.	SED. STRUCTURES	SAMPLES	LITHOLOGIC DESCRIPTION
LOWER OLIGOCENE	P 19 / AG	CP 18 (NP 23) / AM	Barren	Barren				1, 2, 3, CC	0.5, 1.0				*	FORAMINIFERAL OOZE, NANNOFOSSIL OOZE, and NANNOFOSSIL CHALK

FORAMINIFERAL OOZE, NANNOFOSSIL OOZE, and NANNOFOSSIL CHALK

Core seriously disturbed by drilling; consists of a mixture of foraminiferal ooze, nannofossil ooze, and nannofossil chalk, (mainly downhole contamination).
CC: Nannofossil chalk and foraminiferal chalk mixed with one fragment of limestone and some fragments of "cherty limestone."

SMEAR SLIDE AND THIN SECTION SUMMARY (%):

	1, 70 D	3, 5 D	CC M	CC M
TEXTURE:				
Sand	60	—		
Clay	40	100		
COMPOSITION:				
Foraminifers	60	Tr	12	25
Nannofossils	40	100	—	—
Pellets (?)	—	—	—	5
Bioclasts	—	—	—	10
Echinoderm fragments	—	—	—	3
Sponge spicules	—	—	—	10
Bryozoans	—	—	—	12
Spar cement	—	—	—	15
Micrite	—	—	88	20

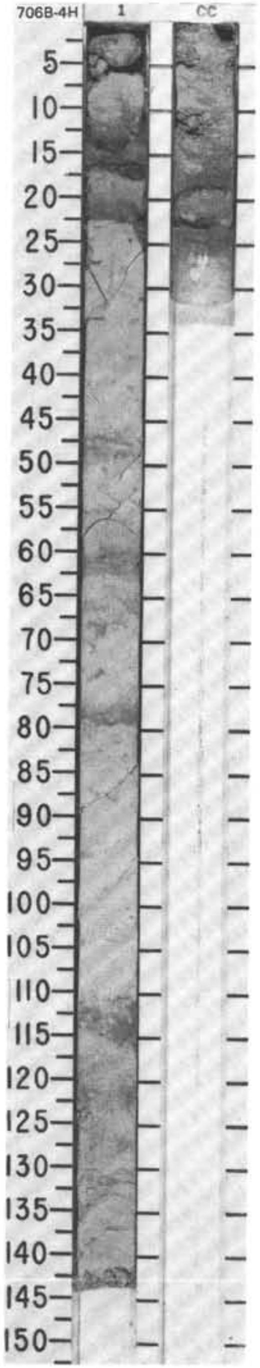

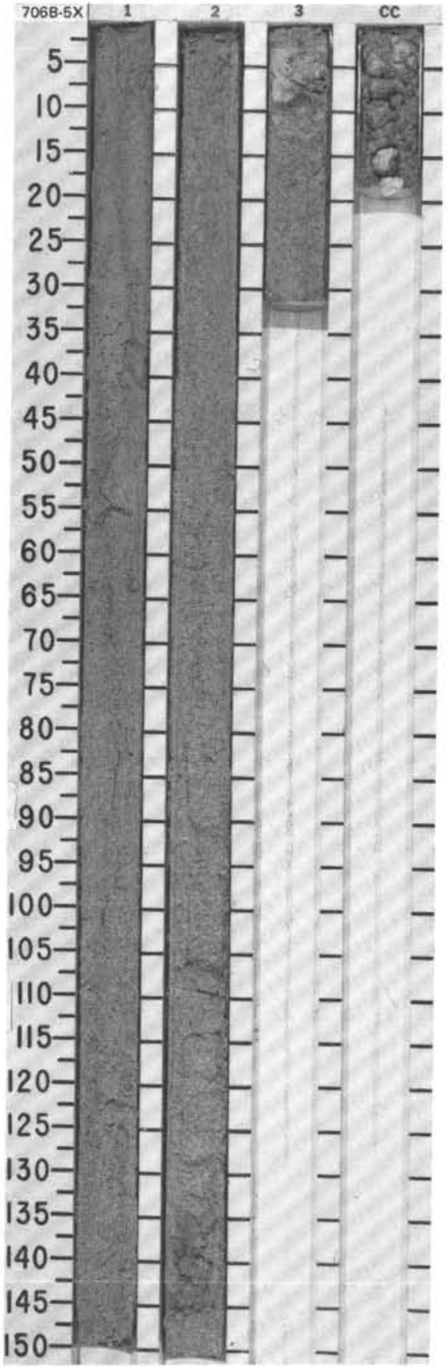

SITE 706 HOLE B CORE 6X CORED INTERVAL 2524.4-2534.0 mbsl; 27.1-36.7 mbsf

TIME-ROCK UNIT	FORAMINIFERS	NANNOFOSSILS	RADIOLARIANS	DIATOMS	PALEOMAGNETICS	PHYS. PROPERTIES	CHEMISTRY	SECTION	METERS	GRAPHIC LITHOLOGY	DRILLING DISTURB.	SED. STRUCTURES	SAMPLES
LOWER OLIGOCENE	P 19	CP 18 (NP 23)	Barren	Barren				1	0.5, 1.0		O O O O X X		#
								2				~ ~ ~	* ** * *
								CC					*
	AG	AM											

(BIOSTRAT. ZONE/FOSSIL CHARACTER: FORAMINIFERS, NANNOFOSSILS, RADIOLARIANS, DIATOMS)

LITHOLOGIC DESCRIPTION

FORAMINIFER-BEARING NANNOFOSSIL OOZE

Major lithology: Foraminifer-bearing nannofossil ooze, greenish gray to light greenish gray (5GY 6/1, 7/1). Section 1, totally disturbed by drilling, contains a chaotic mixture of foraminiferal ooze and nannofossil chalk.

Minor lithologies: Unaltered volcanic ash, Section 2, 86-100 cm, black (N2) at sharp basal contact, grading upward to mottled greenish gray (5GY 5/1). Section 1 disturbed by drilling and contains a mixture of foraminiferal ooze and nannofossil ooze. Section 1, 100-150 cm, contains a drilling breccia of limestone and cherty limestone pebbles in a nannofossil chalk.

SMEAR SLIDE AND THIN SECTION SUMMARY (%):

	1, 123	2, 50 D	2, 85 D	2, 90 M	2, 120 D	CC, 9 D
TEXTURE:						
Sand		10	—	40	5	—
Silt		90	100	40	5	—
Clay		—	—	20	100	100
COMPOSITION:						
Quartz	—	—	—	Tr	—	—
Feldspar	—	—	—	Tr	—	—
Clay	—	—	—	10	—	—
Volcanic glass	—	—	—	60	—	—
Accessory minerals:						
Olivine	—	—	—	Tr	—	—
Opaques	—	—	—	25	—	—
Foraminifers	20	10	Tr	Tr	5	—
Nannofossils	—	90	100	5	95	100
Sponge spicules	—	—	Tr	—	—	—
Bioclasts	12	—	—	—	—	—
Intraclasts	10	—	—	—	—	—
Echinoderm fragments	3	—	—	—	—	—
Bryozoans	15	—	—	—	—	—
Red Algae	15	—	—	—	—	—
Coral (?)	5	—	—	—	—	—
Spar cement	20	—	—	—	—	—

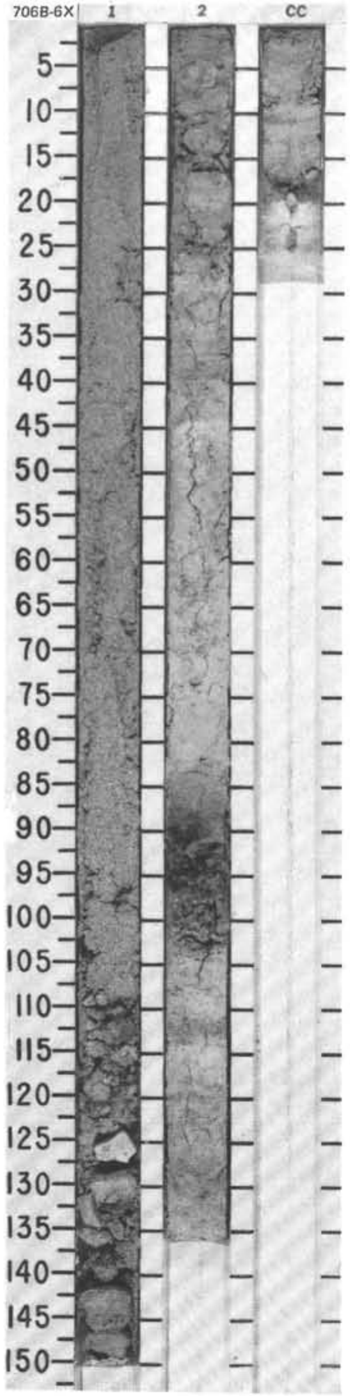

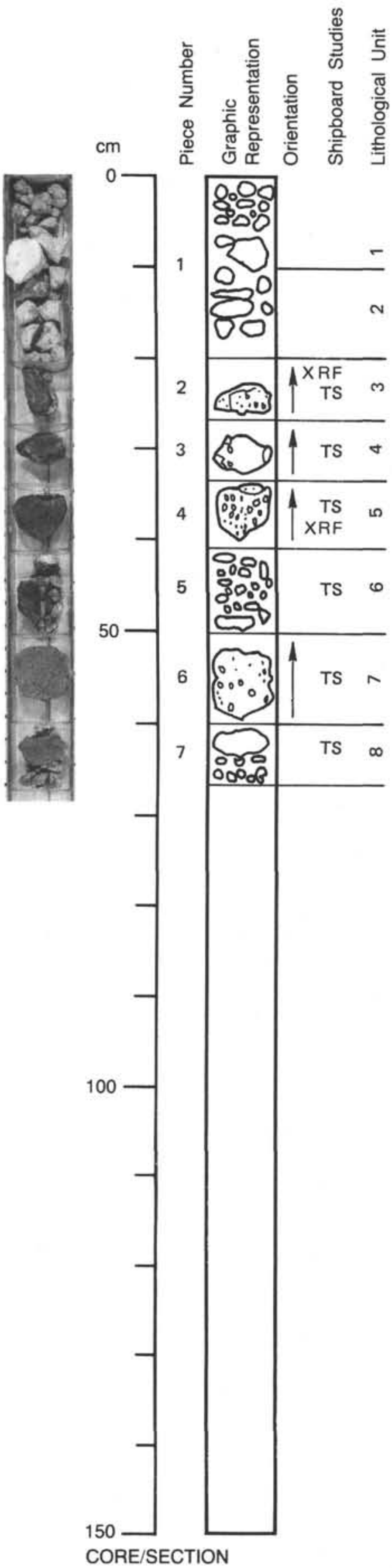

115-706B-7X-CC

UNIT 1: DRILLING RUBBLE (LIMESTONE, MUDSTONE, CHERT, and BASALT)

Piece 1

SIZE: <1 cm to 5 cm.
COLOR: Chert, green.
STRUCTURE: Rubble.

UNIT 2: MASSIVE SULFIDE "NODULES"

Piece 1 (continued)

SIZE: 1 cm thick ×5 cm across.
PIECES: Seven pieces of microbreccia, irregular fragments of glass and rock in matrix of sulfide in cut surface. (Sandstone of basalt grains with sulfide cement.)
COLOR: Dark grayish brown (10YR 4/2) on cut surface.
STRUCTURE: Massive nodules. Pyrite octahedra on surface.

UNIT 3: VESICULAR BASALT

Piece 2

SIZE: 5.5×2.5 cm.
CONTACTS: Altered, chilled glassy margin to upper surface, ≈3 mm thick.
GROUNDMASS: Slightly altered vesicular basalt, phaneritic, fine grained.
COLOR: Dark gray (N4).
VESICLES: Regular, ellipsoidal, internally rimmed by zeolite + chlorite? . Vesicle abundance 20%, 5-20 mm diameter, uniformly distributed.
STRUCTURE: Massive. Interstitial glass developed toward altered glassy margin.
TEXTURE: Intersertal.
ALTERATION: Slightly altered.
VEINS/FRACTURES: Small veins which cut the sample have green plagioclase (celadonite?) margins, infilled with elongate, inward-growing, prismatic, colorless zeolite plagioclase. Veins 1 mm.

UNIT 4: SLIGHTLY VESICULAR BASALT

Piece 3

SIZE: 6×4 cm.
CONTACTS: Right margin of fragment has 2 mm crust of altered glass, now seen as gray-green plagioclase (celadonite?)
GROUNDMASS: Slightly vesicular basalt, phaneritic, fine grained.
COLOR: Dark gray (N4).
VESICLES: 0.2-1.0 mm, ellipsoidal, randomly scattered. Lined with gray green plagioclase + zeolite. Estimated vesicle abundance 2%.
STRUCTURE: Massive.
TEXTURE: Intersertal.
ALTERATION: Slightly altered.

UNIT 5: VESICULAR BASALT

Piece 4

SIZE: 6×5 cm.
CONTACTS: Part of the surface is rimmed by glass.
PHENOCRYSTS: Plagioclase.
GROUNDMASS: Vesicular basalt, phaneritic, fine grained.
COLOR: Dark gray (N4).
VESICLES: <2 mm, homogeneously scattered. Some internally rimmed by zeolites. Amount of vesicles is ≈20%.
STRUCTURE: Massive.
ALTERATION: Slightly altered.

UNIT 6: BASALT (RUBBLE)

Piece 5

SIZE: <5 cm.
PHENOCRYSTS: Plagioclase (microphenocrysts).
GROUNDMASS: Phaneritic fine-grained basalt.
COLOR: Dark gray (N4).
VESICLES: Average size is 1 mm, maximum size 4 mm. Amount of vesicles is ≈20%. Some internally rimmed by zeolite group.
STRUCTURE: Rubble.
ALTERATION: Slightly altered. Part of the surface is covered by dark green minerals (altered glass?).

UNIT 7: HETEROGENEOUS BASALT

Piece 6

SIZE: 6×7 cm.
GROUNDMASS: Heterogenous basalt, composed of two lithologies; one lithology (≈95%) is phaneritic and fine grained and the other (5%) is aphanitic and glassy. Glassy parts are randomly distributed.
COLOR: Dark gray (N4).
VESICLES: Heterogeneously distributed. Vesicles in fine-grained lithology average 1 mm in diameter; vesicles in glassy lithology are <0.5 mm in diameter. Some of the larger vesicles are rimmed with zeolite.
STRUCTURE: Massive.
ALTERATION: Slightly altered.

UNIT 8: FINE-GRAINED PHANERITIC BASALT

Piece 7

SIZE: <5×3 cm.
PHENOCRYSTS: Plagioclase + augite microphenocrysts. Glassy part is distributed.
GROUNDMASS: Phaneritic basalt, fine grained.
COLOR: Dark gray (N4).
VESICLES: Slightly vesiculated, <5%, maximum size is 0.5 mm.
TEXTURE: Intersertal. Glassy part is distributed.
ALTERATION: Slightly altered.

SITE 706 HOLE C CORE 1W CORED INTERVAL 2507.5-2551.8 mbsl; 0.0-44.3 mbsf

TIME-ROCK UNIT	FORAMINIFERS	NANNOFOSSILS	RADIOLARIANS	DIATOMS	PALEOMAGNETICS	PHYS. PROPERTIES	CHEMISTRY	SECTION	METERS	GRAPHIC LITHOLOGY	DRILLING DISTURB.	SED. STRUCTURES	SAMPLES	LITHOLOGIC DESCRIPTION
								CC						

(Column group header: BIOSTRAT. ZONE/ FOSSIL CHARACTER — Foraminifers, Nannofossils, Radiolarians, Diatoms)

NANNOFOSSIL CHALK

Major lithology: Nannofossil chalk, with black altered blebs (basalt?). Material is severely disturbed, with no stratigraphic coherency.

SMEAR SLIDE SUMMARY (%):

	1, 6 D	1, 50 D
TEXTURE:		
Silt	—	50
Clay	100	50
COMPOSITION:		
Feldspar	Tr	2
Volcanic glass	Tr	1
Foraminifers	1	5
Nannofossils	99	85
Unknown	—	7

SITE 706 HOLE C CORE 2R CORED INTERVAL 2551.8-2561.4 mbsl; 44.3-53.9 mbsf

TIME-ROCK UNIT	FORAMINIFERS	NANNOFOSSILS	RADIOLARIANS	DIATOMS	PALEOMAGNETICS	PHYS. PROPERTIES	CHEMISTRY	SECTION	METERS	GRAPHIC LITHOLOGY	DRILLING DISTURB.	SED. STRUCTURES	SAMPLES	LITHOLOGIC DESCRIPTION
LOWER OLIGOCENE		AG CP18						1	0.5, 1.0					
								2						
								3						

(Column group header: BIOSTRAT. ZONE/ FOSSIL CHARACTER — Foraminifers, Nannofossils, Radiolarians, Diatoms)

NANNOFOSSIL CHALK and NANNOFOSSIL LIMESTONE overlying basalt

Major lithology:
a. Nannofossil chalk and nannofossil limestone, light greenish gray (5GY 7/1), in Section 1, 0-56 cm. Nannofossil limestone in Section 1, 52-56 cm, is finely laminated with pale green (5G 6/2) chalk.
b. Fine-grained plagioclase phyric basalt in Section 1, 56 cm, through Section 3, 14 cm. (See hard rock barrel sheets for detailed description of these basalts).

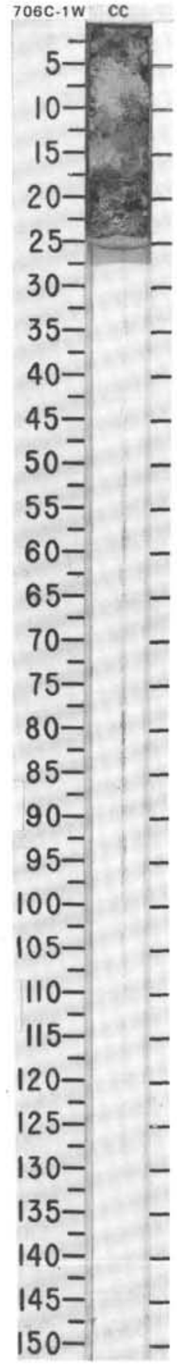

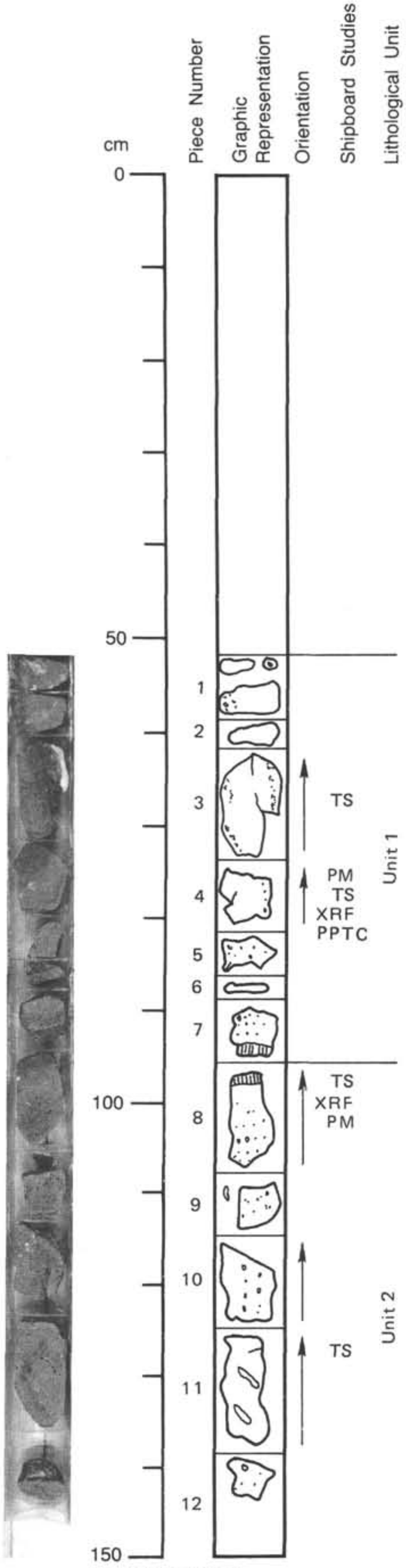

115-706C-2R-1

UNIT 1: FINE-GRAINED, MODERATELY VESICULAR PLAGIOCLASE-PHYRIC BASALT

Pieces 1-7

CONTACTS: Upper contact abrupt but gradational into green sediment, and associated with heavy gray green alteration of uppermost 4 cm. Lower contact with Unit 2 indicated by development of hypocrystalline matrix in lower part of Piece 7.

PHENOCRYSTS: Euhedral, fresh plagioclase up to 2 mm long, forming as much as 15% of rock. Generally randomly distributed.

GROUNDMASS: Generally holocrystalline, but grades to hypocrystalline in Piece 3 towards glass contact on right side.

COLOR: Generally very dark gray (N3), but rapidly changes to olive gray (5/2) at upper contact with sediment.

VESICLES: Irregular to ellipsoidal, 0.1-2.0 mm diameter. Generally decreases in size with development of hypocrystalline texture. Otherwise uniformly distributed, forming ≈5% of rock on upper and lower contacts (Pieces 1 and 7), increasing to maximum of 15% in center (Piece 4). Often infilled by gray green microcrystalline clay, or lined with same. Occasionally empty.

ALTERATION: Generally slightly altered to pale gray-green clay. Upper contact heavily altered to same (Piece 1, upper part).

MODE OF FORMATION: Probably pillow lava unit.

UNIT 2: FINE-GRAINED PLAGIOCLASE-PHYRIC BASALT

Pieces 8-12

CONTACTS: Top: fine-grained, black, glassy or altered, with fewer vesicles than Unit 1. Piece 8 shows gradation from ≈2 cm contact zone as described above, through 1 cm more massive basalt, to more typical black gray vesicular basalt. Bottom: inconspicuous.

PHENOCRYSTS: Plagioclase 10-15%, homogeneous distribution, acicular needles, ≈1 mm, fresh.

GROUNDMASS: Microcrystalline, gray; augite is darker green, uniformly distributed.

COLOR: Uniformly dark gray, except for 2 cm wide blackish zone at upper contact.

VESICLES: Variable, as much as 30% by volume, mostly empty, as large as 5 mm, average 1-2 mm. Greenish celadonite(?) lining to vesicles in Pieces 10 (part), 11, and 12. Piece 11 shows two elongate, as long as 5 cm, lensoid (×5 m) voids, also lined with greenish material, but overall piece more massive. Larger vesicles/voids in Pieces 10 and 12 as well.

ALTERATION: Minimal. Blackish zone at contact may be somewhat altered glass.

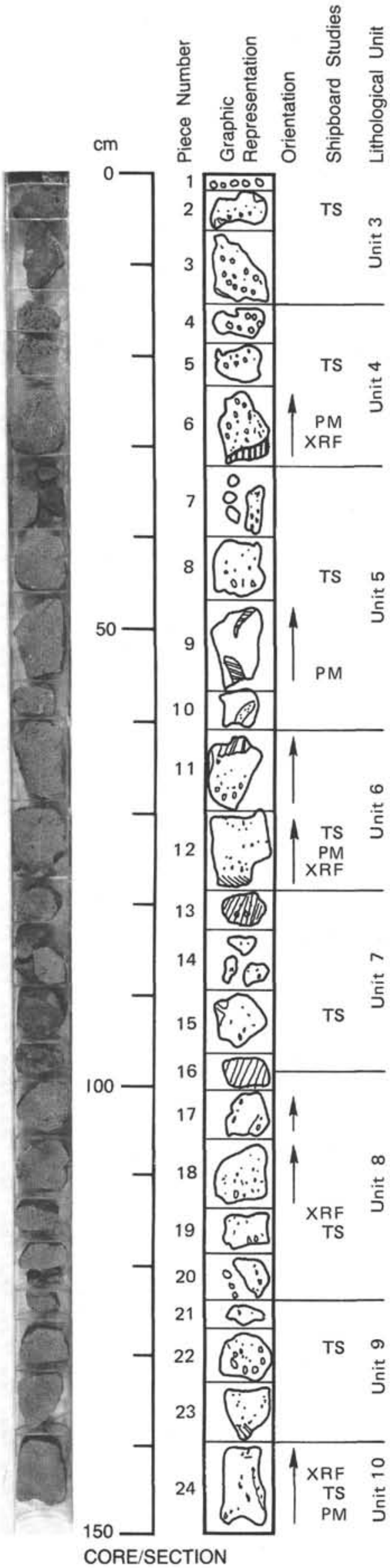

115-706C-2R-2

UNIT 3: FINE-GRAINED, PARTLY GLASSY PLAGIOCLASE-PHYRIC BASALT

Pieces 1-3

PHENOCRYSTS: Plagioclase, <1 mm.
GROUNDMASS: Fine grained to glassy. In Pieces 2 and 3, fresh glass is observed near the surface.
COLOR: Dark gray (N4, N3).
VESICLES: average size 1 mm, maximum size 4 mm, ≈25%. Vesicles near the green surface in Piece 3 are pressed to be elongated. About 60% of vesicles are rimmed by zeolite-group minerals.
ALTERATION: Slightly altered. Part of the surface of Piece 3 is composed of pale green blue minerals. Piece 1 is highly altered.

UNIT 4: FINE-GRAINED, PARTLY GLASSY PLAGIOCLASE-PHYRIC BASALT

Pieces 4-6

CONTACTS: Partly with glassy rim.
PHENOCRYSTS: Plagioclase, <1 mm.
GROUNDMASS: Fine grained to glassy. 1 cm wide glassy rim is attached at base of Piece 6.
COLOR: Dark gray (N4).
VESICLES: Pieces 4 and 6: Homogeneous distribution, highly vesiculated, ≈25%.
Piece 5, upper half: Highly vesiculated, ≈25; lower half, slightly vesiculated, ≈5%. Average size 2 mm, maximum size 4 mm.
ALTERATION: Slightly altered.

UNIT 5: FINE-GRAINED PLAGIOCLASE-PHYRIC BASALT

Pieces 7-10

CONTACTS: The lowest and highest parts of this unit, i.e., Pieces 7 and 10, are glassy.
PHENOCRYSTS: Plagioclase, <1 mm.
GROUNDMASS: Fine grained.
COLOR: Dark gray (N4).
VESICLES: Homogeneous distribution, average size 1 mm, maximum size 5 mm, ≈10%. Vesicles in Pieces 8-10 are rimmed by green-blue minerals.
ALTERATION: Slightly altered.

UNIT 6: FINE-GRAINED PLAGIOCLASE-PHYRIC BASALT

Pieces 11-12

CONTACTS: The top of Piece 11 and the base of Piece 12 are glassy.
PHENOCRYSTS: Plagioclase, <1 mm.
GROUNDMASS: Fine grained.
COLOR: Dark gray (N4).
VESICLES: Piece 11: Homogeneous distribution, average size 1 mm, ≈20%.
Piece 12: A horizontal band, slightly below center, is without vesicles.
ALTERATION: Slightly altered.

UNIT 7: FINE-GRAINED TO GLASSY PLAGIOCLASE-PHYRIC BASALT

Pieces 13–15

PHENOCRYSTS: Plagioclase, <1 mm.
GROUNDMASS: Only the middle part of the unit, Piece 14, is fine grained; other pieces are glassy.
COLOR: Dark gray (N4, N3).
VESICLES: In fine-grained samples, Pieces 14, heterogeneous distribution; in other samples, homogeneous distribution. Average size 1 mm, maximum size 3 mm, ≈20%. Vesicles in Pieces 14 and 15 are rimmed by zeolite-group minerals.
ALTERATION: Slightly altered.

UNIT 8: FINE-GRAINED PLAGIOCLASE-PHYRIC BASALT

Pieces 16–20

CONTACTS: The top and base of the unit, Pieces 16 and 20, are glassy.
PHENOCRYSTS: Plagioclase, <1 mm.
GROUNDMASS: Top and bottom pieces glassy, other pieces are fine grained.
COLOR: Dark gray (N4).
VESICLES: Homogeneous distribution, average size 1 mm, maximum size 3 mm, ≈15%.
ALTERATION: Slightly altered.

UNIT 9: FINE-GRAINED PLAGIOCLASE-PHYRIC BASALT

Pieces 21–23

CONTACTS: Piece 21 and the base of Piece 23 are glassy.
PHENOCRYSTS: Plagioclase, <1 mm.
GROUNDMASS: Fine grained, with top and bottom glassy.
COLOR: Dark gray (N4).
VESICLES: In fine-grained part, very homogeneous, average size 1 mm, ≈20%.
In glassy part, homogeneous, average size <1 mm, ≈5–≈10%.
ALTERATION: Slightly altered.

UNIT 10: FINE-GRAINED TO GLASSY PLAGIOCLASE-PHYRIC BASALT

Piece 24

PHENOCRYSTS: Plagioclase, <1 mm.
GROUNDMASS: Upper right margin of Piece 24 is glassy, the other part is fine grained.
COLOR: Dark gray (N4).
VESICLES: Bottom, moderately vesicular, ≈20%; other part slightly vesicular, average size 1 mm, maximum size 2 mm, ≈5%
ALTERATION: Slightly altered. In glassy part glass may be completely altered.

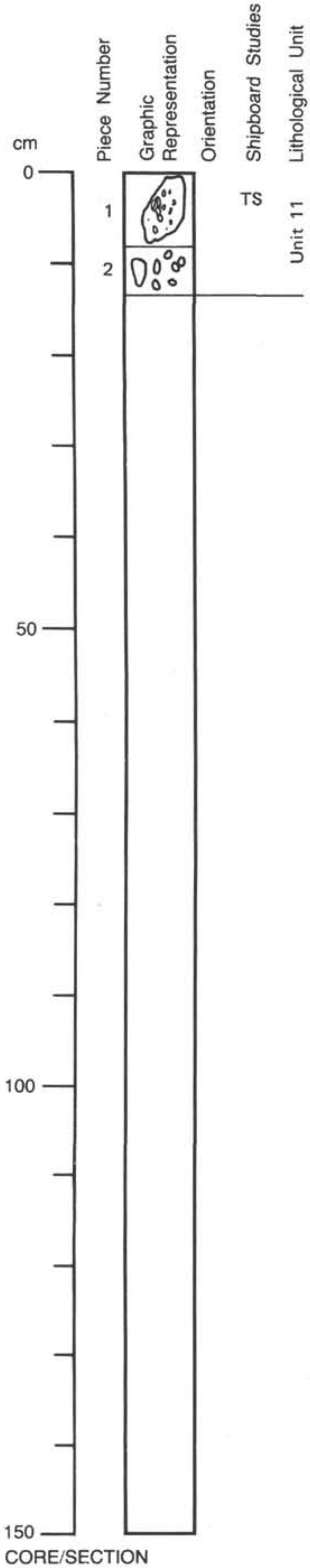

115-706C-2R-3

UNIT 11: FINE-GRAINED PLAGIOCLASE-PHYRIC BASALT

Pieces 1–2

CONTACTS: This unit could be continuous with both Unit 10 in 115-706C-2R-2 and Unit 12 in 115-706C-3R-1.
PHENOCRYSTS: Plagioclase, <1 mm.
GROUNDMASS: Fine grained, with some glass present in the upper left of Piece 1.
COLOR: Dark gray (N4).
VESICLES: Homogeneous distribution, average size 1.5 mm, maximum size 3 mm, ≈20%. Vesicles are rimmed by pale green to gray zeolite-group minerals.
ALTERATION: Slightly altered. Glassy part may be completely altered.

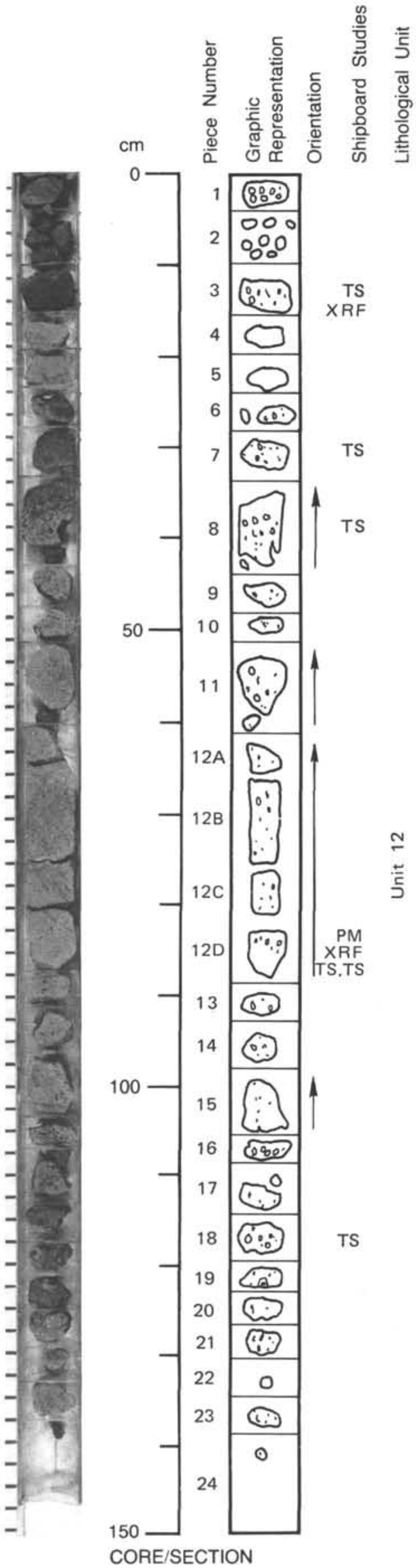

115-706C-3R-1

UNIT 12: SLIGHTLY ALTERED, MODERATELY VESICULATED, PLAGIOCLASE-PHYRIC BASALT

Pieces 1–24

CONTACTS: This unit is continuous with Unit II in 115-706-2R-3. One lithologic boundary between Piece 6 and Piece 7, and another between Piece 17 and Piece 18 (glass).

PHENOCRYSTS: Plagioclase, euhedral to subhedral, fresh, <2 mm, 5–15%, randomly scattered.

GROUNDMASS: Phaneritic intersertal texture. Pieces 7, 19, and 20 are slightly glassy, hypocrystalline. Other pieces are fine-grained, nearly holocrystalline, with small amounts of interstitial glass.

COLOR: Dark gray (N4).

VESICLES: Irregular to ellipsoidal, 5–20%. In the most vesicular piece, Piece 16, vesicles are connected with each other. Sometimes, vesicles are rimmed or filled by green blue clay material, rarely (as in Piece 19) filled with gypsum.

ALTERATION: Slightly altered gray-green-blue clay. Part of glass may be completely altered.

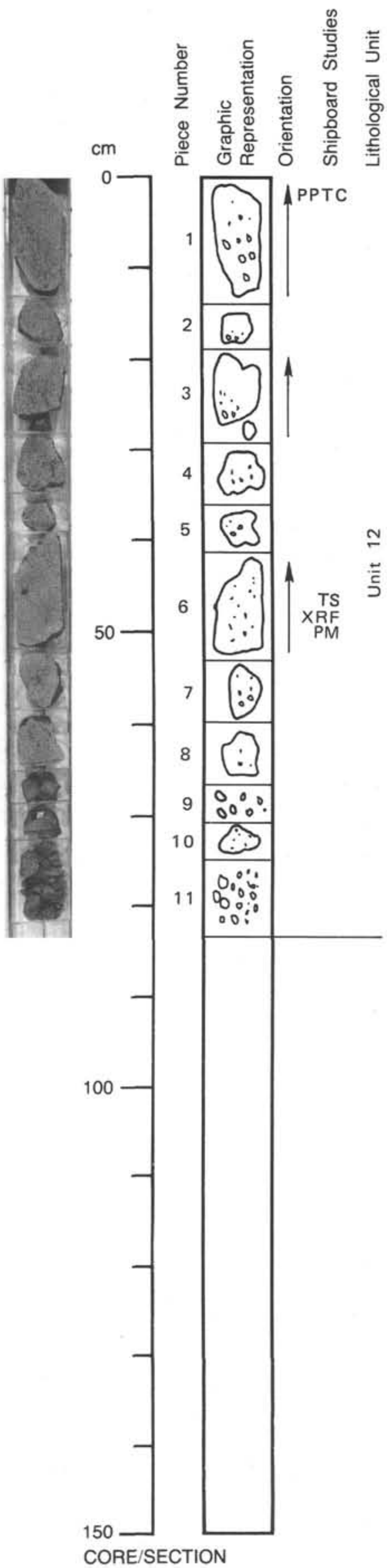

115-706C-3R-2

UNIT 12 (CONTINUED): SLIGHTLY ALTERED, MODERATELY VESICULATED, PLAGIOCLASE-PHYRIC BASALT

Pieces 1–11

Continuous with 115-706C-3R-1, Unit 12

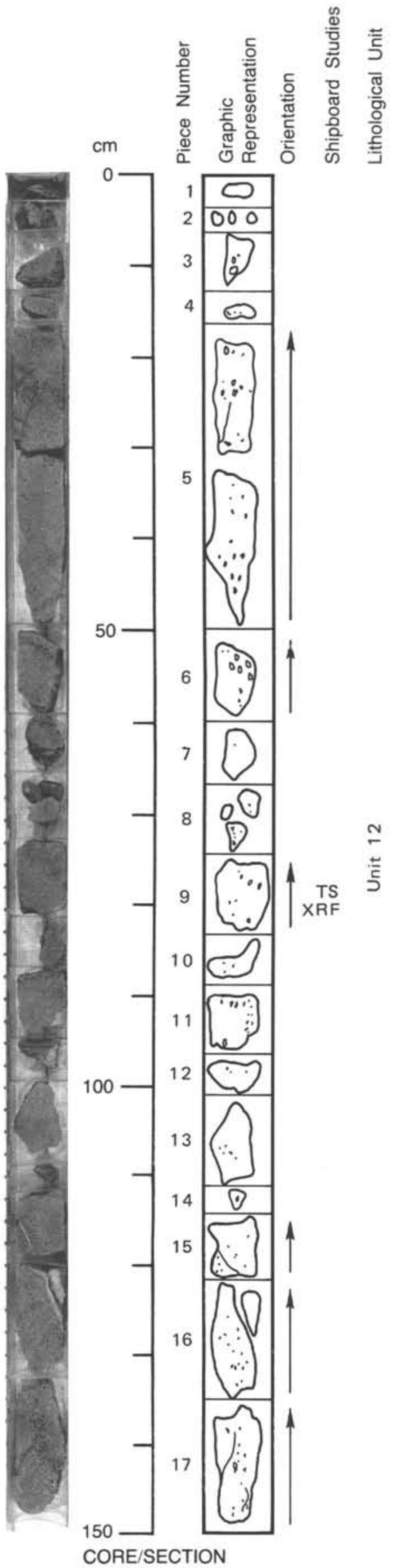

115-706C-4R-1

UNIT 12 (CONTINUED): SLIGHTLY ALTERED, MODERATELY VESICULATED PLAGIOCLASE-PHYRIC BASALT

Pieces 1–17

Continuous with 115-706C-3R-2, Unit 12

PETROGRAPHY: As described in 115-706C-3R-2, Unit 12.

VESICLES: Some filled with pyrite, <1%. Zeolites found in some vesicles. Piece 17 vesicles filled with celadonite and/or limonite, and possible malachite.

VEINS/FRACTURES: Green-gray clay minerals along crack in Pieces 15 and 16. Veins <1% of core. Large grayish green (10G 4/2) veins in Pieces 15, 16, and 17; up to 7 mm across in Piece 16A, dipping 70°. Smaller 1 mm wide veins in Pieces 12 and 13. Possibly celadonite filling, banded with brown limonite(?) alternating with celadonite.

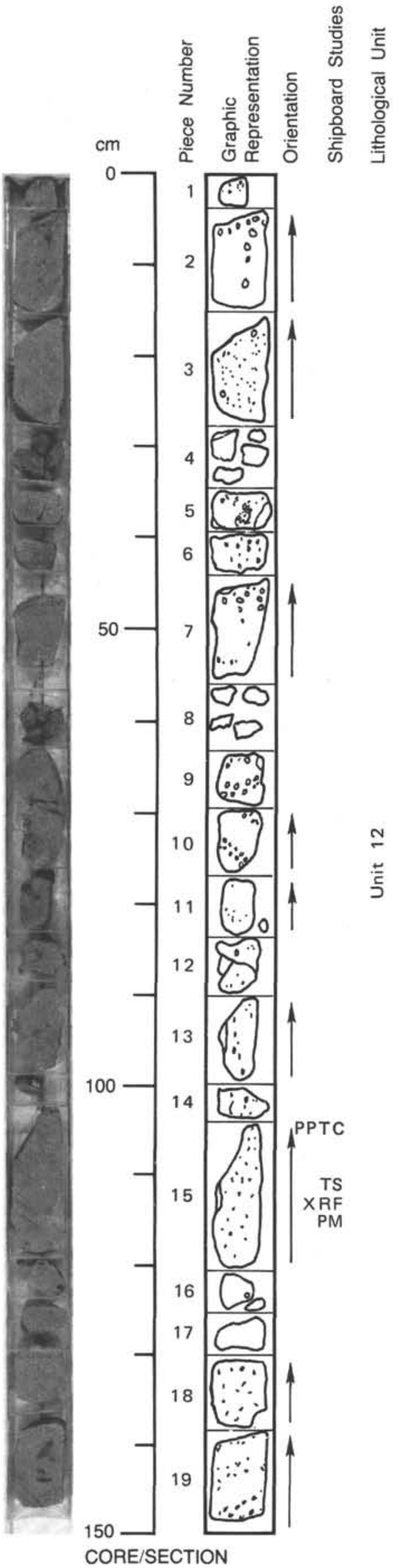

115-706C-4R-2

UNIT 12 (CONTINUED): SLIGHTLY ALTERED, MODERATELY VESICULATED PLAGIOCLASE-PHYRIC BASALT

Pieces 1–19

Continuous with 115-706C-4R-1, Unit 12

CONTACTS: No definite lithologic breaks, but possible lithologic boundary between Pieces 6 and 7.

VESICLES: Pieces 3, 8, and 19: Sulfide in vesicles.
Piece 9: Bands of vesicles.
Piece 10: Two vesicular bands.
Piece 11: Vesicles lined with zeolite minerals and pyrite.
Piece 13: Toward vein filled with green mineral. Vesicles are lined with same alteration mineral.
Piece 15: Very homogenous, with small 1 mm vesicles slightly coated with zeolite (blue when dry), very fresh otherwise, vesicles $<10\%$ by volume.

ALTERATION: Piece 14: relatively unaltered.

VEINS/FRACTURES: Piece 2: Top surface is fractured and filled with grayish green (10G 4/2) mineral.
Piece 4: Fracture filling of celadonite and limonite.
Piece 5: Large void.
Piece 7: Top, fracture surface with zeolites at surface, band of vesicles below.
Piece 12: Two fractures filled with grayish green (10G 4/2) mineral.
Piece 13: Much of outer surface is zeolite-covered vein, filled with green (10G 4/2) mineral.

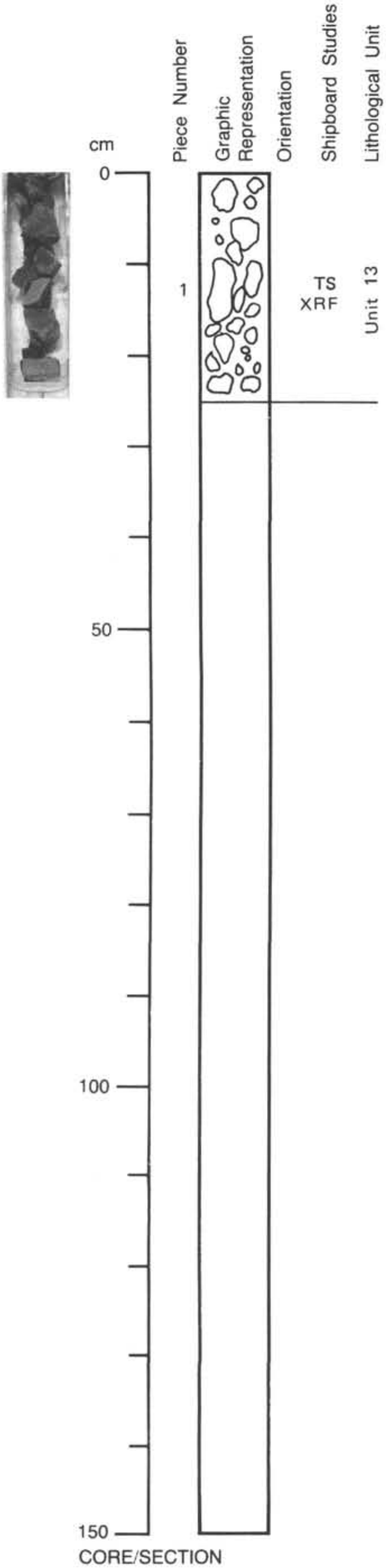

115-706C-4R-3

UNIT 13: MEDIUM-GRAINED AUGITE-PLAGIOCLASE-PHYRIC BASALT

Piece 1

PHENOCRYSTS: Pyroxene, 5%, as large as 1 mm, unaltered.
GROUNDMASS: Pyroxene, plagioclase, olivine(?), and minor sulfide.
COLOR: Black.
TEXTURE: Medium grained.
VESICLES: 3%, vesicles mostly <1 mm, rarely 5 mm.
SECONDARY PHASES: Vesicles coated with light blue mineral 100 cm thick. Also some sulfide and black rounded mineral.
ALTERATION: Slightly altered.
VEINS/FRACTURES: None.

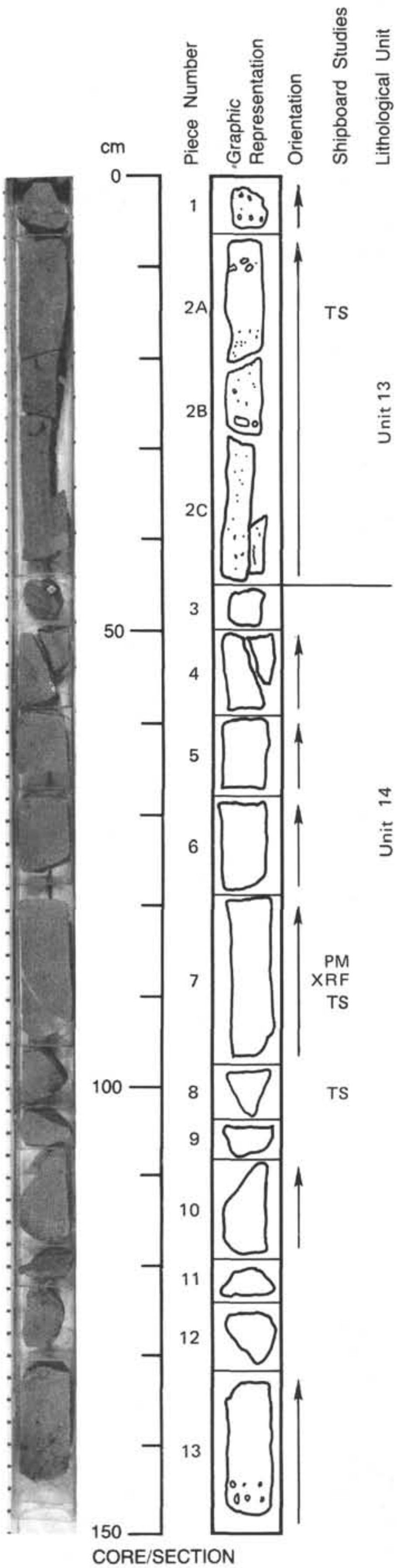

115-706C-5R-1

UNIT 13 (CONTINUED): MEDIUM-GRAINED AUGITE-PLAGIOCLSE-PHYRIC BASALT

Pieces 1–2

Continuous with 115-706C-4R-3, Unit 13

VESICLES: Piece 1: Slightly vesicular, <5%, vesicles unfilled.
Pieces 2: Vesicles contain coating of light blue alteration mineral. In Piece 2A, vesicles small, <1 mm; pyrite fills vesicles, forming layer.
VEINS/FRACTURES: Piece 2C: Vertical fracture contains black to dark green mineral.

UNIT 14: FINE-GRAINED, MODERATELY VESICULAR PLAGIOCLASE-PHYRIC BASALT

Pieces 3–13

CONTACTS: *Bottom appears somewhat glassy.*
PHENOCRYSTS: Euhedral plagioclase forms grains 1 mm long and composes 10–15% of rock. Randomly oriented.
GROUNDMASS: Holocrystalline, but grading to glassy near lower contact (outer 2–5 cm).
COLOR: Generally very dark gray to black.
VESICLES: Generally round to elliptical, <2 mm in diameter. Size tends to decrease very close to contacts. Tends to be "bands" with higher percentages of vesicles, some 10–15%, but generally ≤5%. Usually coated or partially filled with blue gray alteration mineral, or less commonly a greenish mineral (celadonite?), or nothing at all. Rarely pyrite fills vesicles. Piece 13 is slightly more vesicular than other pieces.
ALTERATION: Slightly to moderately altered near cracks filled with alteration minerals. Alteration generally takes form of vesicle infilling.
VEINS/FRACTURES: Sample broke along alteration vein in Piece 3.

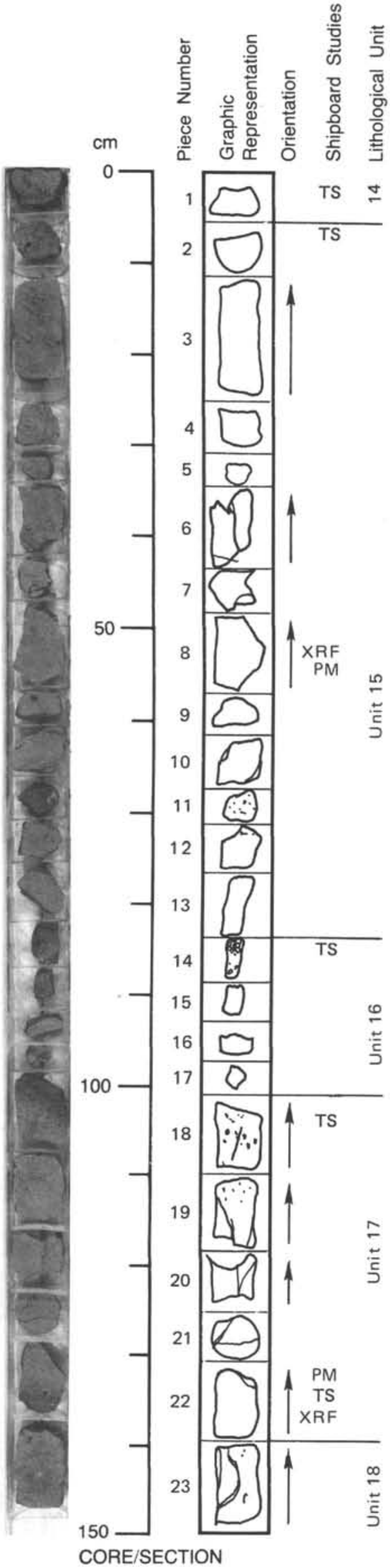

115-706C-5R-2

UNIT 14 (CONTINUED): FINE-GRAINED, MODERATELY VESICULAR PLAGIOCLASE-PHYRIC BASALT

Piece 1

Continuous with 115-706C-5R-1, Unit 14

CONTACTS: Glass at bottom of Piece 1.

UNIT 15: FINE-GRAINED, MODERATELY VESICULAR PLAGIOCLASE-PHYRIC BASALT

Pieces 2-13

CONTACTS: Glassy contact at top of Piece 2 and at bottom of Piece 13.
PHENOCRYSTS: Euhedral plagioclase phenocrysts <1 mm long compose 10-15% of rock.
GROUNDMASS: Holocrystalline but glassy near upper and lower contacts, 3-5 cm.
COLOR: Black, except for grayish green (10G 4/2) alteration minerals.
VESICLES: Occur in "layers." Largest are 5 mm across, but more typically ≈1 mm in diameter, as in Piece 3. Sometimes filled, but most commonly coated with grayish green (10G 4/2) celadonite(?). Vesicles generally make up about 5% of rock, but can locally be as much as 15%.
ALTERATION: Forms veins through much of unit. Main mineral is grayish green (10G 4/2) celadonite(?). These rock infillings are well represented by Piece 6.

UNIT 16: GLASSY TO FINE-GRAINED VESICULAR PLAGIOCLASE-PHYRIC BASALT

Pieces 14-17

CONTACTS: The upper contact is relatively well defined. Abundant glass in Piece 14.
PHENOCRYSTS: Euhedral plagioclase, as long as 2 mm, 15% of rock.
GROUNDMASS: Glassy to holocrystalline fine-grained basalt. Piece 14 contains abundant glass.
VESICLES: As large as 3 mm across. In glassy contact vesicles are filled with black material (Piece 14). In other pieces vesicle interiors are coated with grayish green (10G 4/2) celadonite(?).
ALTERATION: Cracks on surfaces of some pieces (e.g., Piece 15) show alteration, with celadonite(?). The same mineral also fills, or partially fills, vesicles.

UNIT 17: FINE-GRAINED, VESICULAR PLAGIOCLASE-PHYRIC BASALT

Pieces 18-22

CONTACTS: The upper contact shows a well-developed glassy chill margin.
PHENOCRYSTS: Euhedral plagioclase forms phenocrysts, <1 mm in length, <10% of the rock.
GROUNDMASS: Glassy to holocrystalline fine-grained basalt. Glass occurs at both upper (Piece 18) and lower (Piece 22) contacts, but is best developed in the upper contact sample. Glassy bands are about 2-3 cm thick.
VESICLES: Have irregular shapes, as much as 4 mm across, but most vesicles are ≈1 mm in diameter and round to oval in shape. Vesicles tend to be coated, or less commonly filled, with a grayish green mineral (celadonite?). Vesicles in the glassy-contact samples are filled with a black mineral.
ALTERATION: Veins as wide as 2.5 mm occur on the sides or cutting through the middle of all pieces. The main alteration mineral in the veins is grayish green (10G 4/2) celadonite. The same mineral coats the insides of vesicles in most pieces.

UNIT 18: FINE-GRAINED, VESICULAR PLAGIOCLASE-PHYRIC BASALT

Piece 23

PHENOCRYSTS: Euhedral plagioclase 1-2 mm long forms 10–15% of the samples.
GROUNDMASS: Holocrystalline.
COLOR: Black, except alteration mineral veins/coatings.
VESICLES: Large vesicles can be highly irregular in shape and as much as 1 cm across. Most vesicles are ≈ 1 mm across. Vesicles tend to be filled with grayish green (10G 4/2) celadonite(?). Large irregular vesicles appear common.
ALTERATION: Slightly altered. In glassy part glass may be completely altered. The most common evidence for alteration is the almost ubiquitous coating of celadonite(?) over the interior of vesicles.

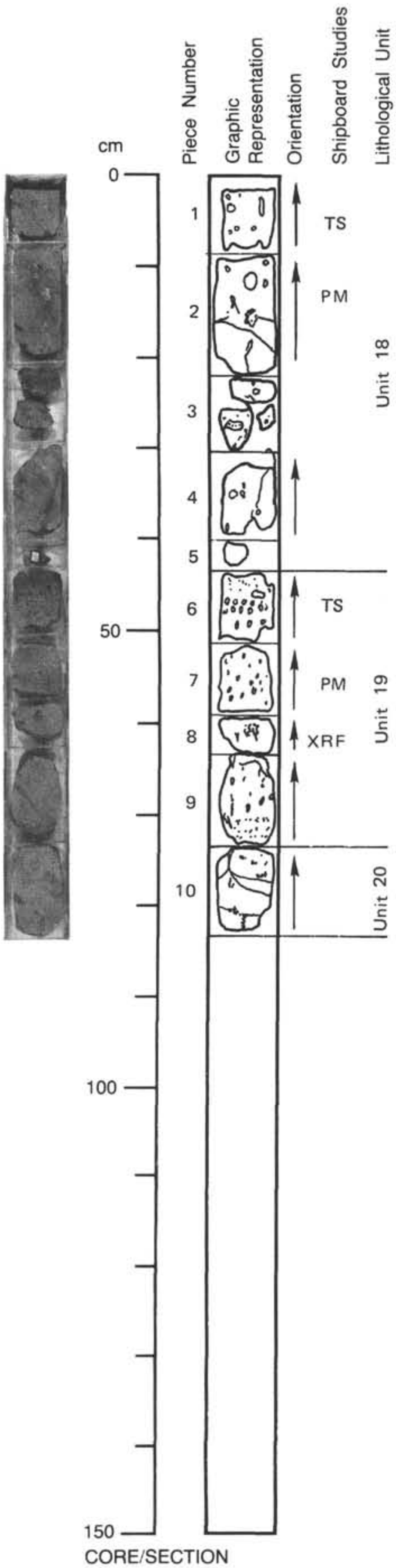

115-706C-5R-3

UNIT 18 (CONTINUED): FINE-GRAINED, VESICULAR PLAGIOCLASE-PHYRIC BASALT

Pieces 1-5

Continuous with 115-706C-5R-2, Unit 18

UNIT 19: FINE-GRAINED, VESICULAR OLIVINE-AUGITE-PLAGIOCLASE PHYRIC BASALT

Pieces 6-9

CONTACTS: Glass at top, possible glass at bottom.
PHENOCRYSTS: Most appear fresh.
Pyroxene - Microphenocrysts 1-2%, 1 mm.
Plagioclase - 2-5%, <1 mm.
Olivine - Rare, <1 mm.
Pyroxene-plagioclase glomerocrysts - Rare, 1-2 mm.
GROUNDMASS: Feldspar and augite, fine grained.
COLOR: Black.
VESICLES: As large as 7 mm, but most are 1 mm, 5% (modal %). 1 cm zone with few vesicles below glass, otherwise uniformly distributed.
SECONDARY PHASES: Green clay completely filling vesicles near glass contact. Open vesicles have ≈60 cm green clay (celadonite?) covered with zeolite. Rare limonite in vesicles.
ALTERATION: Groundmass altered to green clay, 5%; slightly altered, ≈10%.

UNIT 20: FINE-GRAINED OLIVINE-AUGITE PLAGIOCLASE PHYRIC BASALT

Piece 10

PHENOCRYSTS: Augite - Rare, <1 mm.
Plagioclase - Microphenocrysts, grade into groundmass.
Olivine(?) - Rare, <1 mm.
GROUNDMASS: Feldspar and augite, fine grained.
COLOR: Black.
VESICLES: Round, 1 mm diameter, 1-2 modal %. Uniformly distributed, increasing in abundance to 5% down unit. Voids up to 1 cm, irregular shape, rare.
ALTERATION: Groundmass altered to green clay. Cracks and fractures filled with green clay celadonite(?). Phenocrysts unaltered. 10-30% slightly to moderately altered rock.
VEINS/FRACTURES: 1%, filled with celadonite and zeolite.

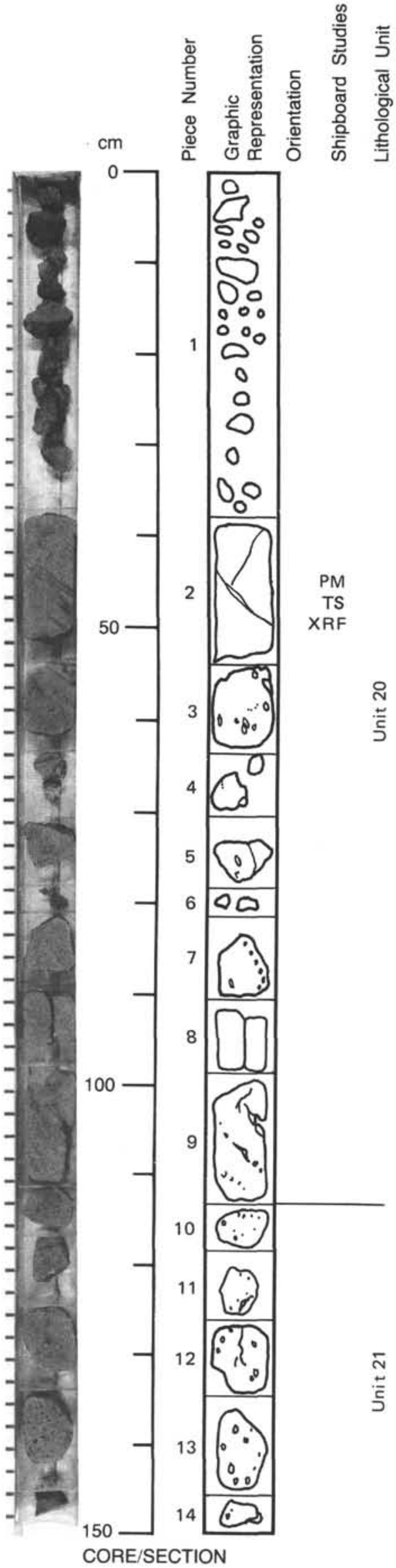

115-706C-6R-1

UNIT 20 (CONTAINED): FINE-GRAINED OLIVINE-AUGITE PLAGIOCLASE-PHYRIC

Piece 1

SIZE: 1-6 cm in diameter.
VESICLES: All pieces are vesicular, some with glassy selvages (1-2 mm). Vesicles generally clean; some with clay-celadonite coatings.
STRUCTURE: Rounded, subhedral basalt pieces (21). Probably infill from previous coring.

Pieces 2-9

Continuous with 115-706C-5R-3, Unit 20

VEINS/FRACTURES: Largest vein, 2-5 mm thick, in Piece 2, is filled with celadonite + limonite at edges.

UNIT 21: SLIGHTLY ALTERED VESICULAR AUGITE-PLAGIOCLASE-PHYRIC BASALT

Pieces 10-14

PHENOCRYSTS: Clinopyroxene - Microphenocrysts, <5%, 1 mm.
Plagioclase - 5-10%, 1 mm.
Remainder is intersertal matrix (plagioclase-clinopyroxene-opaque).
GROUNDMASS: Phaneritic, fine grained. No visible glass.
COLOR: Black.
VESICLES: 0.5-5.0 mm, elliptical, uniformly distributed in most pieces, but some show segregation.
ALTERATION: Groundmass slightly altered to green clay. Vesicles coated with clay, zeolite. Surface (fractures) contain zeolites and rare pyrite.
VEINS/FRACTURES: One hairline fracture in Piece 12, otherwise only on surface.

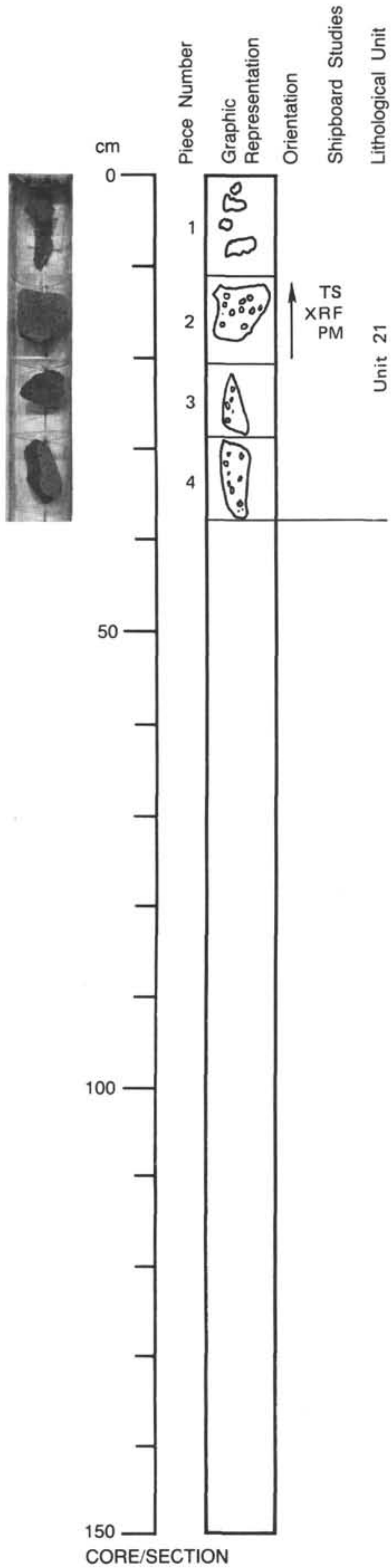

115-706C-6R-2

UNIT 21 (CONTINUED): SLIGHTLY ALTERED VESICULAR AUGITE-PLAGIOCLASE-PHYRIC BASALT

Pieces 1–4

Continuous with 115-706C-6R-1, Unit 21

SITE 706 HOLE C CORE 7R CORED INTERVAL 2600.1-2609.8 mbsl; 92.6-102.3 mbsf

TIME-ROCK UNIT	BIOSTRAT. ZONE/ FOSSIL CHARACTER: FORAMINIFERS	NANNOFOSSILS	RADIOLARIANS	DIATOMS	PALEOMAGNETICS	PHYS. PROPERTIES	CHEMISTRY	SECTION	METERS	GRAPHIC LITHOLOGY	DRILLING DISTURB.	SED. STRUCTURES	SAMPLES	LITHOLOGIC DESCRIPTION
?								1	0.5 1.0		X			**CARBONATE SAND and BASALTIC RUBBLE, overlying BASALT** Major lithology: Fine to coarse basaltic sand and rubble, black (N/2), mixed with coarse carbonate sand, white (N/8), containing pteropods, echinoid spines, bivalves, and coral fragments, in Section 1, 0 cm, through Section 3, 70 cm. Overlies vesicular plagioclase-phyric basalt in the CC. (See hard-rock barrel sheets for detailed description of these basalts).
								2			X			
								3			X			
								CC						

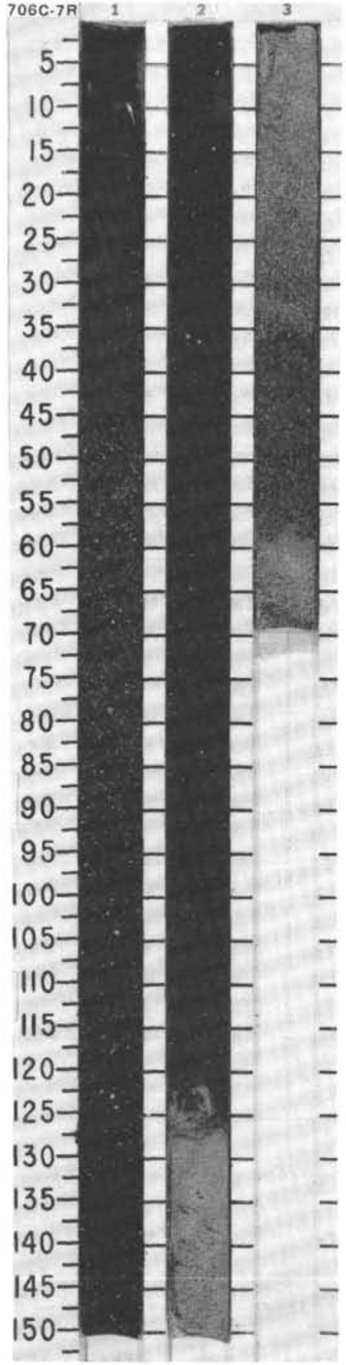

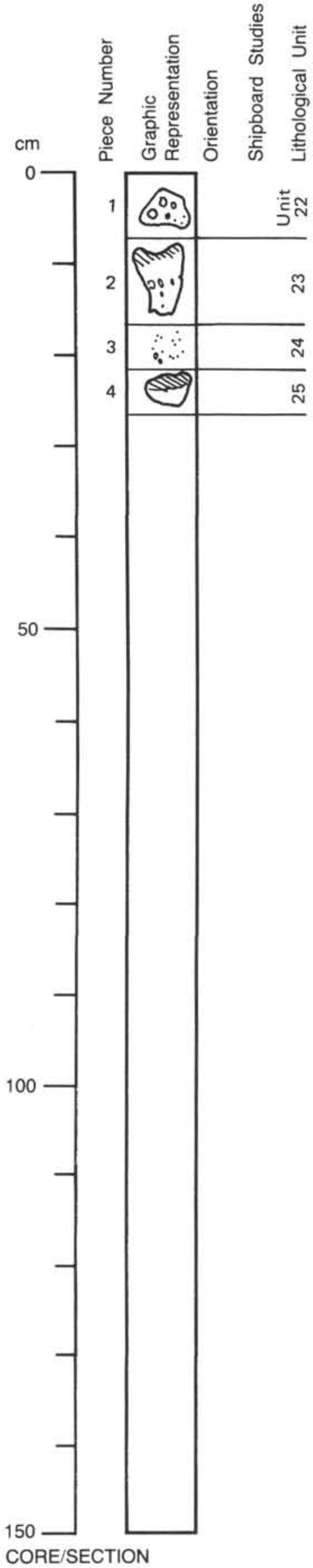

115-706C-7R-CC

UNIT 22: HIGHLY VESICULAR PLAGIOCLASE-PHYRIC BASALT

Piece 1

PHENOCRYSTS: Plagioclase, euhedral, fresh, as long as 1 mm, forms ≈15% of rock.
GROUNDMASS: Middle part of rock is relatively glassy.
COLOR: Dark gray (N4).
VESICLES: Ellipsoidal, ≈20%. Holocrystalline part contains larger amounts of vesicles than glassy part.
ALTERATION: Slightly altered.

UNIT 23: VESICULAR PLAGIOCLASE-PHYRIC BASALT

Piece 2

PHENOCRYSTS: Plagioclase, euhedral, fresh (same as Unit 22).
GROUNDMASS: Top 1 cm is glassy, the other part is fine grained, nearly holocrystalline.
COLOR: Dark gray (N4).
VESICLES: Larger vesicles (≈5 mm, irregular) are scattered heterogeneously. Smaller vesicles (averaging 1 mm, round) are evenly distributed.
ALTERATION: Slightly altered.

UNIT 24: RUBBLE

Piece 3

COLOR: Black (N2).
STRUCTURE: Coarse basaltic rubble, from coring and collapse.

UNIT 25: SLIGHTLY TO MODERATELY VESICULAR PLAGIOCLASE-PHYRIC BASALT

Piece 4

PHENOCRYSTS: Plagioclase, euhedral, fresh (same as Units 22 and 23).
GROUNDMASS: Lower half nearly holocrystalline, upper half glassy.
COLOR: Dark gray (N4, N3).
VESICLES: Homogeneously distributed, round, average size 0.5 mm, ≈10%.
ALTERATION: Slightly altered.

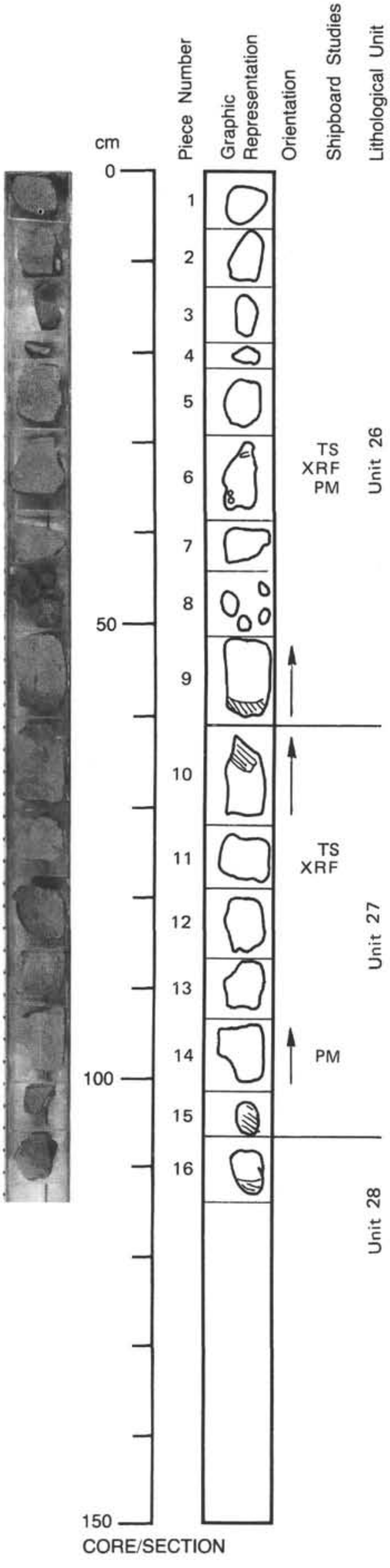

115-706C-8R-1

UNIT 26: SLIGHTLY VESICULAR, FINE-GRAINED PLAGIOCLASE PHYRIC BASALT

Pieces 1-9

CONTACTS: Chilled border at base of Piece 9. The upper core may be absent or in the previous core.

PHENOCRYSTS: Uniformly distributed, euhedral, fresh, as large as 2 mm, ≈15%.

GROUNDMASS: Phaneritic, intersertal, generally holocrystalline. Pieces 2 and 6, and the bottom of Piece 7, are glassy.

COLOR: Dark gray (N3).

VESICLES: Irregular to ellipsoidal, as large as 4 mm, generally uniformly distributed. As much as 15%, often infilled or lined with gray green celadonite(?), otherwise empty.

ALTERATION: Generally slight, but Piece 5 moderate. (Note: Piece 5 is somewhat anomalous with respect to those on either side, and may be misplaced.) Glassy margin on Piece 4 is celadonite.

UNIT 27: SLIGHTLY VESICULAR, FINE-GRAINED PLAGIOCLASE PHYRIC BASALT

Pieces 10-15

PHENOCRYSTS: Plagioclase, as large as 3 mm, fresh, euhedral, uniformly distributed, as much as 15% of rock.

GROUNDMASS: Dominantly intersertal texture. Hypocrystalline in places, especially at upper contact (Piece 10), one margin of Pieces 12 and 13, and a lower contact (Piece 15).

COLOR: Dark gray (N3).

VESICLES: Uniformly distributed, irregularly ellipsoidal, larger vesicles are present away from contacts, <1-4 mm in size, ≈10% byrohime. Vesicles are generally empty, occasionally filled by greenish clay (celadonite?).

ALTERATION: Slight, gray green clay. Top part of upper contact altered to green celadonite (Piece 10).

UNIT 28: SLIGHTLY ALTERED, SLIGHTLY VESICULAR PLAGIOCLASE PHYRIC BASALT

Piece 16

See next core section, 115-706C-8R-2

CONTACTS: Chilled contact border with Unit 27.

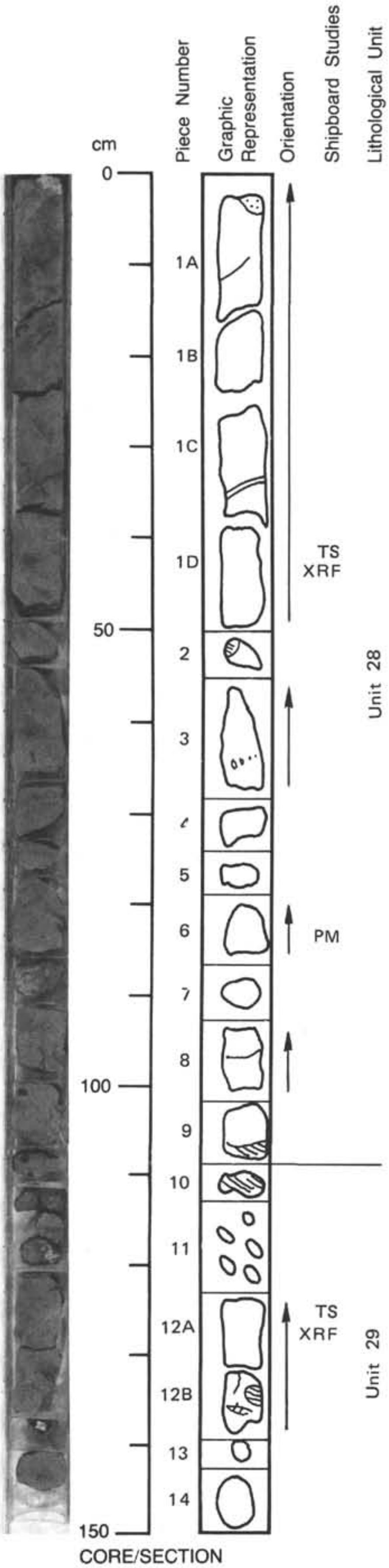

115-706C-8R-2

UNIT 28 (CONTINUED): SLIGHTLY ALTERED, SLIGHTLY VESICULAR PLAGIOCLASE PHYRIC BASALT

Pieces 1-9

Continuous with 115-706C-8R-1, Unit 28

CONTACTS: Chilled contact border, Piece 9.
PHENOCRYSTS: Plagioclase, fresh, euhedral, as large as 3 mm in diameter, uniformly distributed, composes as much as 15% of rock.
GROUNDMASS: Intersertal texture, generally holocrystalline, locally hypocrystalline (top of Piece 1C; Pieces 3 and 6; and Piece 9, lower contact).
COLOR: Generally dark gray (N3).
VESICLES: Slightly vesicular, as much as 5% of rock. Uniformly distributed, as large as 3 mm in diameter. Occasional vesicle trains and blisters developed parallel to high angle fractures in Pieces 1A and 1B. Either empty or lined/infilled with greenish clay (celadonite?).
ALTERATION: Slightly altered, but green phase developed as filling of high angle veins, as thick as 4 mm, which traverse core. Alteration is as wide as 1.5 cm at top of Piece 1A.

UNIT 29: SLIGHTLY ALTERED, SLIGHTLY VESICULAR PLAGIOCLASE PHYRIC BASALT

Pieces 10-14

PHENOCRYSTS: Plagioclase, euhedral, fresh, maximum size 3 mm, ≈15%.
GROUNDMASS: Phaneritic intersertal texture. Piece 12B contains glassy part. Other pieces are generally fine-grained basalt with a small amount of interstitial glass.
COLOR: Dark gray (N3).
VESICLES: Slightly vesicular, ≈5%.
ALTERATION: Slightly altered.

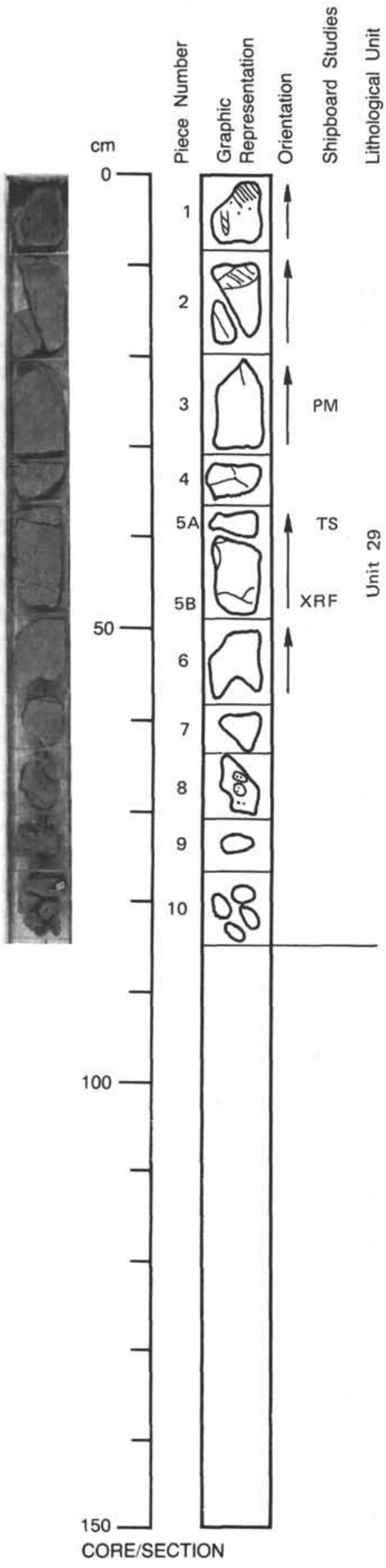

115-706C-8R-3

UNIT 29 (CONTINUED): SLIGHTLY ALTERED, SLIGHTLY VESICULAR PLAGIOCLASE BASALT

Pieces 1–10

Continuous with 115-706C-8R-2, Unit 29

GROUNDMASS: Pieces 1 and 2A contain glassy part.

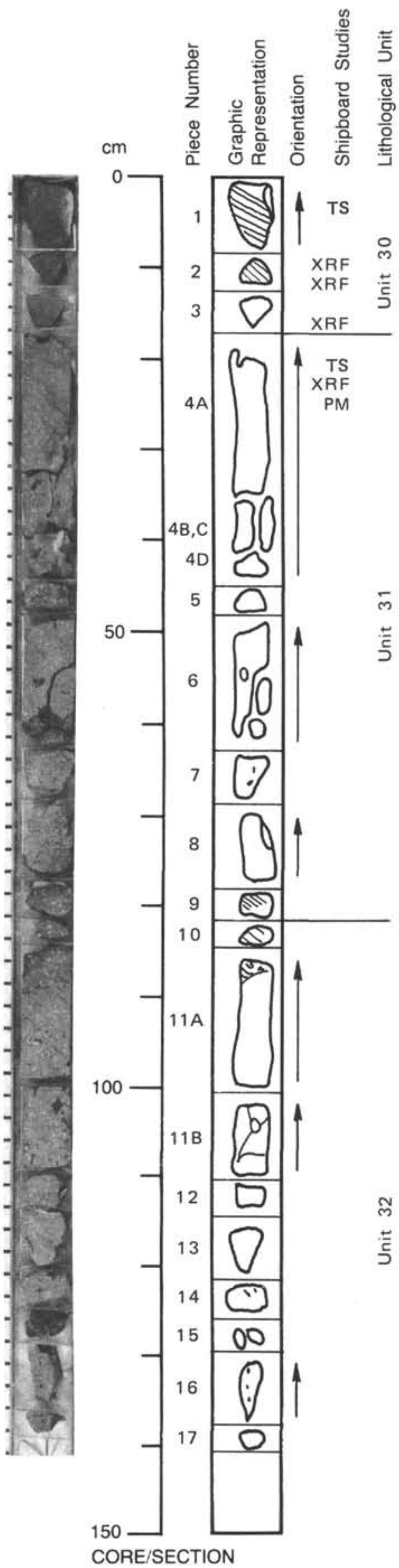

115-706C-9R-1

UNIT 30: FINE-GRAINED, SLIGHTLY VESICULAR HYPOCRYSTALLINE AUGITE-OLIVINE-PLAGIOCLASE-PHYRIC BASALT

Pieces 1–3

PHENOCRYSTS: Plagioclase - Euhedral, fresh, as long as 2 mm, ≈10% of rock, uniformly distributed.
Olivine - Euhedral to subhedral, <0.5 mm in size, less than 5 modal %, completely altered to iddingsite, uniformly distributed.
Augite - Tiny (<0.5 mm), <5 modal %.
GROUNDMASS: Aphanitic to glassy, but partly intergranular.
COLOR: Very dark gray (N3).
VESICLES: Slightly vesicular, irregular, less than 0.5 mm, uniform distribution.
ALTERATION: Very slightly altered gray green clay. Piece 1 has celadonitic chilled rim.

UNIT 31: MODERATELY VESICULAR, PORPHYRITIC AUGITE-OLIVINE-PLAGIOCLASE-PHYRIC BASALT

Pieces 4–9

CONTACTS: Chilled margins at top and bottom.
PHENOCRYSTS: Plagioclase - Euhedral to subhedral, fresh, as large as 1 cm, ≈20% of rock, uniformly distributed.
Olivine - Euhedral to subhedral, smaller than 0.5 mm, much less than 5 modal %, completely iddingsitized, uniformly distributed.
Augite - Fresh, subhedral, smaller than 0.5 mm, much less than 5 modal %, uniformly distributed.
GROUNDMASS: Phaneritic, fine grained, intergranular. Pieces 8 and 9 are glassy.
COLOR: Very dark gray (N3).
VESICLES: Moderately vesicular, as large as 4 mm, ≈10% of rock. Some aggregated (Piece 6C). Generally empty, but some filled with green-gray clay.
ALTERATION: Generally slightly altered. Glassy contact at bottom of Piece 9 and top of Piece 14 is altered to green-gray clay. Alterated in Piece 4 along the high-angle fracture, 6 mm wide.

UNIT 32: MODERATELY VESICULAR, PORPHYRITIC PLAGIOCLASE-PHYRIC BASALT

Pieces 10–17

PHENOCRYSTS: Plagioclase, olivine, and augite.
GROUNDMASS: Phaneritic, fine grained, intergranular.
COLOR: Very dark gray (N3).
VESICLES: Moderately vesicular.
ALTERATION: Generally slightly altered.

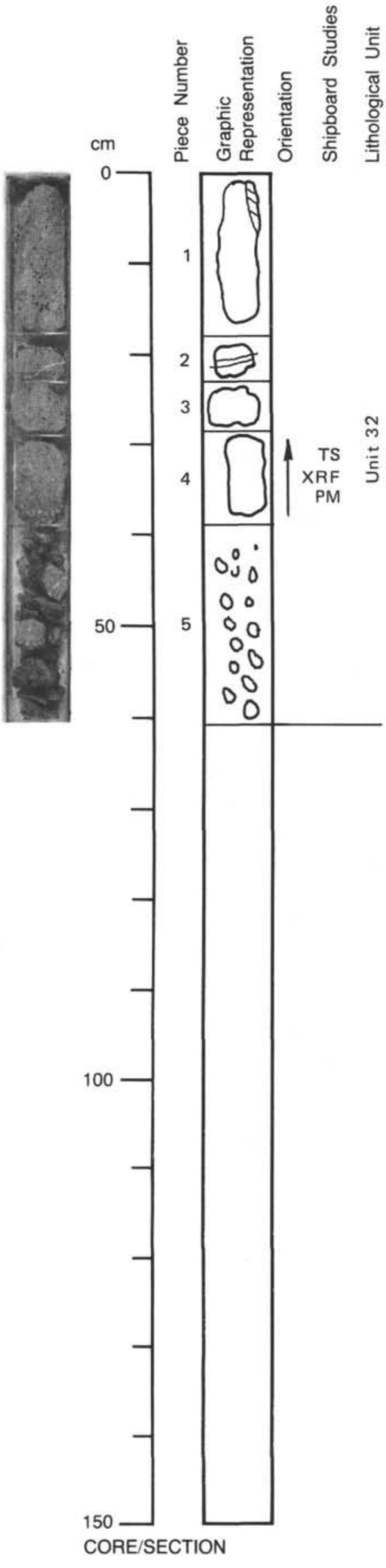

115-706C-9R-2

UNIT 32 (CONTINUED): MODERATELY VESICULAR, PORPHYRITIC AUGITE-OLIVINE-PLAGIOCLASE-PHYRIC BASALT

Pieces 1–5

Continuous with 115-706C-9R-1, Unit 32

CONTACTS: The top of unit (Piece 10) is glassy chilled rim.

THIN SECTION DESCRIPTION

115-706A-6H-CC (Piece 1, 20-27 cm)

ROCK NAME: Highly clinopyroxene plagioclase phyric basalt

WHERE SAMPLED: Unit 3

TEXTURE: Highly porphyritic, vesicular

GRAIN SIZE: Fine, hypocrystalline

OBSERVER: ANB

PRIMARY MINERALOGY	PERCENT PRESENT	PERCENT ORIGINAL	SIZE RANGE (mm)	APPROX. COMPOSITION	MORPHOLOGY	COMMENTS
PHENOCRYSTS						
Plagioclase	15	15	0.2–1.0	An 60	Euhedral–subhedral	Fresh. Quench morphology.
Clinopyroxene	5	5	0.4–0.8	Augite	Subhedral	Subophitic.
GROUNDMASS						
Plagioclase	5	5	0.05–0.20	An 44-60		
Clinopyroxene	5	5	0.04–0.08	Augite		
Spinel	5	5	0.04–0.08	Magnetite		
Glass	—	65				Interstitial. Completely devitrified to cpx + magnetite + plag + clay.

SECONDARY MINERALOGY	PERCENT	REPLACING/ FILLING	COMMENTS
Clays	10	Glass	Devitrification alteration product.
Magnetite	5	Glass	Devitrification product.
Clinopyroxene	35	Glass	Augite. Devitrification products.
Plagioclase	15	Glass	Devitrification products.

VESICLES/ CAVITIES	PERCENT	LOCATION	SIZE RANGE (mm)	FILLING	SHAPE	COMMENTS
Vesicles	20	Even	0.02–8 .00	Glass	Irregular	Essentially two generations: fine vesicles in groundmass, always filled with celadonite; larger vesicles lined with glass.

THIN SECTION DESCRIPTION

115-706B-7X-CC (Piece 2, 20-27 cm)

ROCK NAME: Highly olivine-bearing clinopyroxene plagioclase phyric basalt
WHERE SAMPLED: Unit 3
TEXTURE: Highly porphyritic, vesicular
GRAIN SIZE: Fine
OBSERVER: YT

PRIMARY MINERALOGY	PERCENT PRESENT	PERCENT ORIGINAL	SIZE RANGE (mm)	APPROX. COMPO-SITION	MORPHOLOGY	COMMENTS
PHENOCRYSTS						
Olivine	Tr	3	0.2–0.3	Fo 80(?)	Euhedral	Only one crystal is fresh. Other crystals are completely altered to clays(?).
Plagioclase	15	15	0.2–0.8	An 60	Euhedral	Fresh. An 70-55.
Clinopyroxene	7	7	0.2–0.4	Augite	Euhedral–subhedral	Fresh.
GROUNDMASS						
Plagioclase	2	2	<0.2		Euhedral, acicular	
Clinopyroxene	1	1	<0.2	Augite		
Quench crystals, glass	72	72	<0.1		Dendritic	Magnetite + cpx.

SECONDARY MINERALOGY	PERCENT	REPLACING/ FILLING	COMMENTS
Clays	Tr	Glass	
Clays	3	Ol	Possibly iddingsite.

VESICLES/ CAVITIES	PERCENT	LOCATION	SIZE RANGE (mm)	FILLING	SHAPE	COMMENTS
Vesicles	30	Even	0.1–4.0		Irregular, elliptical	Vesicles near the crack are filled with pale green clays.

COMMENTS: Glass is brown and fresh except for glass near the crack which is altered to clays. Crack is filled with brown and green clays. Brown core may be devitrification products. Green clay also possibly devitrification product.

THIN SECTION DESCRIPTION

115-706B-7X-CC (Piece 3, 27-34 cm)

ROCK NAME: Highly olivine clinopyroxene plagioclase phyric basalt

WHERE SAMPLED: Unit 4

TEXTURE: Highly porphyritic, vesicular

GRAIN SIZE: Fine

OBSERVER: YT

PRIMARY MINERALOGY	PERCENT PRESENT	PERCENT ORIGINAL	SIZE RANGE (mm)	APPROX. COMPOSITION	MORPHOLOGY	COMMENTS
PHENOCRYSTS						
Olivine	—	3	≈0.3		Euhedral–subhedral	Completely altered to iddingsite.
Plagioclase	10	10	0.2–0.8	An 60	Euhedral	Fresh. Zoned approximately An 70 to An 80.
Clinopyroxene	10	10	0.2–0.4	Augite	Euhedral–subhedral	Zoned, fresh crystals.
GROUNDMASS						
Plagioclase	5	5	<0.2		Acicular, euhedral	
Clinopyroxene	5	5	<0.2	Augite		
Glass	—	30				Altered or devitrified to clay.
Quench crystals	37	37	<0.6	Magnetite + cpx	Acicular	Quench product.

SECONDARY MINERALOGY	PERCENT	REPLACING/FILLING	COMMENTS
Clays	30	Glass	Unidentifiable fine-grained aggregate.
Clays	3	Ol	Possibly iddingsite.

VESICLES/CAVITIES	PERCENT	LOCATION	SIZE RANGE (mm)	FILLING	SHAPE
Vesicles	15	Even	0.1–2.0	None	Irregular

THIN SECTION DESCRIPTION

115-706B-7X-CC (Piece 4, 34-41 cm)

ROCK NAME: Highly olivine clinopyroxene plagioclase phyric basalt

WHERE SAMPLED: Unit 5

TEXTURE: Highly porphyritic, vesicular

GRAIN SIZE: Fine

OBSERVER: YT

PRIMARY MINERALOGY	PERCENT PRESENT	PERCENT ORIGINAL	SIZE RANGE (mm)	APPROX. COMPOSITION	MORPHOLOGY	COMMENTS
PHENOCRYSTS						
Olivine	—	2	0.2–0.4		Euhedral	Completely altered to clays.
Plagioclase	15	15	0.2–0.8	An 55	Euhedral	Fresh. Zoned approximately An 70 to An 40.
Clinopyroxene	7	7	0.2–0.5	Augite	Euhedral–subhedral	Fresh. Some zoned crystals.
GROUNDMASS						
Plagioclase	5	5	<0.2		Acicular, euhedral	Fresh.
Clinopyroxene	5	5	<0.2	Augite		Fresh.
Glass		—	20			Devitrified to fine minerals.
Quench crystals	46	46	<0.6	Magnetite, cpx	Acicular	Quench products.

SECONDARY MINERALOGY	PERCENT	REPLACING/FILLING	COMMENTS
Clays	20	Glass	Composed of unidentifiable fine-grained crystals.
Clays	2	Ol	Possibly iddingsite.

VESICLES/CAVITIES	PERCENT	LOCATION	SIZE RANGE (mm)	FILLING	SHAPE
Vesicles	25	Even	0.1–2.0	None	Irregular

THIN SECTION DESCRIPTION

115-706B-7X-CC (Piece 5, 41-50 cm)

ROCK NAME: Highly olivine clinopyroxene plagioclase phyric basalt

WHERE SAMPLED: Unit 6

TEXTURE: Highly porphyritic

GRAIN SIZE: Fine, aphanitic to phaneritic

OBSERVER: ANB

PRIMARY MINERALOGY	PERCENT PRESENT	PERCENT ORIGINAL	SIZE RANGE (mm)	APPROX. COMPO-SITION	MORPHOLOGY	COMMENTS
PHENOCRYSTS						
Olivine	—	3	<0.5		Subhedral–anhedral	Iddingsite + green clay pseudomorphs after ol.
Plagioclase	15	15	0.1–1.0	An 60	Euhedral–subhedral	
Clinopyroxene	3	3	0.2–0.5	Augite	Subhedral	
GROUNDMASS						
Glass	—	44				Interstitial. Filled with quench phases and olive green clays.
Spinel	15	15	<0.1	Magnetite	Laths	Quench laths in glass.
Clinopyroxene	15	15	<0.1	Augite	Prisms	Quench prisms in glass.
Plagioclase	5	5	<0.1	An 60(?)	Needles	Quench needles in glass.

SECONDARY MINERALOGY	PERCENT	REPLACING/ FILLING	COMMENTS
Clays	44	Glass	Associated with quench phases in glass.
Clays	3	Ol	Pseudomorphs after ol.
Zeolites	Tr	Vesicles	Tabular primarily white to colorless crystals with straight extinction. Possibly gypsum.

VESICLES/ CAVITIES	PERCENT	LOCATION	SIZE RANGE (mm)	FILLING	SHAPE	COMMENTS
Vesicles	5	Even	0.2–4.0	Glass, clays	Irregular, elliptical	Large vesicles empty or lined with glass + brown alteration products ± zeolites. Small vesicles filled with brown-green alteration clays.

THIN SECTION DESCRIPTION

115-706B-7X-CC (Piece 6, 50-60 cm)

ROCK NAME: Highly clinopyroxene plagioclase phyric basalt

WHERE SAMPLED: Unit 7

TEXTURE: Highly porphyritic, vesicular

GRAIN SIZE: Fine

OBSERVER: YT

PRIMARY MINERALOGY	PERCENT PRESENT	PERCENT ORIGINAL	SIZE RANGE (mm)	APPROX. COMPO-SITION	MORPHOLOGY	COMMENTS
PHENOCRYSTS						
Plagioclase	15	15	0.3–0.8	An 50-60	Euhedral	Fresh, zoned crystals.
Clinopyroxene	5	5	0.2–0.5	Augite	Subhedral	Fresh. Subophitic.
GROUNDMASS						
Plagioclase	10	10	<0.2	An 50		
Clinopyroxene	10	10	<0.1	Augite		Quench products.
Opaques	10	10	<0.6	Magnetite	Dendritic	Quench products.
Glass	—	50				Completely altered to brown clay.

SECONDARY MINERALOGY	PERCENT	REPLACING/ FILLING	COMMENTS
Clays	50	Glass	Devitrification and alteration products.

VESICLES/ CAVITIES	PERCENT	LOCATION	SIZE RANGE (mm)	FILLING	SHAPE	COMMENTS
Vesicles	20	Even	<2	Clay	Round	Partially filled by green and brown clays.

THIN SECTION DESCRIPTION

115-706B-7X-CC (Piece 7, 60-67 cm)

ROCK NAME: Highly olivine clinopyroxene plagioclase phyric basalt
WHERE SAMPLED: Unit 8, bottom of unit
TEXTURE: Highly porphyritic, vesicular
GRAIN SIZE: Aphanitic, holohyaline
OBSERVER: ANB

PRIMARY MINERALOGY	PERCENT PRESENT	PERCENT ORIGINAL	SIZE RANGE (mm)	APPROX. COMPOSITION	MORPHOLOGY	COMMENTS
PHENOCRYSTS						
Olivine	—	2	0.1–0.3		Subhedral–anhedral	Completely altered to iddingsite.
Plagioclase	15	15	0.2–1.0	An 60	Subhedral–euhedral	Fresh. Quench terminations. Larger crystals are poikilitic, enclosing glass.
Clinopyroxene	8	8	0.1–0.5	Augite	Subhedral	Fresh. Tendency to form glomerocrysts. Zoning to brown Fe-rich margins.
GROUNDMASS						
Glass	70	75				Occasional devitrified patches with magnetite + cpx. Some alteration to yellow clays.

SECONDARY MINERALOGY	PERCENT	REPLACING/ FILLING
Clays	5	Glass
Iddingsite	2	Ol

VESICLES/ CAVITIES	PERCENT	LOCATION	SIZE RANGE (mm)	FILLING	SHAPE	COMMENTS
Vesicles	15	Even	0.02–0.80	Clays	Irregular	Olive-yellow clays.

THIN SECTION DESCRIPTION

115-706C-2R-1 (Piece 3, 70-72 cm)

ROCK NAME: Highly olivine clinopyroxene plagioclase phyric basalt
WHERE SAMPLED: Unit 1
TEXTURE: Highly porphyritic, hypocrystalline
GRAIN SIZE: Aphanitic
OBSERVER: JDG

PRIMARY MINERALOGY	PERCENT PRESENT	PERCENT ORIGINAL	SIZE RANGE (mm)	APPROX. COMPOSITION	MORPHOLOGY	COMMENTS
PHENOCRYSTS						
Olivine	—	2				
Plagioclase	15	15	<0.7	An 62	Euhedral	Unoriented. Slightly zoned.
Clinopyroxene	10	10	<0.3	Augite		Often slightly zoned with rings of opaque inclusions.
GROUNDMASS						
Glass	55	55				Spectacularly well-preserved glass. Cryptocrystalline. Opaque. The glass in half of the slide is devitrified.

SECONDARY MINERALOGY	PERCENT	REPLACING/ FILLING	COMMENTS
Clays	20	Ol, vesicles	Brown and green clays (3:1 ratio) line vesicles. Zoning from edge to center of vesicles: dark brown, nearly isotropic mineral; light olive green fibrous anisotropic mineral; light olive green fibrous mineral with higher birefringence (first order yellow); dark brown, nearly isotropic mineral.

VESICLES/ CAVITIES	PERCENT	LOCATION	SIZE RANGE (mm)	FILLING	SHAPE	COMMENTS
Vesicles	35		1.6	Various	Oval	Vesicles are more oval in glassy areas. Alteration minerals filling vesicles are zoned inward. Vesicle centers are empty.

COMMENTS: Half of the slide has a glassy groundmass. Other half has cryptocrystalline groundmass.

THIN SECTION DESCRIPTION

115-706C-2R-1 (Piece 4, 76-80 cm)

ROCK NAME: Highly olivine clinopyroxene plagioclase phyric basalt

WHERE SAMPLED: Unit 4

TEXTURE: Highly porphyritic, hypocrystalline

GRAIN SIZE: Aphanitic

OBSERVER: JDG

PRIMARY MINERALOGY	PERCENT PRESENT	PERCENT ORIGINAL	SIZE RANGE (mm)	APPROX. COMPO-SITION	MORPHOLOGY	COMMENTS
PHENOCRYSTS						
Olivine	—	5			Euhedral	Altered to brown clays.
Plagioclase	15	15	51	An 60		Zoned. Some glomerocrysts.
Clinopyroxene	10	10	<0.5	Augite		Zoned.
Opaques	(?)	(?)				Possibly some opaque inclusions in cpx.
GROUNDMASS						
Fine crystals	40	40				Cryptocrystalline, opaque + cpx(?).

SECONDARY MINERALOGY	PERCENT	REPLACING/ FILLING	COMMENTS
Clays	30	Vesicles	Brown clays. Show dark to tan color zonation inward toward vesicle center.
Clays	5	Ol	Pseudomorph after ol.

VESICLES/ CAVITIES	PERCENT	LOCATION	SIZE RANGE (mm)	FILLING	SHAPE	COMMENTS
Vesicles	35		52	Clays	Oval, irregular	Large variation in size, from <0.1 mm to 2 mm. Filled with brown clays.

COMMENTS: One end of sample contains unaltered glass. Vesicles in glass tend to be more regular (oval) in shape; tiny vesicles are absent.

THIN SECTION DESCRIPTION

115-706C-2R-1 (Piece 8, 98-101 cm)

ROCK NAME: Highly olivine clinopyroxene plagioclase phyric basalt

WHERE SAMPLED: Top of Unit 2

TEXTURE: Highly porphyritic, vesicular

GRAIN SIZE: Fine

OBSERVER: YT

PRIMARY MINERALOGY	PERCENT PRESENT	PERCENT ORIGINAL	SIZE RANGE (mm)	APPROX. COMPO-SITION	MORPHOLOGY	COMMENTS
PHENOCRYSTS						
Olivine	—	4	0.2–0.4		Euhedral	Completely altered to clay.
Plagioclase	15	15	0.2–0.7	An 55	Euhedral	Fresh. Zoned An 65 to An 40. Some glomerocrysts with other phenocrysts.
Clinopyroxene	7	7	0.2–0.5	Augite	Euhedral–subhedral	Fresh. Zoned crystals. Some glomerocrysts with other phenocrysts.
GROUNDMASS						
Plagioclase	1	1	<0.2			
Clinopyroxene	1	1	<0.2			
Glass	47	47				Cpx (<<0.1 mm) shows radial quench texture in glass. Fresh brown glass near the top of the section.

SECONDARY MINERALOGY	PERCENT	REPLACING/ FILLING	COMMENTS
Clays	4	Ol	Looks like the same clay lining vesicles.
Clays	25	Vesicles	Looks like the same clay replacing ol.

VESICLES/ CAVITIES	PERCENT	LOCATION	SIZE RANGE (mm)	FILLING	SHAPE	COMMENTS
Vesicles	25	Even	0.1–1.0	Clay	Irregular	Rimmed by dark brown clay minerals.

THIN SECTION DESCRIPTION

115-706C-2R-1 (Piece 11, 127-128 cm)

ROCK NAME: Highly olivine clinopyroxene plagioclase phyric basalt

WHERE SAMPLED: Unit 2

TEXTURE: Highly porphyritic

GRAIN SIZE: Fine, aphanitic to phaneritic

OBSERVER: ANB

PRIMARY MINERALOGY	PERCENT PRESENT	PERCENT ORIGINAL	SIZE RANGE (mm)	APPROX. COMPO-SITION	MORPHOLOGY	COMMENTS
PHENOCRYSTS						
Olivine	—	2	<0.5		Subhedral–anhedral	Completely altered to green clay ± iddingsite.
Plagioclase	21	21	0.1–1.0	An 60	Euhedral–subhedral	Normal zoning.
Clinopyroxene	5	5	0.2–0.5	Augite	Subhedral	Concentric zoning to more Fe-rich margins.
GROUNDMASS						
Plagioclase	14	14	<0.1		Quench	Quench phases in altered glass.
Clinopyroxene	21	21	<0.1	Augite	Quench	Quench phases in altered glass.
Glass	—	21				Interstitial. Devitrified and quench phases altered to clays.
Spinel	16	16	<0.5	Magnetite	Quench	Quench phases in altered glass.

SECONDARY MINERALOGY	PERCENT	REPLACING/ FILLING	COMMENTS
Clays	21	Glass	Associated with quench phases in altered glass.

VESICLES/ CAVITIES	PERCENT	LOCATION	SIZE RANGE (mm)	FILLING	SHAPE	COMMENTS
Vesicles	15	Even	0.2–3.0	Green clays	Irregular, elliptical	Small vesicles invariably completely filled. Large vesicles are generally lined.

THIN SECTION DESCRIPTION

115-706C-2R-2 (Piece 2, 2-4 cm)

ROCK NAME: Highly olivine-bearing clinopyroxene plagioclase phyric basalt

WHERE SAMPLED: Unit 3, near top of unit

TEXTURE: Highly porphyritic

GRAIN SIZE: Fine

OBSERVER: YT

PRIMARY MINERALOGY	PERCENT PRESENT	PERCENT ORIGINAL	SIZE RANGE (mm)	APPROX. COMPO-SITION	MORPHOLOGY	COMMENTS
PHENOCRYSTS						
Olivine	—	<1	<0.2		Euhedral–subhedral	Completely altered to iddingsite and/or clays.
Plagioclase	7	7	0.2–0.7	An 60	Euhedral	Fresh.
Clinopyroxene	5	5	0.2–0.5		Euhedral–subhedral	Some sector-zoned crystals. Fresh.
GROUNDMASS						
Plagioclase	1	1	<0.2		Euhedral	
Clinopyroxene	1	1	<0.2	Augite	Euhedral	
Glass, quench crystals	76	76			Needles, dendritic	Quench products are probably cpx + magnetite. Some fresh brown glass at one end of slide.

SECONDARY MINERALOGY	PERCENT	REPLACING/ FILLING	COMMENTS
Clays	10	Vesicles	Green to pale brown clays.

VESICLES/ CAVITIES	PERCENT	LOCATION	SIZE RANGE (mm)	FILLING	SHAPE	COMMENTS
Vesicles	30	Even	<2	Clay	Round, irregular	Vesicles more abundant in glassy areas. Green to brown clay filling.

COMMENTS: One end of sample contains unaltered glass.

THIN SECTION DESCRIPTION

115-706C-2R-2 (Piece 5, 20-24 cm)

ROCK NAME: Highly olivine clinopyroxene plagioclase phyric basalt

WHERE SAMPLED: Unit 4, middle of unit

TEXTURE: Highly porphyritic, vesicular

GRAIN SIZE: Fine, hypocrystalline

OBSERVER: ANB

PRIMARY MINERALOGY	PERCENT PRESENT	PERCENT ORIGINAL	SIZE RANGE (mm)	APPROX. COMPO-SITION	MORPHOLOGY	COMMENTS
PHENOCRYSTS						
Olivine	—	2	0.1–0.3		Subhedral	Completely altered to iddingsite. Very difficult to distinguish from small infilled vesicles.
Plagioclase	10	10	0.04–1.00	An 62	Subhedral–euhedral	Fresh. Quench forms. Inclusions of glass.
Clinopyroxene	3	3	0.1–0.5	Augite	Subhedral	Fresh. Zoned.
GROUNDMASS						
Plagioclase	1	1	<0.4		Subhedral	Often as microlites.
Glass	—	84				Interstitial. Extensively devitrified and altered to clays.

SECONDARY MINERALOGY	PERCENT	REPLACING/ FILLING
Clays	34	Glass
Magnetite	10	Glass
Clinopyroxene	40	Glass
Iddingsite	2	Ol

VESICLES/ CAVITIES	PERCENT	LOCATION	SIZE RANGE (mm)	FILLING	SHAPE	COMMENTS
Vesicles	20	Even	0.1–4.0	Clays	Irregular, elliptical	Olive-yellow clays. Only small vesicles in groundmass are infilled. Larger, apparently later vesicles are empty or thinly lined with the same clays.

THIN SECTION DESCRIPTION

115-706C-2R-2 (Piece 8, 42-47 cm)

ROCK NAME: Highly olivine-bearing clinopyroxene plagioclase phyric basalt

WHERE SAMPLED: Unit 5, middle of unit

TEXTURE: Highly porphyritic

GRAIN SIZE: Fine

OBSERVER: YT

PRIMARY MINERALOGY	PERCENT PRESENT	PERCENT ORIGINAL	SIZE RANGE (mm)	APPROX. COMPO-SITION	MORPHOLOGY	COMMENTS
PHENOCRYSTS						
Olivine	—	1	0.1–0.2		Subhedral	Completely altered to brown clay or iddingsite.
Plagioclase	10	10	0.1–1.0	An 60	Euhedral–subhedral	Fresh.
Clinopyroxene	5	5	0.1–0.8	Augite	Euhedral–subhedral	Fresh. Zoned.
GROUNDMASS						
Plagioclase	1	1	<0.1		Subhedral	Fresh.
Clinopyroxene	1	1	<0.1			Fresh.
Opaque	3	3	<0.3		Dendritic	Quench products.
Glass	—	79				Completely altered to clays.

SECONDARY MINERALOGY	PERCENT	REPLACING/ FILLING	COMMENTS
Clays	79	Glass	Very fine-grained aggregate from glass devitrification/alteration.
Iddingsite	1	Ol	Brown clay or iddingsite.

VESICLES/ CAVITIES	PERCENT	LOCATION	SIZE RANGE (mm)	FILLING	SHAPE	COMMENTS
Vesicles	20	Even	<3	Clay	Irregular	Filled by brown and green clays.

THIN SECTION DESCRIPTION

115-706C-2R-2 (Piece 12, 77-80 cm)

ROCK NAME: Highly olivine-bearing clinopyroxene plagioclase phyric basalt
WHERE SAMPLED: Unit 6
TEXTURE: Microporphyritic
GRAIN SIZE: Fine
OBSERVER: RBH

PRIMARY MINERALOGY	PERCENT PRESENT	PERCENT ORIGINAL	SIZE RANGE (mm)	APPROX. COMPOSITION	MORPHOLOGY	COMMENTS
PHENOCRYSTS						
Olivine	—	Tr	0.1			Completely altered to iddingsite or clay.
Plagioclase	12	12	<1	An 70	Subhedral, laths	Average crystal is 0.5 mm. Some skeletal terminations. Zoned.
Clinopyroxene	6	6	≈0.2		Subhedral, prisms	Almost equant crystals, partially enclosing plag. Zoned. Some synneusis texture. Glomerophyric texture.
GROUNDMASS						
Cryptocrystalline groundmass	62	62				Cryptocrystalline (opaque + cpx(?)).

SECONDARY MINERALOGY	PERCENT	REPLACING/ FILLING	COMMENTS
Clays	19	Vesicles, ol	Greenish brown, pale green at one end of section, probably celadonite. Concentrically lining smaller vesicles which are generally filled.
Glass	1	Groundmass	Brownish with pelitic crack.

VESICLES/ CAVITIES	PERCENT	LOCATION	SIZE RANGE (mm)	FILLING	SHAPE	COMMENTS
Vesicles	35	Even		Celadonite		Larger vesicles are empty. Smaller vesicles are filled with celadonite.

COMMENTS: Extremely fresh microporphyritic basalt with conspicuous vesicles. Smaller vesicles filled with greenish celadonite.

THIN SECTION DESCRIPTION

115-706C-2R-2 (Piece 15, 93-94 cm)

ROCK NAME: Highly olivine clinopyroxene plagioclase phyric basalt
WHERE SAMPLED: Unit 7
TEXTURE: Highly porphyritic
GRAIN SIZE: Aphanitic, hyaline
OBSERVER: ANB

PRIMARY MINERALOGY	PERCENT PRESENT	PERCENT ORIGINAL	SIZE RANGE (mm)	APPROX. COMPOSITION	MORPHOLOGY	COMMENTS
PHENOCRYSTS						
Olivine	—	5	<0.5		Subhedral	Completely replaced by olive green clays. Quench textures.
Plagioclase	15	15	0.1-1.0	An 65	Euhedral–subhedral	Quench terminations.
Clinopyroxene	5	5	<0.7	Augite	Subhedral	Hourglass and concentric zoning. Synneusis texture.
GROUNDMASS						
Glass	45	75				Oxidized to opaque-rich amorphous material. Much fresh brown glass still present.

SECONDARY MINERALOGY	PERCENT	REPLACING/ FILLING	COMMENTS
Clays	5	Ol	Olive green clays.
Altered glass	30	Glass	Oxidized and altered glass. Magnetite-rich amorphous material.

VESICLES/ CAVITIES	PERCENT	LOCATION	SIZE RANGE (mm)	FILLING	SHAPE	COMMENTS
Vesicles	20	Even	0.5-2.0	Clays	Subspherical	Variously filled or lined with olive green clays and brown clays.

THIN SECTION DESCRIPTION

115-706C-2R-2 (Piece 19, 115-118 cm)

ROCK NAME: Highly clinopyroxene plagioclase phyric basalt

WHERE SAMPLED: Unit 8

TEXTURE: Highly porphyritic, vesicular

GRAIN SIZE: Fine

OBSERVER: YT

PRIMARY MINERALOGY	PERCENT PRESENT	PERCENT ORIGINAL	SIZE RANGE (mm)	APPROX. COMPO-SITION	MORPHOLOGY	COMMENTS
PHENOCRYSTS						
Olivine	—	5	0.2–0.3		Euhedral	Completely altered to iddingsite. Some inclusions of picolite.
Plagioclase	15	15	0.2–1.0	An 70	Euhedral	Fresh. Zoned An 70 to An 55.
Clinopyroxene	7	7	0.2–0.5	Augite	Euhedral–subhedral	Fresh. Concentric and sector zoning.
GROUNDMASS						
Glass	—	42				Completely replaced by fine-grained minerals.
Opaque + clinopyroxene	30	30			Acicular	Quench products.
Plagioclase	1	1	<0.2			Fresh.
Clinopyroxene	Tr	Tr	<0.2	Augite		Fresh. Groundmass minerals.

SECONDARY MINERALOGY	PERCENT	REPLACING/ FILLING	COMMENTS
Clays	5	Ol	Brown clays. Possibly iddingsite.
Clays	42	Glass	Aggregate of unidentifiable fine-grained minerals. Devitrification and alteration products.

VESICLES/ CAVITIES	PERCENT	LOCATION	SIZE RANGE (mm)	FILLING	SHAPE
Vesicles	20	Even	<2	Brown clay	Irregular, elliptical

THIN SECTION DESCRIPTION

115-706C-2R-2 (Piece 22, 129-133 cm)

ROCK NAME: Highly olivine clinopyroxene plagioclase phyric basalt

WHERE SAMPLED: Unit 9

TEXTURE: Highly porphyritic, holocrystalline

GRAIN SIZE: Aphanitic

OBSERVER: JDG

PRIMARY MINERALOGY	PERCENT PRESENT	PERCENT ORIGINAL	SIZE RANGE (mm)	APPROX. COMPO-SITION	MORPHOLOGY	COMMENTS
PHENOCRYSTS						
Olivine	—	2				Completely altered to green clays.
Plagioclase	28	28	<0.6	An 63		Distinctly zoned.
Clinopyroxene	15	15	<0.5	Augite		Zoned. Contain rings of opaque inclusions. Some glomerocrysts.
GROUNDMASS						
Groundmass	53	53			Anhedral	Augite + plag + opaques. Very fine grained to cryptocrystalline. Percentages of each phase are difficult to accurately estimate. Opaques form needles that tend to radiate; possibly devitrification or quench texture.

SECONDARY MINERALOGY	PERCENT	REPLACING/ FILLING	COMMENTS
Clays	<2	Cracks	Yellow-brown clay mineral fills crack that runs across the thin section.
Clays	2	Ol	

VESICLES/ CAVITIES	PERCENT	LOCATION	SIZE RANGE (mm)	FILLING	SHAPE	COMMENTS
Vesicles	15		<2.5		Irregular	Generally empty. Close to vesicle is phenocryst-free, black opaque cryptocrystalline material.

COMMENTS: Except for small crack filled with green clay minerals, the sample appears very fresh.

THIN SECTION DESCRIPTION

115-706C-2R-2 (Piece 24, 141-144 cm)

ROCK NAME: Highly olivine clinopyroxene plagioclase phyric basalt

WHERE SAMPLED: Unit 10

TEXTURE: Highly porphyritic

GRAIN SIZE: Aphanitic

OBSERVER: JDG

PRIMARY MINERALOGY	PERCENT PRESENT	PERCENT ORIGINAL	SIZE RANGE (mm)	APPROX. COMPOSITION	MORPHOLOGY	COMMENTS
PHENOCRYSTS						
Olivine	—	5	0.2			Completely altered to chlorite(?) + iddingsite.
Plagioclase	29	29	<0.35	An 70	Euhedral	Slightly zoned. Very fresh. Unoriented.
Clinopyroxene	19	19	<0.45	Augite		Zoned. Brownish, especially at edges. Some glomerocrysts.
Spinel	5		<0.30		Needles	Quench or devitrification texture. Tend to radiate from phenocrysts.
GROUNDMASS						
Groundmass	32					Cryptocrystalline, opaque groundmass.

SECONDARY MINERALOGY	PERCENT	REPLACING/ FILLING	COMMENTS
Clays	5	Vesicles	Brown clays. Line the interior of vesicles.
Clays	5	Vesicles, ol	Green clays. Line the interior of vesicles. Formed after brown clays; green clay sometimes occurs further inside vesicles.
Iddingsite	5	Ol	Together with green clays.

VESICLES/ CAVITIES	PERCENT	LOCATION	SIZE RANGE (mm)	FILLING	SHAPE	COMMENTS
Vesicles	5		≈1	Clays	Irregular	Rimmed with brown and green clays.

COMMENTS: A dark band of opaque cryptocrystalline material, largely devoid of phenocrysts but with many (7%) small, somewhat oval vesicles, cuts across the middle of the thin section. Brown color of augite indicates high Ti.

THIN SECTION DESCRIPTION

115-706C-2R-3 (Piece 1, 1-3 cm)

ROCK NAME: Highly olivine-bearing clinopyroxene plagioclase phyric basalt

WHERE SAMPLED: Unit 11

TEXTURE: Highly porphyritic

GRAIN SIZE: Fine

OBSERVER: RBH

PRIMARY MINERALOGY	PERCENT PRESENT	PERCENT ORIGINAL	SIZE RANGE (mm)	APPROX. COMPOSITION	MORPHOLOGY	COMMENTS
PHENOCRYSTS						
Olivine	—	Tr			Subhedral	Completely altered to clay.
Plagioclase	30	30	<1		Subhedral, prismatic, laths	Fresh. Zoned crystals.
Clinopyroxene	15	15	<1		Subhedral, equant	Fresh. Zoned crystals; some sector zoning.
GROUNDMASS						
Opaques	5	5	<0.5		Needles, skeletal	Skeletal/Dendritic crystals from devitrification of glass or quench. Cannot determine if low temperature alteration effects are present.
Glass(?)	—	50				Completely altered to clays.

SECONDARY MINERALOGY	PERCENT	REPLACING/ FILLING	COMMENTS
Clays	50	Glass, plag	Brown to greenish brown clay.
Clays	Tr	Ol	Brown clay + iddingsite.

VESICLES/ CAVITIES	PERCENT	LOCATION	SIZE RANGE (mm)	FILLING	SHAPE	COMMENTS
Vesicles	15	Even		Clay	Elliptical	Mostly empty. Smaller vesicles filled with greenish-brown clay (or celadonite?).

THIN SECTION DESCRIPTION

115-706C-3R-1 (Piece 3, 12-15 cm)

ROCK NAME: Highly olivine clinopyroxene plagioclase phyric basalt

WHERE SAMPLED: Unit 11

TEXTURE: Highly porphyritic, vesicular

GRAIN SIZE: Fine

OBSERVER: YT

PRIMARY MINERALOGY	PERCENT PRESENT	PERCENT ORIGINAL	SIZE RANGE (mm)	APPROX. COMPO-SITION	MORPHOLOGY	COMMENTS
PHENOCRYSTS						
Olivine	—	5	0.1–0.3		Euhedral	Completely altered to iddingsite + chlorite (brown-green clays).
Plagioclase	25	25	0.2–1.0	An 55	Euhedral	Fresh. Zoned, An 70 to An 50.
Clinopyroxene	10	10	0.2–0.5		Euhedral–subhedral	Fresh. Some zoned crystals.
GROUNDMASS						
Plagioclase	1	1	<0.1		Euhedral	
Clinopyroxene	Tr	Tr	<<0.1			
Opaques	25	25	<0.7		Acicular	Shows needle-like texture. Quench products.
Glass	—	34				Completely devitrified to clays + unidentifiable fine-grained minerals.

SECONDARY MINERALOGY	PERCENT	REPLACING/ FILLING	COMMENTS
Clays	5	Ol	Possibly iddingsite + chlorite.
Clays	34	Glass	Aggregates of unidentifiable fine minerals.

VESICLES/ CAVITIES	PERCENT	LOCATION	SIZE RANGE (mm)	FILLING	SHAPE
Vesicles	35	Even	0.2–4	None	Irregular, elliptical

THIN SECTION DESCRIPTION

115-706C-3R-1 (Piece 7, 28-30 cm)

ROCK NAME: Highly olivine clinopyroxene plagioclase phyric basalt
WHERE SAMPLED: Unit 12, top of unit
TEXTURE: Highly porphyritic
GRAIN SIZE: Aphanitic
OBSERVER: ANB

PRIMARY MINERALOGY	PERCENT PRESENT	PERCENT ORIGINAL	SIZE RANGE (mm)	APPROX. COMPO-SITION	MORPHOLOGY	COMMENTS
PHENOCRYSTS						
Olivine	—	5	<0.7		Subhedral–anhedral	Quench forms with axial cavities common. Completely replaced by iddingsite + pale green clays.
Plagioclase	15	15	0.1–1.0	An 60	Euhedral–subhedral	Fresh. Quench terminations common.
Clinopyroxene	5	5	<0.6	Augite	Subhedral	Sub-ophitic in places.
GROUNDMASS						
Glass	25	80				Amorphous brown glass, largely altered to magnetite-rich amorphous material.

SECONDARY MINERALOGY	PERCENT	REPLACING/ FILLING	COMMENTS
Altered glass	55	Glass	Magnetite-rich altered glass.

VESICLES/ CAVITIES	PERCENT	LOCATION	SIZE RANGE (mm)	FILLING	SHAPE	COMMENTS
Vesicles	20	Even	0.3–4.0	Clays	Elliptical	Variously lined or filled with green-brown clays.

THIN SECTION DESCRIPTION

115-706C-3R-1 (Piece 8, 35-38 cm)

ROCK NAME: Highly olivine clinopyroxene plagioclase phyric basalt
WHERE SAMPLED: Unit 12, close to top
TEXTURE: Highly porphyritic
GRAIN SIZE: Aphanitic, hyaline
OBSERVER: ANB

PRIMARY MINERALOGY	PERCENT PRESENT	PERCENT ORIGINAL	SIZE RANGE (mm)	APPROX. COMPO-SITION	MORPHOLOGY	COMMENTS
PHENOCRYSTS						
Olivine	—	3	<0.5		Subhedral–anhedral	Completely altered to iddingsite.
Plagioclase	10	10	0.2–1.0	An 60	Euhedral–subhedral	Fresh. Often with quench terminations.
Clinopyroxene	3	3	<0.8	Augite	Subhedral	Larger crystals contain subophitic plag.
GROUNDMASS						
Glass	—	84				Completely replaced.

SECONDARY MINERALOGY	PERCENT	REPLACING/ FILLING	COMMENTS
Clays	24	Glass	Brown clay often crowded with plag microlites. Associated with alteration of glass to magnetite.
Altered glass	60	Glass	Sometimes crowded with plag microlites.
Zeolites	Tr	Vesicle	Colorless, prismatic primarily gray crystals, 0.5 mm long, with straight extinction. Radiate off vesicle wall.

VESICLES/ CAVITIES	PERCENT	LOCATION	SIZE RANGE (mm)	FILLING	SHAPE	COMMENTS
Vesicles	15	Even	0.2–5.0	Clay, zeolites	Subelliptical	Small vesicles in glass filled with green-brown clays. Much larger vesicle lined with same clay and rare zeolites.

THIN SECTION DESCRIPTION

115-706C-3R-1 (Piece 12D, 83-85 cm)

ROCK NAME: Highly olivine clinopyroxene plagioclase phyric basalt

WHERE SAMPLED: Unit 12

TEXTURE: Highly porphyritic

GRAIN SIZE: Fine, aphanitic, hyaline

OBSERVER: ANB

PRIMARY MINERALOGY	PERCENT PRESENT	PERCENT ORIGINAL	SIZE RANGE (mm)	APPROX. COMPO-SITION	MORPHOLOGY	COMMENTS
PHENOCRYSTS						
Olivine	—	2	<0.4		Subhedral–anhedral	Completely replaced by iddingsite, brown clays and oxides.
Plagioclase	20	20	0.2–1.0	An 60	Euhedral–subhedral	Fresh crystals with quench terminations.
Clinopyroxene	5	5	<0.1	Augite	Subhedral	Zoned to Fe-richer cpx near margins. Subophitic intergrowths with plag in some places.
GROUNDMASS						
Plagioclase	5	5	<0.1		Acicular	Quench products.
Clinopyroxene	5	5	<0.1	Augite	Granular	Quench products.
Glass	—	63				Interstitial. Completely replaced by brown clays + magnetite-rich material.

SECONDARY MINERALOGY	PERCENT	REPLACING/ FILLING	COMMENTS
Clays	20	Glass	Brown clays.
Clays	2	Ol	Iddingsite + brown clays.
Altered glass	43	Glass	Magnetite + unidentifiable fine-grained minerals.

VESICLES/ CAVITIES	PERCENT	LOCATION	SIZE RANGE (mm)	FILLING	SHAPE	COMMENTS
Vesicles	15	Even	<4	Chlorite(?)	Elliptical	Large vesicles lined by green celadonite or chlorite. Small vesicles completely filled by celadonite or chlorite. One exceptional vesicle measures >1 cm in diameter.

THIN SECTION DESCRIPTION

115-706C-3R-1 (Piece 12D, 85-88 cm)

ROCK NAME: Highly olivine clinopyroxene plagioclase phyric basalt

WHERE SAMPLED: Unit 12

TEXTURE: Highly porphyritic, vesicular

GRAIN SIZE: Fine

OBSERVER: YT

PRIMARY MINERALOGY	PERCENT PRESENT	PERCENT ORIGINAL	SIZE RANGE (mm)	APPROX. COMPO-SITION	MORPHOLOGY	COMMENTS
PHENOCRYSTS						
Olivine	—	2	0.2–0.4		Euhedral	Completely altered to iddingsite.
Plagioclase	22	22	0.2–1.0	An 55	Euhedral–subhedral	Fresh. Zoned An 65 to An 50.
Clinopyroxene	13	13	0.2–0.5	Augite	Subhedral	Fresh. Sector or concentrically zoned.
GROUNDMASS						
Plagioclase	19	19	<0.2			
Clinopyroxene	13	13	<0.2	Augite		
Opaques	6	6	<0.5		Needles	Quench texture.
Glass	—	25				Completely replaced by fine-grained minerals.

SECONDARY MINERALOGY	PERCENT	REPLACING/ FILLING	COMMENTS
Clays	25	Glass	Aggregates of unidentifiable fine-grained minerals.
Clays	2	Ol	Possibly iddingsite.

VESICLES/ CAVITIES	PERCENT	LOCATION	SIZE RANGE (mm)	FILLING	SHAPE	COMMENTS
Vesicles	20	Even	0.1–5.0	Clay	Irregular, elliptical	Filled by green-brown clays.

THIN SECTION DESCRIPTION

115-706C-3R-1 (Piece 18, 114-117 cm)

ROCK NAME: Highly olivine clinopyroxene plagioclase phyric basalt

WHERE SAMPLED: Unit 12

TEXTURE: Highly porphyritic, vesicular

GRAIN SIZE: Fine

OBSERVER: YT

PRIMARY MINERALOGY	PERCENT PRESENT	PERCENT ORIGINAL	SIZE RANGE (mm)	APPROX. COMPO-SITION	MORPHOLOGY	COMMENTS
PHENOCRYSTS						
Olivine	—	5	0.2–0.5		Euhedral	Completely replaced by brown (iddingsite?) and green clays (chlorite?).
Plagioclase	10	10	0.2–0.8	An 55	Euhedral	Fresh. Zoned An 40 to An 65.
Clinopyroxene	5	5	0.2–0.6	Augite	Euhedral–subhedral	Fresh.
GROUNDMASS						
Glass }	80	80				Part of the glass is fresh brown glass. Mostly filled with acicular quenched cpx.
Clinopyroxene(?) }			<0.1			

SECONDARY MINERALOGY	PERCENT	REPLACING/ FILLING	COMMENTS
Clays	5	Ol	Iddingsite + chlorite.

VESICLES/ CAVITIES	PERCENT	LOCATION	SIZE RANGE (mm)	FILLING	SHAPE	COMMENTS
Vesicles	30	Even	0.1–3.0	Clay	Round, irregular	Pale green to brown clay filling.

THIN SECTION DESCRIPTION

115-706C-3R-2 (Piece 6, 45-47 cm)

ROCK NAME: Highly olivine clinopyroxene plagioclase phyric basalt

WHERE SAMPLED: Unit 12

TEXTURE: Highly porphyritic, vesicular

GRAIN SIZE: Fine

OBSERVER: YT

PRIMARY MINERALOGY	PERCENT PRESENT	PERCENT ORIGINAL	SIZE RANGE (mm)	APPROX. COMPO-SITION	MORPHOLOGY	COMMENTS
PHENOCRYSTS						
Olivine	—	3	0.1–0.3		Euhedral	Completely altered to brown clay.
Plagioclase	14	14	0.2–0.7	An 55	Euhedral	Fresh. Zoned An 50 to An 60.
Clinopyroxene	5	5	0.2–0.5	Augite	Euhedral	Fresh. Sector zoning.
GROUNDMASS						
Plagioclase	1	1	<0.2		Euhedral	Fresh.
Clinopyroxene	Tr	Tr	<<2		Subhedral	
Clinopyroxene(?)	34	34	<0.5		Acicular	Needle-like quench products.
Glass	—	43				Completely replaced by aggregate of unidentifiable, fine-grained phases.

SECONDARY MINERALOGY	PERCENT	REPLACING/ FILLING	COMMENTS
Clays	3	Ol	Brown clay.
Altered glass	43	Glass	Aggregate of unidentifiable, fine-grained phases.

VESICLES/ CAVITIES	PERCENT	LOCATION	SIZE RANGE (mm)	FILLING	SHAPE
Vesicles	25	Even	<1	None	Irregular, elliptical

THIN SECTION DESCRIPTION

115-706C-4R-1 (Piece 9, 78-80 cm)

ROCK NAME: Highly olivine magnetite clinopyroxene plagioclase phyric basalt

WHERE SAMPLED: Unit 12

TEXTURE: Microporphyritic, vesicular

GRAIN SIZE: Fine to medium

OBSERVER: RBH

PRIMARY MINERALOGY	PERCENT PRESENT	PERCENT ORIGINAL	SIZE RANGE (mm)	APPROX. COMPOSITION	MORPHOLOGY	COMMENTS
PHENOCRYSTS						
Olivine	—	<1	<1		Euhedral	Completely altered to iddingsite.
Plagioclase	25	25	1		Subhedral, laths	
Clinopyroxene	15	15	1		Subhedral, equant	Subophitically encloses plag.
Spinel	2	2	0.5	Titano-magnetite	Skeletal, subhedral	Crystals look homogeneous. May show low temperature alteration.
GROUNDMASS						
Opaques	3	3	0.5		Needles	Probably quench product.
Glass(?)	—	55			Amorphous	Completely altered to brownish-green clay.

SECONDARY MINERALOGY	PERCENT	REPLACING/ FILLING	COMMENTS
Clays	55	Glass(?)	Brownish clay replacing glass(?) and/or cryptocrystalline groundmass.
Iddingsite(?)	<1	Ol	

THIN SECTION DESCRIPTION

115-706C-4R-2 (Piece 15, 117-119 cm)

ROCK NAME: Highly olivine-bearing clinopyroxene plagioclase phyric basalt

WHERE SAMPLED: Unit 12

TEXTURE: Highly porphyritic

GRAIN SIZE: Fine

OBSERVER: ANB

PRIMARY MINERALOGY	PERCENT PRESENT	PERCENT ORIGINAL	SIZE RANGE (mm)	APPROX. COMPOSITION	MORPHOLOGY	COMMENTS
PHENOCRYSTS						
Olivine	—	Tr	<0.2		Subhedral–anhedral	Completely altered to iddingsite or brown clay.
Plagioclase	20	20	<0.7	An 60	Euhedral–subhedral	Fresh crystals. Quench terminations.
Clinopyroxene	2	2	<0.8	Augite	Subhedral	Zoned to slightly titaniferrous margins.
GROUNDMASS						
Plagioclase	5	5			Acicular	Acicular quench crystals.
Clinopyroxene	20	20			Prismatic	Prismatic quench crystals and granules in matrix. Slightly titaniferrous.
Spinel	10	10			Octahedra	Quench octahedra and combs.
Glass	—	43				Completely altered to brown clays. Largely interstitial. Often concentrated around vesicles.

SECONDARY MINERALOGY	PERCENT	REPLACING/ FILLING	COMMENTS
Clays	43	Glass, ol	Brown clays replacing interstitial glass and ol, and possibly filling intercrystalline cavities.

VESICLES/ CAVITIES	PERCENT	LOCATION	SIZE RANGE (mm)	FILLING	SHAPE	COMMENTS
Vesicles	20	Even	<4	Clay	Irregular, elongate	Lined or infilled by brown clays.

THIN SECTION DESCRIPTION

115-706C-4R-3 (Piece 1, 10-13 cm)

ROCK NAME: Highly clinopyroxene plagioclase phyric basalt
WHERE SAMPLED: Unit 13
TEXTURE: Highly porphyritic, vesicular, ophitic
GRAIN SIZE: Fine to medium
OBSERVER: YT

PRIMARY MINERALOGY	PERCENT PRESENT	PERCENT ORIGINAL	SIZE RANGE (mm)	APPROX. COMPO-SITION	MORPHOLOGY	COMMENTS
PHENOCRYSTS						
Plagioclase	25	25	0.2–1.5	An 45	Euhedral–subhedral	Fresh. Zoned An 60 to An 40. Larger phenocrysts (>1 mm) have honeycomb texture; inclusions in these crystals could be glass + quenched magnetite.
Clinopyroxene	25	25	0.2–0.8	Augite	Subhedral	Fresh. Zoned crystals. Ophitic texture.
GROUNDMASS						
Plagioclase	1	1	<0.2		Acicular	
Clinopyroxene	Tr	Tr				
Glass	—	29				Completely replaced by aggregate of fine-grained unidentifiable minerals.
Opaques	20	20	<0.3		Acicular	Quench products.

SECONDARY MINERALOGY	PERCENT	REPLACING/ FILLING	COMMENTS
Altered glass	29	Glass	Aggregate of fine-grained unidentifiable minerals.

VESICLES/ CAVITIES	PERCENT	LOCATION	SIZE RANGE (mm)	FILLING	SHAPE
Vesicles	10	Even	0.2–2.0	Brown clays	Round, elliptical

THIN SECTION DESCRIPTION

115-706C-5R-1 (Piece 2A, 14-16 cm)

ROCK NAME: Highly olivine-bearing clinopyroxene plagioclase phyric basalt
WHERE SAMPLED: Unit 14, top of unit
TEXTURE: Highly porphyritic, vesicular, ophitic
GRAIN SIZE: Fine to medium
OBSERVER: YT

PRIMARY MINERALOGY	PERCENT PRESENT	PERCENT ORIGINAL	SIZE RANGE (mm)	APPROX. COMPO-SITION	MORPHOLOGY	COMMENTS
PHENOCRYSTS						
Olivine	—	Tr	0.2		Subhedral	Completely altered to brown clay.
Plagioclase	26	26	0.2–1.5	An 45	Euhedral–subhedral	Fresh. Zoned An 50 to An 65.
Clinopyroxene	26	26	0.2–0.8	Augite	Subhedral–euhedral	Fresh. Micro-ophitic.
Spinel	3	3	0.1–0.2	Magnetite	Euhedral–subhedral	Occurs as inclusions in plag and cpx and as discrete crystals.
GROUNDMASS						
Plagioclase	1	1	<0.2			
Clinopyroxene	Tr	Tr	<<1			
Glass	—	25				Completely altered to aggregates of fine-grained unidentifiable crystals.
Opaques	19	19	<0.3		Acicular	Quench products. Easily distinguished from opaque phenocrysts by morphology.

SECONDARY MINERALOGY	PERCENT	REPLACING/ FILLING	COMMENTS
Altered glass	25	Glass	Aggregate of fine-grained unidentifiable crystals.

VESICLES/ CAVITIES	PERCENT	LOCATION	SIZE RANGE (mm)	FILLING	SHAPE
Vesicles	10	Even	0.2–1.0	None	Irregular, elliptical

THIN SECTION DESCRIPTION

115-706C-5R-1 (Piece 7, 83-85 cm)

ROCK NAME: Highly olivine-bearing clinopyroxene plagioclase phyric basalt

WHERE SAMPLED: Unit 14

TEXTURE: Highly porphyritic, vesicular

GRAIN SIZE: Fine

OBSERVER: RBH

PRIMARY MINERALOGY	PERCENT PRESENT	PERCENT ORIGINAL	SIZE RANGE (mm)	APPROX. COMPO- SITION	MORPHOLOGY	COMMENTS
PHENOCRYSTS						
Olivine	—	Tr	0.5		Subhedral	Completely altered to greenish clay.
Plagioclase	20	20	<1		Subhedral, tabular	Lath-like crystals with swallow tail terminations.
Clinopyroxene	20	20			Subhedral, equant	Glomerocrysts common. Ophitic texture.
Spinel	2	2	0.1-0.2		Dendritic, skeletal	Beautiful skeletal crystals. Needles in groundmass. Laths are quench morphology. All very homogeneous with no signs of any alteration (or completely altered).
GROUNDMASS						
Cryptocrystalline groundmass	—	50				Opaque + quench cpx.
Glass(?)	—	8				

SECONDARY MINERALOGY	PERCENT	REPLACING/ FILLING	COMMENTS
Clays	58	Groundmass, glass(?), ol	Greenish brown clays with concentric color variations. Seems to have completely replaced glass(?) and/or cryptocrystalline groundmass. Fe-Ti oxides. Homogeneously distributed. Also fills smaller vesicles and replaces ol.
Pyrite	Tr	Vesicles	Rounded blobs filling 3 vesicles. Contain blebs of an isotropic phase.

VESICLES/ CAVITIES	PERCENT	LOCATION	SIZE RANGE (mm)	FILLING	SHAPE	COMMENTS
Vesicles	10			Clays, pyrite		Partially lined with greenish brown clay. Three vesicles are filled with pyrite.

COMMENTS: This slide is good for Fe-Ti oxides and identifying sulfides.

THIN SECTION DESCRIPTION

115-706C-5R-1 (Piece 8, 98-100 cm)

ROCK NAME: Highly olivine-bearing clinopyroxene plagioclase phyric basalt
WHERE SAMPLED: Unit 14
TEXTURE: Highly porphyritic, hypocrystalline
GRAIN SIZE: Fine, aphanitic
OBSERVER: ANB

PRIMARY MINERALOGY	PERCENT PRESENT	PERCENT ORIGINAL	SIZE RANGE (mm)	APPROX. COMPOSITION	MORPHOLOGY	COMMENTS
PHENOCRYSTS						
Olivine	—	Tr	<0.5		Subhedral–anhedral	Completely altered to brown clay.
Plagioclase	15	15	<1.0	An 62	Euhedral–subhedral	Fresh. Often with quench terminations.
Clinopyroxene	7	7	<0.8	Augite	Subhedral	Some hourglass zoning. Brownish Fe-rich zoned margins.
GROUNDMASS						
Plagioclase	5	5	<0.1		Subhedral	
Clinopyroxene	15	15	<0.2	Augite	Anhedral	
Spinel	10	10	<0.1	Magnetite	Subhedral–anhedral	Groundmass octahedra and quench material from interstitial glass.
Glass	—	48				Interstitial. Variously altered to brown clays.

SECONDARY MINERALOGY	PERCENT	REPLACING/ FILLING
Clays	48	Glass, ol

VESICLES/ CAVITIES	PERCENT	LOCATION	SIZE RANGE (mm)	FILLING	SHAPE
Vesicles	10	Even	<2	Brown clay	Subelliptical

THIN SECTION DESCRIPTION

115-706C-5R-2 (Piece 1, 2-5 cm)

ROCK NAME: Highly clinopyroxene plagioclase phyric basalt
WHERE SAMPLED: Unit 14
TEXTURE: Highly porphyritic
GRAIN SIZE: Fine
OBSERVER: RBH

PRIMARY MINERALOGY	PERCENT PRESENT	PERCENT ORIGINAL	SIZE RANGE (mm)	APPROX. COMPOSITION	MORPHOLOGY	COMMENTS
PHENOCRYSTS						
Plagioclase	10	10	<1		Subhedral, bladed	
Clinopyroxene	5	5	<0.8		Equant, subhedral–anhedral	
GROUNDMASS						
Clinopyroxene	70	70				Feathery quench texture in reflected light. Possibly partially altered to clay.
Opaques	<1	<1	0.05			Very fine uniformly distributed grains and needles.

SECONDARY MINERALOGY	PERCENT	REPLACING/ FILLING	COMMENTS
Clays	15	Vesicles.	Greenish varicolored clay.

VESICLES/ CAVITIES	PERCENT	LOCATION	SIZE RANGE (mm)	FILLING	SHAPE	COMMENTS
Vesicles	Tr		<2	Clays	Round	Vesicles all filled.

THIN SECTION DESCRIPTION

115-706C-5R-2 (Piece 2, 7-11 cm)

ROCK NAME: Highly olivine-bearing clinopyroxene plagioclase phyric basalt

WHERE SAMPLED: Unit 15

TEXTURE: Highly porphyritic, vesicular

GRAIN SIZE: Fine

OBSERVER: YT

PRIMARY MINERALOGY	PERCENT PRESENT	PERCENT ORIGINAL	SIZE RANGE (mm)	APPROX. COMPO-SITION	MORPHOLOGY	COMMENTS
PHENOCRYSTS						
Olivine	—	3	0.2–0.3		Euhedral	Completely altered to green and brown clays.
Plagioclase	15	15	0.2–0.7	An 50	Euhedral	Fresh. Zoned An 60 to An 40.
Clinopyroxene	10	10	0.2–0.5	Augite	Subhedral	Fresh, zoned crystals. Some glomerocrysts with plag.
GROUNDMASS						
Plagioclase	<1	<1			Acicular	
Glass	—	42				Completely altered to unidentifiable fine-grained crystals.
Opaques	30	30				Quench products.

SECONDARY MINERALOGY	PERCENT	REPLACING/ FILLING	COMMENTS
Altered glass	42	Glass	Unidentifiable fine-grained crystals.
Clays	3	Ol	Green and brown clays.

VESICLES/ CAVITIES	PERCENT	LOCATION	SIZE RANGE (mm)	FILLING	SHAPE	COMMENTS
Vesicles	20	Even	0.2–1.2	Clay	Irregular, elliptical	Rimmed by green clay.

THIN SECTION DESCRIPTION

115-706C-5R-2 (Piece 14, 87-89 cm)

ROCK NAME: Highly olivine clinopyroxene plagioclase phyric basalt

WHERE SAMPLED: Unit 16

TEXTURE: Highly porphyritic

GRAIN SIZE: Fine, aphanitic, hyaline

OBSERVER: ANB

PRIMARY MINERALOGY	PERCENT PRESENT	PERCENT ORIGINAL	SIZE RANGE (mm)	APPROX. COMPO-SITION	MORPHOLOGY	COMMENTS
PHENOCRYSTS						
Olivine	—	2	<0.4		Subhedral	Completely altered to green clays.
Plagioclase	15	15	<4	An 60	Euhedral–subhedral	Fresh. Quench terminations. Glass inclusions. Strong oscillatory zoning, An 65 at margins.
Clinopyroxene	5	5	<0.6	Augite	Euhedral–subhedral	Hourglass zoning.
GROUNDMASS						
Glass	30	78				Large areas of fresh glass grading into magnetite-rich opaque altered areas.

SECONDARY MINERALOGY	PERCENT	REPLACING/ FILLING	COMMENTS
Clays	2	Ol	Green clay replacing ol.
Altered glass	48	Glass	Alteration of interstitial glass. Magnetite-rich.

VESICLES/ CAVITIES	PERCENT	LOCATION	SIZE RANGE (mm)	FILLING	SHAPE
Vesicles	15	Even	<4	Brown clays	Irregular

THIN SECTION DESCRIPTION

115-706C-5R-2 (Piece 18, 102-105 cm)

ROCK NAME: Highly olivine clinopyroxene plagioclase phyric basalt

WHERE SAMPLED: Unit 17

TEXTURE: Highly porphyritic, vesicular

GRAIN SIZE: Fine

OBSERVER: YT

PRIMARY MINERALOGY	PERCENT PRESENT	PERCENT ORIGINAL	SIZE RANGE (mm)	APPROX. COMPO-SITION	MORPHOLOGY	COMMENTS
PHENOCRYSTS						
Olivine	—	3	0.2–0.3		Euhedral	Completely altered to brown and pale brown clays.
Plagioclase	10	10	0.2–0.6	An 50	Euhedral	Fresh. Zoned An 40 to An 60.
Clinopyroxene	10	10	0.2–0.5	Augite	Euhedral–subhedral	Fresh. Glomerocrysts with plag, and monomineralic glomerocrysts.
Spinel	<1	<1	<0.1	Magnetite(?)	Euhedral	Distinct morphology from groundmass spinel.
GROUNDMASS						
Plagioclase	Tr	Tr	<<1		Acicular	
Clinopyroxene	Tr	Tr	<<1			
Glass	77	77				Fresh brown glass exists in some areas. Dendritic cpx crystals exist.

SECONDARY MINERALOGY	PERCENT	REPLACING/ FILLING	COMMENTS
Clays	3	Ol	Brown and pale brown clays.

VESICLES/ CAVITIES	PERCENT	LOCATION	SIZE RANGE (mm)	FILLING	SHAPE	COMMENTS
Vesicles	25	Even	0.2–2.0	Clay	Elliptical, irregular	Especially elliptical in the brown glass.

THIN SECTION DESCRIPTION

115-706C-5R-2 (Piece 22, 135-137 cm)

ROCK NAME: Highly olivine clinopyroxene plagioclase phyric basalt

WHERE SAMPLED: Unit 17

TEXTURE: Highly porphyritic, vesicular

GRAIN SIZE: Fine

OBSERVER: YT

PRIMARY MINERALOGY	PERCENT PRESENT	PERCENT ORIGINAL	SIZE RANGE (mm)	APPROX. COMPO-SITION	MORPHOLOGY	COMMENTS
PHENOCRYSTS						
Olivine	—	5	0.3		Euhedral	Completely altered to pale brown clay.
Plagioclase	10	10	0.2–0.6	An 50	Euhedral	Fresh. Zoned An 40 to An 60.
Clinopyroxene	10	10	0.2–0.5	Augite	Euhedral–subhedral	Fresh. Sector and normal zoning. Some crystals contain dusty inclusions. Some monomineralic glomerocrysts and some glomerocrysts with plag.
GROUNDMASS						
Plagioclase	Tr	Tr	<<1		Acicular	
Glass	75	75				Opaque-like cpx quench crystals sometimes rim phenocrysts. This opaque-like rim could consist of more than one phase (magnetite + cpx).

SECONDARY MINERALOGY	PERCENT	REPLACING/ FILLING	COMMENTS
Clays	5	Ol	Chlorite(?).

VESICLES/ CAVITIES	PERCENT	LOCATION	SIZE RANGE (mm)	FILLING	SHAPE
Vesicles	15	Even	<1.5	Pale brown clay	Irregular, elliptical

THIN SECTION DESCRIPTION

115-706C-5R-3 (Piece 1, 1-4 cm)

ROCK NAME: Highly olivine-bearing clinopyroxene plagioclase phyric basalt
WHERE SAMPLED: Unit 18
TEXTURE: Highly porphyritic
GRAIN SIZE: Aphanitic, microcrystalline, glassy
OBSERVER: ANB

PRIMARY MINERALOGY	PERCENT PRESENT	PERCENT ORIGINAL	SIZE RANGE (mm)	APPROX. COMPOSITION	MORPHOLOGY	COMMENTS
PHENOCRYSTS						
Olivine	—	Tr	<0.5		Subhedral–anhedral	Completely altered to green clays.
Plagioclase	15	15	<0.8	An 60	Euhedral–subhedral	Incipient fine-scale alteration developed on crystal margins and cleavage traces.
Clinopyroxene	5	5	<0.5	Augite	Subhedral	Subophitic aggregates with plag common.
GROUNDMASS						
Plagioclase	5	5	<0.5		Anhedral	Quench phase in altered glass.
Clinopyroxene	5	5	<0.1	Augite	Anhedral	Quench phase in altered glass.
Spinel	5	5	<0.1	Magnetite	Subhedral	Quench phase in altered glass.
Glass	—	65				Interstitial. Altered to brownish clay aggregates.

SECONDARY MINERALOGY	PERCENT	REPLACING/ FILLING	COMMENTS
Clays	65	Glass	Unidentifiable brownish alteration product of interstitial glass.

VESICLES/ CAVITIES	PERCENT	LOCATION	SIZE RANGE (mm)	FILLING	SHAPE	COMMENTS
Vesicles	15	Even	<2	Clay	Irregular, sub-elliptical	Large vesicles lined with brown clays, which are then rimmed by green celadonite(?). Small vesicles are totally filled by green celadonite(?).

THIN SECTION DESCRIPTION

115-706C-5R-3 (Piece 6, 44-48 cm)

ROCK NAME: Highly olivine clinopyroxene plagioclase phyric basalt
WHERE SAMPLED: Unit 19, glassy contact
TEXTURE: Highly porphyritic
GRAIN SIZE: Fine, microcrystalline
OBSERVER: MRF

PRIMARY MINERALOGY	PERCENT PRESENT	PERCENT ORIGINAL	SIZE RANGE (mm)	APPROX. COMPOSITION	MORPHOLOGY	COMMENTS
PHENOCRYSTS						
Olivine	<1	1–2	0.1–0.2		Euhedral	Spinel inclusions.
Plagioclase	10	10	0.05–1.00		Euhedral, laths	Intergrown with ol, augite, spinel.
Clinopyroxene	2	2	0.1–1.0		Subhedral	Rims show reaction with glass.
Spinel	<1	<1		Titano-magnetite(?)	Subhedral, skeletal	Titanomagnetite(?) in groundmass and glass.
GROUNDMASS						
Cryptocrystalline groundmass, glass	80	80				Dark brown opaque. Contains Fe-Ti oxide needles and some subhedral grains. Distinct plumose texture apparent in reflected light—probably silicate (cpx).

SECONDARY MINERALOGY	PERCENT	REPLACING/ FILLING	COMMENTS
Clays	8	Vesicles	Greenish clay. Filling smaller vesicles. Probably replacing some ol.

THIN SECTION DESCRIPTION

115-706C-6R-1 (Piece 2, 46-50 cm)

ROCK NAME: Highly olivine-bearing clinopyroxene plagioclase phyric basalt

WHERE SAMPLED: Unit 20

TEXTURE: Highly porphyritic

GRAIN SIZE: Aphanitic, microcrystalline

OBSERVER: ANB

PRIMARY MINERALOGY	PERCENT PRESENT	PERCENT ORIGINAL	SIZE RANGE (mm)	APPROX. COMPOSITION	MORPHOLOGY	COMMENTS
PHENOCRYSTS						
Olivine	—	*Tr*	<0.3		Subhedral–anhedral	*Completely altered to brown-green clays.*
Plagioclase	10	10	<0.8	An 62	Euhedral–subhedral	Fresh. Quench terminations. Incipient alteration to clays along fractures, cleavage traces, and crystal edges.
Clinopyroxene	5	5	<0.5	Augite	Subhedral	
GROUNDMASS						
Plagioclase	5	5	<0.05		Anhedral	Altering to microcrystalline clays. Quench phase in glass.
Clinopyroxene	5	5	<0.05	Augite	Anhedral	Quench phase.
Spinel	7	7	<0.1	Magnetite(?)	Subhedral	Quench phase. Combs and granules.
Glass	—	68				Interstitial. Completely altered to microcrystalline clays of uncertain composition.

SECONDARY MINERALOGY	PERCENT	REPLACING/ FILLING	COMMENTS
Clays	68	Glass	Indeterminate glass alteration product associated with quench phases.

VESICLES/ CAVITIES	PERCENT	LOCATION	SIZE RANGE (mm)	FILLING	SHAPE	COMMENTS
Vesicles	5	Even	<3	Glass, clay	Irregular, elliptical	Linings of altered glass. Some small vesicles filled with green celadonite(?) and indeterminate brown clays.

COMMENTS: 4 mm wide vein of bright green celadonite(?) tranverses the slide. Associated with indeterminate brown-orange clays. Vesicles occur ≈0.5 mm either side of the vein contact, and are filled with the same clays. Contact is sharp, but locally irregular, and clearly truncates some phenocrysts.

THIN SECTION DESCRIPTION

115-706C-6R-2 (Piece 2, 16-18 cm)

ROCK NAME: Highly olivine clinopyroxene plagioclase phyric basalt

WHERE SAMPLED: Unit 21

TEXTURE: Highly porphyritic

GRAIN SIZE: Fine

OBSERVER: YT

PRIMARY MINERALOGY	PERCENT PRESENT	PERCENT ORIGINAL	SIZE RANGE (mm)	APPROX. COMPO-SITION	MORPHOLOGY	COMMENTS
PHENOCRYSTS						
Olivine	—	2	<0.2		Euhedral	Completely altered to brown clays.
Plagioclase	25	25	0.2-0.8	An 45	Euhedral	Fresh. Zoned (approximately) An 30 to An 50.
Clinopyroxene	15	15	0.2-0.5	Augite	Euhedral, skeletal	Fresh. Some glomerocrysts.
GROUNDMASS						
Glass	—	25				Completely altered to aggregates of fine-grained unidentifiable phases.
Opaques	18	18	<0.2	Magnetite	Euhedral, cubic	
Clinopyroxene	15	15	<0.4		Acicular	Needle-like quench products.

SECONDARY MINERALOGY	PERCENT	REPLACING/ FILLING	COMMENTS
Clays	2	Ol	Brown clay.
Clays	25	Glass	Aggregates of fine-grained unidentifiable phases.

VESICLES/ CAVITIES	PERCENT	LOCATION	SIZE RANGE (mm)	FILLING	SHAPE
Vesicles	15	Even	<2	Brown clay	Irregular, elliptical

THIN SECTION DESCRIPTION

115-706C-8R-1 (Piece 6, 40-42 cm)

ROCK NAME: Highly olivine-bearing clinopyroxene plagioclase phyric basalt

WHERE SAMPLED: Unit 26

TEXTURE: Microporphyritic, vesicular

GRAIN SIZE: Fine

OBSERVER: RBH

PRIMARY MINERALOGY	PERCENT PRESENT	PERCENT ORIGINAL	SIZE RANGE (mm)	APPROX. COMPO-SITION	MORPHOLOGY	COMMENTS
PHENOCRYSTS						
Olivine	—	≈1(?)	0.3			Possibly present.
Plagioclase	12	12	0.2-3.0		Subhedral laths	Laths and quench needles.
Clinopyroxene	12	12	0.25-1.00		Subhedral, equant	Glomerocrysts. Some ophitic texture.
GROUNDMASS						
Clinopyroxene, plagioclase	59	59				Plumose quench texture, possible cpx(?) and plag needles.
Opaques	<2	<2	<0.08	Fe-Ti	Needles, dendritic	Dendritic needles and fine needles only. Distinctly different habits. No skeletal cubes. Quench texture. Very fine opaques common in groundmass.

SECONDARY MINERALOGY	PERCENT	REPLACING/ FILLING	COMMENTS
Clays	15	Vesicles	Bright green celadonite(?) filling smaller vesicles.

VESICLES/ CAVITIES	PERCENT	LOCATION	SIZE RANGE (mm)	FILLING	SHAPE	COMMENTS
Vesicles	10		<2	Clays		Lined with greenish celadonite(?).

THIN SECTION DESCRIPTION

115-706C-8R-1 (Piece 11, 74-77 cm)

ROCK NAME: Highly olivine-bearing clinopyroxene plagioclase phyric basalt

WHERE SAMPLED: Unit 27

TEXTURE: Highly porphyritic

GRAIN SIZE: Aphanitic, microcrystalline

OBSERVER: ANB

PRIMARY MINERALOGY	PERCENT PRESENT	PERCENT ORIGINAL	SIZE RANGE (mm)	APPROX. COMPOSITION	MORPHOLOGY	COMMENTS
PHENOCRYSTS						
Olivine	—	Tr	<0.3		Subhedral	Completely altered to brown clay of indeterminate composition.
Plagioclase	10	10	<1	An 60	Euhedral–subhedral	Fresh. Quench terminations.
Clinopyroxene	7	7	<0.6	Augite	Subhedral–anhedral	Subophitic clots common. Glomerocrysts with cpx common.
GROUNDMASS						
Plagioclase	10	10	<0.1		Anhedral	Groundmass crystals. Subordinate quench forms from glass.
Clinopyroxene	10	10	<0.2	Augite	Anhedral	
Spinel	10	10	<0.2	Magnetite	Subhedral	Octahedra and quench combs from glass.
Glass	—	53				Interstitial. Completely altered to clays of indeterminate composition.

SECONDARY MINERALOGY	PERCENT	REPLACING/ FILLING	COMMENTS
Clays	53	Glass, ol	Alteration phase of indeterminate composition.

VESICLES/ CAVITIES	PERCENT	LOCATION	SIZE RANGE (mm)	FILLING	SHAPE	COMMENTS
Vesicles	7	Even	7	Clay	Irregular, elliptical	Lined with brown clays. Small vesicles are completely filled by same clays. Oxidized magnetite-rich glass surrounds some vesicles.

THIN SECTION DESCRIPTION

115-706C-8R-2 (Piece 1D, 44-47 cm)

ROCK NAME: Highly olivine clinopyroxene plagioclase phyric basalt

WHERE SAMPLED: Unit 28

TEXTURE: Highly porphyritic, vesicular

GRAIN SIZE: Fine to medium

OBSERVER: YT

PRIMARY MINERALOGY	PERCENT PRESENT	PERCENT ORIGINAL	SIZE RANGE (mm)	APPROX. COMPOSITION	MORPHOLOGY	COMMENTS
PHENOCRYSTS						
Olivine	—	2	0.2–0.3		Euhedral	Completely replaced by green-gray clay + carbonate.
Plagioclase	15	15	0.2–2.0	An 40-50	Euhedral	Fresh. Zoned An 60 to An 35. Two larger plag 'xenocrysts' measure 2 and 3 mm; these have typical dusty inclusions.
Clinopyroxene	15	15	0.2–0.8	Augite	Euhedral–subhedral	Fresh. Some glomerocrysts.
GROUNDMASS						
Plagioclase	1	1	<0.2		Acicular	
Glass	—	41				Completely replaced by aggregates of fine-grained unidentifiable phases.
Clinopyroxene	27	27	<0.4		Dendritic	Needle-like quench products.

SECONDARY MINERALOGY	PERCENT	REPLACING/ FILLING	COMMENTS
Clays	1	Ol	Green-gray clays.
Altered glass	41	Glass	Aggregates of fine-grained unidentifiable phases.
Carbonate	1	Ol	

VESICLES/ CAVITIES	PERCENT	LOCATION	SIZE RANGE (mm)	FILLING	SHAPE	COMMENTS
Vesicles	15	Even	0.1–1.5	Clay	Irregular	Green clays.

THIN SECTION DESCRIPTION

115-706C-8R-2 (Piece 12A, 125-128 cm)

ROCK NAME: Highly olivine-bearing clinopyroxene phyric basalt

WHERE SAMPLED: Unit 29

TEXTURE: Microporphyritic

GRAIN SIZE: Fine

OBSERVER: RBH

PRIMARY MINERALOGY	PERCENT PRESENT	PERCENT ORIGINAL	SIZE RANGE (mm)	APPROX. COMPOSITION	MORPHOLOGY	COMMENTS
PHENOCRYSTS						
Olivine	—	Tr				
Plagioclase	8	8	<1.5		Subhedral, laths, needles	Average crystal size = 0.5 mm.
Clinopyroxene	8	8	0.3		Equant, subhedral	
Spinel	2	2	0.05–0.20	Fe-Ti Oxide	Skeletal, dendritic	Cruciformdendrites. Largely quench and ubiquitous fine 5μm particles.
GROUNDMASS						
Plagioclase	2	2			Needles	
Clinopyroxene	2	2			Granules	
Opaque	68	78				Incipient crystals of cpx, plag, and opaques in opaque to near opaque groundmass.

SECONDARY MINERALOGY	PERCENT	REPLACING/ FILLING	COMMENTS
Clays	10	Opaque	Replacing opaque groundmass and lining vesicles.

VESICLES/ CAVITIES	PERCENT	LOCATION	SIZE RANGE (mm)	FILLING	SHAPE
Vesicles	20		<2	None	Rounded

COMMENTS: Heterogeneous. Several bands and patches of darker chilled material with sparse phenocrysts cut across the slide. Also some rounded very fine basalt microcrystalline droplets with plag + cpx growing around and nucleating on it. Some larger plag crystals are filled with inclusions.

THIN SECTION DESCRIPTION

115-706C-8R-3 (Piece 5A, 45-47 cm)

ROCK NAME: Highly olivine clinopyroxene plagioclase phyric basalt

WHERE SAMPLED: Unit 29

TEXTURE: Highly porphyritic

GRAIN SIZE: Fine

OBSERVER: YT

PRIMARY MINERALOGY	PERCENT PRESENT	PERCENT ORIGINAL	SIZE RANGE (mm)	APPROX. COMPOSITION	MORPHOLOGY	COMMENTS
PHENOCRYSTS						
Olivine	—	3	0.2–0.3		Euhedral	Completely replaced by brown clay (crystal margins) + carbonate (crystal interiors).
Plagioclase	24	24	0.2–1.0	An 60	Euhedral	Fresh, zoned. Larger crystals have honeycomb structure.
Clinopyroxene	23	23	0.2–0.5	Augite	Euhedral–subhedral	Fresh, zoned. Some glomerocrysts.
GROUNDMASS						
Plagioclase	Tr	Tr	<0.1		Acicular	
Clinopyroxene	Tr	Tr	<0.1			
Glass	—	30				Completely replaced by carbonate and brown clays.
Quench crystals	20	20	<0.4	Magnetite(?), cpx	Acicular	Quench products.

SECONDARY MINERALOGY	PERCENT	REPLACING/ FILLING	COMMENTS
Clays	1	Ol	
Carbonate	2	Ol, glass	
Clays	30	Glass	Brown clays.

VESICLES/ CAVITIES	PERCENT	LOCATION	SIZE RANGE (mm)	FILLING	SHAPE	COMMENTS
Vesicles	2	Even	<0.1	Clay	Irregular	Filled by brown clay.

THIN SECTION DESCRIPTION

115-706C-9R-1 (Piece 1, 5-8 cm)

ROCK NAME: Highly olivine clinopyroxene plagioclase phyric basalt

WHERE SAMPLED: Unit 30

TEXTURE: Highly porphyritic, slightly vesicular

GRAIN SIZE: Fine

OBSERVER: YT

PRIMARY MINERALOGY	PERCENT PRESENT	PERCENT ORIGINAL	SIZE RANGE (mm)	APPROX. COMPOSITION	MORPHOLOGY	COMMENTS
PHENOCRYSTS						
Olivine	—	9	0.2–1.2		Euhedral–subhedral	Completely altered to brown clays. Subhedral crystals indicate growth morphology (arrow-like).
Plagioclase	11	11	0.2–1.0	An 60	Euhedral	Fresh, zoned.
Clinopyroxene	10	10	0.2–0.5	Augite	Euhedral–subhedral	Fresh, zoned.
GROUNDMASS						
Plagioclase	Tr	Tr				
Glass, quench crystals	70	70				Brown fresh glass.

SECONDARY MINERALOGY	PERCENT	REPLACING/ FILLING	COMMENTS
Clays	9	Ol	Generally iddingsite. Some green clay (chlorite?).

VESICLES/ CAVITIES	PERCENT	LOCATION	SIZE RANGE (mm)	FILLING	SHAPE	COMMENTS
Vesicles	10	Even	<0.2	Clay	Elliptical, round	Pale brown clay.

COMMENTS: This rock is possibly the most Mg-rich rock in Site 706C.

THIN SECTION DESCRIPTION

115-706C-9R-1 (Piece 4A, 27-29 cm)

ROCK NAME: Highly clinopyroxene plagioclase phyric basalt
WHERE SAMPLED: Unit 31
TEXTURE: Highly porphyritic
GRAIN SIZE: Medium to coarse
OBSERVER: RBH

PRIMARY MINERALOGY	PERCENT PRESENT	PERCENT ORIGINAL	SIZE RANGE (mm)	APPROX. COMPO-SITION	MORPHOLOGY	COMMENTS
PHENOCRYSTS						
Plagioclase	15	15	20–30	An60-73	Subhedral	
Clinopyroxene	1	1	2		Subhedral, equant	Occasional crystal attached to plag.
GROUNDMASS						
Plagioclase	35	35	0.8		Subhedral, laths	Medium to fine grained.
Clinopyroxene	25	25	0.6		Anhedral, equant	Equant grains, sometimes aggregated.
Opaque	5	5	0.2		Skeletal, needles	Probably magnetite + ilmenite.
Glass(?)	—	19				Completely altered to clays.

SECONDARY MINERALOGY	PERCENT	REPLACING/ FILLING	COMMENTS
Clays	19	Glass(?)	Green to brown clays.

VESICLES/ CAVITIES	PERCENT	LOCATION	SIZE RANGE (mm)	FILLING	SHAPE
Vesicles	5	Even	<1	None	Round

THIN SECTION DESCRIPTION

115-706C-9R-2 (Piece 4, 36-38 cm)

ROCK NAME: Highly olivine clinopyroxene plagioclase phyric basalt

WHERE SAMPLED: Unit 32

TEXTURE: Highly porphyritic

GRAIN SIZE: Aphanitic, microcrystalline/hypocrystalline

OBSERVER: ANB

PRIMARY MINERALOGY	PERCENT PRESENT	PERCENT ORIGINAL	SIZE RANGE (mm)	APPROX. COMPO-SITION	MORPHOLOGY	COMMENTS
PHENOCRYSTS						
Olivine	—	1	<1.0		Subhedral	Completely replaced by calcite. Occasional aggregates.
Plagioclase	15	15	<7.0	An 60-65	Euhedral–subhedral	Two generations: large phenocrysts An 60-65 zoned to An 55(+) at margins; smaller phenocrysts ≈An 60.
Clinopyroxene	10	10	<0.8	Augite	Subhedral–anhedral	Sub-ophitic aggregates common.
GROUNDMASS						
Plagioclase	5	5	<0.05		Acicular	Quench phase in glass.
Spinel	5	5	<0.05	Magnetite	Octahedra	Quench octahedra and combs in glass.
Glass	—	64				Interstitial. Completely altered to indeterminate clay grade phases, largely colorless to gray clay with some bright orange-red phase.

SECONDARY MINERALOGY	PERCENT	REPLACING/ FILLING	COMMENTS
Clays	64	Glass	Indeterminate clays, colorless to gray.
Carbonate	1	Ol	Probably calcite.

VESICLES/ CAVITIES	PERCENT	LOCATION	SIZE RANGE (mm)	FILLING	SHAPE	COMMENTS
Vesicles	10	Even	<1.5	Clay		Various glass linings, celadonite linings and infills, clay linings and infills. Occasional late calcite infills.

COMMENTS: Plag phenocrysts in this unit are an order of magnitude larger than in other Units. Aggregates common. Large crystals often poikilitically enclose smaller (but still large) crystals. Associated with usually smaller plag phenocrysts.
Unlike other rock units, calcite is a relatively common alteration phase. It exclusively replaces ol and occurs as late-stage infills in some large vesicles, where it post-dates glass linings. Also occurs as granular infill in an irregular, 2-mm-wide vein which cuts the slide transversely.
Zoned inclusion-rich areas occur in the cores of some large plag phenocrysts.